Altered Expression Profiles and Defects in a Group of Cell Cycle Regulators and Tumor Suppressor Genes (INK4) and Evaluation of Comprehensive Expression Profiles of Canine miRNAs in Spontaneous Canine Breast Cancer Models

by

Farruk Mohammad Lutful Kabir

A dissertation submitted to the Graduate Faculty of
Auburn University
in partial fulfillment of the
requirements for the Degree of
Doctor of Philosophy

Auburn, Alabama
December 13, 2014

Approved by

R. Curtis Bird, Chair and Graduate Advisor, Professor of Pathobiology
Bruce F. Smith, Professor of Pathobiology
Frederik W. van Ginkel, Associate Professor of Pathobiology
Jacek Wower, Professor of Animal Sciences

Abstract

The cyclin-dependent kinase inhibitors (CKIs) act as powerful cell cycle regulators and endogenous tumor suppressors. Defects in members of the INK4A/B CKI tumor suppressors have been associated with human and canine cancers. Most of the cancer-associated genetic alterations that are known to play roles in mammary tumor development and progression are similar in both species. The objectives of this study were to evaluate genetic regulation and defects in INK4 genes as well as the comprehensive expression profiles and altered regulation of miRNAs in spontaneous canine mammary tumor (CMT) and malignant melanoma (CML) models. Gene expression profiles and sequencing of INK4 genes have been evaluated by RT-PCR, rapid amplification of cDNA ends (RACE)-PCR, and touchdown-PCR assays as well as subsequent cloning experiments. The sequences were analyzed by Vector NTI and bioinformatics tools. The comprehensive miRNA expression profile was evaluated by miRNA qPCR arrays. Members of the INK4 genes are differentially expressed while genes encoded by the p16/INK4A/B locus (p16, p14 and p15) have been found most frequently defective in CMT and CML models. A novel frameshift mutation has been discovered in p16 exon1α resulting in altered mRNA and protein expression in the CMT28 cell line derived from canine mammary adenocarcinoma. These altered expression profiles for the INK4 tumor suppressor genes were also demonstrated in CML cell lines and primary canine mammary tumors and found to be highly correlated with those found in common human breast cancer cell lines. For the

first time, the 277 most abundantly expressed miRNAs in the canine genome have been screened in three CMT cell lines (CMT12, CMT27 and CMT28) that were characterized for INK4 gene defects. Several miRNAs that were altered in the CMT cell lines could potentially target these INK4 genes and also correlated to orthologous miRNAs identified in human breast cancer. Particularly, the miR-141 was validated by functional 3'-UTR reporter assay for binding of the INK4A 3'-UTR target sequence. These altered miRNAs and their target genes may represent unique and critical regulatory features in CMT models that can be used to better understand the conserved cell cycle regulatory mechanisms in human breast cancer.

Acknowledgements

First of all, I would like to sincerely acknowledge my Graduate Mentor and Advisor, Dr. R. Curtis Bird for his benevolent support, help and scholarly guidance throughout my PhD study in the field of Cancer Molecular Genetics. I would also like to acknowledge my doctoral research advisory committee members Dr. Bruce F. Smith, Dr. Frederik W. van Ginkel, and Dr. Jacek Wower for their constructive suggestions, academic support and scientific inputs in my PhD research.

I would like to deeply thank Patricia DeInnocentes for being a wonderful senior colleague and for all assistance, guiding and training the basic laboratory practices since the beginning of my PhD. I would also like to thank Allison Church Bird for her kind help and support for all the flow cytometry works. I would like to acknowledge Dr. Bruce F. Smith and all the past and present members of his lab for their support and help with essential techniques, training and for providing me the primary biopsy samples from different dogs. I would like to thank Dr. Payal Agarwal Sandey, Dr. Maninder Sandey and Dr. Jeremy Foote for their help, suggestions and training in my graduate research. My sincere gratitude is for all the professors, staff, fellow senior and junior students of the Department of Pathobiology for their timely support and help.

I would like to thank Auburn University Research Initiative in Cancer (AURIC) and Dr. Frank Bartol, Department of Pathobiology and Cellular and Molecular Biosciences (CMB) Graduate Program for all funding and academic support.

Finally, I would like to gratefully mention my beloved parents, younger brother, grandparents and my wife (being a constant supporter in personal life by any cost) for giving me the core inspiration and incentive in attaining the position at this level and for my all outstanding achievements.

Dedication

I dedicate my PhD work to those human beings who suffered from cancers and fought until the last breath of their lives. Here I would like to mention my late grandmother who died in metastatic breast cancer. And this work is dedicated to those as well who are currently suffering from cancers because the lifesaving cure is still out of their reach.

I also dedicate this work to my parents (Dr. A. Latif Talukder and Mrs. Farida Akter), my wife (Jishan Zaman) and my late grandfather (Mohammad Ali).

Table of Contents

Abstract ii

Acknowledgments iv

Dedication vi

List of Tables x

List of Figures xi

List of Abbreviations xiii

Chapter 1: Literature Review

Section 1. Dog as a Tumor Model 1

Section 2. Canine Mammary Tumors (CMTs)

Tumor Incidence 2

Comparative Genomics of Human and Canine Breast Cancers 3

Classification/Subtypes of CMTs 4

Development of an *in vivo* Tumor Model of CMTs 5

Section 3. Cell Cycle Regulators: A Classic Repertoire of Tumor Suppressors

Cell Cycle and Cancer are Connected 6

Cell Cycle Machinery 7

Two Families of CDK Inhibitors 8

CDK Inhibitors Form a Repertoire of Tumor Suppressor Proteins 9

Section 4. Gene Location, Mapping, Structure and Functions of the p16/INK4A/ARF Locus....10

Evolutionary History and Alternative Splicing of the INK4/ARF Locus from a Common Ancestor....11

Roles of INK4A/ARF in the Cell Cycle and Cancers....18

p16/INK4A and p14ARF have Non-overlapping Distinct Functions....18

The INK4A/ARF Locus Functions in Cell Senescence, and is a Barrier to Tumorigenesis....22

Alteration of the INK4A/ARF Locus in Cancers....25

Section 5. Regulatory, Small Non-coding RNAs: miRNAs in Cancers....31

Long Non-coding RNAs in Cancers....32

How Many miRNAs are There?....33

miRNA Biosynthesis and Regulation of Gene Expression....34

OncomiRs: Roles in Cancers....35

Regulation of miRNAs in Breast Cancers....37

miRNAs Regulate Cell Cycle by Targeting Multiple Genes....38

Chapter 2: Altered Expression of p16/INK4A from the INK4A/ARF Locus Due to the Novel Frameshift Mutation and Frequent Loss of p16 in Spontaneous CMT Models

Section 1. Introduction....41

Section 2. Methods and Materials....45

Section 3. Results....50

Section 4. Discussion and Conclusions....63

Chapter 3: Recurrent Loss of the p16/INK4A Locus in Primary Canine Mammary Tumors, Melanomas, and Human Breast Cancer Cell Lines

Section 1. Introduction....67

Section 2. Methods and Materials....71

Section 3. Results.....77

Section 4. Discussion and Conclusions 88

Chapter 4: Comprehensive Expression Profile and Regulation of miRNAs in Spontaneous Canine Mammary Tumor Models with INK4 Tumor Suppressor Defects

Section 1. Introduction.....92

Section 2. Methods and Materials.....97

Section 3. Results.....116

Section 4. Discussion and Conclusions 149

Chapter 5: Conclusions.....154

References.....159

Appendix 1: GenBank accession numbers for INK4 proteins from different species.....186

Appendix 2: miRNA CDKN2A 3' UTR target clone and miR-141 precursor clone datasheet.....187

Appendix 3: List of the 277 miRNAs from the canine genome 195

Appendix 4: List of total altered miRNAs (220) identified in 3 CMT cell lines.....202

Appendix 5: Heat map visualization of log2 (fold-change) level of expression of miRNAs in 3 CMT cell lines (for array plates 2, 3 and 4).....210

Appendix 6: Comparison of miRNA relative normalized expression between CMEC and CMT cells.....213

Appendix 7: 3D profile showing fold difference in expression of miRNAs in CMT12 and CMT28 cell lines.....214

Appendix 8: Volcano plot for CMT cell lines 216

Appendix 9: Single cell sorting of normal canine mammary epithelial cells 217

List of Table

Table 1: Primer sequences designed for INK4 genes 46

Table 2: INK4 and p53 primers designed from human genome.....74

Table 3: Prediction of miRNA targets by using TargetScan 111

Table 4: Deregulated miRNAs targeting oncogene growth factors and hormone receptors in the context of CMT models 147

Table 5: Altered expression of miRNAs that are associated with canine and human breast cancers.....153

List of Figures

Figure 1. Proposed evolutionary history of the mammalian INK4 genes.....12

Figure 2. INK4/CDKN2 dendrogram 14

Figure 3. Evolutionary model showing the gene duplication events postulated to have given rise to generate INK4A and ARF exon 1β.....16

Figure 4. Cell cycle regulation by p16/INK4A and p14ARF in two different pathways ..20

Figure 5. Representative human chromosome 9p21 and the genomic organization and mapping of the INK4A/ARF locus.....27

Figure 6. INK4 CKI expression in CMT cells.....51

Figure 7. Amplification of p16 from NCF and CMT28 by TD-PCR.....53

Figure 8. Alignment of canine and other mammalian p16 sequences 55

Figure 9. Comparison of predicted CMT28 p16mut protein sequence with wild type sequences from NCF and other mammals 57

Figure 10. Mutation of the CMT28 p16 sequence alters the reading frame of exon 2 to p14ARF.....59

Figure 11. Comparative analysis of INK4 protein motifs and folding structures.....61

Figure 12. Isolation and development of normal CMEC and primary CMT cells 78

Figure 13. Expression of INK4 mRNAs in primary CMT cells.....80

Figure 14. INK4 mRNA expression in CML cell lines 82

Figure 15. Expression of p21/Cip1, p27/Kip1, p53 and Rb tumor suppressor genes in a panel of two representative CML cell lines CML-7C and CML-10P 83

Figure 16. Alignment of canine p16 sequences and other mammalian p16 sequences.....85

Figure 17. INK4 expression profile in human breast cancer cell lines 87

Figure 18. miRNA PCR array plate layout 99

Figure 19. Amplification of mature miRNAs in qPCR arrays 103

Figure 20. Calculation of fold-change in expression 106

Figure 21. 4% high resolution agarose gel electrophoresis of selected miRNA qPCR array products showing relative banding patterns 109

Figure 22. Vector backbone of the miRNA 3'-UTR target clone 114

Figure 23. 2% formaldehyde denaturing gel electrophoresis for miRNAs 116

Figure 24. Comprehensive expression profile of dog miRNome 118

Figure 25. Heat map visualization of log2 (fold-change) level of expression of miRNAs in CMT cell lines 120

Figure 26. Comparison of miRNA relative normalized expression between CMEC and CMT27 cells 122

Figure 27. Scatter plots of CMT vs CMEC log ($2^{-\Delta Ct}$) showing fold-change in miRNA expression 123

Figure 28. Representative 3D profile showing fold difference in expression of miRNAs in CMT27 cell line 127

Figure 29. Altered miRNA expression profiles in CMT cell lines 129

Figure 30. Prediction of miRNA target binding sites in p16 mRNA sequence 133

Figure 31. Amplification of exon2-3'UTR (E2-3'UTR) sequence in CMECs, CMT9, CMT12, CMT28, and CMT27 cell lines 137

Figure 32. Sequencing and alignment of the longer 3'-UTR of INK4A or p14ARF mRNA amplified in CMEC, CMT9 and CMT28 138

Figure 33. Transfection of CMEC and CMT cell lines by miR-141 141

Figure 34. Validation of miR-141 target binding by 3'-UTR luciferase assay 143

Figure 35. Prediction of miRNA targets among key cell cycle regulatory genes 146

Figure 36. Novel targets of miR-429 and miR-200c predicted by TargetScan 148

List of Abbreviations

Ago2	Argonaut Proteins
ARF	Alternative Reading Frame
BLAST	Basic Local Alignment Search Tool
BSA	Bovine Serum Albumin
BTB	A Canine Mammary Epithelium-derived Cell Line
CDK	Cyclin-dependent Kinase
CDKN2	Cyclin-dependent Kinase Inhibitor 2
cDNA	Complementary DNA
Cip/Kip	CDK Interacting Protein/ Kinase Inhibitory Protein
CKI	Cyclin-dependent Kinase Inhibitor
CMEC	Canine Mammary Epithelial Cell
CML	Canine Melanoma
CMT	Canine Mammary Tumor
CMV	Cytomegalovirus
DNA	Deoxyribo Nucleic Acid
ΔΔCt	ΔΔ Cycle Threshold
EGFR	Epidermal Growth Factor Receptor
EMT	Epithelial to Mesenchymal Transition
ER/ESR	Estrogen Receptor
ERBB1/2/3	Epidermal Growth Factor Receptor 1/2/3
ERRFI1	ERBB Receptor Feedback Inhibitor 1
FBS	Fetal Bovine Serum

GAPDH	Glyceraldehyde-3-Phosphate Dehydrogenase
HER2	Human Epidermal Growth Factor Receptor 2
HOTAIR	HOX antisense intergenic RNA
IFN	Interferon
IL-2R	Interleukin-2 Receptor
INK4	Inhibitor of Cyclin-dependent Kinase 4
IVIS	*in vivo* Imaging System
lncRNA	Long Non-coding RNA
LOH	Loss of Heterozygosity
MDM2	A p53 Ubiquitin Protein Ligase
miRNA	mircoRNA
miRTC	miRNA Reverse Transcription Control
MOPS	Morpholino Propanesulfonic Acid Buffer
mRNA	Messenger RNA
MTAP	Methylthioadenosine Phosphorylase
NCF	Normal Canine Fibroblasts
NK	Natural Killer
NOD-SCID	Non-obese Diabetic-SICD
NSG	NOD-SCID IL-2R Gamma Chain -/-
PBL	Peripheral Blood Lymphocytes
PBS	Phosphate Buffered Saline
PCR	Polymerase Chain Reaction
PDCD4	Programmed Cell Death 4
PPC	Positive PCR Control
PR	Progesterone Receptor
PTEN	Phosphatase and Tensin Homolog
qPCR	Quantitative Polymerase Chain Reaction

RACE	Rapid Amplification of cDNA End
Rb	Retinoblastoma
RISC	RNA-induced Silencing Complex
RT-PCR	Reverse Transcription Polymerase Chain Reaction
SCID	Severe Combined Immunodeficient
snoRNA	Small Nucleolar RNA
snRNA	Small Nuclear RNA
SPS	Seed-pairing Stability Contribution
sqRT-PCRs	Semi-quantitative Reverse Transcription PCR
SV40	Simian Vacuolating virus 40
TD-PCR	Touch Down PCR
TPM1	Tropomyosin 1
TRBP	Transactivator RNA Binding Protein
3’-UTR	3´-Untranslated Regions

Chapter 1: Literature Review

Section 1. Dog as a Tumor Model

In the field of human cancer research, there is an intense interest in development of appropriate model systems for the advancement of future therapeutic inventions. Companion animals such as domesticated dogs (*Canis lupus familiaris*) are considered excellent preclinical models of cancers and other complex human diseases for many reasons, including their easy accessibility and living status in diverse cultures (Rowell et al., 2011). Since they are treated as pet animals, most of the dog population share the same environment, risk factors or disease characteristics with the human population (American Veterinary Medical Association, 2008; Smith and Bird, 2010) which provides an added advantage for scientists to investigate cancer etiologies. Additionally, dogs represent a more outbred population than inbred laboratory animals providing a genetic diversity similar to that observed in humans (Lindblad-Toh et al., 2005).

Canine models address two important issues in cancer research. First, in terms of similarities, dogs spontaneously develop cancers in the context of a natural immune system with a clinical presentation, tumor genetics and heterogeneity, disease progression and response to conventional therapies (Khanna et al., 2006) that better define and simulate the complex biology of cancers in human patients. The similarities between the dog and human genomes have also greatly revolutionized the comparative genomic analysis. With the advent of the high resolution 2.4 billion bp canine genome sequence and the identification

of nearly all of its genes as clear orthologs of known human genes (Lindblad-Toh et al., 2005), the dog has emerged as a valuable comparative and intermediate model for the study of human cancers. Secondly, using dogs as animal models may contribute to the development of cancer therapeutics for, not only human and dog, but also other species – a promising theme lately coined as "One Medicine" that campaigns under a unified scientific platform where discoveries in one species may ameliorate health in all species. Canine tumors with potential relevance for human cancer biology include osteosarcoma, mammary carcinoma, lymphoma, melanoma, lung carcinoma, and soft tissue sarcomas (Vail and MacEwen, 2000).

Section 2. Canine Mammary Tumors (CMTs)

Tumor Incidence

Mammary tumors are the most common neoplasm in sexually intact female dogs. The severity of canine mammary tumors (CMT) can be comprehended from a number of studies that reported increased rates of incidence in the dog population globally. Breast cancer represents the second most frequent neoplasm in humans and dogs after lung and skin cancers, respectively, although many reports indicate that dogs are 2 to 4 times more susceptible to mammary cancers than women in certain geographical areas (Cullen et al., 2002; Jemal et al., 2007; Owen, 1979; Sorenmo, 2003). Nearly 50% of all these neoplasms are diagnosed as malignant and more than 95% of these malignant CMTs are carcinomas (Ahern et al., 1996; Misdorp, 2002; Withrow and MacEwen, 1996).

Comparative Genomics of Human and Canine Breast Cancers

Because CMTs are considered predictive models for human breast cancer (Vail and MacEwen, 2000), similarities in genetic alterations and cancer predisposition between humans and dogs have raised interest even further. A large number of studies have demonstrated that CMTs have many similarities in molecular and clinical features with human breast cancer. Most of the cancer-associated genetic defects critical to mammary tumor development and oncogenic determinants of metastasis have been reported to be similar in both species. Comparative gene expression analysis has revealed a significant overlap in canine and human genes that are deregulated in mammary tumors compared to normal mammary tissue (Uva et al., 2009). Although CMTs have not yet been intrinsically classified based on genetic markers like human breast cancer subtypes, the expression profile of vital genes involved in cellular proliferation, angiogenesis, apoptosis, cell cycle regulation, DNA damage repair, signal transduction, and survival pathways, firmly correlate to those in human breast cancer (Rao et al., 2008; Uva et al., 2009). These studies characterized CMTs, based on genome-wide gene expression changes, comparing to human breast cancer, suggesting that mutations and alterations in the cancer genome may promote deregulation of individual genes in mammary cancers.

Comparative analysis of deregulated gene sets or cancer signaling pathways showed that a significant proportion of orthologous genes are comparably up- and down-regulated in both human and dog breast tumors. Prominent oncogenic pathways and related genes such as PI3K/AKT, KRAS, MAPK, Wnt-β catenin, BRCA2, ESR1 and P-cadherin are commonly up-regulated while representative tumor suppressive pathways such as p53, p16/INK4A, PTEN and E-cadherin are down-regulated in human and dog breast cancer

(Haga et al., 2001; Klopfleisch and Gruber, 2009; Lutful Kabir et al., 2013; Ressel et al., 2009; Saal et al., 2007; Sweet-Cordero et al., 2005; Uva et al., 2009; van 't Veer et al., 2002).

Classification/Subtypes of CMTs

Canine mammary tumors are biologically heterogeneous neoplasms offering several ways to classify such tumors on the basis of histopathological characteristics or expression of molecular markers (Shinoda et al., 2014). Despite the appearance of histomorphological variations between human and canine breast cancers due to various prognostic indicators, a number of studies reported that there are significant similarities regarding molecular marker expression, hormone dependency and cancer phenotypes (Misdorp, 2002; Shinoda et al., 2014; Sleeckx et al., 2011; Thuroczy et al., 2007). It is important to classify breast cancer in order to correlate clinical phenotypes, invasion or grade of progression and to develop prognostic markers. The human classification of breast cancers based on expression profile of luminal epithelial specific genes and hormone receptors including estrogen receptor 1 (ESR1), progesterone receptor (PR) and proto-oncogenes such as epidermal growth factor receptors (EGFR/HER2), have also identified similar molecular subtypes in CMTs, but unlike human subtypes, these are not routinely investigated for CMTs during clinical diagnosis (Beck et al., 2013; Gama et al., 2008). Recently, in more refined studies employing immunohistochemical approaches and based on the characteristic expression patterns of ESR1, PR and EGFR (ERBB1/HER1, ERBB2/HER2, ERBB3 and ERBB4), human-like breast cancer phenotypes for CMTs have been developed and classified as luminal A, luminal B, HER2 positive and triple negative (basal like) (Sassi et al., 2010) (DeInnocentes et al., 2014, manuscript in preparation). Such

standard classification therefore, strongly supports canine mammary tumors as valuable intermediate models for human breast cancer that should be well-placed for developing diagnostic and treatment strategies.

Development of an *in vivo* Tumor Model of CMTs

In addition to comparative genomics studies demonstrating similarities with human breast cancers, canine mammary tumors have been used for the development of *in vivo* tumor models. For this strategy severe combined immunodeficient (SCID) mouse strains have been ideally used for engrafting cells from higher animals (Jenkins et al., 2005; Meyerrose et al., 2003). SCID mice have defects in T and B cell development but they can generate natural killer (NK) cells that are capable of destroying tumor cell xenografts. Recently, genetically modified strains called non-obese diabetic-SICD mice with targeted mutations in the interleukin-2 receptor (IL-2R) γ-chain locus (NOD-SCID *Il-2rg*$^{-/-}$ or NSG) that completely prevent NK-cell development in addition to the absence of T and B cells, are considered a more appropriate model system for hematopoietic cells, tissues or tumor engraftment (Shultz et al., 2007). Different studies engrafted human and canine stem cell precursors, various immune cells, hematopoietic cells or peripheral blood lymphocytes (PBL) to generate a humanized mouse or an NSG mouse model of the canine immune system. These mice provide a promising model to study canine immune functions and cancers *in vivo* (Foote et al., 2014; Ishikawa et al., 2005; King et al., 2008; Niemeyer et al., 2001; Shultz et al., 2005; Watanabe et al., 2007).

Like established human breast cancer cell lines, CMT cells transfected with plasmids expressing fluorescent protein are able to develop primary tumors in NSG mice that can be detected several weeks post-subcutaneous injection by *in vivo* imaging using

an IVIS protocol (Jenkins et al., 2005) (Foote et. al., 2014, unpublished data). This *in vivo* tumor model of CMTs requires further investigation for stable transfection of cells using appropriate vectors and for optimum tumor growth.

Section 3. Cell Cycle Regulators: A Classic Repertoire of Tumor Suppressors

Cell Cycle and Cancer are Connected

From simple eukaryotes like yeast to higher mammals, the cell cycle serves as a prime biological process by which cells progress and divide. Paradoxically it is also central to cancer mechanisms. Cancer can be distinguished from many other diseases because its fundamental cause is not a lack of or reduction in cell function. However, cancers occur due to an alteration of the normal process of cell division. But how are these two spontaneous biological processes connected? Cell cycle is a highly regulated and controlled process governed by large and complex protein machineries (Pines and Hunter, 1991). Whereas cancer is a disease of uncontrolled cellular proliferation. The excessive cell growth in cancer is in fact associated with a vicious cycle where cells divide through unchecked cell cycle progression with a reduction in sensitivity to signals that normally guide cells to adhere, become quiescent, terminally differentiate or die (Collins et al., 1997). This combination of altered properties is caused by malignant transformations forming a cancerous mass that can eventually develop the ability to spread and migrate throughout the body – a process called metastasis (Mareel and Leroy, 2003). One such group of genetic alterations that contribute to cancer development are termed 'gain-of-function' mutations that largely define oncogenes and result from the mutated versions of normal cellular proto-oncogenes. Oncogenic mutations appear to destroy the integrity of growth factors and other positive regulators of cell cycle that function in highly coordinated

and regulated signaling pathways normally required for cellular proliferation (Aaronson, 1991). The other major genetic alteration involves 'loss of function' mutations in so-called tumor suppressor genes (Weinberg, 1991). They encode proteins that can negatively regulate cell cycle progression but when mutated are highly likely to promote a large number of spontaneous as well as hereditary forms of cancers (Sherr, 1996). The best examples of such genetic alterations, with respect to loss of function in cell cycle regulation, are the mutations in retinoblastoma (Rb) and p16/INK4A tumor suppressors (Bates et al., 1994; Okamoto et al., 1994; Otterson et al., 1994). Loss of function of these tumor suppressor gene products liberate the E2F transcription factors that consequently remove the control for exit from G1 phase out of the cell cycle and result in abnormal cellular proliferation (Sherr, 1996).

Cell Cycle Machinery

The eukaryotic cell cycle, also called the cellular life cycle, consists of four discrete phases: G1, S, G2 and M. Cell cycle progression is driven by the sequential activation of a family of serine-threonine kinases called cyclin-dependent kinases (CDKs) whose functions are controlled by a complex network of regulatory proteins including cyclins and a phosphorylation cascade of CDK substrates (Fig. 1A) (Morgan, 1997; Pines and Hunter, 1991; Santamaria and Ortega, 2006). The activity of the cyclin-CDK complex is critically regulated at different stages of the cell cycle, often termed 'checkpoints', that decide whether the events of the cell cycle should proceed or stop under certain physiological conditions (Elledge, 1996). Mammalian cells generally remain in a quiescent or G_0 state and are only committed to enter the cell cycle and proliferate when instructed by extracellular stimuli. In the constant presence of growth factors and proliferation signals

the cells will grow logarithmically, indicating the requirement of controlling mechanisms in the cell cycle (Pardee, 1989). A group of inhibitory proteins called CDK inhibitors (CKIs) control the cyclin-CDK activity thereby restraining cell cycle progression in response to extracellular and intracellular signals (Harper and Elledge, 1996; Vidal and Koff, 2000). The orderly progression of the cell cycle is fine-tuned by the genes encoding such negative regulators or CKIs and positive regulators including the cyclins and CDKs. Dysregulation of these genes can lead to premature entry into the next phase of the cell cycle leaving the previous phase unchecked and frequently this occurs prior to completion of critical molecular events such as repair of DNA damage or replication errors. Such dysfunction frequently triggers genomic instability and neoplastic transformation (Hartwell, 1992).

Two Families of CDK Inhibitors

Based on their structural similarities and specific roles in cell cycle regulation, CKIs are divided into two distinct groups: the INK4, or CDKN2, and the Cip/Kip, or CDKN1, families (Morgan, 1997; Sherr and Roberts, 1999; Vidal and Koff, 2000). The first group representing the INK4 proteins (**In**hibitors of CD**K4**) are so named because of their ability to specifically inhibit the catalytic subunits of CDK4 and CDK6. It has been reported that INK4 compete with cyclin D for binding to the CDK4/6 subunit (McConnell et al., 1999; Parry et al., 1999). The members of the INK4 protein family that share common structural features, are p16/INK4A (and p14ARF, an alternatively spliced product), p15/INK4B, p18/INK4C and p19/INK4D (Fig. 1A) (Chan et al., 1995; Guan et al., 1994; Hannon and Beach, 1994; Hirai et al., 1995; Ruas and Peters, 1998; Serrano, 1997; Serrano et al., 1993; Sharpless, 2005; Sharpless and DePinho, 1999).

The Cip/Kip family (for **C**DK **i**nteracting **p**rotein/ **K**inase **i**nhibitory **p**rotein) consists of 3 members, including p21/Cip1, p27/Kip1 and p57/Kip2, all of which share a common inhibitory domain that enables them to bind CDK complexes (el-Deiry et al., 1993; Gu et al., 1993; Harper et al., 1993; Matsuoka et al., 1995; Polyak et al., 1994; Toyoshima and Hunter, 1994; Xiong et al., 1993). These proteins of the Cip/Kip family have broad specificity for binding and inhibiting a number of cyclin-CDK complexes compared to that of INK4 members. They also inhibit the activity cyclin cyclin D-CDK4 preventing Rb phosphorylation during G1 to S phase transition. In addition they inhibit cyclin A-CDK2 in late G1 phase and cyclin E-CDK2 in early S phase (Fig. 1A) (Harper et al., 1993; Matsuoka et al., 1995; Toyoshima and Hunter, 1994). Therefore, both CKI families are important modulating components of the complex network of cell cycle regulatory mechanisms.

CDK Inhibitors Form a Repertoire of Tumor Suppressor Proteins

Many studies stress the fact that CDKs are positive regulators and CKIs are negative regulators of cell proliferation based on their distinct inhibitory actions in the eukaryotic cell cycle (Okamoto et al., 1994; Serrano et al., 1993). Besides their specific roles in cell cycle regulation, differentiation and development, CKIs are proven tumor suppressors or likely highly considered to have this potential as mutations in these genes promote malignant phenotypes (Harper and Elledge, 1996; Kamb et al., 1994; Matsuoka et al., 1995; Ruas and Peters, 1998; Serrano, 1997). In some clinical trials, CKI tumor suppressors promote aggressively cancer cell growth by inducing p53 function and stability and increasing anti-proliferative activity thereby inhibiting cell cycle progression (Wesierska-Gadek and Schmid, 2006). Among all the CKIs, p16/INK4A is the founder

member and was the first classified as a major tumor suppressor gene (only preceded by p53 for many human malignancies) because the mutations in the INK4A/ARF locus and loss of heterozygosity of the chromosomal region encoding this gene have been reported in a wide range of cancers including melanomas, leukemias, gliomas, lung, breast and bladder cancers (Kamb et al., 1994; Ruas and Peters, 1998). The loss of expression of the neighboring p15/INK4B gene, due to promoter hypermethylation, also occurs in a number of leukemias and lymphomas (Serrano, 2000; Sharpless and DePinho, 1999). The p16/INK4A locus has also been found to be frequently mutated in canine malignant melanomas, mammary carcinomas and fibrosarcomas (Aguirre-Hernandez et al., 2009; DeInnocentes et al., 2009; Koenig et al., 2002; Lutful Kabir et al., 2013; Migone et al., 2006).

Section 4. Gene Location, Mapping, Structure and Functions of the INK4A/ARF Locus

A locus on the short arm of human chromosome 9p21 (also known multiple tumor suppressor locus) encodes three products called p16/INK4A, p14ARF and p15/INK4B, all of which regulate cell proliferation by inhibiting the cyclin-CDK complex at the G1 to S phase transition in the cell cycle (Kamb et al., 1994; Ruas and Peters, 1998). The organization of the INK4A/ARF/INK4B (or INK4A/ARF) locus in the mammalian genome is highly conserved. Orthologous sequence searches and comparative genomics analysis demonstrated that this locus in human (chromosome 9) is syntenic to that of chimp (chromosome 9), dog (chromosome 11) (Fig. 5B), cat (chromosome D4), mouse (chromosome 4) and rat (chromosome 5) and this region encoding several tumor suppressor genes is highly susceptible to genetic instability and mutations in many cancers (Gilley and Fried, 2001; Ruas and Peters, 1998; Sharpless, 2005). The close similarities

between the INK4A and INK4B genes and two other members of the INK4 CKI gene family, INK4C and INK4D based on their structure, biochemical properties and functions in the cell cycle, suggest that they arose as a result of gene duplication during the course of evolution. This is most likely true since a number of studies have demonstrated that all four INK4 CKIs share a common structural feature called ankyrin repeats used as a structural scaffold facilitating protein-protein interactions (Byeon et al., 1998; Guan et al., 1994; Serrano et al., 1993; Venkataramani et al., 1998). As well as these structural similarities among the INK4 gene family, it has been reported that these four CKIs are also functionally related (Ruas and Peters, 1998).

Evolutionary History and Alternative Splicing of the INK4/ARF Locus from a Common Ancestor

The evolutionary history of the INK4A/ARF/INK4B locus suggests the INK4 genes to have evolved through tandem gene duplication events. One of the most interesting findings for the evolutionary descent of INK4 genes was the complete absence of ARF-like gene products in the Japanese puffer fish *Fugu rubripes* and in the Zebrafish (Gilley and Fried, 2001; Sharpless, 2005) suggesting that p14ARF was introduced into the vertebrate or mammalian genome following INK4 duplication. Moreover, only two INK4 genes representing INK4A or B and INK4C or D were identified in the fugu genome (Fig. 2). Evolutionarily, p16/INK4A and p15/INK4B may share a common ancestor while p18/INK4C and p19INK4D appear to have evolved from another ancestor gene (Fig. 1B) (Gilley and Fried, 2001; Sharpless, 2005). Cross-species comparative analysis suggested that a single common ancestral INK4 gene was present and a series of duplication and rearrangement events first gave rise to INK4A/B and INK4C/D-like elements in a common vertebrate ancestor and after the divergence of higher vertebrates from tetrapods and fish

approximately 350 million years ago (MYA) giving rise to the individual INK4 genes in the genome (Sharpless, 2005).

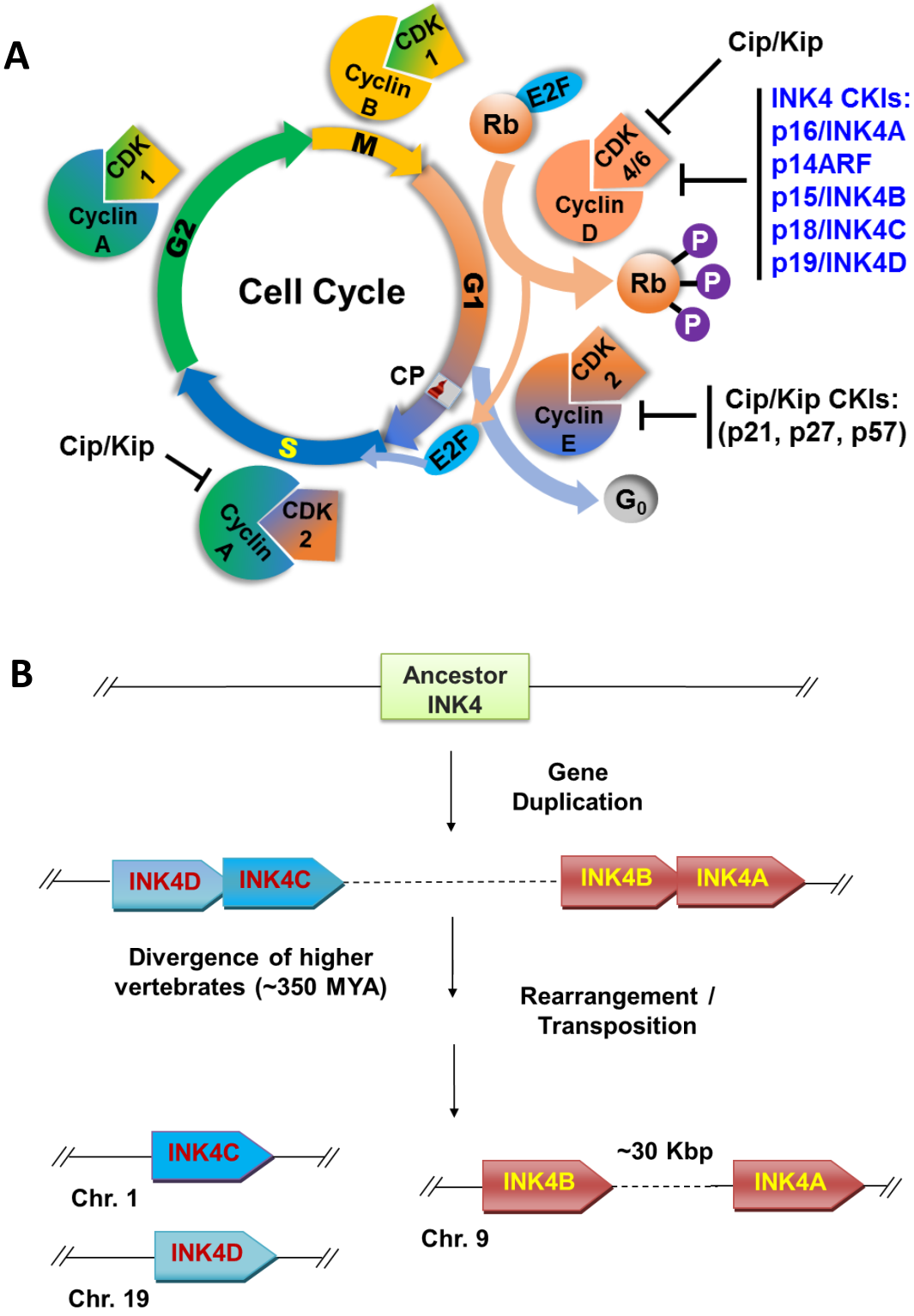

Fig. 1. (A) Cell cycle regulatory mechanisms. Cell cycle phases, major regulatory proteins or protein complexes including cyclins, CDKs, INK4 and Cip/Kip inhibitors and their targets have been shown in this diagram. CP = G1 checkpoint or major restriction point. (B) Proposed evolutionary history of the mammalian INK4 genes. Schematic representation of proposed gene duplication events and the subsequent evolution of p16/INK4A, p15/INK4B, p18/INK4C and p19/INK4D from a single common ancestor INK4 gene. During the course of evolution, INK4C and INK4D were integrated into different chromosomes through rearrangement and transposition while INK4A and INK4B remained located on the same chromosome approximately 30 Kbp apart. Here placement of these genes in the human chromosomes is depicted.

The evolutionary changes placed p16/INK4A and p15/INK4B about 30 kbp apart in the same transcriptional orientation on chromosome 9p21 whereas p18/INK4C and p19/INK4D were split into different chromosomes which were later mapped to human chromosomes 1p32 and 19p13, respectively (Fig. 1B) (Ruas and Peters, 1998). A phylogenetic tree based on the amino acid sequences of INK4 proteins indicates their high similarities among the groups and divergence from the common ancestor (Fig. 2). Two important observations can be inferred from such phylogenetic analysis that could support the evolutionary model of INK4 genes. First, this evolutionary relationship clearly suggests that the p16/INK4A and p15/INK4B from mammals represent a paralogous group that was once related with p16/15 in *Fugu* while p18/INKC and p19/INK4D shared the same group with p19/INK4D in *Fugu*. Secondly, the evolution and divergence of individual INK4

genes through gene duplication most likely took place just before the divergence of placental mammals from marsupials (Fig. 2)

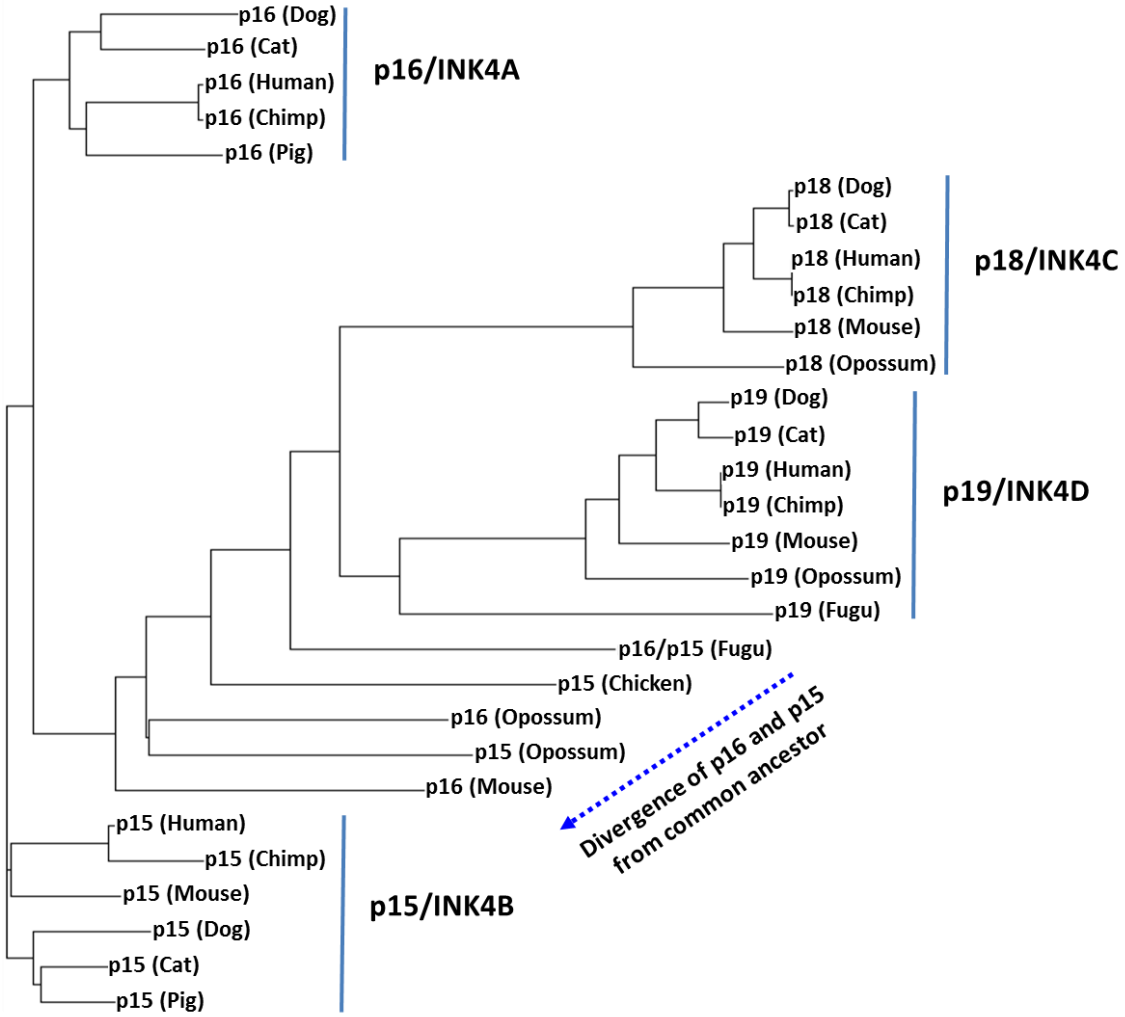

Fig. 2. INK4/CDKN2 dendrogram. A neighbor-joining algorithm was used to calculate the rooted relationship dendrogram and phylogenetic tree for INK4 proteins. The dendrogram was generated from a large alignment of all published INK4 proteins from different species (GenBank accession numbers for all 29 INK4 protein entries are listen in Appendix 1) using ClustalW program. The phylogenetic

analysis demonstrates the high similarity and conservation among INK4 proteins as well as their evolutionary descent from the common ancestor.

During the evolution of p16/INK4A and p15/INK4B through gene duplication, an additional exon appeared when comparing the two genes. This alternative exon is designated exon 1β which is spliced to exon 2 and 3 of p16INK4A making a novel p14ARF transcript (Fig. 3B) (Sharpless, 2005). Previously it was postulated that exon 1β was the original exon 1 of the INK4A locus but later it was determined that this alternative exon was transcribed from its own separate promoter and not from the promoter of p16/INK4A exon 1α (Mao et al., 1995). The presence of such a separate promoter for p14ARF suggests that its transcription is regulated independently of p16/INK4A. In fact, another mechanism of gene duplication has been proposed for the evolution of the exon 1β in the INK4A/ARF/INK4B locus (Fig. 3A). The modified evolutionary model proposed that a single ancestral INK4A/B gene similar to that found in fugu and early common vertebral ancestors, and a pre-ARF gene occurred at different chromosomal positions. Gene duplication, rearrangement and deletion resulted in a duplicated exon 1β located in the intergenic region between the two INK4A/B genes that later diverged from each other. The ancestral pre-ARF sequence has been lost and the splice donor of the exon 1β that usually encodes all the ARF biological activity is now spliced to the closest splice acceptor site in the second exon of the INK4A gene producing the p14ARF mRNA transcript that gives rise to a new protein of the INK4 family in mammals (Fig. 3B) (Gilley and Fried, 2001; Mao et al., 1995; Stone et al., 1995).

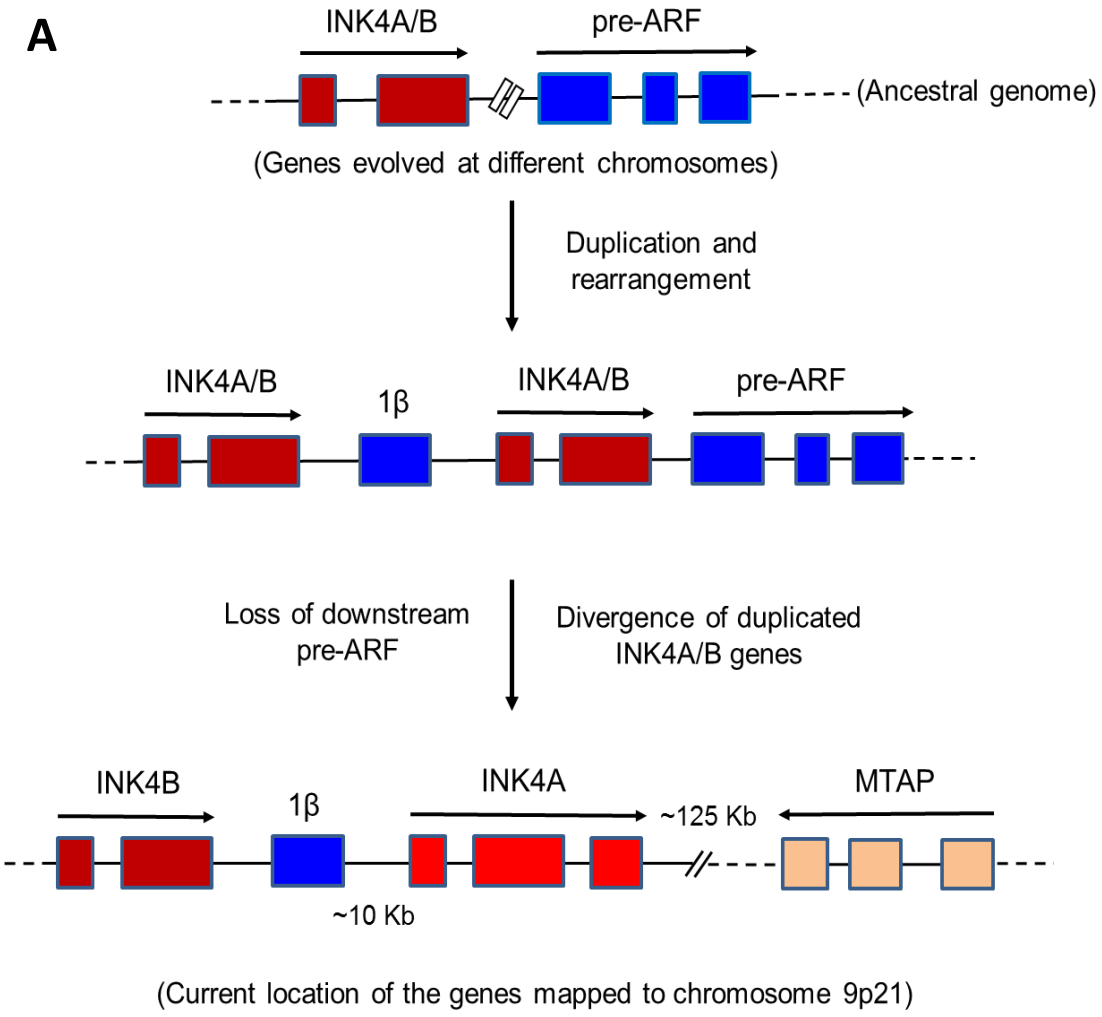

Fig. 3. (A) Evolutionary model showing the gene duplication events postulated to have given rise to INK4A and ARF exon 1β. At the beginning, a single ancestral INK4A/B gene (as found in fugu) and a pre-ARF like element with multiple exons appeared in different chromosomal positions. Gene duplication and rearrangement translocated the transcriptional promoter (exon 1β) of the pre-ARF gene to the upstream of a duplicated INK4A/B gene. The duplicated INK4A gene diverged from INK4B acquiring a third exon and the ancestral pre-ARF sequence was lost. The splice donor of exon 1β of the pre-ARF gene encodes the entire biological function of p14ARF

(Sharpless, 2005). An important neighboring gene MTAP has been mapped downstream on the same chromosomal band 9p21 (Model is based on and redrawn from, Gilley and Fried, 2001).

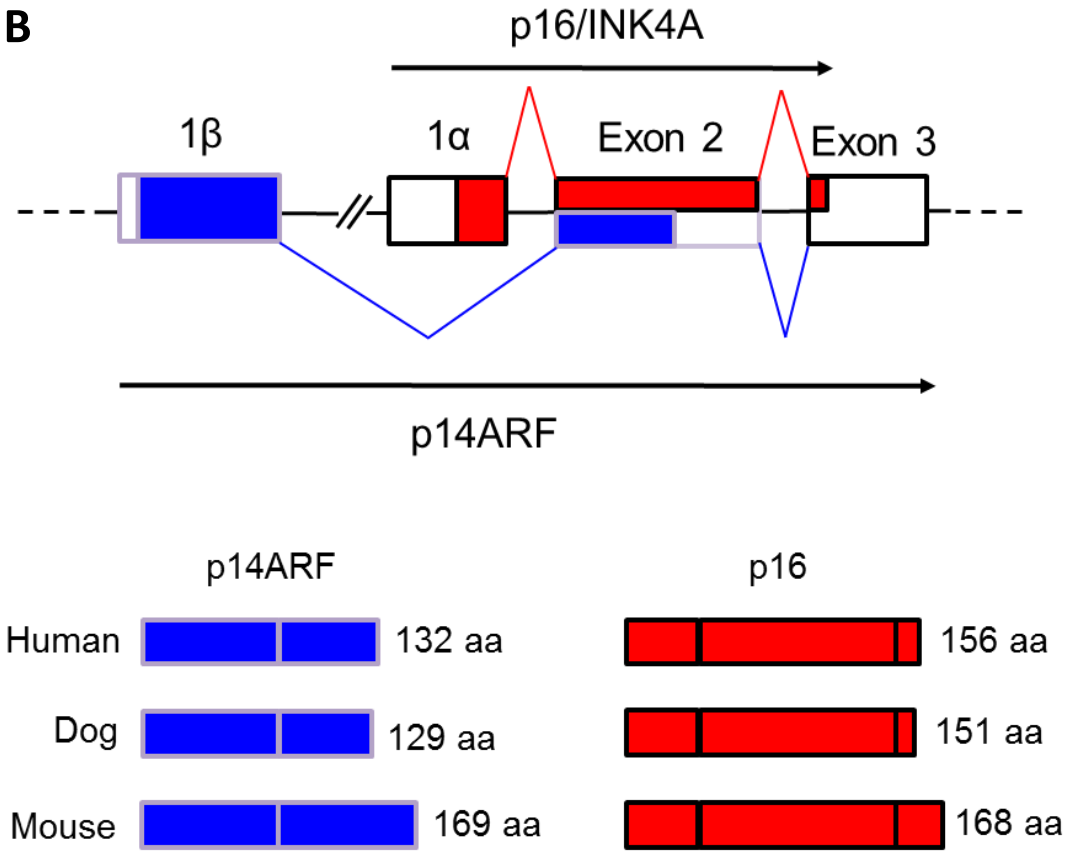

Fig. 3. (B) Alternative splicing results in two different transcripts and products from the modern INK4A/ARF locus. The exons are shown as boxes and the sequences encoding p16/INK4A are shown as red shading while those encoding the ARF transcript are colored blue. Exon 1α is spliced to INK4A exon 2 and 3 forming the p16 mature transcript whereas exon 1β is alternatively spliced to the same exon 2 and 3 generating the mature p14ARF transcript. The latter produces a different protein from p16 because translation occurs from an alternative reading frame. The sizes of

the respective human, dog and mouse p16 and ARF proteins are shown in the bottom panel (see Appendix 1 for GenBank accession numbers). The schematic is modified and redrawn from Ruas and Peters, 1998. (p14ARF in mouse is named p19ARF due to its increased length but should not be compared to p19/INK4D).

Roles of INK4A/ARF in the Cell Cycle and Cancer

The existence of p16/INK4A protein was first discovered as a binding partner of cyclin D-dependent CDK4 by the co-immunoprecipitation assay. In cells transformed by SV40 virus, CDK4 was found to be predominantly associated with p16 rather than cyclin D unraveling an important function of this founder member of the INK4 family and suggesting that p16 can directly bind to the catalytic CDK4 subunit in the absence of regulatory cyclin D (Xiong et al., 1993). Other INK4 members (p15, p18 and p19) were subsequently found to interact with CDK4 and CDK6 by two-hybrid screening (Guan et al., 1994). Both *in vitro* and *in vivo* studies have reported that all the four INK4 proteins directly bind the kinase subunits (CDK4/6) rather than the cyclin subunit (cyclin D) as they act as competitive inhibitors of the cyclins (Chan et al., 1995; Guan et al., 1994; Guan et al., 1996; Hirai et al., 1995; Serrano et al., 1993). This specific interaction with CDKs distinguishes the INK4 family from the Cip/Kip family of CKIs (Ruas and Peters, 1998).

p16/INK4A and p14ARF have Non-overlapping Distinct Functions

Because there is no sequence similarity between exon 1β of p14ARF and exon 1α of p16 and alternative splicing of exon 1β to the shared exon 2 allows translation to continue from the -1 nucleotide of the open reading frame of p16, p14ARF encodes a completely different protein compared to p16 (Fig. 4). These two proteins function in

distinct biological pathways. As Fig. 4 shows, Rb is a critical substrate for cyclin D-dependent kinases (Hunter and Pines, 1994; Sherr, 1994) and its phosphorylation is required to release and activate the E2F transcription factor switching on gene expression involved in the G1 to S phase transition (Weinberg, 1995). p16/INK4A and the three other INK4 members prevent Rb phosphorylation by inhibiting CDK4/6 binding with cyclin D (McConnell et al., 1999; Parry et al., 1999). This cascade pathway in turns leads to E2F repression that inhibits the transcription of many genes required for exit from G1 and initiation of S phase eventually resulting in growth arrest (Sharpless, 2005; Weinberg, 1995).

The ability of p16 protein to limit Rb phosphorylation by cyclin D-dependent kinases was examined in proliferating cells where ectopic overexpression of INK4 proteins was shown to inhibit cyclin-D-CDK4/6 inducing G1 arrest (Guan et al., 1994; Hirai et al., 1995; Lukas et al., 1995; Medema et al., 1995; Quelle et al., 1995) and revert cell transformation in normal diploid fibroblasts by ras and c-myc (Serrano et al., 1995). In comparison, naturally occurring and tumor-derived p16 mutants, lacking CDK4 inhibitory activity, have no effect in cell cycle regulation and proliferation (Koh et al., 1995; Lukas et al., 1995; Ranade et al., 1995; Shultz et al., 2007). Similar effects from exogenously introduced wild-type p16 rescues the normal cellular phenotype and recurrent defects in the p16 gene have been observed in highly transformed canine mammary carcinoma cell lines (DeInnocentes et al., 2009; Lutful Kabir et al., 2013). Moreover, inactivation of both p16 and Rb in tumor cells were found to be mutually exclusive since a large number of human cancer cell lines expressing p16 protein rarely had detectable levels of Rb protein or vice versa (Bates et al., 1994; Okamoto et al., 1994; Otterson et al., 1994). This inverse

relationship suggested that mutations in either Rb or p16 are sufficient to block the G1 checkpoint and therefore both proteins, as well as cyclin D-CDK-4/6, function in a single anti-proliferative pathway (Sherr and Roberts, 1995).

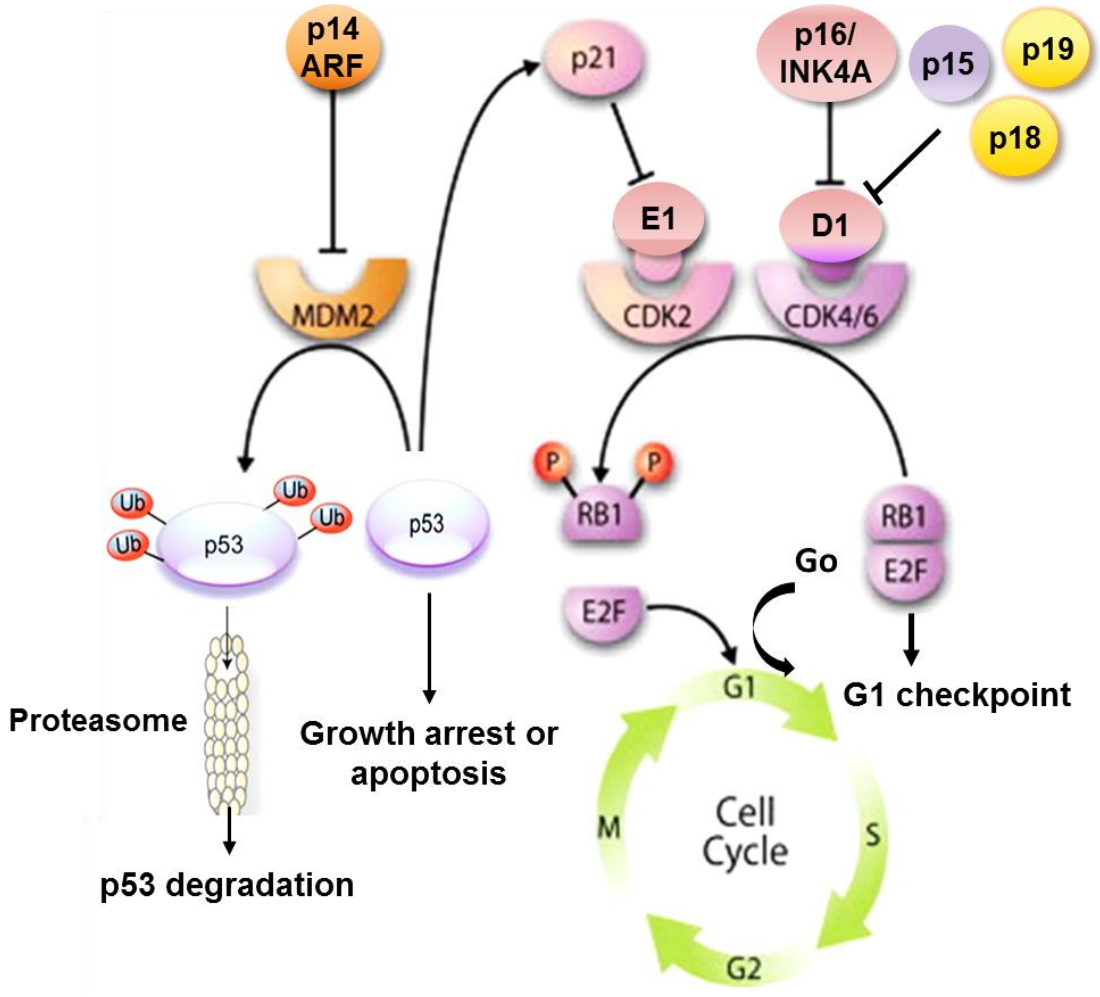

Fig. 4. Cell cycle regulation by p16/INK4A and p14ARF in two different pathways. p14ARF prevents MDM2 mediated p53 degradation allowing its transcriptional activation of p21 that inhibits CDK2-cyclin E1 complex. In the other pathway, p16 and other three members of INK4 family (p15, p18, and p19) inhibit CDK4/6 binding with cyclin D1 preventing Rb phosphorylation that in turn blocks G1 to S phase

transition in the cell cycle. The G1 check point is controlled by these pathways. Defects in p16 and p14 pathways allow cells to enter G1 from Go and proceed to the next S phase thereby driving cell cycle progression and cell proliferation. [Redrawn from (Lomas et al., 2008; Perez-Sayans et al., 2011)].

On the other hand, p14ARF is highly unlikely to act as a direct inhibitor of CDK4/6 because of its structural differences from other INK4 proteins. A great number of studies that used mouse models and human cancer cells differentiated the functions and regulation of p14ARF from that of p16. The initial evidence for its anti-proliferative roles came from observations that expression of p19ARF (p14ARF ortholog in mouse) in embryonic fibroblasts or NIH 3T3 cells induced cell cycle arrest but no direct interaction with CDK complexes was detected in immunoprecipitation assays (Quelle et al., 1995). It has been reported that loss of p19ARF obviates the requirement of p53 inactivation to immortalize mouse embryonic fibroblasts and tumors including melanomas in vivo (Chin et al., 1997; Kamijo et al., 1997). This understanding was further refined by other studies demonstrating that suppression of oncogenic transformation in primary cells by p19ARF is abrogated when p53 is inactivated by viral oncoproteins or dominant p53 mutants (Pomerantz et al., 1998) implying that p19ARF functions upstream of the p53 pathway. Moreover, some groups reported that p19ARF can associate with MDM2 (a p53 ubiquitin protein ligase) or inhibit the E3-ligase activity of MDM2 to prevent MDM2-induced p53 degradation (Kamijo et al., 1998; Llanos et al., 2001; Pomerantz et al., 1998; Zhang et al., 1998) suggesting that these proteins – p19ARF, MDM2 and p53 exist in a common regulatory pathway (Fig. 4). In addition to p53 stabilization, p14ARF regulates p53 transactivation activity. p53 acts as a strong transcriptional activator of p21/Cip1 protein (el-Deiry et al.,

1993). Expression of p19ARF in primary mouse cells expressing functional p53 results in the induction of p21 that plays essential roles in G1 to S phase arrest, apoptosis and tumor growth suppression (Gartel and Tyner, 2002; Pomerantz et al., 1998). Investigating mutations and gene expression profiles of cell cycle regulatory proteins in many human cancer cell lines and primary tumors provided evidence that p53 mutations do not directly correlate with either p16 or Rb expression (Okamoto et al., 1994) stressing the fact that p14ARF (in the p53 pathway) and p16 (in the Rb pathway) have distinct or non-overlapping, important biological functions in cell cycle regulation and cancers (Ruas and Peters, 1998; Sharpless, 2005).

The INK4A/ARF Locus Functions in Cell Senescence and is a Barrier to Tumorigenesis

Cell senescence is a permanent cell post-proliferation phase related to cell aging (Smith and Pereira-Smith, 1996). Senescence can be either induced by DNA replication stress or by oncogene expression but is most often the result of replicative senescence, driven by telomere shortening (Campisi, 2001; Smith and Pereira-Smith, 1996). This irreversible growth arrest can be distinguished from another cellular fate called quiescence. In contrast to terminally differentiated or senescent cells, the quiescent cells retain the ability to resume proliferation following prolonged cell cycle arrest characterized by an absence of DNA synthesis, lower metabolism, and smaller cell size (Yusuf and Fruman, 2003) (Yusuf and Fruman, 2003) and can be induced experimentally by serum-starvation, contact inhibition, and loss of adhesion (Coller et al., 2006). There are numerous factors that perturb the normal cellular environment, ranging from DNA damaging agents and radiation to oncogenes and tumor suppressors that can induce both cell cycle arrest and senescence. In adult organisms, the majority of the cells remain in the quiescent or

differentiated state and are often temporarily arrested but are not senescent (Blagosklonny, 2011). As cellular senescence irreversibly arrests cell growth, it provides a major barrier that cells must overcome in order to progress to complete malignancy (Campisi, 2000; Smith and Pereira-Smith, 1996). Therefore, it is possible that the senescence mechanism evolved to protect higher organisms from developing cancers.

Several lines of evidence have suggested that cellular senescence is regulated by tumor suppressor genes of the cell cycle (Bringold and Serrano, 2000; Campisi, 2001; Lundberg et al., 2000; Sharpless et al., 2001). Three principal tumor suppressive barriers appear to be involved in the cellular senescence mechanism, namely – the p16-Rb pathway, p14ARF-p53 pathway and telomere length regulation in DNA replication. Although senescence requires activation of Rb and/or p53 in many cancers and human fibroblasts, induction of their upstream CDK inhibitors such as p16, p14ARF as well as p21 (a downstream regulator) is also critical in this process (Alcorta et al., 1996; Kamijo et al., 1997; Sage et al., 2003; Stein et al., 1999). There is a widely held view that while cyclins and CDKs are actively promoting cell proliferation, the CDK inhibitors might be important for cells to exit the cell division cycle in order to differentiate or arrest normal growth. In fact, the CDK inhibitors of the INK4A/ARF locus have evolved to function in potent anti-proliferative pathways as well as link the mechanisms that limit the lifespan of proliferative cells leading to replicative senescence and contributing to aging (Campisi, 2001; Sharpless and DePinho, 2004). Classical cell fusion experiments provided the primary evidence that CKIs from the INK4A/ARF loci are responsible for driving senescent cell phenotypes. When mortal (normal) and immortal (malignant) cells were fused, the resulting hybrid cells acquired growth suppression and senescence by introducing individual chromosomes such

as human chromosome 9 or mouse chromosome 4 where the respective INK4A/ARF loci mapped (England et al., 1996; Harris, 1988; Smith and Pereira-Smith, 1996; Vojta and Barrett, 1995).

Many reports have indicated that upregulation of p16 and p21 allow cells to enter the senescent state while loss of p16 leads to immortalization (England et al., 1996; Loughran et al., 1996; Reznikoff et al., 1996; Serrano et al., 1996). The importance of the role of p16 in replicative senescence can be perceived from the observations that this gene is more susceptible to mutation or deletion in established human and canine cancer cell lines than in the corresponding primary tumors (Cairns et al., 1994; Lutful Kabir et al., 2013; Spruck et al., 1994) suggesting some selection for loss of p16 function can occur during the immortalization process (Loughran et al., 1994; Okamoto et al., 1994) though cell lines derived from metastatic tumors showed similar p16 defects compared to their tumor origins (Yeudall et al., 1994). Cell senescence in culture can be characterized by loss of proliferative potential after the accumulation of a limited number of cell doublings that is proportional to the maximal lifespan of the species from which they were explanted (Goldstein, 1990; Hayflick, 1965). A group of studies have provided more obvious evidence from human diploid fibroblasts or keratinocyte cultures suggesting that accumulation of p16 is associated with increased number of population doublings and p16 accumulation continues until cessation of cell division (Alcorta et al., 1996; Hara et al., 1996; Loughran et al., 1996; Wong and Riabowol, 1996).

Alteration of the INK4A/ARF Locus in Cancer

There is compelling genetic evidence from numerous cancer studies that p16/INK4A is a critical tumor suppressor gene whose direct inactivation by point mutation, deletion, or promoter hypermethylation is observed in nearly one third of human cancers, establishing its loss as one of the most frequent lesions promoting human malignancy (Sharpless, 2005). The p16/INK4A gene was independently isolated as a candidate tumor suppressor gene located at human chromosome 9p21, the region which is highly conserved across mammals, was found to be frequently deleted in many human tumors and linked to hereditary susceptibility to melanoma (Hussussian et al., 1994; Kamb et al., 1994a; Ranade et al., 1995). The emergence of human chromosome 9p21 as a site of a major tumor suppressor gene was deduced from extensive cytogenetic and loss of heterozygosity (LOH) studies on a wide range of tumors such as leukemias, melanomas, gliomas, pancreatic adenocarcinomas, as well as breast, lung and bladder cancers (Caldas et al., 1994; Dreyling et al., 1995; Hatta et al., 1995; Kamb et al., 1994a; Nobori et al., 1994; Ogawa et al., 1994; Quesnel et al., 1995). LOH of chromosome 9p21 that encodes the INK4/ARF locus was also deleted in the study of a neighboring gene called methylthioadenosine phosphorylase (MTAP) that also mapped to the same chromosomal region (Fig. 5A) (Carrera et al., 1984). MTAP, a regulatory gene for purine and polyamine biosynthesis, is frequently deleted in different malignant cancer cell lines that also have homozygous deletion of p16 suggesting that loss of MTAP in malignant cells is primarily due to linkage between the MTAP and p16 genes on the same chromosomal region and so they were co-deleted (Nobori et al., 1996). Furthermore, some malignant cells were found to have homozygous deletion of p16 and MTAP but retained an intact p15 gene. These findings of homozygous deletion of p16

and its neighbor in cancer cells also revealed the gene order on chromosome 9p21 starting from the centromeric end which is p15, (p14ARF) p16, MTAP, IFNA and IFNB (interferon alpha and beta) (Fig. 5) (Nobori et al., 1996).

Like p16, p14ARF expression from the same INK4A/ARF locus has been demonstrated to be altered in melanomas and astrocytomas (Randerson-Moor et al., 2001; Rizos et al., 2001). Epigenetic silencing of p14ARF by promoter hypermethylation has also been reported to disrupt the MDM2-p53 pathway in colon cancer (Esteller et al., 2001; Esteller et al., 2000). But in most cases, p14ARF loss in human cancers occurs in the course of genetic deletion that is concomitant with loss of p16 and p15 from chromosome 9p21 (Sharpless, 2005).

Another striking example is the down-regulation of miR-31, a potent tumor suppressor miRNA, in many human tumors including breast cancer (Valastyan S, 2009). While studying the anti-proliferative role of miR-31 in the cell cycle (Creighton et al., 2010), it was discovered that miR-31 is located at the same chromosomal region 9p21 that encodes INK4/ARF (Fig. 5B) suggesting their co-deletion was likely in many cancers. Two other important genes located near the same chromosomal region (9p21) called interferon alpha and beta (IFNA and IFNB) (Fig 5B), have been reported to be frequently lost in a number of human neoplasms such as leukemias, lymphomas and gliomas during homozygous deletion (Diaz et al., 1988; James et al., 1991). This evidence reaffirms and verifies that this chromosomal region harboring multiple tumor suppressor loci is highly tumor prone.

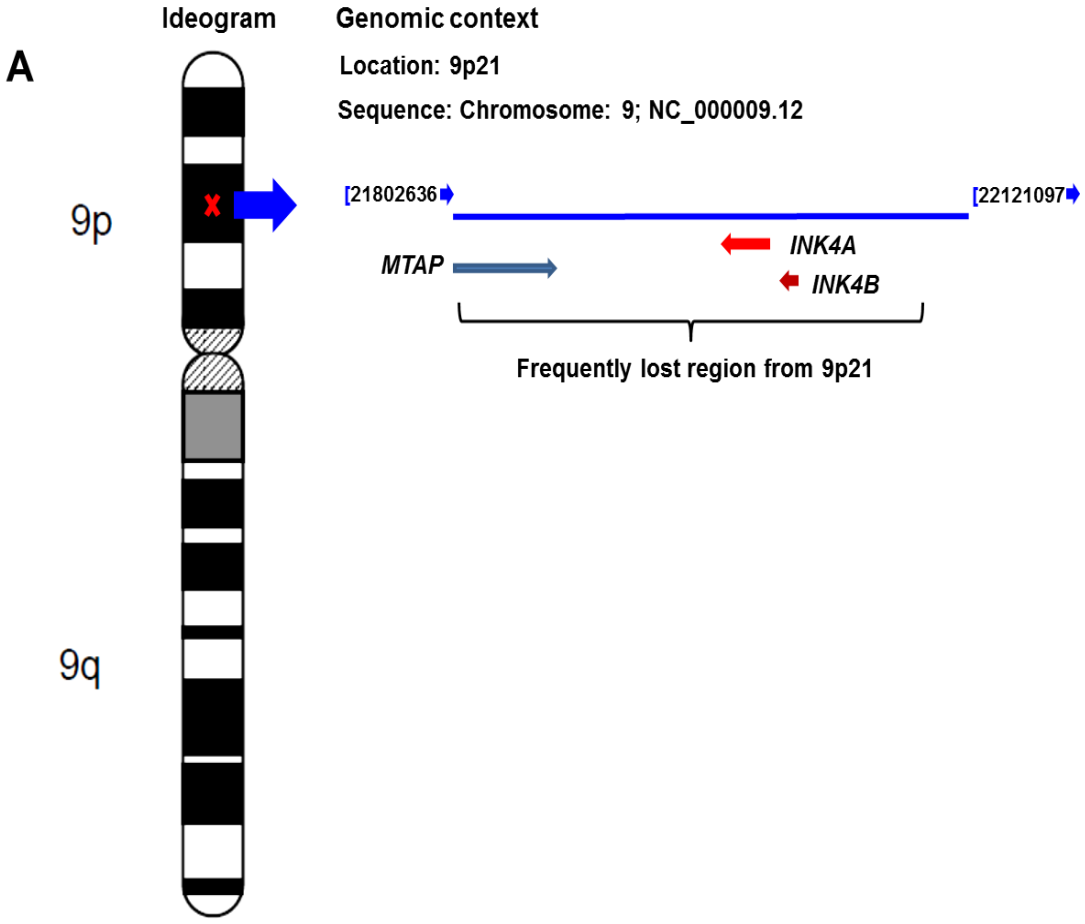

Fig. 5. (A) Representative human chromosome 9p21 and the genomic organization and mapping of the INK4A/ARF locus. The ideogram of human chromosome 9 shows the band 21 on its short arm p. The linear map with genomic context on the right shows relative locations of INK4A, INK4B and MTAP genes based on the NCBI map view of the 9p21 region. The 'X' indicates the region where the deletion/mutation frequently occurred in many cancers.

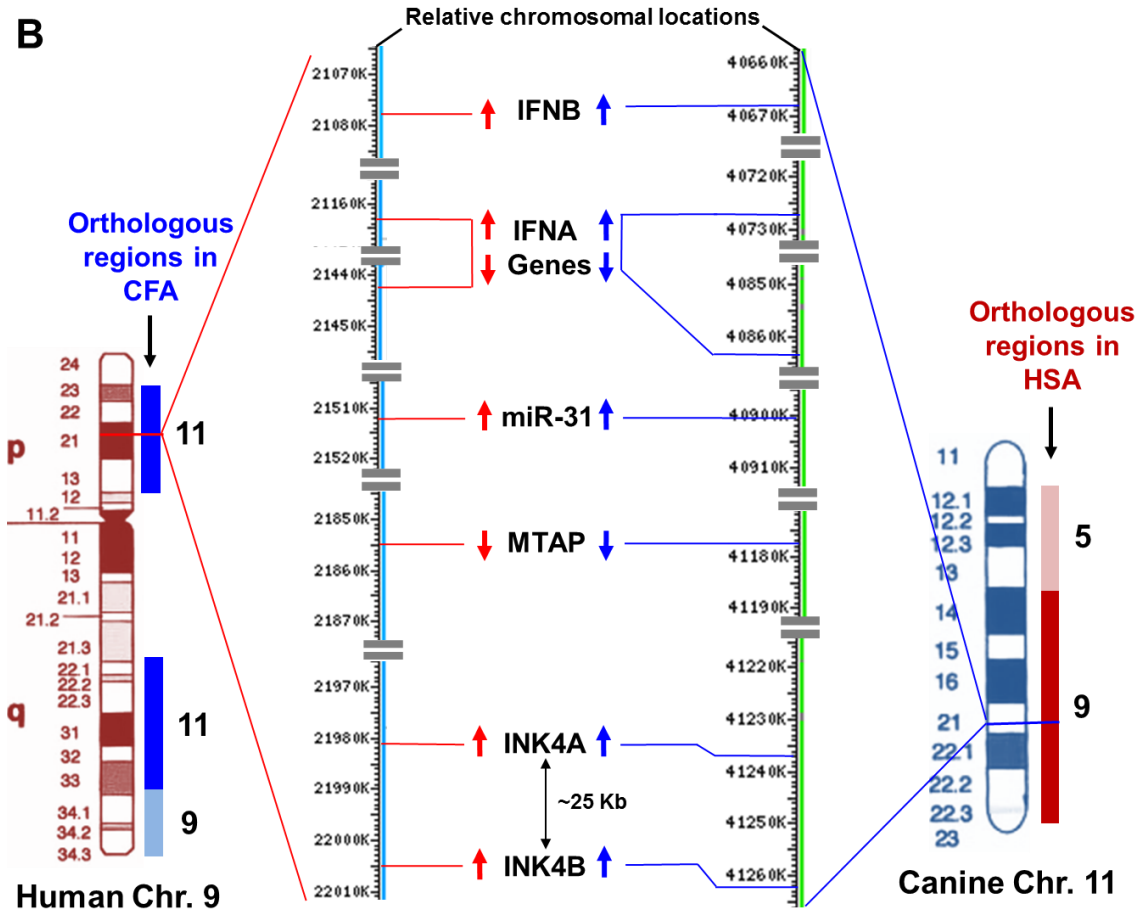

Frequently deleted regions in human chr. 9p21 and orthologous canine chr. 11

Fig. 5. (B) Relative molecular and cytogenetic mapping of the INKA/ARF locus and closely related genes with their positions on human and canine chromosome 9 and 11, respectively. The regions at human chromosome 9 and canine chromosome 11 that are frequently deleted in cancers are completely orthologous to each other. The molecular mapping shows the exact chromosomal position of these genes extrapolated from the NCBI map view of each chromosome represented by the current human and canine annotation releases 106 and 103, respectively. The red and blue arrows indicate the transcriptional orientation of genes in the human and dog chromosomes,

respectively. Transcription of genes from the '+ strand' is indicated by down arrows and from the '- strand' by up arrows. [CFA = *Canis lupus familiaris;* HSA = *Homo sapiens;* Chr. = Chromosome].

Studies with non-human animal models of cancers have also reported genetic defects in the INK4A/ARF locus. The *in vivo* role of p16 in tumorigenesis was initially indicated from mapping tumor susceptibility alleles in common BALB/c mouse strains. This mouse model is prone to tumor development such as plasmacytoma (tumors of the plasma cells) and lung adenocarcinoma in which the major genetic determinant responsible for a strong cancer predisposition also mapped to the INK4A/ARF locus (Herzog et al., 1999; Zhang et al., 1998). Mice with targeted deletions of p16, p19ARF or both were investigated by several groups suggesting that mouse strains with specific inactivation of p16 or p19ARF were tumor prone but neither genetic loss alone was as severe as those with double knockouts of both of these genes (Kamijo et al., 1997; Krimpenfort et al., 2001; Serrano et al., 1996; Sharpless et al., 2001). Mutant mice that were deficient for p16 and heterozygous for p19ARF spontaneously develop a wide range of tumors including melanoma (Krimpenfort et al., 2001). Moreover, in the mouse model, defects in the INK4/ARF locus, with loss of exon 2 and 3 affecting both p16 and p14ARF, lead to overexpression of an activated *H-ras* transgene in melanocytes inducing aggressive melanomas with high penetrance and shorter tumor latency (Chin et al., 1997; Sharpless and Chin, 2003).

INK4A/ARF locus is also associated with cancer predisposition in certain fish species. A strain of fish named *Xiphophorus* including platyfish-swordtails, can develop spontaneous melanoma due to the presence of a cancer-susceptible gene mapped to a locus

closely linked to the chromosomal INK4A region (Nairn et al., 1996). Importantly, primary melanomas, mammary carcinomas and osteosarcomas from dogs have also been reported to harbor frequent defects in p16/INK4A (DeInnocentes et al., 2009; Koenig et al., 2002; Levine and Fleischli, 2000; Lutful Kabir et al., 2013). Altered expression profiles from p16/INK4A/ARF have been recurrently observed in a number of canine breast cancers, melanomas and other primary tumors that highly correlate to lesions in humans and mice (Okamoto et al., 1994; Sharpless, 2005; Yeudall et al., 1994). In fact, altogether, the deletions or point mutations causing shifting of reading frame and altered expression located mostly in exon 1α have been found in cancers from humans, dogs and mice suggesting that specific mutation mapping in p16/INK4A and its regulation are not only limited to cancer type (for example melanomas and breast cancers) but also in other tumors commonly encountered in mammalian species with neoplasms or uncontrolled cellular growth (Herzog et al., 1999; Lutful Kabir et al., 2013; Yeudall et al., 1994; Zhang et al., 1998; Zhang et al., 2001).

Furthermore, the region at canine chromosome 11 (Orthologous to human chromosome 9p21) encoding INK4A/ARF, MTAP and close neighbors including miR-31, as shown in the comparative chromosomal mapping (Fig. 5B), is also highly susceptible and subjected to concomitant deletion in many cancers in dogs (Beck et al., 2013). Reports from several studies suggested that a haplotype spanning MTAP and INK4A/ARF loci showed susceptibility to naturally occurring canine sarcomas (Shearin et al., 2012). The miR-31, one of the highly cited tumor suppressor miRNAs in human breast cancer, was also found to be down-regulated and differentially expressed in canine osteosarcoma and mammary tumors, respectively (Melkamu et al., 2010; Chapter 4). Therefore, the

comparative analysis of cytogenetic and molecular mapping of the genetic defects at human chromosome 9p21 and the corresponding canine chromosome 11 elucidates the frequently deleted regions encoded by the INK4A/ARF/INK4B locus with a highly conserved order of genes (Fig. 5B) that are concurrently lost in many cancers recapitulating the strong similarities in genetic alternations and cancer predisposition between human and dog.

Section 5. Regulatory, Small Non-Coding RNAs: microRNAs in Cancers

It is increasingly apparent that a significant portion of the mammalian genome (estimated to be >70%) encodes regulatory information that is largely carried out by non-coding RNAs (Birney et al., 2007; Costa, 2010; Prensner and Chinnaiyan, 2011). These non-coding RNAs consist of two major classes: small non-coding RNAs (<200 bp, including miRNAs) and long noncoding RNAs or lncRNAs (>200 to ~100 kb) (Cheetham et al., 2013; Gibb et al., 2011). The discovery of microRNAs (miRNAs) established a new era in translational research and for understanding post-transcriptional regulation of genes as well as their critical regulatory roles in diverse biological processes including cell cycle, cell proliferation, differentiation, development and apoptosis as well as in disease pathogenesis (Jovanovic and Hengartner, 2006; Lee et al., 1993; Schickel et al., 2008; Stefani and Slack, 2008). miRNAs are evolutionarily conserved, endogenous small structural RNA molecules (~22 nucleotides) that post-transcriptionally suppress gene expression in a sequence specific manner (Lagos-Quintana et al., 2001). Expression of these small structural RNAs is tightly regulated during development and in normal tissues and is frequently altered in cancer (Esquela-Kerscher and Slack, 2006). Strikingly, more than 50% of miRNA genes are located in cancer associated genomic regions or fragile sites

that are also preferential sites for translocation, deletion, amplification, and integration of exogenous genome fragments suggesting that miRNAs play an important role in the pathogenesis of many human cancers (Calin et al., 2004; Garzon et al., 2009). Since miRNAs are encoded by highly conserved naturally occurring genes across mammalian species, evaluation of their expression profiles in cancer models shows great promise for advancing the development of future therapeutic reagents and diagnostic or prognostic analysis.

Long Non-coding RNAs in Cancers

lncRNAs share many features of mRNAs but in contrast to mRNAs they are found within introns of protein coding genes or intergenic regions of the genome (Prensner and Chinnaiyan, 2011) demonstrating developmental and tissue-specific expression patterns (Mercer et al., 2008). The lncRNAs play a number of important regulatory functions that affect epigenetic changes including chromatin remodeling, transcriptional co-activation and repression, post-transcriptional modification of mRNAs as well as cellular functions including differentiation and homeostasis (Cheetham et al., 2013). Dysregulated expression of lncRNAs causes disruption of these biological functions and plays a critical role in cancer development (Gibb et al., 2011). To date a number of lncRNAs have been implicated in breast cancer development and metastasis. One of the most well-known and first identified lncRNAs is a HOX antisense intergenic RNA that is commonly abbreviated as *HOTAIR*. This lncRNA, located in the mammalian HOXC locus, has been demonstrated to be associated with polycomb repressive complex 2 that mediates transcriptional repression of numerous genes involved in differentiation pathways during development and stem cell pluripotency (Gupta et al., 2010; Morey and Helin, 2010; Tsai et al., 2010;

Zhang et al., 2011). Importantly, *HOTAIR* has been reported to be highly upregulated in both primary and metastatic breast cancers and its overexpression is a strong predictor of metastasis and poor survival (Gupta et al., 2010). Recent studies have also revealed an interplay between miRNAs and lncRNAs within cancer regulatory networks. For example, miR-141 suppresses HOTAIR expression and functions in human renal carcinoma cells (Chiyomaru et al., 2014) while HOTAIR can inhibit a tumor suppressor miRNA, miR-7, in breast cancer stem cells (Zhang et al., 2014). In addition, lncRNAs and transcribed pseudogenes can act as 'natural decoys' inhibiting miRNA expression in cancer through epigenetic silencing (Ebert et al., 2007). However, unlike the rapid advances in miRNA research, including the well-established mechanisms of miRNAs in gene silencing and strong sequence conservation of miRNAs across mammals, knowledge regarding the molecular mechanisms of lncRNA function in cancer are still growing. Most lncRNAs are poorly conserved and, their mechanism of action remain unclear and need to be explored further (Cheetham et al., 2013; Prensner and Chinnaiyan, 2011).

How Many miRNAs are there?

miRNAs and their associated proteins appear to be one of the most abundant biomolecules in the cell. Due to cutting-edge amplification technologies and improvement in prediction algorithms, miRNA discovery from model organisms as well as non-model species has greatly advanced, with 30,424 mature miRNAs in 206 species putatively identified to date (miRBase v20.0). Based on this latest estimate, the human, mouse and canine genomes account for 2578, 1908 and 291 mature miRNAs, respectively. The number of experimentally validated miRNAs from each species is smaller than the predicted number. However, both bioinformatics and empirical evidence suggests that

more than 30% of protein-coding genes in the human genome are subjected to regulation by miRNAs, indicating their prominence as global regulators of gene expression (Bartel, 2004; Fabian et al., 2010; Friedman et al., 2009; Kent and Mendell, 2006).

miRNA Biosynthesis and Regulation of Gene Expression

In mammals mature miRNAs generated from sequential processing of primary miRNA transcripts by Drosha and Dicer miRNA processing complexes associate with 3´untranslated regions (3´UTR) of specific target messenger RNAs (mRNAs) to suppress translation and may also induce their degradation (Bartel, 2004; Carthew, 2006; Du and Zamore, 2005). In the nucleus, the RNase III–type enzyme Drosha processes the long primary transcripts (pri-miRNA that is initially transcribed by RNA polymerase II from the cellular genome), yielding 60-70 nucleotide hairpin precursors called pre-miRNA (Cullen, 2004; Lee et al., 2003). The resulting pre-miRNA hairpins are translocated to the cytoplasm by Exportin-5. In the cytoplasm the pre-miRNAs are further cleaved and processed into 19-25 nucleotide miRNA duplex structures by the RNase Dicer and transactivator RNA binding protein (TRBP) (Lund et al., 2004; Yi et al., 2003). The functional strand (or guide strand) of the mature miRNA is loaded together with Argonaut (Ago2) proteins into an RNA-induced silencing complex (RISC), where it guides RISC to silence target mRNAs through mRNA cleavage, translational repression or deadenylation, whereas the passenger strand (the complementary strand of the double stranded pre-miRNA following Dicer processing) is typically degraded (Hutvagner and Zamore, 2002; Winter et al., 2009).

The mature miRNAs usually target the 3’ UTR of mRNAs and make complementary base pairing with their seed (core orthologous target) sequences (located

at 2-8 bases from the 5'-end of the miRNA) (Garzon et al., 2009). The seed sequence, by which miRNAs bind to their targets, is only several nucleotides long, suggesting that each miRNA may potentially bind to a large number of genes thereby regulating their expression. miRNAs can direct the RISC complex to downregulate target gene expression by either of two post-transcriptional mechanisms: mRNA cleavage or translational repression (Bartel, 2004; Chendrimada et al., 2005; Hammond et al., 2000). The execution of one of these mechanisms is primarily determined by the degree of complementarity between the miRNA and its target mRNA. The miRNA will promote the cleavage of the target message if its seed region is sufficiently complementary to the target sequences (Hutvagner and Zamore, 2002; Zeng et al., 2002). After degradation of the mRNA, the miRNA remains intact and can guide the RISC to target other messages. Interestingly, miRNAs can regulate their own expression or biosynthesis by targeting the miRNA processing machinery. For example, miR-103/107 family can inhibit DICER and induce epithelial to mesenchymal transition (EMT) promoting metastasis in human breast cancer (Martello et al., 2010).

OncomiRs: Roles in Cancers

The association of miRNAs with the initiation, progression and key control pathways of human malignancies holds great potential for new developments in advanced diagnostic and therapeutic strategies in the management of most common cancers. The expression of miRNAs are deregulated in cancer by a variety of mechanisms including amplification, deletion, mutation or epigenetic silencing (Calin et al., 2002; Chang et al., 2007; Saito et al., 2006). Epigenetic regulation of miRNAs is mediated by promoter hypermethylation in certain human cancers. For example, miR-127, which is

downregulated in human cancer cells, has been reported to be located within a CpG island and highly up-regulated by DNA demethylation and histone acetylation (Saito et al., 2006).

Many groups have discovered ‘miRNA signatures’ in both hematological and solid tumors that discriminate cancers from normal cells and might be key to improving prognosis, progression and possibly suppression of cancer (Calin et al., 2005; Garzon et al., 2009; Iorio et al., 2005; Lu et al., 2005; Volinia et al., 2006; Yanaihara et al., 2006). miRNAs are often regarded as ‘oncomiRs’ meaning miRNAs involved in dominant cancer regulatory mechanisms. OncomiRs can be categorized as tumor oncogenes and tumor suppressors or anti-oncomiRs. miR-155 was one of the first identified oncomiRs that has been demonstrated to be highly expressed in several well-known lymphomas, leukemias, breast, colon and lung cancers (Iorio et al., 2005; Kluiver et al., 2005; Metzler et al., 2004; Volinia et al., 2006; Yanaihara et al., 2006). Like miR-155, other oncogenic miRNAs usually target tumor suppressor genes and cell cycle inhibitors, or anti-proliferative genes and they can also serve as potential therapeutic targets. Another strong oncogenic candidate miRNA is miR-21 which is upregulated in a wide variety of blood related and solid tumors including myeloid leukemia, lymphocytic leukemia, gliobalstoma and cancers of the pancreas, prostate, stomach, colon, lung, liver and breast (Calin et al., 2005; Ciafre et al., 2005; Garzon et al., 2008; Meng et al., 2007; Volinia et al., 2006). Overexpression of miR-21 in these cancers inhibits the apoptotic pathway and allowing abnormal proliferation. miR-21 was one of the first miRNAs identified in the human genome that showed strong evolutionary conservation across a wide range of vertebrate species. Three major targets of miR-21 include prominent tumor suppressors such as PTEN (phosphatase and tensin homolog) an important regulator of cardiovascular disease, PDCD4 (programmed cell

death 4) and TPM1 (tropomyosin 1) (Chan et al., 2005; Frankel et al., 2008; Meng et al., 2007; Zhu et al., 2007).

let-7 was one of the first characterized anti-oncomiRs or tumor suppressor miRNAs, which is highly conserved among mammalian species, and is downregulated in many tumors including lung and breast cancer (Iorio et al., 2005; Johnson et al., 2005; Yanaihara et al., 2006). The let-7 miRNA family functionally inhibits a number of well-characterized oncogenes such as *ras*, *c-myc* and *HMGA2* and induces apoptosis and cell cycle arrest in human colon cancer cells (Akao et al., 2006; Johnson et al., 2005; Lee and Dutta, 2007; Sampson et al., 2007). This miRNA targets the *ras* oncogene in lung cancer by being abnormally expressed promoting cell cycle progression (Johnson et al., 2005). In addition, let-7 also downregulates the expression of c-*myc*, a transcriptional activator of many tumor promoting genes that are dysregulated in lymphomas. Thus, anti-oncomiRs control the expression of oncogenes and their transcription factors.

Regulation of miRNAs in Breast Cancers

The association between altered miRNA expression signatures and breast cancer metastasis has been described by many studies (Reviewed in Harquail et. al., 2012; Zhang and MA, 2012). And, a large number of miRNAs have been identified as deregulated in human breast cancer compared to normal breast tissue. The overexpression of certain oncogenic miRNAs (miR-21, miR-27a, miR-155, miR-9, miR-10b, miR-373/miR-520c, miR-206, miR-18a/b, miR-221/222) and the loss of several tumor suppressor miRNAs (miR-205/200, miR-125a, miR-125b, miR-126, miR-17-5p, miR-145, miR-200c, let-7, miR-20b, miR-34a, miR-31, miR-30) lead to loss of regulation of vital cellular functions

that are involved in breast cancer pathogenesis (Harquail et al., 2012; Zhang and Ma, 2012).

In human breast cancer, miR-21 upregulates the EMT, the PI3K/ATK signaling pathway, the anti-apoptotic pathway and induces proliferation by targeting very well-characterized tumors suppressors such as PTEN, TPM1, and PDCD4 (Frankel et al., 2008; Qi et al., 2009; Zhu et al., 2007; Zhu et al., 2008). Strikingly, all of these miR-21 targets have been reported to be deregulated in canine mammary tumors. In this regard, expression of selected miRNAs associated with human breast cancers were investigated in canine malignant mammary tumors. Almost all of the miRNAs followed the same expression profile observed in human breast cancers when compared to normal canine mammary tissue. This investigation revealed that miR-21 and miR-29b were significantly up-regulated and miR-15b, miR-16 were significantly down-regulated in breast cancers in both species (Boggs et al., 2008).

miRNAs Regulate Cell Cycle by Targeting Multiple Genes

One of the important functions of miRNAs is to regulate cell cycle progression and arrest by targeting multiple cell cycle regulatory genes. They regulate cell proliferation by specifically targeting cyclin-CDK complexes and CDK inhibitors. One of the first discoveries that connected miRNAs and cell cycle regulation, was the anti-proliferative potential of the miR-15a/16-1 family that target multiple cell cycle genes involved in cellular proliferation and growth arrest (Linsley et al., 2007; Liu et al., 2008; Takeshita et al., 2010; Wang et al., 2009). The miR-16 family act as tumor suppressors that induce cell cycle arrest at the G1 phase by targeting several cyclin-CDK genes including CDK6, cyclin D1, D3, E2F3 and WEE1 and all the miRNAs in this family are downregulated in a wide

variety of tumors (Bueno and Malumbres, 2011). Additionally, miR-34 and other family members, target CDK4/6, cyclin D1, cyclin E2, E2F1/3 and c-myc, indicating their strong anti-proliferative roles (Sun et al., 2008). These miRNAs are transcriptionally activated by p53 and are involved in the p53 signaling pathway thereby acting as mediators of tumor growth suppression (He et al., 2007). However, these tumor suppressive miRNAs involved in cell cycle regulation are inactivated in tumors by epigenetic mechanisms, such as hypermethylation, that lead to overexpression of their target genes (Lujambio et al., 2007).

Members of the miR-290 family positively regulate G1 to S phase transition by inhibiting cyclin-dependent kinase inhibitors such as p21, during embryonic stem cell differentiation (Wang and Blelloch, 2009). The Cip/Kip family CKIs are targeted by miR-17-92, miR-106b, the miR-221 family and miR-25 in many different carcinomas (Bueno and Malumbres, 2011). The expression of p16/INK4A is repressed by miR-24 and miR-31 which are also involved in the regulation of cell proliferation and progression of cell cycle in many cancers (Lal et al., 2008; Malhas et al., 2010). It has been reported that miR-21 negatively regulates cell cycle during G1 to S phase transition in response to DNA damage and inhibits Cdc25A expression affecting G2/M progression in colon cancer cells (Wang et al., 2009). Another study showed that miR-322/424 and miR-503 are upregulated during myogenensis and they promote cell cycle arrest at G1 phase by down-regulating Cdc25A (Sarkar et al., 2010). All these reports clearly suggest that the cell cycle G1 to S phase transition is tightly regulated by several families of miRNAs. Therefore, miRNAs regulate cell cycle either positively or negatively by targeting the expression of many genes at different stages and most of these regulatory pathways have been implicated in different pathological or developmental conditions.

In conclusion, the strong similarities in genome sequence, along with highly similar characteristics for spontaneous tumor models, have raised great promise for further comparative genomic research between humans and dogs. Comparing spontaneous mammary carcinomas in female dogs with breast cancer in women has significantly improved our understanding in deciphering the molecular mechanisms, relevant risk factors, genetic profiles of these types of cancer and novel strategies for future therapeutic inventions. However, although there is great potential in canine cancer models, a large number of cancer associated genes such as cell cycle regulators, including the INK4 tumor suppressor genes and emerging miRNAs in the canine genome, have not been well studied in such models. Additionally, the high correlation between tumor suppressor gene expression and miRNAs due to post-transcriptional regulation is one of the central areas in cancer research which also needs to be further explored. In this dissertation, INK4 tumor suppressor gene expression and the aberrant regulation by miRNAs have been elucidated in spontaneous canine cancer models in order to further enrich our understanding of the complex genetic mechanisms in regulating human and canine cancers.

Chapter 2: Altered Expression of p16/INK4A from the INK4A/ARF/ INK4B Locus Due to the Novel Frameshift Mutation and Frequent Loss of p16 in Spontaneous CMT Models

Section 1. Introduction

Canine mammary carcinomas comprising approximately 50% of all neoplasms in unspayed female dogs, provide a high level of similarity in genetics, pathology and environmental exposure, when compared to human breast cancer (Ahern et al., 1996; DeInnocentes et al., 2006; Migone et al., 2006; Withrow and MacEwen, 1996). The factors in canine mammary tumor (CMT) development and pathogenesis that strongly recapitulate human breast cancers are spontaneous tumors, hormonal etiology, age of onset (after 6 years comparable to 40 years for women), tumor size, clinical stages and response to conventional therapies (Khanna et al., 2006; Paoloni and Khanna, 2008; Strandberg and Goodman, 1974; Vail and MacEwen, 2000). These clinical features along with high incidence rate of CMTs could provide considerable advantages in pre-clinical trials with animal models and might be applicable in comparative medicine. CMTs are mostly of epithelial origin suffixing the term adenoma or adenocarcinoma (Misdorp, 2002; Withrow and MacEwen, 1996). Cell proliferation in normal epithelium is tightly controlled by several regulators of the cell cycle check points (Sarli et al., 2002). Uncontrolled cellular proliferation is the hallmark of neoplastic transformation of mammary tissue. In this regard, CMT cells might have defective cell cycle regulatory mechanisms including increased expression levels of hyperactive growth promoting genes or proto-oncogenes and down-

regulation of growth inhibiting genes or tumor suppressors that lead to abnormal cellular transformation and tumor development (Klopfleisch et al., 2010). Like human breast cancer, expression of canine cell proliferation and cell cycle regulatory genes are frequently altered in CMTs (Ahern et al., 1996; DeInnocentes et al., 2006; Lutful Kabir et al., 2013).

Tumor suppressor genes play vital roles in controlling cell cycle, replication, recombination, signal transduction, differentiation and aging (Oesterreich and Fuqua, 1999). They can directly control cell proliferation by regulating cell cycle check-points but promote neoplasia when they acquire mutations (Kinzler and Vogelstein, 1997; Tripathy and Benz, 1992). Cell cycle progression is regulated by cyclin/cyclin-dependent kinases (CDKs) whose activities are regulated by CKIs (Morgan, 1997; Pines and Hunter, 1991). The INK4 family, consisting of p16/INK4A, p15/INK4B, p18/INK4C and p19/INK4D (Vidal and Koff, 2000), inhibits assembly of CDK4/6 with cyclin D preventing Rb phosphorylation and inactivating E2F transcription factors required for S phase (Fig. 4, Chapter 1) (Weinberg, 1995). As already discussed in the previous chapter, genes of the INK4 family are evolutionarily and functionally related and are thought to have evolved from a common ancestor through gene duplication (Sharpless, 2005). The INK4A/ARF/INK4B locus (belongs to human chromosome 9p21 and corresponding canine chromosome 11) encodes two different transcripts (p16 and p14ARF) that are alternatively spliced and translated to make different proteins with distinct cell cycle regulatory and tumor suppressor functions (Agarwal P et al., 2012; Fosmire et al., 2007; Ruas and Peters, 1998). The p16 and p14ARF share a large overlapping sequence encoded by exon 2 and 3 but different alternatively spliced first exons (exon 1α and 1β, respectively)

resulting in two different reading frames (Fig. 2B, Chapter 1) suggesting that their expression may be affected by either common or unique mutation events.

Both p16 and p14ARF are tumor suppressor genes but they function in two different anti-proliferative pathways; p16 in cyclin D-CDK4/6 and Rb pathway and p14ARF in p53 pathway (Fig. 4, Chapter 1) (Hunter and Pines, 1994; Sherr, 1994). Functional effects of p14ARF are not limited to p53 as p14ARF has been implicated in vascular regression in developing eye (McKeller et al., 2002) and arrest of cell cycle in embryo fibroblasts in the absence of p53 (Weber et al., 2000). Previous studies have demonstrated that p16 can suppress proliferation when transfected into human and canine tumor cell lines (Campbell et al., 2000; DeInnocentes et al., 2009; Jin et al., 1995; Spillare et al., 1996). Defects in INK4 genes have been associated with cancers in humans and dogs including melanoma, osteosarcoma and mammary carcinoma (Koenig et al., 2002; Levine and Fleischli, 2000).

Defective expression of p16 mRNA has been previously reported in three established canine mammary tumor cell lines (CMT12, CMT27, CMT28) (DeInnocentes et al., 2009). Although CMT28 cells express p16 mRNA they do not express detectable protein (Agarwal et al., 2013) however, the cause of this defect is unknown and pinpointing the defect is complicated due to the presence of highly GC rich repeats within the coding region and the missing full-length p16 mRNA sequence from the published canine genome (CanFam genome assembly). This causes difficulty in primer design and PCR amplification (Lindblad-Toh et al., 2005). The major objective of this study was to develop powerful molecular biology strategies for mapping INK4A/ARF genetic defects and analysis of mRNA and protein sequences important for the evaluation of p16 gene expression in the development of canine breast cancer. This is the first evidence of full-

length canine p16 coding sequence and mutation from a CMT model. In addition, the expression profiles and defects for all INK4 gene family members have also been evaluated in a panel of independently-derived spontaneous canine breast cancer cell lines.

Section 2. Methods and Materials

Cell Lines

Six stable CMT cell lines were derived from female dogs of different breeds with spontaneous mammary carcinomas or adenocarcinomas. CMT9 and CMT12 were developed from Poodle, CMT 27 from German Shepherd, CMT28 from mixed breed, CMT47 from Miniature Schnauzer and CMT119 from Golden Retriever. Normal thoracic canine fibroblasts (NCF) and a canine mammary epithelium-derived cell line (BTB) were used as control for normal cells. NCF cultures were derived from primary fibroblasts grown directly from sterile explants of subcutaneous loose connective tissue using standard primary culture procedures (DeInnocentes et al., 2006).

Cell Culture and RNA Extraction

Cell lines were grown in Leibovitz's L-15 Medium with 1% antibiotic and 10% fetal bovine serum. Cells were grown at 100% humidity at 37 °C with 5% CO2, changing the medium every two days (DeInnocentes et al., 2006; Wolfe et al., 1986). Total RNA was isolated from cells (with 70-80% confluence) by phenol-chloroform extraction according to the manufacturer's instructions (RNA STAT-60; Tel-Test, Inc). RNA pellets were air-dried and stored (-80ºC). Pellets were resuspended in diethylpyrocarbonate-treated water for PCR assays. Concentration and purity of RNA was determined by absorbance at 260 nm (You and Bird, 1995).

Primer design

Primers were designed for INK4 genes using Vector NTI primer design software (Invitrogen, Table 1). Published canine INK4 sequences were aligned with sequences from other mammalian species and primers designed from highly conserved unique regions.

Table 1: Primer sequences designed for INK4 genes

Gene	Primers (Forward/Reverse)	Primer Sequences (5′ to 3′)
p16	F1 (3′-RACE gene specific outer/forward primer)	CAGCATGGAGCCTTCGGCTGACTG
	F2 (3′-RACE gene specific inner/forward primer)	CAGCACCACCAGCGTGTCCAGGAAG
	R1 (Reverse)	CAGGTCATGATGATGGGCAGC
p14ARF	R2 (5′-RACE gene specific inner/reverse primer)	TCGGCACAGTTGGGCTC
	R3 (5′-RACE gene specific outer/reverse primer)	CCACCAGCGTGTCCAGGAAG
	Forward	CGAGTGAGGGCTTTCGTGGTG
	Reverse	ACCACCAGCGTGTCCAGGAAG
p15	Forward	GTGCGGCAGCTCCTGGAAG
	Reverse	CCAGCGTGTCCAGGAAGCC
p18	Forward	CGCTGCAGGTTATGAAACTT
	Reverse	GCAGGTTCCCTTCATTATCC
p19	Forward	GCTGCAGGTCATGATGTTTG
	Reverse	GAGCATTGACATCAGCACCA
L37	Forward	AAGGGGACGTCATCGTTCGG
	Reverse	AGGTGCCTCATTCGACCGGT

Semi-Quantitative Reverse Transcription-PCR (sqRT-PCR) and Touchdown-PCR (TD-PCR) Assays

Gene expression was analyzed by sqRT-PCR using mRNA templates in semi-quantitative assays at limiting template dilution and minimum amplification number (DeInnocentes et al., 2009). sqRT-PCR was performed in one reverse transcription (RT) step (Icycler, Bio-Rad) and then amplification using specific primers. PCR protocol consisted of RT (48ºC, 45 min), denaturation (94ºC, 2 min) and amplification cycles (p18 and p19 25 cycles, p15 30 cycles, 35 cycles for TD-PCR) composed of denaturation (94ºC, 1 min), annealing for 30 sec (67ºC for p14ARF and p15; 60ºC for p18 and p19) and elongation (68ºC, 1 min). Amplification was followed by extension (68ºC, 7 min).

The TD-PCR protocol was RT (48ºC, 45 min), denaturation (94ºC, 2 min), and 10 cycles of denaturation (94ºC, 1 min), annealing 1 min (primer annealing temperature plus 10ºC decreasing 1ºC/cycle) and elongation (68ºC, 1 min) followed by 25 cycles PCR amplification as described (annealing 65ºC for p16, 60ºC for p14ARF). TD-annealing temperature range for p16 was 75-65ºC and 70-60ºC for p14ARF (36). PCR products were analyzed semi-quantitatively on 2.5% agarose electrophoresis gels comparing L37 control gene and 100 bp DNA markers.

Rapid Amplification of cDNA Ends (RACE)

RNA was extracted from NCF and CMT28 cells and 3′-RACE-PCR performed (RLM-RACE kit, Ambion) according to the manufacturer's instructions. First stand cDNA was synthesized from RNA by RT (48ºC 1 hr) using the 3′-RACE adapter ligated to the 3′-poly(A) mRNA tails. cDNA was amplified using primers (F1 and F2) and 3′-RACE primers (r´1 and r´2) complementary to anchored 3´-RACE adapters (Fig.7A). Outer 3′-

RACE-PCR was first performed using F1 and r′1 primers. Inner nested 3′-RACE-PCR was performed using nested primers F2 and r´2 and outer 3′-RACE product as template. In 5′-RACE, adapters were ligated to 5′- RNA ends prior to RT. 5′-RACE-PCRs were performed using reverse primers (R2 and R3) and 5′-RACE primers (f´1 and f´2) complementary to anchored 5′-RACE adapters.

RACE-PCRs were optimization by using thermostable GC-rich template-adapted polymerase (AccuPrime GC-rich DNA polymerase, Invitrogen) in TD-PCR. RACE-TD-PCR cycle profiles were denaturation (95ºC, 3 min), TD (10 cycles of denaturation 95ºC, 30 sec, annealing at temperature of Tm plus 10ºC and decreasing 1ºC/cycle 30 sec, elongation at 72ºC, 30 sec) followed by 25 amplification cycles (denaturation at 95ºC, 30 sec, annealing at temperature from previous TD step 30 sec, elongation 72ºC, 30 sec) and extension at 72ºC, 7 min. Inner 3′/5′-RACE-PCR products were analyzed by 2.0% agarose gel electrophoresis.

TA-cloning, Sequencing and Alignment

Amplicons (identified by apparent molecular weight) were gel purified and cloned into TA-cloning vector pCR2.1 according to manufacturer's instruction (Invitrogen). Successfully propagated clones were identified by restriction endonuclease digestion and 1.5% agarose gel electrophoresis. Cloned amplicons were isolated, processed and sequenced (MGH DNA Sequencing, Cambridge, MA). Amplicon sequences were subjected to BLAST analysis (http://blast.ncbi.nlm.nih.gov/) to confirm authenticity. Canine p16 and p14ARF sequences were aligned with published p16 and p14ARF sequences using Vector NTI AlignX (Invitrogen). Dendrograms were generated from multiple alignments applying a neighbor-joining algorithm (ClustalW, Vector NTI).

Protein Structural Analysis

Protein sequences were predicted from coding sequences and aligned and instability indices calculated (ExPASy ProtParam algorithm) (Gasteiger et al., 2005). Protein motifs and native folding were predicted and compared using motif/structure prediction and fold recognition databases including Phyre V0.2 protein fold recognition server, 3D-PSSM Fold Recognition Server and Swiss-Model InterproScan (Kelley et al., 2000; Kelley and Sternberg, 2009; Zdobnov and Apweiler, 2001).

Section 3. Results

Differential Expression of INK4 Tumor Suppressors in CMT Models

First, the four members of INK4 genes including p14ARF were evaluated for their expression and genetic defects in CMT models. INK4 mRNA expression was analyzed for a panel of six different CMT cell lines derived from canine primary carcinoma and adenocarcinomas (DeInnocentes et al., 2006; Wolfe et al., 1986). Following extensive optimization of PCR assays, expression profiles for INK4 genes were determined for CMT cells (Fig. 6). Expression of 1 or more of p16, p14ARF, and p15 mRNAs were absent in most CMT cell lines. p16 mRNA expression was defective in all CMT cell lines except CMT28 cells compared to p14ARF and p15, which were expressed in 2 or 3 of the CMT cell lines, respectively. p16 and p14ARF share common exons 2 and 3 requiring that PCR reactions include primers specific for each gene designed from the unique first exons. Primers had to avoid repeated and common sequences and also employed noncoding strand primers from shared exon 2. The success of this strategy was demonstrated by the ability to discriminate each transcript in different CMT cell lines where only 1 of p16 and p14ARF was expressed or where only p15 was expressed among these cell lines. CMT9 expressed p14ARF and p15 but not p16 while CMT47 expressed p15 but not p16 or p14ARF (Fig.6). These results demonstrate that each primer pair amplified only the transcript intended and could distinguish expression of each gene particularly that of alternatively spliced p14ARF from p16. This was confirmed by sequencing multiple reactions from each CMT cell line that expressed a specific gene. Where p16 and p15 were expressed, levels detected in CMT cells were comparable to levels observed in NCF.

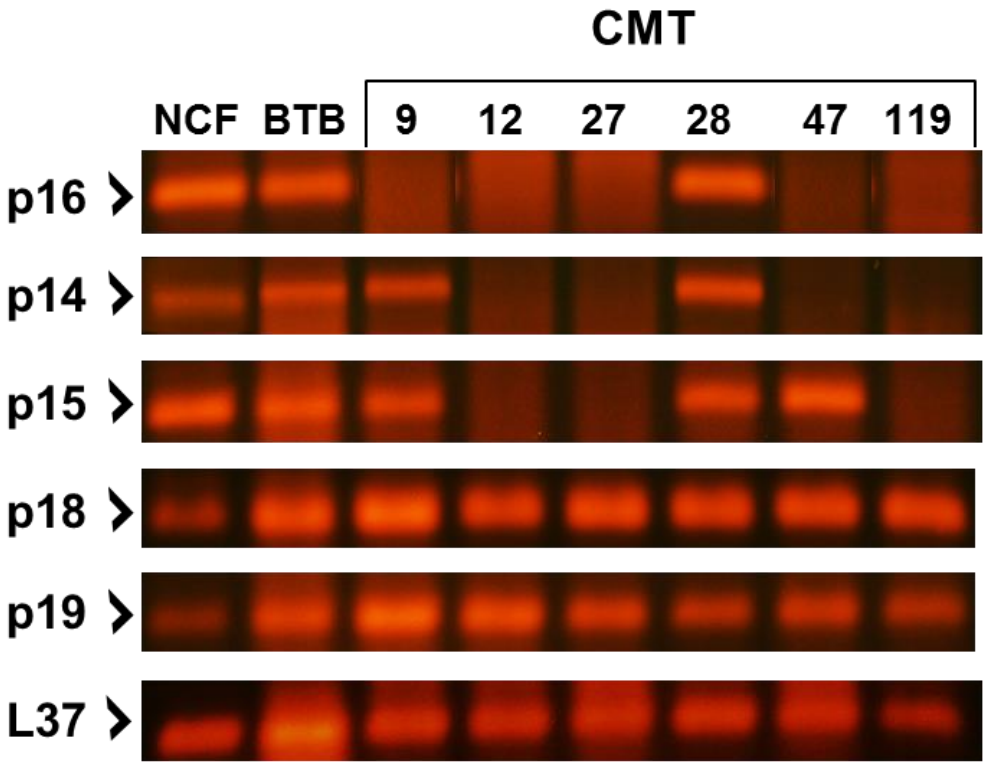

Fig. 6. INK4 CKI expression in CMT cells. RNA extracted from each cell line was used as templates in sqRT-PCR to amplify INK4-encoded mRNAs. Expression of 5 INK4 genes (p16, p14ARF, p15, p18, p19) in 8 canine cell lines (CMT9, 12, 27, 28, 47, 119, and NCF, BTB) were evaluated. L37 was used as internal control transcript.

Expression of p18 and p19 were both upregulated in all of the CMT cell lines evaluated when compared to NCFs (Fig. 6). This supports a previous report that human tumor-derived cell lines, also frequently mutated for p16 and p15, expressed few detectable defects in p18 and p19 (Zariwala and Xiong, 1996). A canine mammary epithelium-derived cell line (BTB) expressed all of the INK4 genes at comparable levels to those observed in CMT cells and at levels frequently higher than those in NCFs. NCFs expressed all of the

INK4 genes except p14ARF, which was expressed at a lower level. Moreover, levels for the expressed genes in NCFs were conspicuously lower compared to CMT cells with the exception of p16 and p15.

Similar differential expression patterns for the INK4 genes, including expression defects in p16, were also observed in primary canine cells directly isolated from several breast carcinoma biopsy samples (discussed in details in the next chapter) implying that these genetic defects are not likely an artifact of culture *in vitro*. These results suggested that p16, among all members of the INK4 gene family, was the most frequently defective in almost all of the CMT cell lines tested, followed by p14ARF and then p15. CMT9 and CMT47 cells provided examples where malignant cells were defective for p16 alone or combined with p14ARF.

Amplification of Full-length p16 Transcript from CMT28

In order to amplify the full-length p16 transcript, RACE strategy was applied in addition to conventional RT-PCR. The coding sequence of canine p16 is incomplete in the published canine genome (AF234176) so RACE-strategies to discover missing exon 1α sequences were employed (Fig.7A). Since p16 and p14ARF share the exon 2-3 region, primers were designed from conserved unique upstream p16 sequences avoiding overlapping sequence with p14ARF. Optimized touchdown (TD) sqRT-PCR generated p16 amplicons of ~270 bp from NCF and CMT28 cells (Fig.7B top) that were isolated and cloned. To amplify p16 transcript 3'-ends, 3'-RACE-TD-PCR was performed using gene-specific forward primers (F1 and F2) and 3'-RACE reverse primers (r'1 and r'2, Fig.7A). Outer 3'-RACE-TD-PCR was performed using gene-specific outer primer F1 and 3'-RACE outer primer r'1 from cDNA templates. Inner (nested) 3'-RACE-TD-PCR was then

carried out (primers F2 and r'2). 3'-RACE primers (r'1 and r'2) were complementary to adapter sequences ligated to mRNA poly(A)tails (Fig.7A). Nested 3'- RACE-PCR generated an amplicon of ~400 bp (Fig.7B bottom) covering most of the downstream region of p16 mRNA including the 3'-terminal poly(A) tail.

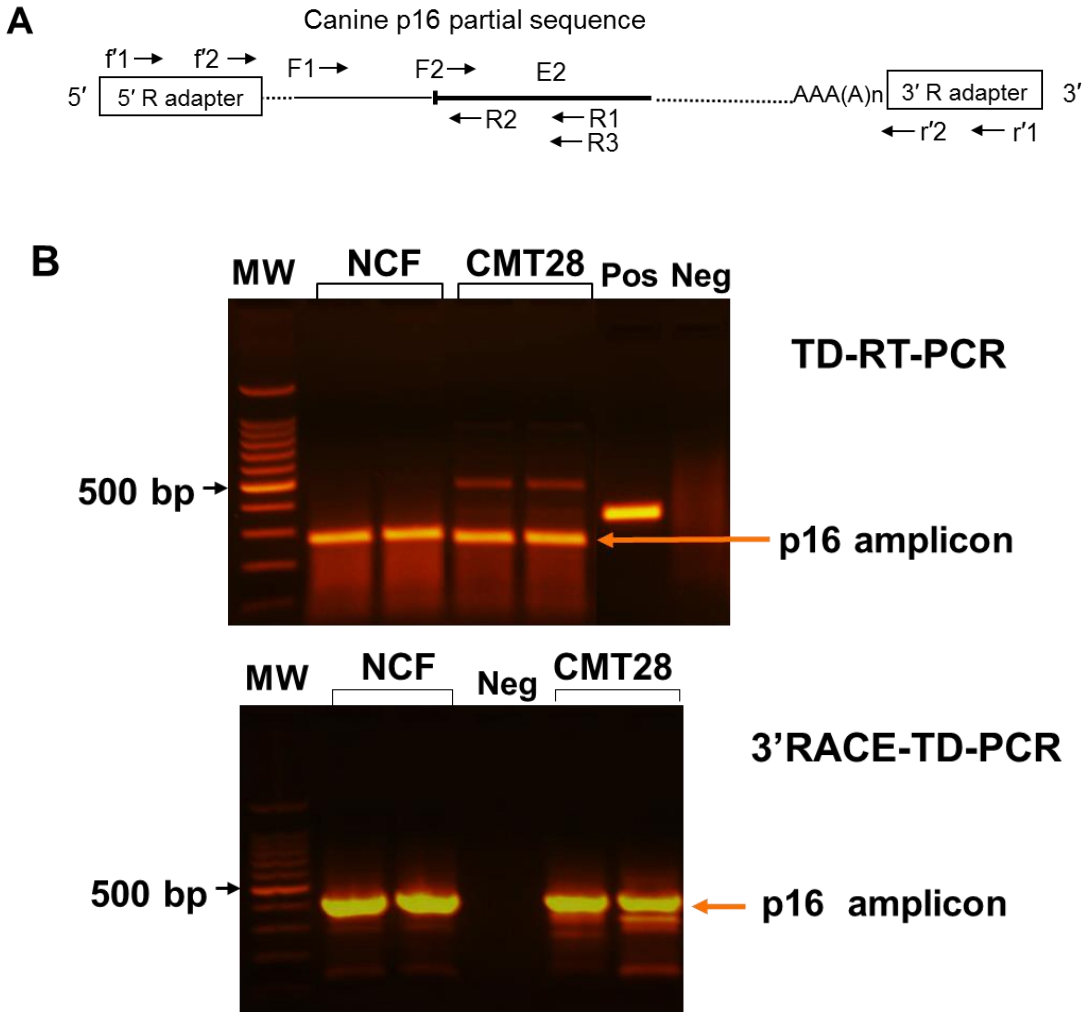

Fig. 7. Amplification of p16 from NCF and CMT28 by TD-PCR. (A) Schematic representing experimental design indicating p16 PCR primers. Primer pair F1 (forward) and R1 (reverse) were designed for amplification of 5'-upstream region by sqRT-TD-PCR. 3'-RACE PCRs were designed for amplification of downstream

region of the gene using primer pairs F1, r'1 and F2, r'2. 50-RACE reactions employed different primer pairs f'1, R3 and f'2, R2. Continuous line indicates partial canine p16 sequence including partial exon 2 (E2 thick line). Dotted line represents sequence absent from published p16 sequences. Arrows indicate position/orientation of primers on the canine p16 sequence. (B) Top: Expression of p16 upstream region (right arrows) in two passages of NCF and CMT28 cells evaluated by sqRT-TDPCR. Bottom: Amplification of 3'-region of p16 in the same cells by 3'-RACE-TD-PCR. MW: 100 bp molecular weight markers, left arrow: 500 bp fragment. Positive (Pos) and negative (Neg) control PCR reactions.

Alignments of Amplified Transcript Sequences Reveal a Frameshift Mutation in p16 Exon 1α from CMT28 Cells

Cloned amplicons and 3'-RACE-PCR products were sequenced and authenticity of p16 sequences were confirmed by NCBI BLAST analysis. Complete p16 sequences from NCF and CMT28 cells were generated from separate upstream and downstream sequences that aligned with published p16 sequences derived from other mammals and partial canine p16 sequences (Fig.8). Alignment allowed identification of conserved ATG start codons, three exon regions and 3'-poly(A) tails of canine p16 from both cell lines. Most strikingly, p16 from CMT28 but not from NCF, was found to encode a 17 bp deletion in 5' region of exon 1α, providing direct evidence for a genetic defect in p16 in canine mammary cancer that would result in a frameshift mutation.

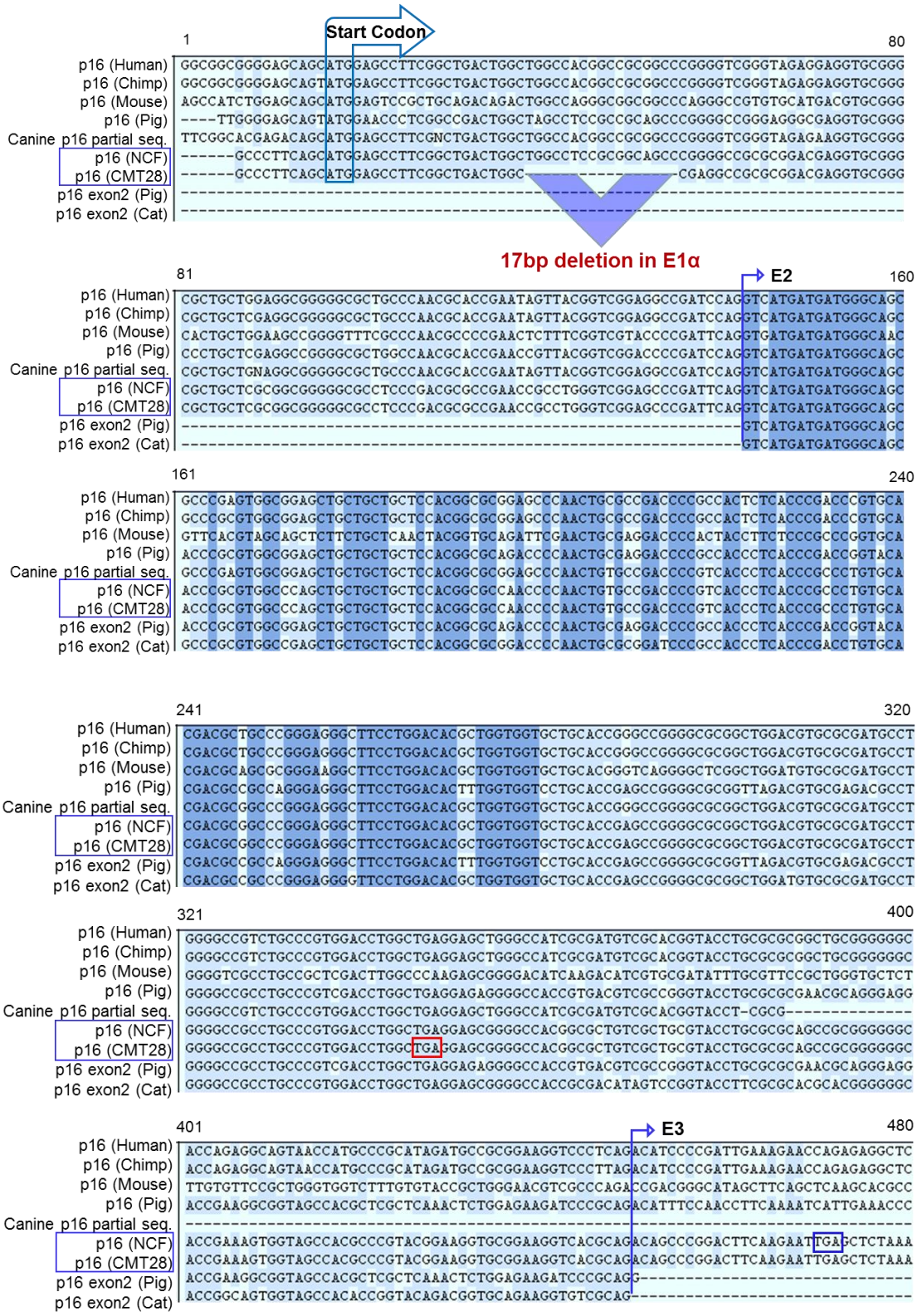
Start Codon
17bp deletion in E1α
E2
E3
p16 (Human)
p16 (Chimp)
p16 (Mouse)
p16 (Pig)
Canine p16 partial seq.
p16 (NCF)
p16 (CMT28)
p16 exon2 (Pig)
p16 exon2 (Cat)

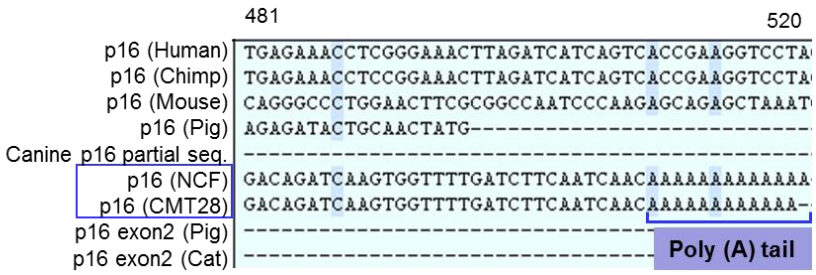

Fig. 8. Alignment of canine and other mammalian p16 sequences. Canine p16 amplicon sequences from NCF (#JQ796919) and CMT28 (#JQ796920) were aligned and compared to published p16 sequences (human #L27211, chimpanzee #NM_001146290, mouse #AF044336, pig #AJ316067), p16 exon 2 sequences (human #U12819, pig #AJ242787, cat #AB010807) and predicted partial p16 sequences from the canine genome (#AF234176). Alignments revealed a highly conserved ATG start codon, identical (boxed bent arrow), and conserved (light shaded background) regions. Exon 2 (E2) and exon 3 (E3) boundaries are indicated (bent arrows). A 17 bp deletion was identified in CMT28 exon 1a (E1a) from p16 alignments (large shaded arrow). p16 sequences from both cell lines terminated in 3' end poly(A) tails but included different stop codons (boxed TGA codons). p16 sequences from NCF and CMT28 (as denoted by a rectangular box on the left panels) indicate canine p16 mRNAs that were sequenced in this study.

Evolutionary relationships between p16 coding sequences from NCF, CMT28 cells, and other vertebrates were determined (Fig.2). Dendrograms comparing p16 sequences revealed evolutionary relationships among mammalian species rooted on distant chicken or fugu. Mouse and opossum sequences were clustered separately from human and canine sequences. Canine p16 sequences (NCF, CMT28) were closely related to published

p16 sequences from human, chimp and other higher mammals suggesting high levels of conservation among these species. Predicted p16 protein sequences were also aligned and were highly conserved. Unlike p16 mRNAs, the CMT28 p16mut protein sequence was poorly aligned with other p16 protein sequences after the first 7 amino acids resulting in premature termination with a truncated sequence compared to other p16 proteins including NCF (Fig. 9).

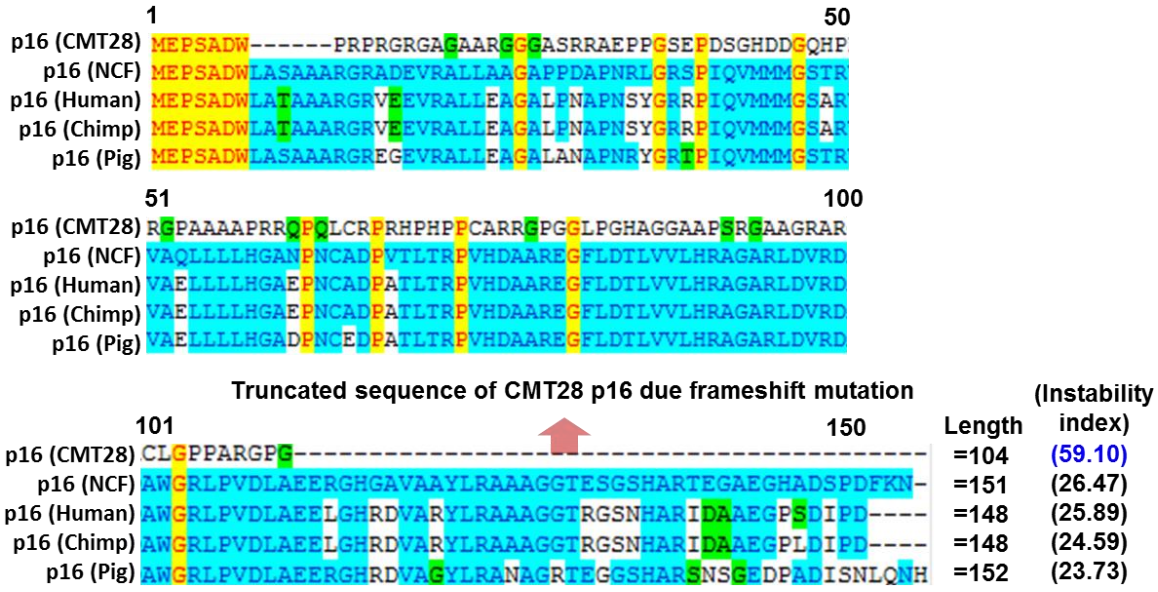

Fig. 9. Comparison of predicted CMT28 p16mut protein sequence with wild type sequences from NCF and other mammals. p16 sequences from NCF, CMT28 cells, and other p16 sequences were translated and aligned. Instability index of each p16 protein sequence (ExPASyProtParam algorithm) is indicated (parentheses) after the length of each protein sequence (amino acid number). Instability indices less than 40 were predicted to be relatively stable whereas indices greater than 40 indicated relatively unstable proteins.

Mutation in p16 Exon 1α from CMT28 Changes the Reading Frame to p14ARF Exon 2 Resulting in Unstable Hybrid Protein

CMT28 p16mut was predicted to translate an altered reading frame due to a 17 bp deletion in exon 1α (Fig.10A). The first 22 base pairs of p16 exon 1α were conserved followed by the remainder of exon 1α, which was read out of frame generating a unique sequence. Following the exon 2 boundary, reading frame was shifted to that of p14ARF exon 2 (Fig.10A) suggesting that CMT28 p16mut is predicted to translate into a hybrid-protein composed of p16 (mutated exon 1α) and p14ARF (exon 2) resulting in an aberrant and likely dysfunctional protein (Fig.10B-C). Translation of CMT28 p16mut would result in shorter peptide sequences (104 amino acids) compared to wild type NCF p16 (151 amino acids, Fig.9). The CMT28 p16mut protein sequence was predicted to be unstable compared to wild type protein (high calculated instability index, ProtParam algorithm) (Gasteiger et al., 2005) suggesting that if CMT28 cells produced a truncated/altered p16/p14ARF fusion protein it would most likely be rapidly degraded. This supports previous experimental evidence that CMT28 cells do not express detectable p16 protein by Western blot (Agarwal et al., 2013). Since the majority of the CMT28 p16mut peptide sequence would be identical to p14ARF exon 2 and the remainder of exon 1α was unique, except the first 7 amino acids, it is unlikely that p16 antibodies would recognize the CMT28 p16mut peptide (Fig.10B). A schematic of CMT28 p16mut protein indicates how different it is from wild type p16 and p14ARF consisting of an initial short amino acid sequence from p16 exon 1α (E1'α), a large conserved region from p14ARF exon 2 (due to the frameshift mutation) and a middle unique sequence (E1'αmut) unique to the putative fusion peptide (Fig.10C).

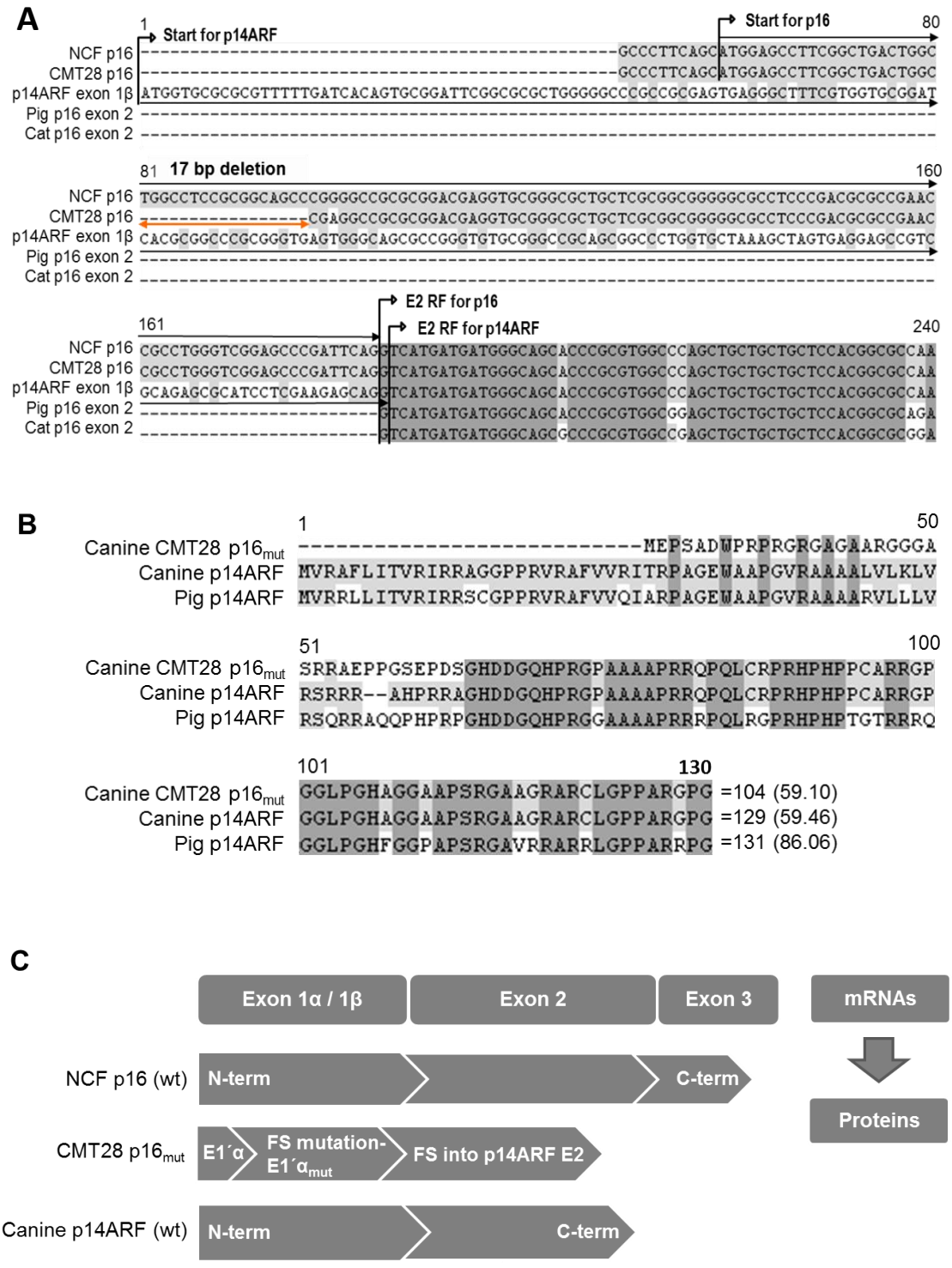

Fig. 10. Mutation of the CMT28 p16 sequence alters the reading frame of exon 2 to p14ARF. (A) NCF and CMT28 p16 sequences were compared with p14ARF. Horizontal arrows indicate p16 exon 1a and p14ARF exon 1b reading frames starting

from initiation codons (bent arrows labeled ATG). Exon 2 reading frames (bent arrows labeled E2) for NCF p16 or p14ARF are indicated and double-ended arrow indicates CMT28 exon 1a deletion mutation. Alignments of p16, p14ARF and p16 exon 2 are shown. (B) Predicted canine (#FM883643) and pig (#AJ510264.1) p14ARF were translated and aligned with CMT28 p16mut and exon 2 boundary noted (bent arrow E2). (C) Schematic comparing exon structure of CMT28 p16mut with wild type (wt) canine NCF p16 and p14ARF proteins (FS-frameshift; E10a-partial exon 1a; N/C term-nitrosal/carboxyl protein termini).

Frameshift Mutation in CMT28 p16 Exon 1α Disrupts Predicted Protein Structural and Functional Integrity

Because frameshift mutation was predicted to cause deletion and truncation of CMT28 p16mut protein, both wild-type and mutant p16 protein sequences were analyzed using the protein motif/structure prediction tool (Phyre V0.2) (Kelley and Sternberg, 2009) to predict functional protein folding motifs (Fig.11). Amino acid sequences were further analyzed characterizing wild type canine p16 protein obtained from NCF as encoding a family of beta-hairpin–alpha-hairpin ankyrin repeats and predicting a model of folded structure (3D-PSSM, InterProScan and ScanProsite tools) (Kelley et al., 2000; Zdobnov and Apweiler, 2001) (Fig.11A-B). No recognizable hairpin or repeat structures were identified in the CMT28 p16mut protein. Moreover, wild type NCF p16, but not CMT28 p16mut protein models, revealed potential ligand binding sites (3DLigandSite server) (Wass et al., 2010). Because CMT28 p16mut protein shares a large overlapping amino acid sequence with canine p14ARF, it was investigated whether the mutant protein could undergo p14ARF-like structural folding or form similar functional motifs using the same protein motif and fold recognition bioinformatics tools. Wild type p14ARF sequences

predicted a folded structure and a unique N-terminal motif not shared with p16mut protein (Fig. 11A-B). The CMT28 p16mut sequence revealed neither the folded structure with ankyrin repeats comparable to p16 nor p14ARF-like N-terminal folding (Fig.11).

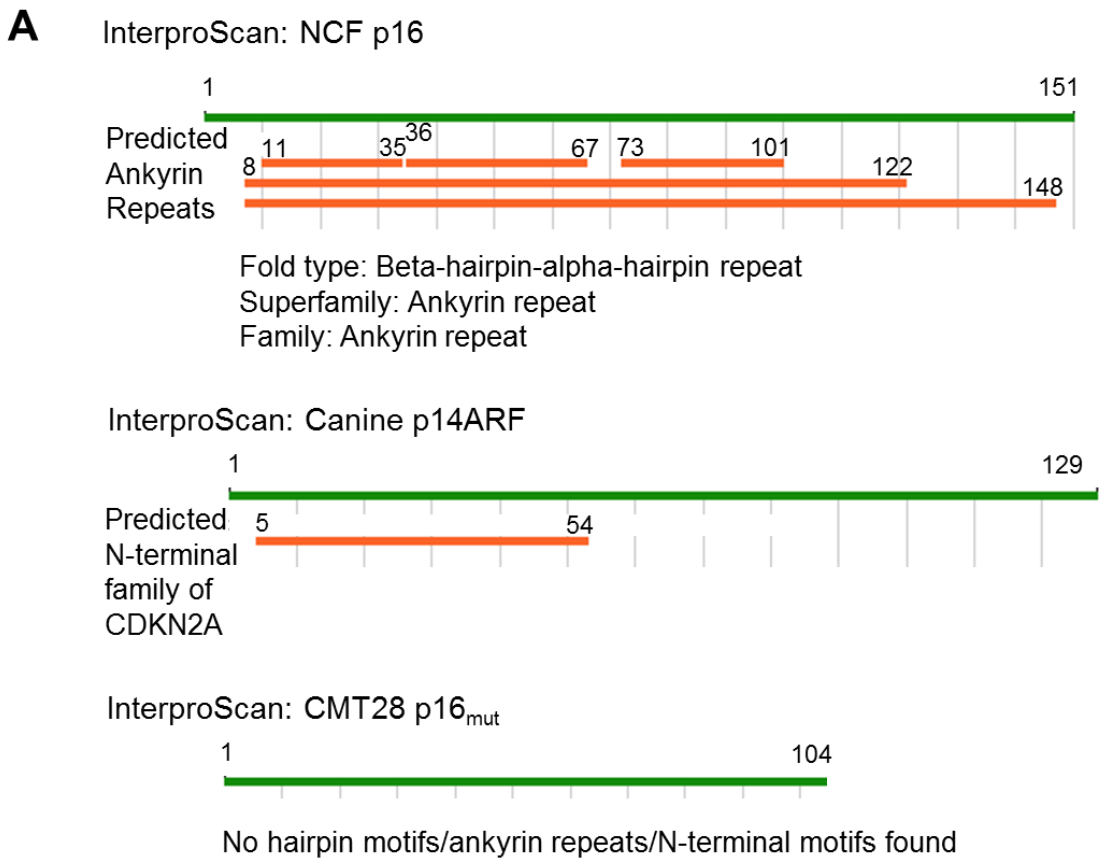

Fig. 11. Comparative analysis of INK4 protein motifs and folding structures. (A) NCF p16, CMT28 p16mut, and canine p14ARF protein sequences were analyzed by fold/motif recognition tools. Predicted ankyrin repeats and N-terminal motifs are indicated (lines/numbers indicate respective amino acid positions).

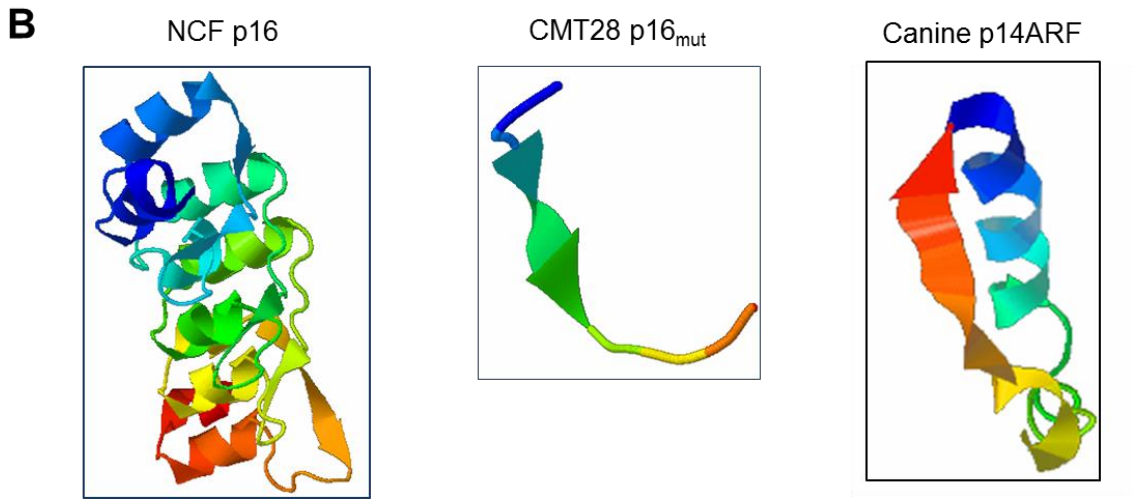

Fig. 11. (B) Three dimensional models for NCF, p16, CMT28 p16mut, and canine p14ARF proteins generated by protein motif recognition tools predicted each protein's folded structure and three dimensional model (Phyre V0.2, 3D-PSSM protein fold recognition servers and Swiss-Model InterProScan tools).

Section 4. Discussion and Conclusions

Canine cancers are excellent intermediate models for the study of human cancers because cancer etiologies in dogs are nearly similar to those of human cancers and dogs share the same environments with their owners. Spontaneous canine cancers bridge biological distances between induced mouse tumors and human cancers (Bird et al., 2008). Canine mammary tumor models, representing canine mammary carcinomas are the most frequently observed spontaneous neoplasms in dogs and provide a high level of similarity to human breast cancer. They have been characterized for tumor suppressor gene expression defects including p16, and other members of INK4 and Cip-Kip gene families and for defects in oncogenes such as c-erbB-2 and c-yes (Bird et al., 2008; DeInnocentes et al., 2009; DeInnocentes et al., 2006). It is important to characterize these defects to determine how closely they reflect defects found in human breast cancer. Continued research on CMT models builds validation and reinforces the strength of the model particularly for development of novel therapeutic strategies.

All canine mammary tumor cell lines used in this study are highly transformed lines derived from different dog breeds with clinical cases of spontaneous mammary carcinoma (DeInnocentes et al., 2006; Wolfe et al., 1986). Evaluation of INK4 expression profiles in the canine mammary tumor model suggested defects in these genes were extremely common. Because p16, p14ARF and p15 encode repetitive GC-rich sequences, the design and optimization of unique primers and protocols for RT-PCR was challenging, but sqRT-PCRs (following optimization by TD-PCR) were established and uniquely detected INK4 transcripts (DeInnocentes et al., 2006). The study has demonstrated that while p16, p14ARF, and p15 expression were defective or absent in most CMT cell lines, p18 and p19

were overexpressed in these tumor cell lines compared to NCF. This is consistent with previous reports of a lack of mutations in p18 and p19 in primary human tumors and tumor derived cell lines, which harbored p16 and p15 mutations (Zariwala and Xiong, 1996). Defects in INK4 genes would remove cell cycle check-point control, particularly in G1/S phase transition, promoting uncontrolled proliferation. This cancerous phenotype can be at least partially reversed by transfection of human p16 expression constructs into CMT28 cells altering cell phenotype to a less transformed state (DeInnocentes et al., 2009). The importance of p16/INK4A tumor suppressor defects in promoting CMT28 cell malignancy has been established and appeared coincident with defects in p14ARF and p15. This data suggests that while defects in expression of p16 mRNA in CMT cells are common they may not be sufficient to account for canine mammary neoplasia. Defects in p14ARF and/or p15 in other CMT cell lines suggested further investigation of this locus was warranted as frequency of defects in p15 in human tumors is also lower than p16 (Stone et al., 1995a).

Amplification and sequencing of the entire p16 coding sequence from CMT28 and NCF cells revealed a deletion mutation in p16 exon 1α in CMT28 cells suggesting a transforming mechanism in this canine mammary tumor model. The mutation in CMT28 p16 would cause failure in expression, as the 17 bp deletion caused a frameshift extending into exon 2. We determined that CMT28 p16mut has an altered reading frame that shifted to that of p14ARF in exon 2 predicting that p16mut would translate into a hybrid protein composed of a short p16 region, a new unique out-of-frame region and a large p14ARF overlapping region. The resulting truncated p16/p14 fusion sequence would likely be unstable (index >40) compared to wild type p16 protein (Gasteiger et al., 2005). Although this is a theoretical estimate of stability, it has provided a close approximation of stability

in vivo (Guruprasad et al., 1990) and likely predicts rapid degradation. This is consistent with reports that CMT28 does not express any detectable p16 protein (Agarwal et al., 2013). Moreover, artificially INK4A constructs made from exon 2 (skipping exon 1 or deleting N-terminal amino acids) showed that the amino-terminally truncated form of p16 or p14 would be functionally inactive and loses the inhibitory activity in the cell cycle (Lilischkis et al., 1996). This suggests that biological functions are mostly encoded by their first exons. Two important conclusions can be deduced from comparative protein structure and functional analyses. A loss of function mutation in CMT28 p16mut is likely to disrupt protein's functional integrity including native folding, which is essential for interaction with other proteins. Analysis of p16 and p14ARF suggested that the remarkable co-evolution of these two overlapping transcripts has evolved to generate two different proteins, largely derived from common nucleotide sequence, that both uniquely contribute to cell proliferation control.

In conclusion, sequencing of open reading frames from the wild-type and mutant canid INK4 locus revealed important aspects of its expression and genetic defects in canine mammary cancer. In addition to frequent loss of p16/INK4A locus, critical mutation in exon 1α altered the reading frame generating an aberrant fusion protein of p16 and p14ARF, that is predicted to be truncated, unstable, and devoid of functional motifs. The loss of function mutation in exon 1α of CMT28 p16 confirmed the critical importance of the INK4A locus in canine mammary cancer. Importantly, this mutation strongly correlate to those in human cancers. In a variety of human cancers, the altered expression of p16/INK4A gene results from the deletion mutations mostly occurred in exon 1α (Okamoto et al., 1994; Yeudall et al., 1994). Finally, the mapping of p16 defects and aberrant

expression profiles in the canine breast cancer model should shed light on the mechanisms regulating neoplasia and this important tumor suppressor gene is perhaps providing therapeutic insights for human breast cancer.

Chapter 3: Recurrent Loss of the p16/INK4A Locus in Primary Canine Mammary Tumors, Melanomas, and Human Breast Cancer Cell Lines

Section 1. Introduction

Spontaneous tumors in dogs serve as intermediate models for human cancer biology and translational cancer therapeutics. Canine malignancies have been established as strong comparative models for several types of human cancers, including melanoma and mammary carcinoma, based mainly on prognostic factors, lesions, morphologic characteristics, biologic behavior and epidemiologic features in both species (Bergman, 2007; Gilbertson et al., 1983; MacEwen, 1990; Owen, 1979; Taylor et al., 1976). Mammary carcinomas and melanomas in dogs are two naturally occurring tumors that have comparative relevance in molecular and histopathologic features especially when compared to their human counterparts (Hahn et al., 1994; MacEwen, 1990; Merlo et al., 2008). Canine malignant melanoma offers a clinically faithful model of human melanoma because it develops naturally in both inbred and outbred dogs with the background of an intact immune system where tumor, host and tumor microenvironment remain syngeneic (Bergman, 2007). Canine mammary tumors have been investigated as an increasingly powerful model to study human breast cancer because of significant similarities between dog and human in terms of breast cancer biology, pathogenesis, critical gene expression profiles and signaling pathways involved in cancer development (Pinho et al., 2012). The highest incidence rates for canine mammary cancer have been reported by epidemiological studies. The overall cancer incidence in female dogs was estimated to be three times higher

than in male dogs (272 versus 99 per 100,000 dogs), a difference largely accounted for by the increased prevalence of mammary carcinoma (Merlo et al., 2008; Vail and MacEwen, 2000).

Besides the cancer biological resemblance and clinical features, the dog provides an excellent spontaneous model for the identification and the study of cancer-associated loci. The dog became only the fifth mammal whose entire genome was sequenced after the completion of human genome sequencing. This paved the way for comparative genomics analysis drawing considerable attention as a model system to study evolution, structure and function of genes, genetic susceptibility and etiology of many human diseases including cancers (Lindblad-Toh et al., 2005). Extensive genetic similarities in gene order and functions have further revolutionized this area of research. In this context, a highly conserved region in canine chromosome 11 containing a cluster of tumor suppressor genes, has been found to be orthologous to the region in human chromosome 9p21 and is frequently deleted in a wide spectrum of cancers in both species (discussed in chapter 1, Fig. 5). A gene locus from this chromosomal region, known as CDKN2A/B or INK4A/ARF/INK4B, encodes important cell cycle regulators that play critical roles in controlling cell cycle progression and also act as potent tumor suppressors (Kamb et al., 1994a; Ruas and Peters, 1998; Sharpless, 2005).

The orderly progression of cells through the cell cycle is governed by genes encoding proteins that form a complex network of regulatory signals. These large cell cycle regulatory protein complexes are composed of cyclins, cyclin-dependent kinases (CDK) and their inhibitors called CDK-inhibitors (CKIs) (Hunter and Pines, 1994; Sherr, 1993). Dysregulation of these genes can allow premature entry into the next phase of the cell cycle

leading to neoplastic transformation (Hartwell, 1992). Therefore, cells acquire negative regulation at the transitions between cell cycle phases often known as checkpoints. In this mechanism of cell cycle control, the inhibitors of cyclin-CDK complexes or CKIs play important roles. One of the classes of CKI genes, called CDKN2 or the INK4 family, consists of four members, including p16/INK4A, p15/INK4B, p18/INK4C and p19/INK4D which actively regulate the retinoblastoma (Rb) pathway of the G1 to S phase transition of the cell cycle (Vidal and Koff, 2000; Weinberg, 1995). The expression of p16/INK4A, or other INK4 members, causes decreased activity of CDK4/6 kinase thereby promoting Rb hypo-phosphorylation which in turn leads to E2F repression and growth arrest (Russo et al., 1998; Serrano et al., 1993). As previously discussed in chapter 1 and 2, p14ARF, also known as alternative reading frame (ARF) of the p16 gene, is encoded and alternatively spliced from the same INK4A/ARF locus, but reads from a distinct first exon called exon 1β producing a different protein with separate regulatory functions in the cell cycle (Fig. 3B) (Gilley and Fried, 2001; Mao et al., 1995; Stone et al., 1995). This member of the INK4 family acts as a major upstream regulator of p53 and p21/Cip1 and is involved in p53 mediated growth suppression or cell cycle arrest (Fig. 4) (Gartel and Tyner, 2002; Kamijo et al., 1998; Pomerantz et al., 1998; Ruas and Peters, 1998; Sharpless, 2005; Zhang et al., 1998).

The INK4A/ARF/INK4B locus located on chromosome 9p21 in the human and the orthologous region of chromosome 11 in the dog encodes three important tumor suppressor genes including - p16, p14ARF, and p15 and is among the most frequent site of genetic loss in both human and canine cancers (Aguirre-Hernandez et al., 2009; DeInnocentes et al., 2009; Kamb et al., 1994; Kamb et al., 1994a; Koenig et al., 2002; Lutful Kabir et al.,

2013; Ruas and Peters, 1998; Serrano, 2000). Particularly, the inactivation of p16 is so important that evidence from the genetic analysis of numerous tumors have reported its defect in almost one-third of human cancers and identified p16 loss as one of the most recurrent lesions in human malignancies (Sharpless, 2005). Later, such genetic defects were also identified in other non-human species. Although altered p16 expression, due to deletion and mutations, was initially reported in the case of familial melanomas (Hussussian et al., 1994; Liu et al., 1995; Zuo et al., 1996), a higher frequency of p16 loss was observed in most common human cancers, such as, greater than 60% in the case of lung cancer (non-small cell lung cancer), pancreatic adenocarcinoma, leukemia, head and neck cancer, esophageal cancer, multiple myeloma and 20-40% of bladder carcinomas, as well as Non-Hodgkin's lymphoma, and stomach, colorectal, ovarian, and breast cancers (Rocco and Sidransky, 2001; Ruas and Peters, 1998; Sharpless and Chin, 2003; Sharpless and DePinho, 1999). All these estimates of p16 inactivation were based only on studies with primary tumors rather than cell line data. However, cell lines derived from metastatic tumors can reproduce similar p16 defects (Yeudall et al., 1994). The current study emphasizes an important correlation between human breast cancer and canine primary breast tumors, canine mammary tumors (CMTs) and malignant melanomas by evaluating regulatory mechanisms involving p16 and other INK4 gene defects and their recurrent deletion from cancer-associated tumor suppressor loci.

Section 2. Methods and Materials

Cell Lines

Five established canine malignant melanoma cell lines (CMLs) derived from different dog breeds, mammary tumor cells (CMTs, as described in the previous chapter) and three human breast cancer cell lines including MDA-MB-231, MCF7 and ZR-75 obtained from American Type Culture Collection (ATCC, Manassas, VA, USA) were used in this study. All the melanomas and mammary tumors were developed from spontaneous primary tumors. The sources of primary specimens were canine patients admitted to the Small Animal Clinic, College of Veterinary Medicine, Auburn University, AL for diagnosis and treatment of spontaneous tumors. CML2, 3 and 11 were originated from Poodle, CML7C from Scottish Terrier and CML10P from a mixed breed dog. All the CML cell lines were derived from primary oral melanomas except CML10P which was developed from a primary skin melanoma. The histologic pattern of these canine melanomas was composed of epitheloid or spindle-shaped cells (Wolfe et al., 1987).

A number of primary canine breast tumor cells were established from the biopsy samples collected directly from different dog patients. Among a number of confirmed positive cases, four spontaneous mammary carcinomas were selected for this study and numbered as CMT106, CMT110, CMT111 and CMT112. The CMT106 cells were derived from an English Springer Spaniel, CMT110 from a Bull Mastiff and CMT111 and 112 were derived from Labrador Retrievers. The average age range of these female dogs was 7-11 years and is comparable to the typical breast cancer onset in humans. Normal canine mammary epithelial cells (CMECs) were cultured and developed from dogs and beagles with no history of mammary carcinomas and were verified by histopathological

examination. RNA was extracted from these primary cells immediately after establishing the monolayer cultures to select for live cells.

Processing of Primary Tumor Biopsy Tissues and Preparation of Single-cell Suspensions

Tumor biopsy samples excised surgically were placed immediately in chilled transport medium consisting of tissue culture medium with 10% heat inactivated serum and 2% antibiotics (Wolfe et al., 1986). Tissues were carefully cut into small pieces with a sterile scalpel blade and tissue fragments were then incubated in L-15 medium containing 200-250 U collagenase/ml for 1.5 to 2 hours with gentle shaking. The resultant cell suspensions were filtered through 50 μm sterile filters, washed and resuspended in L-15 medium enriched with 10% fetal bovine serum (FBS) and 2-3X antibiotics. About 5 million cells in 5 ml culture medium were dispensed into 25 cm^2 cell culture flasks or in 6-well plates and grown at 100% humidity at 37 °C with 5% CO_2 for 2-3 days (You and Bird, 1995). Cultured cells had to be free from mycoplasma and fungal contamination based on ultra-structural observation before they were ready for subculture.

Single Cell Sorting of Normal Canine Mammary Epithelial Cells (CMEC)

Primary mammary gland biopsy tissue samples were collected from dogs and processed to generate single cell suspensions according to the previously discussed protocol. A mixed cell population was observed in primary cell cultures that included fibroblasts and mammary epithelial cells (Fig. 12A upper panel). Single cell sorting was employed to isolate mammary epithelial cells from fibroblasts based on their specific morphologies. The cultured cells were trypsinized and resuspended in flow wash buffer (FWB = 1% bovine serum albumin or BSA in PBS). Following 3X wash in FWB, cells

were filtered through 50 μm sterile filters (Partec CellTrics) and prepared for flow cytometry analysis. Epitheloid single cell populations were isolated using side scatter by size analysis and single cell sorted into 96-well culture plates containing 100 μl growth media per well in a MoFlo XDP Cell Sorter (Beckman Coulter, CA) (Appendix 9).

Cell Culture and RNA Extraction

All primary tumor cells and established cancer cell lines were grown in Leibovitz's L-15 Medium (GIBCO, Invitrogen Co) with 1% antibiotics and 10% fetal bovine serum. Human breast cancer cell line ZR-75 was grown in Roswell Park Memorial Institute medium (RPMI, GIBCO, Invitrogen Co). Cells were grown at 100% humidity at 37 °C with 5% CO_2, changing the medium every two days (DeInnocentes et al., 2006; Wolfe et al., 1986). Total RNA was isolated from cells (70-80% confluence) by phenol-chloroform extraction according to the manufacturer's instructions (RNA STAT-60; Tel-Test, Inc). RNA pellets were air-dried and stored (-80ºC). Pellets were resuspended in diethylpyrocarbonate-treated water for PCR assays. Concentration and purity of RNA was determined by absorbance at 260 nm (You and Bird, 1995).

Primer design

Primers were designed for INK4 (Chapter 2, Table 1), Cip/Kip (DeInnocentes et al., 2009), Rb (Bird et al., 2008) and p53 (DeInnocentes et al., 2006) genes using Vector NTI primer design software (Invitrogen). Published canine CKI sequences were aligned with sequences from other mammalian species and primers designed from highly conserved unique regions. A new set of primers for INK4 genes (Table 2) were designed

and derived from published human sequences. The additional canine p53 primers were designed and based on GenBank AF060514.

Table 2: INK4 and p53 primers designed from human genome

Genes	Primers (Forward/Reverse)	Primer Sequences (5′ to 3′)
p16	Forward	ATGGAGCCTTCGGCTGACTGGCTGG
	Reverse	TGGAGCAGCAGCAGCTCCGCCAC
p14ARF	Forward	CGAGTGAGGGTTTTCGTGGTTC
	Reverse	ACCACCAGCGTGTCCAGGAAG
	Forward	AGTGAGGGTTTTCGTGGTTCACATCC
	Reverse	ACCACCAGCGTGTCCAGGAAGC
p15	Forward	GTGCGACAGCTCCTGGAAGC
	Reverse	CCAGCGTGTCCAGGAAGCC
p19	Forward	ATGCTGCTGGAGGAGGTTCG
	Reverse	TGCGATGGAGATCAGATTCAGC
p53	Forward1	ATCTATAAGAAGTCGGAGTTCGTGACC
	Forward2	ATGGCCATCTATAAGAAGTCGGAGTTCG
	Reverse1	GTAGTTGTAGTGGATGGTGGTATAGTCAGA
	Reverse2	GAGTCTTCCAGGGTGATGATAGTGAGGAT

Formaldehyde Denaturing Gel Electrophoresis

Denaturing 1% agarose gels were prepared using formaldehyde and N-morpholino Propanesulfonic acid buffer (MOPS) in deionized water. The gel composition was 0.5 gram agarose, 5 ml 10X MOPS buffer (pH 7.0), 8.1 ml 2.2 M formaldehyde (37%) and water to make the final volume 50 ml. Agarose in MOPS buffer was melted in a microwave oven until the solution became homogeneous. Melted gel was cooled to 60^{o}C in water bath. In a fume hood, 37% formaldehyde was measured into a screw-capped tube and heated up to

60°C in a water bath. Melted agarose and formaldehyde were carefully mixed and the gel was poured under the fume hood and allowed to become a cool semi-solid matrix. Denaturation of RNA was carried out by incubation at 60°C in the presence of formaldehyde denaturation buffer. The composition of denaturation buffer was 250 µl deionized formamide, 92 µl 37% formaldehyde, 50 µl 10X MOPS and 100 µl RNase free ethidium bromide. For each sample, 1-3 µg RNA was mixed with 3 volumes of denaturation buffer. To monitor sample migration in the gel, dye solution containing 0.25% bromophenol blue and 0.25% xylene cyanol was mixed with denaturation buffer in a 1 to 3 ratio (5 µl dye in 15 µl buffer).

Reverse Transcriptase (RT) PCR

Gene expression was evaluated by optimized RT-PCR as described previously (Chapter 2) using mRNA templates in semi-quantitative assays at limiting template dilution and minimum amplification number (DeInnocentes et al., 2009). The basic PCR protocol consisted of RT (48ºC, 45 min), denaturation (94ºC, 2 min) and amplification cycles (usually 30) composed of denaturation (94ºC, 1 min), annealing for 30 sec (65ºC for p53) and elongation (68ºC, 1 min). Amplification was followed by extension (68ºC, 7 min).

For some difficult templates, including p16 and p14, the touch-down (TD) RT-PCR method was employed. The TD-PCR protocol was RT (48ºC, 45 min), denaturation (94ºC, 2 min), and 10 cycles of denaturation (94ºC, 1 min), annealing 1 min (primer annealing temperature plus 10ºC decreasing 1ºC/cycle) and elongation (68ºC, 1 min) followed by 25 cycles PCR amplification as described (Korbie and Mattick, 2008). PCR products were analyzed semi-quantitatively on 2% or 2.5% agarose electrophoresis gels compared with L37 or GAPDH internal control genes and 100 bp DNA markers.

TA-Cloning, Sequencing and Alignment

All the amplicons (obtained from each PCR assay) were verified by DNA sequencing. Amplicons (identified by apparent molecular weight) were subjected to gel purification and TA-cloning as described previously (Chapter 2) for sequencing. Cloned (or gel-purified) amplicons were isolated, processed and sequenced (MGH DNA Sequencing, Cambridge, MA). Canine p16 sequences were aligned with published p16 sequences from other species using the Vector NTI AlignX tool (Invitrogen).

Section 3. Results

Processing and Development of Normal CMEC and Primary Mammary Tumor Cell Lines

Both primary tumors and normal mammary biopsy tissue samples from dogs were processed to generate single cell suspensions according to the previously discussed protocol (Methods and Materials). Most primary mammary tumor cells in culture shared the morphology of smaller cuboidal and epithelial-like cells and subsequently acquired a cuboidal to spindle shaped morphology with higher nuclear to cytoplasmic ratios (Fig. 12B). In the case of normal canine mammary epithelial cells (CMECs), fibroblasts overgrew during prolonged periods in culture. For this reason, single cell sorting was carried out to isolate mammary epithelial cells from fibroblasts based on their specific morphologies. Another cell type observed was likely to be long spindle-shaped fibroblasts which was sorted from primary cultures of canine mammary epithelial cells (Fig. 12A). These cells can be defined as canine mammary fibroblasts that predominate among mammary stromal populations and are closely associated with other inflammatory and endothelial cells in the surrounding breast microenvironment (Ronnov-Jessen et al., 1996).

Cellular morphologies and growth patterns of the primary tumor cells remained unchanged when grown in culture but they were characterized by individual distinct features typical of mammary epithelial cells. They grew with variable physical shapes and in close contact with one another and could be readily distinguishable from normal CMECs (Fig. 12). The primary tumor cells and mammary fibroblasts were grown in culture for maximum number of passages unless they reach senescent state. While the CMECs growth could be slowed down in culture after several passages. For this reason the RNA was

extracted from all these cells at the beginning of primary culture or before seeding the cells in the subsequent passages. As shown in Fig. 12, the primary canine breast tumor cells, normal CMECs and mammary fibroblasts have distinct morphological features, growth potentials as well as gene expression profiles (discussed in later sections).

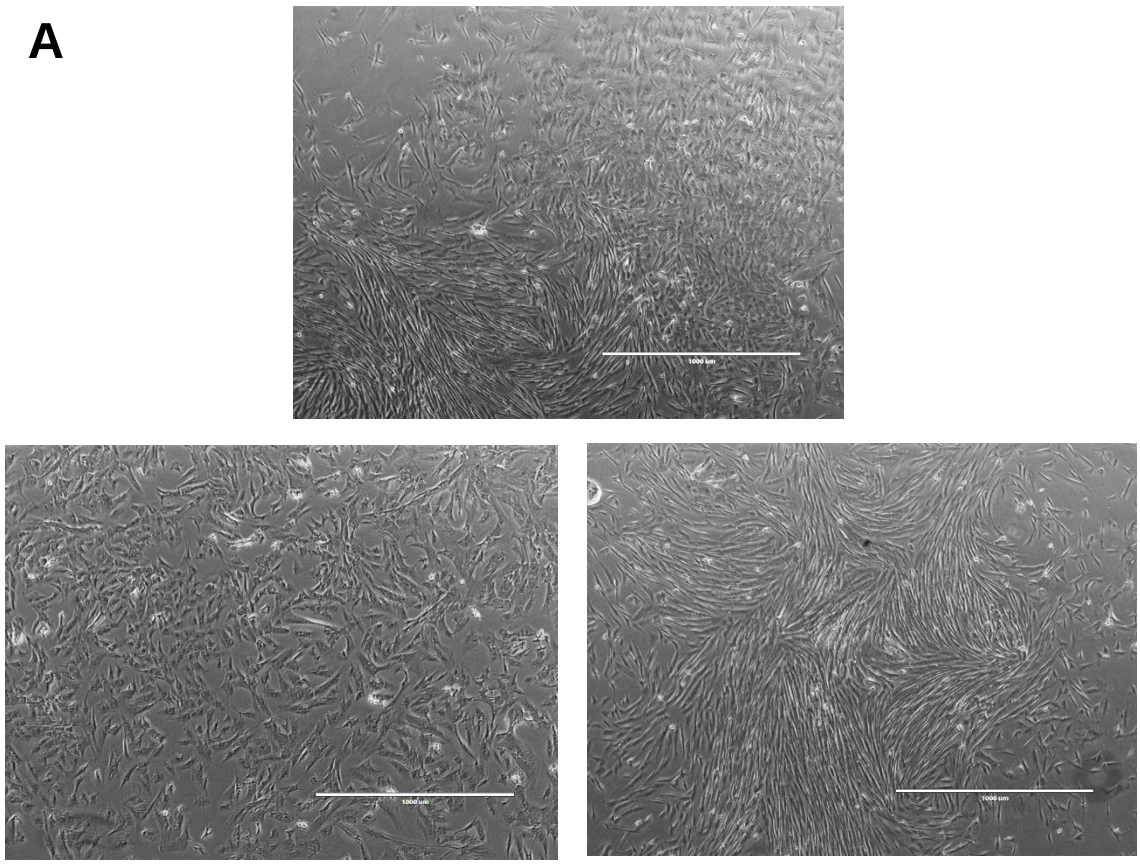

Fig. 12. Isolation and development of normal CMEC and primary CMT cells. (A) Isolation of normal CMECs and canine mammary fibroblasts based on their morphologies and growth potentials. Live cultures of normal CMECs have been shown. Mixed population (fibroblasts and mammary epithelial like) in the primary

culture (upper panel), sorted canine mammary epithelial cells (CMECs) (bottom left) and sorted canine mammary fibroblasts (CMF) (bottom right).

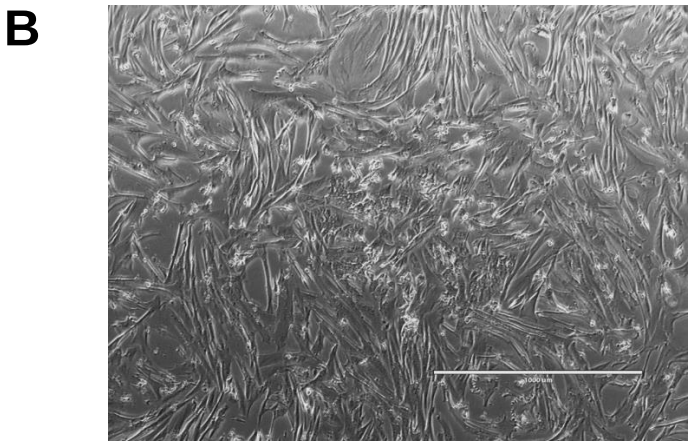

Fig. 12. (B) Selected primary canine mammary tumor cells (CMT110). Cells were examined under phase contrast microscopy using 4X (for CMEC) and 10X (for CMT110) objectives (magnification bars indicate scale for each; 1000 µm for 4X and 400 µm for 10X magnification) and photographed. Representative fields of cells are shown for each cell type from culture when cell growth had achieved confluence of 70-80%.

Differential Expression Profiles of INK4 Genes in Primary Canine Mammary Carcinomas

All INK4 gene expression was evaluated in a panel of four primary canine mammary tumors (CMT106, CMT110, CMT111 and CMT112) and normal CMECs. Using optimized assays of semi-quantitative RT-PCR or touch-down RT-PCR, mRNA expression of all 4 INK4 gene family members as well as p14ARF were measured in these cells (Fig. 13). Like established CMT models (Chapter 2), primary canine mammary tumors were most frequently defective for p16 compared to other INK4 tumor suppressor

genes. p14ARF and p15 were differentially expressed while p18 and p19 expression were found to be normal in all of the cell lines analyzed. The expression profile for all the INK4 genes in CMECs and canine mammary fibroblasts are comparable to that in normal canine fibroblasts (NCF) (Fig. 13 and Fig. 6, Chapter 2). Defects evident in p16, p14ARF and p15 in these primary breast tumors suggest that their altered expression is not likely an artifact of CMT culture *in vitro*. In addition, the immortalization of CMTs appears not to be a mere outcome from loss of the p16/INK4A locus during cell culture but a consequence of aberrant cell cycle regulatory mechanisms in canine breast cancers.

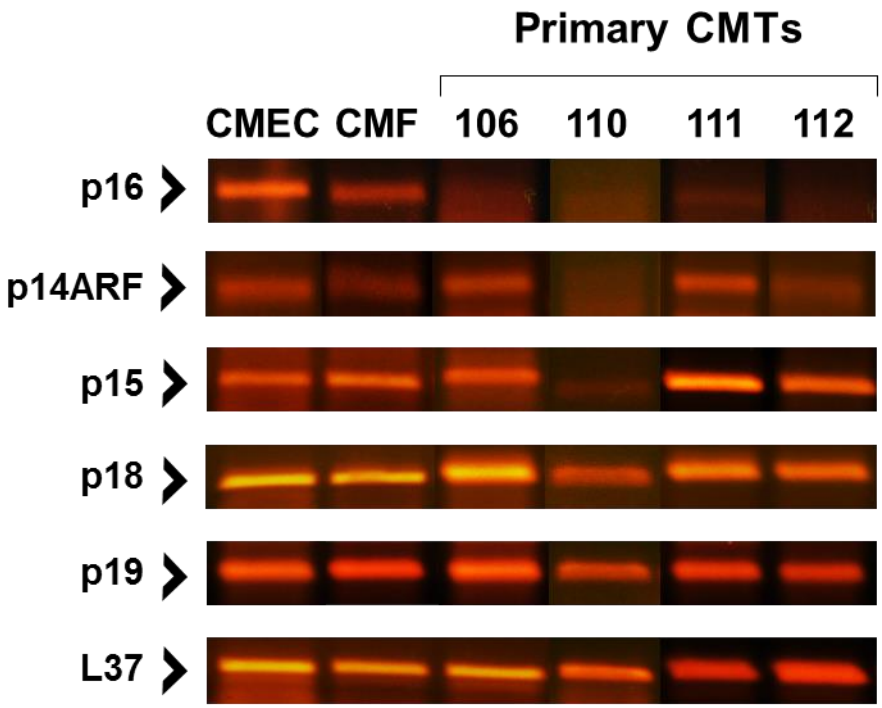

Fig. 13. Expression of INK4 mRNAs in primary CMT cells. Total RNA extracted from each primary cell culture was used as template in touch-down (TD) RT-PCR or conventional RT-PCR to amplify INK4 transcripts. INK4 genes p16, p14ARF, p15, p18, and p19 were evaluated in 4 canine breast cancer cell lines (CMT106, 110, 111,

and 112) derived from fresh tumor biopsies and CMEC. Canine mammary fibroblasts (CMF) were used to compare INK4 expression with those in normal CMEC. L37 was used as an internal control transcript.

The INK4A/ARF/INK4B Locus is Highly Susceptible to Frequent Loss in CMLs

The expression of INK4 gene members was also investigated in canine malignant melanoma models. Five CML cell lines (CML-7C, CML-10P, CML2, CML3 and CML11) were established from spontaneous primary melanomas derived from different dog breeds (Wolfe et al., 1987). Three members of the INK4 gene family including p16, p15 and p14ARF were highly defective and completely lost in these melanoma models except CML-7C that expressed both the p16 and p14 messages (Fig. 14). Subsequently DNA sequencing analysis revealed that p16 mRNA from CML-7C, although expressed, harbored a large deletion mutation that disrupted the gene and protein expression (Fig. 16). This expression data, demonstrating loss of the INK4A/ARF/INK4B locus in canine chromosome 11, establishes a strong correlation with the frequent loss of orthologous region in chromosome 9p21 in human melanomas (Fig. 5, Chapter 1) (Hussussian et al., 1994; Kamb et al., 1994a; Ranade et al., 1995).

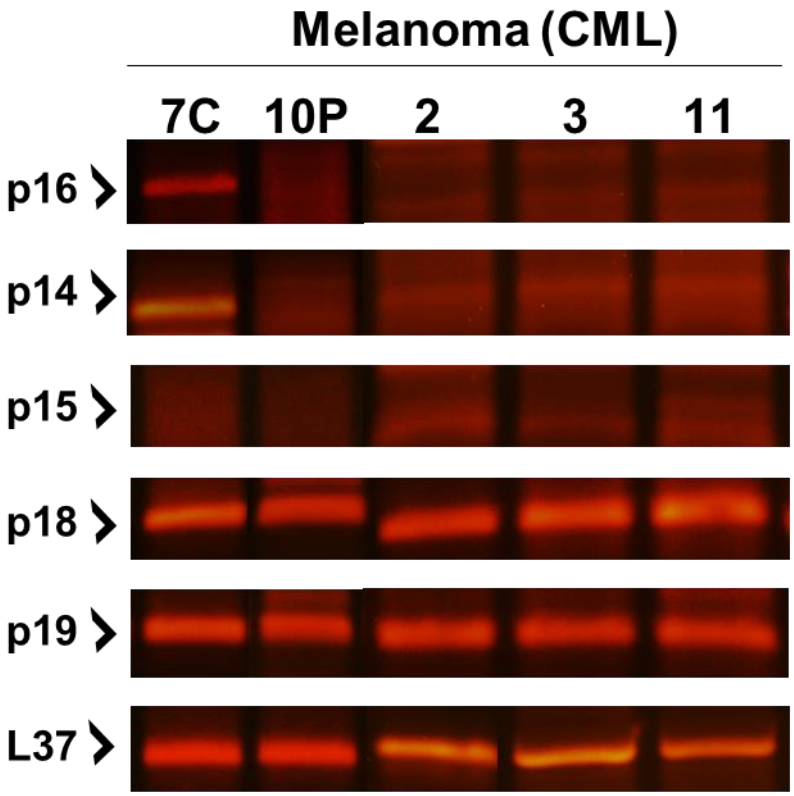

Fig. 14. INK4 mRNA expression in CML cell lines. Expression of all INK4 members in a panel of 5 canine malignant melanoma cell lines were evaluated using optimized TD-RT-PCR and conventional RT-PCR approaches.

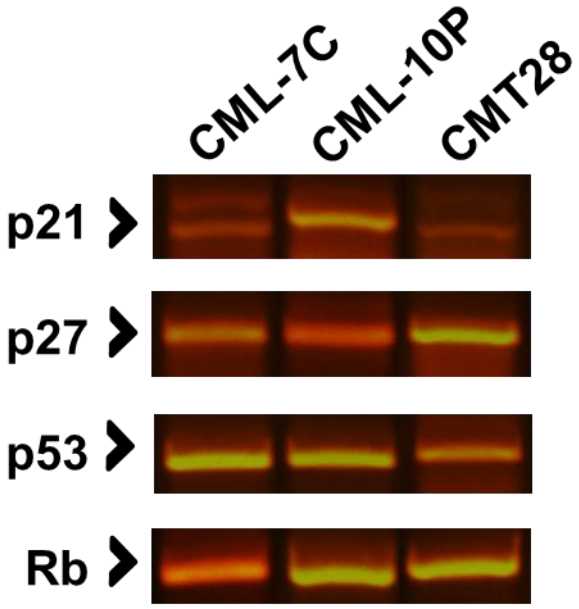

Fig. 15. Expression of p21/Cip1, p27/Kip1, p53 and Rb tumor suppressor genes in a panel of two representative CML cell lines CML-7C and CML-10P. Two CML cell lines were selected based on their INK4 expression pattern and defects. CMT28 was used to compare the gene expression with those in CML cell lines.

Because p16 and p14ARF function in two distinct anti-proliferative pathways regulating Rb and p53-p21, respectively, the expression of these critical tumor suppressor genes as well as the Cip-Kip genes including p21/Cip1 and p27/Kip1, were evaluated in CML cell lines and compared to those in the CMT28 model (Fig. 15). The p53, Rb and p27 tumor suppressor genes were normally expressed in these tumor cell lines as verified by sequencing each amplified transcript. p21 expression was moderately downregulated in CMT28 and one of the CML cell lines (CML-7C) but its sequence remained intact in contrast to the deletion mutation detected in p16 from these tumors. These expression profiles of the downstream regulatory members of p16 and p14ARF suggest that defects in

either p16 or Rb and p14ARF or p53 might be sufficient to circumvent the G1 checkpoint and cell cycle arrest thereby promoting cell proliferation in CMT and CML cells. This expression analysis further supports similar evidence from human cancers validating the non-overlapping regulatory functions of p16 and p14ARF in regulating the cell cycle (Bates et al., 1994; Okamoto et al., 1994; Otterson et al., 1994; Ruas and Peters, 1998; Sherr and Roberts, 1995).

Sequencing and Alignments of Amplified p16 Transcripts from CML-7C Reveal a Large Deletion Mutation in Exon 1α

Gene expression analysis identified p16 expression in only one of the CML cell lines (CML-7C). The amplicon was sequenced and the authenticity of the p16 sequence was confirmed by NCBI Blast analysis (http://blast.ncbi.nlm.nih.gov/Blast.cgi). The amplified sequence covering exon 1α and exon 2 of p16 obtained from the CML-7C cell line was aligned with several published p16 sequences from dog and other mammalian species. The alignment allowed identification of conserved ATG start codons, exon 1-2 boundary and highly conserved regions among all of the mammalian p16 sequences (Fig. 16). Strikingly, a large deletion of 69 bp was found in exon 1α of p16 from CML-7C, providing obvious evidence explaining the loss of p16 message in canine malignant melanoma. In addition, this deletion comprising a major portion of exon 1α critical for native folding and biological functions of p16 protein (Lutful Kabir et al., 2013) suggests that the mutant p16 mRNA from CML-7C is highly unlikely to be translated into functional protein. Like CMT28, the CML-7C model also expressed the p14ARF mRNA suggesting that these cell lines have a functional p14-p53 pathway while they are likely deficient in a functional p16-Rb pathway for cell growth suppression.

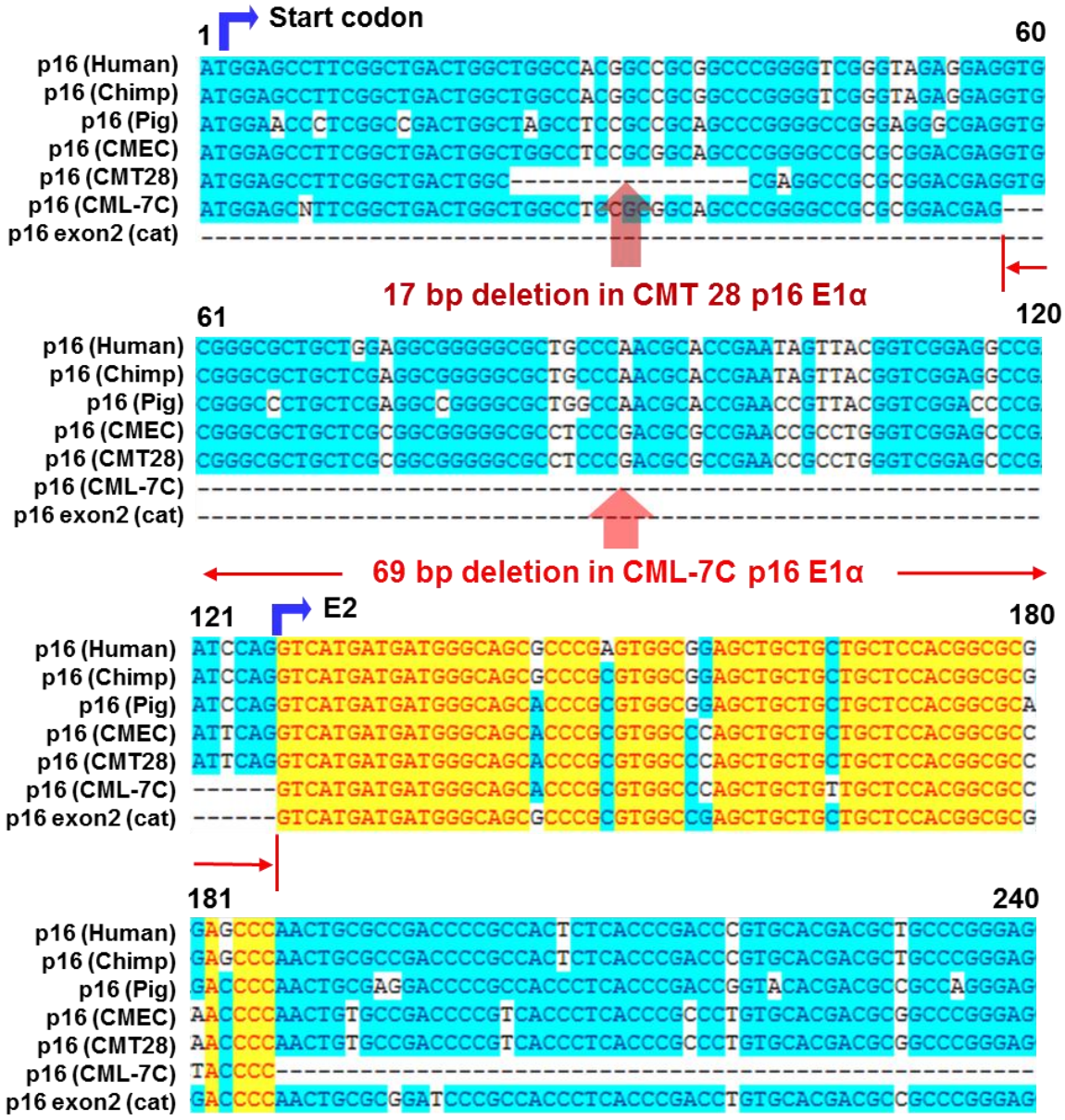

Fig. 16. Alignment of canine p16 sequences and other mammalian p16 sequences. Canine p16 amplicon sequences from NCF/CMEC (#JQ796919) and CMT28 (#JQ796920) were aligned and compared to published p16 sequences (human #L27211, chimpanzee #NM_001146290 and pig #AJ316067), p16 exon 2 sequence (Cat #AB010807). Alignments revealed a highly conserved ATG start codon at the beginning of the sequences, identical (bent arrow), and conserved (blue and yellow

shaded background) regions. The exon 1 and exon 2 (E2) boundary is indicated (bent arrows). A previously identified 17 bp deletion in CMT28 and a large 69 bp deletion in CML-7C p16 exon 1α are shown (large shaded arrows).

Human Breast Cancer Models Harbor Similar INK4A/ARF/INK4B Defects

In order to correlate the genetic defects in the INK4A/ARF/INK4B locus between canine and human cancers, three well-established human breast cancer cell lines, including MDA-MB-231, MCF7 and ZR-75, were investigated for INK4 gene expression. These cell lines represent three major subtypes of human breast cancer reflecting human breast cancer heterogeneity. Molecular classification of human breast carcinoma identified MDA-MB-231 as triple negative, i.e., negative for the three receptors including estrogen receptor alpha (ER1), progesterone receptor (PR) and human epidermal growth factor receptor 2 (HER2), MCF7 as luminal A or ER+, PR+/-, HER2- and ZR-75 as luminal B or ER+, PR+/- and HER2+ (Holliday and Speirs, 2011; Kao et al., 2009).

Prior to PCR assays, the integrity of total RNA extracted from each human breast cancer cell line was verified by formaldehyde denaturing gel electrophoresis. The clearly visible bands for 28S and 18S ribosomal RNAs (at an apparent ratio of approximately 2:1) were indicative of intact RNA (Fig. 17A). One or more of the p16, p14ARF and p15 genes were differentially expressed in all three breast cancer cell lines (Fig. 17B). The expression defects in the INK4A/ARF/INK4B locus in human breast cancer models highly correlate to those found in CMT cell lines suggesting the canine breast tumor cell lines are appropriate models of human disease in terms of aberrant regulation and defects in cancer associated gene loci.

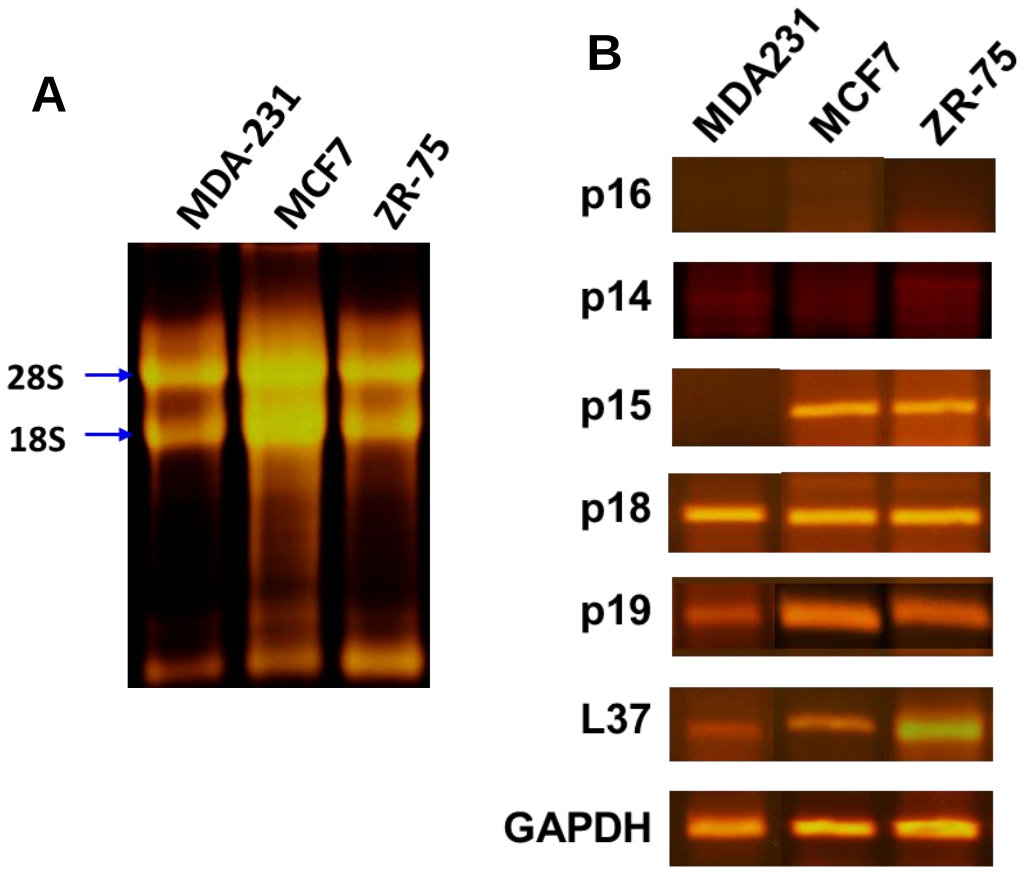

Fig. 17. INK4 expression profile in human breast cancer cell lines. (A) 1% formaldehyde denaturing gel electrophoresis for total RNA extracted from 3 human breast cancer cell lines MDA-MB-231, MCF7 and ZR-75. Two distinct ribosomal bands of 28S and 18S with relative molecular weight and brightness indicate the integrity of RNAs. (B) Evaluation of INK4 gene family expression in 3 human breast cancer cell lines. L37 and GAPDH were used as endogenous control transcripts.

Section 3. Discussion and Conclusions

Cancers in domestic dogs develop spontaneously and tumor growth occurs over long periods of time within a syngeneic host followed by recurrent incidence and metastasis to other parts of the body (Paoloni and Khanna, 2008). Canine cancer cell lines have been used as models to study the molecular pattern and regulatory mechanisms in corresponding human cancers. Although questions have been raised for using cancer cell lines as models of human cancers, they still remain powerful experimental tools for studying many features of cancers in humans and in some instances the findings have translated into clinical benefits (Gottardis et al., 1988; Osborne et al., 1985). A number of critical target genes and signaling pathways have been evaluated for comparative analysis, showing a significant overlap of human and canine genes that are deregulated in cancers, supporting the use of canine models for cancer research (Pinho et al., 2012). Determining the close similarities in terms of aberrant regulation in molecular signaling pathways and altered gene expression profiles in both canine and human cancers would further validate the use of canine cancer models for the study of human cancer biology.

Several established canine cancer cell lines including mammary tumors, melanomas and primary breast cancer cells as well as normal canine mammary epithelial cells or CMECs were investigated to characterize the defects in INK4 tumor suppressor genes and to determine how directly they compare to lesions found in human breast cancer. Although it was challenging to develop and culture merely normal CMECs, as they are highly differentiated and closely associated with other cell types in the surrounding breast microenvironment, we were able to sort the single mammary epithelial population from mammary fibroblasts using a high-speed cell sorting approach. To create a genetic

correlation based on gene expression profiles and defects between canine and human breast cancers, three highly characterized human cancer cell lines, including MDA-MB-231, MCF7 and ZR-75, were also used in this study. These cell lines have been well-defined based on their luminal-basal classification derived from their molecular expression profiles of luminal epithelial-specific genes or proto-oncogenes and hormone receptors. They represent subtype-specific breast cancer pathobiologies (Kao et. al., 2009). The established CMT cell lines, derived from a number of primary canine mammary carcinomas are currently in the process of a human breast cancer-like classification (DeInnocentes et. al., 2014 – unpublished data; also discussed in Chapter 1). Therefore, this comparative analysis of INK4 gene expression defects will better characterize the future characterization and stratification of CMTs.

All primary canine breast cancer cells and normal CMECs were processed and prepared during the primary culture for RNA extraction in order to maintain as faithfully as possible the gene expression pattern *in vivo*. The INK4 primers that were designed previously based on canine genome, were also applied for gene expression analysis in human breast cancer cell lines. But these primers did not specifically identify human INK4 genes because either forward or reverse primers for each INK4 gene (except p18) encoded a few base pair mismatches with respect to the human p16 mRNA sequence. This problem occurred where primers were designed based on the species of interest avoiding highly repeated GC-rich region of INK4 genes. For this reason, several unique primer sets were designed based on the human genome to investigate INK4 gene expression in human breast cancer cell lines (Table 2). All human breast cancer cell lines and primers were stored and used separately from canine cells and their primers.

The INK4 gene expression profile in primary canine breast cancer cells closely reflected expression profiles in CMT cell lines (previously reported in Lutful Kabir et. al., 2013; DeInnocentes et. al., 2009). Three INK4 members, p16, p14ARF and p15 were most frequently defective in both CMT cell lines and primary cancers providing strong evidence for the loss of the INK4A/ARF/INK4B locus in canine breast cancer. The p16 defects in primary canine mammary tumors were more frequently compared to p14ARF and p15. The p16 protein could not be detected in CMT cell lines (Agarwal et al., 2013) consistent with the predictions that the altered protein expression was due to the deletion mutation or frequent loss of the message in these cell lines (Lutful Kabir et al., 2013). Similar recurrent loss of p16, p14ARF and p15 expression was observed in the panel of human breast cancer cell lines suggesting that the INK4A/ARF/INK4B locus encoding p16, p14ARF and p15 is one of the major determinants of tumor suppressors in both canine and human breast cancers.

The gene expression profile in canine malignant melanoma cell lines demonstrated that p16, p14ARF and p15 were even more frequently defective compared to their loss of expression in CMT cell lines and primary tumors. Moreover, p16 from one of the CML cell lines CML7C, was found to harbor a large deletion of 69 bp coding region that nearly disrupted the entire exon 1α of p16. This recurrent loss of p16 in canine melanoma models also recapitulated the frequently deleted region in human chromosome 9 encoding the INK4A/ARF/INK4B locus thought to confer hereditary susceptibility to melanoma in humans (Hussussian et al., 1994; Kamb et al., 1994a; Ranade et al., 1995).

Interestingly, the remaining two INK4 members, p18 and p19 were normally expressed or, in some CML cell lines, their expression were detectably upregulated

compared to CMEC and normal canine fibroblasts (NCF) (Fig. 6, 13) suggesting a potential compensatory activities in cell cycle G1 checkpoint regulation, their precise tumor suppressive roles are yet to be investigated. However, this upregulated expression of p18 and p19 in canine cancer models are consistent with a previous report in which p18 and p19 survived with fewer mutations while expression of p16 and p15 were frequently lost by harboring many mutations in primary human tumors and tumor-derived cell lines (Zariwala and Xiong, 1996).

In conclusion, this study identified gene expression defects that could frequently be attributed to large deletion mutations in three INK4 genes encoded by the INK4A/ARF/INK4B locus in spontaneous canine cancer models and primary tumor biopsies. The defects and loss of function mutations in this locus are recurrent in different cancers from dog and strongly correlated to those found in human breast cancer cell lines and also melanomas that have been widely studied identifying INK4A/ARF/INK4B deletions in the orthologous region of human chromosome 9p21. This novel genetic interrelation in cancer regulatory mechanisms involving INK4 proteins between human and dog strongly supports the use of canine cancers as exceptional comparative intermediate models and contribute to the promising advances in the development of new therapeutics and treatments for these cancers.

Chapter 4: Comprehensive Expression Profiles and Regulation of miRNAs in Spontaneous Canine Mammary Tumor Models with INK4 Tumor Suppressor Defects

Section 1. Introduction

After the completion of human genome sequencing, the best estimates of protein coding genes accounted for 30,000 genes representing as low as 1% of the genome with the current prediction of 20,000 to 25,000 genes (Human Genome Project Information Archive, http://web.ornl.gov/sci/techresources/Human_Genome/project/info.shtml). A significant remaining fraction of the genome, however, is being transcribed into RNAs that do not encode proteins, which are classified as non-coding RNAs (Wright et al., 2001). The latest reference human genome annotation identified 57,820 genes and more than 50% of these genes were found to encode non-coding RNAs including small non-coding RNAs and microRNAs (miRNAs) (http://www.gencodegenes.org/) (Harrow et al., 2012). The advent of high-throughput technologies led to the discovery that miRNAs have added a new layer of controls to the traditional complex regulatory network composed of epigenetic regulation and post-translational modifications. Since their discovery in 1993 in *C. elegans* (Lee et al., 1993) and later in humans (Lagos-Quintana et al., 2001), the expression of miRNAs has been reported by numerous studies and shown to regulate diverse and vital cellular processes including cell cycle, cell proliferation, differentiation, development and apoptosis as well as disease pathogenesis (Ambros, 2003; Croce and Calin, 2005; Hatfield et al., 2005; Jovanovic and Hengartner, 2006; O'Donnell et al., 2005; Schickel et al., 2008;

Stefani and Slack, 2008). Experimental evidence and the latest miRNA target predictions suggest that more than 60% of protein-coding genes in the human genome are subjected to regulation by miRNAs, making them the most abundant single class of regulatory biomolecules (Bartel, 2004; Esteller, 2011; Fabian et al., 2010; Friedman et al., 2009; Kent and Mendell, 2006; Lewis et al., 2005). To date, 2578 mature miRNAs have been annotated in the human genome while mouse and canine genomes account for 1908 and 291 miRNAs, respectively (miRBase Release 20, June 2013).

miRNAs are evolutionarily conserved, endogenous small structural RNA molecules of 20-22 nucleotides that post-transcriptionally suppress gene expression in a sequence specific manner (Lagos-Quintana et al., 2001). The miRNA genes are assembled as mono- or polycystronic transcriptional units in the genome located mostly in intergenic and intronic regions encoding ~95% of miRNAs and in exonic regions encoding ~5% of miRNAs (Hsu et al., 2006). As discussed in Chapter 1, the biogenesis and effector functions of miRNAs involve complex sequential processing of long primary miRNA transcripts by the RNase III enzyme Drosha and Dicer miRNA processing complexes. The resulting functional strand of the mature miRNA is loaded together with Argonaut family (Ago2) protein into an RNA-induced silencing complex (RISC), where it guides RISC to target mRNAs 3′untranslated regions (3'-UTR) through translational repression or their degradation (Bartel, 2004; Carthew, 2006; Du and Zamore, 2005). The mRNA cleavage or translational repression functions by miRNAs are primarily determined by the degree of complementarity between the miRNA and its target mRNA. The miRNA will promote the cleavage of the target message if its seed region is sufficiently complementary to the target sequences (Hutvagner and Zamore, 2002; Zeng et al., 2002). An increasing body of

experimental data and online-based bioinformatics prediction tools underscore this property of miRNA-target binding by the 2-7 nucleotide seed region of the 5'-end of mature miRNAs. Since this short complementary site is highly conserved across mammals, thousands of genes appear to be under the regulation of miRNAs which in fact represents more than 5300 genes that are potential miRNA targets (Lewis et al., 2005).

There is an inherent relationship between miRNAs and cancer, because more than 50% of miRNA genes are located at cancer associated genomic regions or fragile sites that are also preferential sites for translocation, deletion, amplification, and integration of exogenous genome fragments (Calin et al., 2004a; Garzon et al., 2009). It is widely accepted that miRNAs can act as dual regulators in cancer mechanisms by either promoting or suppressing malignant processes resembling mechanisms of classical oncogenes or tumor suppressors. For this reason, some miRNAs are often regarded as onco-miRs that are involved in dominant gain of function, cancer regulatory mechanisms and therefore this group has been categorized as tumor oncogenes (Esquela-Kerscher and Slack, 2006). Whereas, a contrasting group of cancer-associated miRNAs are termed anti-onco-miRs and they act as tumor suppressors. This group of miRNAs (anti-onco-miRs) can target mRNAs encoding proteins that promote tumor initiation and progression while oncomiRs target mRNAs coding for tumor suppressors (Esquela-Kerscher and Slack, 2006). Overexpression of these oncogenic miRNAs causes down-regulation of target tumor suppressors which contributes to malignant transformation (Rovira et al., 2010). miR-155 and let-7 are the two miRNAs first characterized that were identified experimentally to act as an onco-miR and anti-onco-miR, respectively, and reported to be expressed in a number of human malignancies including lymphomas and leukemias, as well as breast, colon and

lung cancers (Iorio et al., 2005; Johnson et al., 2005; Kluiver et al., 2005; Metzler et al., 2004; Volinia et al., 2006; Yanaihara et al., 2006).

Since miRNAs are encoded by highly conserved naturally occurring genes across mammalian species, evaluation of their expression profiles in cancer models would greatly advance our understanding of regulatory mechanisms involving many critical cancer associated genes. Development of high-throughput approaches have greatly facilitated the investigation of cancer pathway-specific expression of hundreds of miRNAs. Besides, miRNA profiling studies have also further classified human cancers, such as leukemias, based on the developmental lineage and differentiation state of tumors and identified gene expression patterns that correlated with distinct mechanisms of cellular transformation (Lu et al., 2005). Global miRNA expression profiles of cancer versus normal cells may provide the characteristic regulatory features of up- and down-regulated miRNAs that can be correlated to altered expression of tumor-associated genes. For genome-wide miRNA profiling different array-based high-throughput analysis including miRNA microarrays, serial analysis of gene expression or quantitative PCR arrays for miRNAs have been employed in many cancer studies (Calin et al., 2004a; Cummins et al., 2006; Nelson et al., 2004; Schmittgen et al., 2004).

An increasing number of studies have characterized the comprehensive miRNA expression profiles in human solid and blood-related cancers. But little has been accomplished in non-human cancer models and therefore, miRNA expression and deregulation profiles and regulatory mechanisms in animal cancer models remain largely unknown. Studies with canine breast cancer models have shown a strong genetic correlation with their human counterparts particularly in terms of altered gene expression

profiles and frequent loss of INK4 cell cycle regulatory genes in breast cancers (Chapters 2 and 3). In this study, the comprehensive expression profile of the 277 most abundantly expressed and highly characterized miRNAs from the canine genome have been evaluated in canine mammary tumor (CMT) models. Importantly, groups of miRNAs or miRNA families have been identified as potential regulators for INK4 tumor suppressor genes in CMT cells providing an additional regulatory mechanism for their altered expression induced by post-transcriptional silencing. miR-141, identified as one of the critical members of the altered miRNA panel, was primarily predicted to target p16/INK4A mRNA in CMT cell lines. The miR-141 binding to the 3'-UTR target sequence, which is common to p16/INK4A and p14ARF mRNAs, has been validated by functional 3'-UTR reporter assay. These deregulated miRNAs could be predicted to target critical biomarker genes and other cell cycle regulators that have been investigated and found to be defective in CMT cells. Additionally, altered regulation of miRNAs in CMT models are highly conserved in their relationship with orthologous miRNA expression profiles in human breast cancer.

Section 2. Methods and Materials

Extraction of small RNAs including miRNAs from CMTs and CMECs

Small RNAs including miRNAs were extracted from three selected CMT cell lines, including CMT12, CMT27, and CMT28, and normal canine mammary epithelial cells (CMECs) according to the manufacturer's instructions (QIAGEN, miRNeasy Mini-extraction Method). CMT cells grown in culture and counted (3×10^6 to 1×10^7 cells) were used for miRNA extraction. Briefly, cells were properly homogenized in phenol-guanidine lysis reagent. After addition of chloroform, the homogenate was separated into aqueous and organic phases by centrifugation. RNA was separated to the upper, aqueous phase, while DNA partitioned to the interphase and proteins to the lower, organic phase or the interphase. The upper, aqueous phase was extracted, and ethanol was added to provide appropriate binding conditions for all RNA molecules from 18 nucleotides (nt) upwards. The sample was then applied to a mini-spin column where the total RNA including all mRNAs and ribosomal RNAs bound to the silica membrane and phenol and other contaminants were efficiently washed away. At this stage high quality RNA was eluted in RNase-free deionized water.

To promote enrichment of miRNAs and other small RNAs (less than ~200 nt) in a separate fraction, the upper aqueous phase from the previous step was transferred to a new reaction tube. The separated aqueous phase was mixed with 1 volume of 70% ethanol in mini-spin column and centrifuged to collect the flow-through. At this step, all small RNAs, including miRNAs, were separated in the eluted volume while the larger RNAs (>200 nt long) were retained on the mini-spin column. The flow-through containing the miRNAs

was then washed several times by ethanol and purification buffers and eluted in RNase-free water.

Formaldehyde Denaturing gel electrophoresis for small RNAs

Denaturing 2% agarose gels were prepared for analysis of small RNAs including miRNAs extracted from CMEC and CMT cells. Total RNA extracted from CMT cell lines was also analyzed on denaturing gels for comparison. The gel composition and preparation followed the previously described protocol (Chapter 3).

qPCR Array Plate Layout

miRNA qPCR array was organized in a 96-well plate format. For dog-specific miRNA expression profiles, 4 X 96-well plates were used to analyze all 277 canine miRNAs and controls. Each plate template was designed for mature miRNA specific assays and several control assays (Fig. 18). This plate format is suitable for analysis on a Bio-Rad CFX96 qPCR instrument.

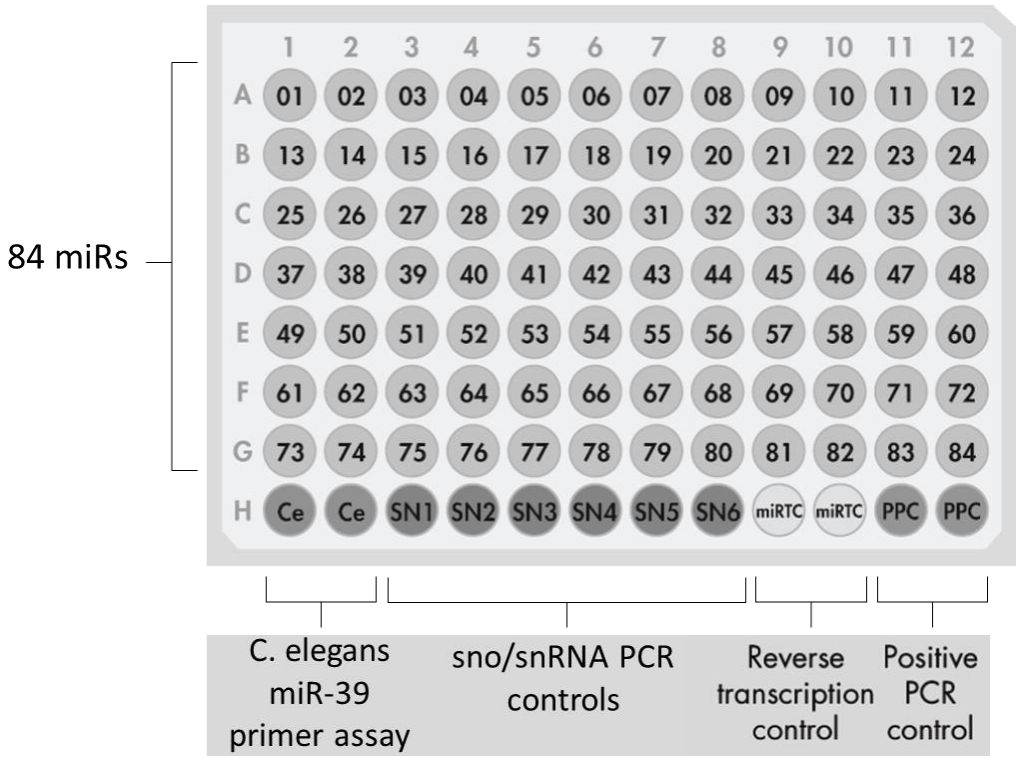

Fig. 18. miRNA PCR array plate layout. Each plate contained 84 mature miRNA specific forward primer assays in wells A1 to G12 (except plate-4 that contained the remaining 25 miRNAs of that total). The last row of each plate (wells H1 to H12) contained a panel of endogenous controls including small nucleolar or small nuclear RNAs (snoRNAs/snRNAs) as indicated by SN1-SN6, positive PCR control (PPC), miRNA reverse transcription control (miRTC) and *C. elegans* miR-39 (Ce) primer assay as negative controls.

miRNA qPCR Array Controls

As shown in Fig. 18, the last row of each miRNA PCR array plate contained all control assays. For accurate and reproducible results in miRNA quantification by using qPCR arrays, it is necessary to normalize the amount of target miRNA by using suitable

endogenous reference RNAs – an approach known as relative quantification. For data normalization using the ΔΔCT method of relative quantification, 6 snoRNA/snRNA primer assays were arrayed in each qPCR plate (wells H3 to H8). These primers were designed to quantify a panel of 5 snoRNAs (SNORD61, SNORD68, SNORD72, SNORD95, and SNORD96A) and the snRNA RNU6B (RNU6-2) as indicated by SN1-SN6, respectively, in the plate. These endogenous controls or reference genes are highly conserved in human, mouse, rat, and dog and have been validated to have relatively stable expression levels across tissues and cell types.

The miRNA reverse transcription control (miRTC) is an assay that assesses the performance of a reverse transcription reaction by detecting template (cDNA) synthesized from the kit's built-in control RNA. This control monitors for any variables that may inhibit the reverse transcription reaction. The positive PCR control (PPC) wells contain a pre-dispensed artificial DNA sequence and the assay that detects it. This control monitors for any variables that may inhibit the PCR reaction. If the RNA sample is of high quality, the cycling program is correctly run and the thresholds are correctly defined, the value of $Ct^{\mathbf{PPC}}$ should be 19 ± 2 (discussed below in detail).

To provide an alternative data normalization method, *C. elegans* miR-39 (ce-miR-39) primer assay can be employed particularly for serum and plasma samples. A mimic for cel-miR-39 can be added to the samples to control for variations during the preparation of total RNA and subsequent steps. After purification, qPCR detection of the *C. elegans* miRNA mimic can be performed and results can then be used for data normalization of endogenous miRNAs in each sample.

Reverse Transcription of miRNAs and small RNAs isolated from CMTs and CMECs

The first step of the qPCR array protocol begins with the reverse transcription (RT) of miRNAs. Approximately 100-200 ng miRNA isolated from cells was used as starting material. If total RNA was used as starting material, the recommended RNA input would be 500 ng or higher depending on cell type and optimization of the assay. The RT step was performed according to manufacturer's instructions (QIAGEN, miScript miRNA PCR Array). Briefly, 4 µl 5X HiSpec buffer, 2 µl 10X nucleics mix, 2 µl reverse transcriptase mix, RNase-free water ~11.5 µl (adjusted depending on RNA concentration) and template miRNA were added to make a 20 µl reaction and gently mixed on ice. Reactions were incubated for 60 min at 37ºC and finally for 5 min at 95ºC to inactivate reverse transcriptase. The cDNA synthesized by RT was diluted by adding 90 µl RNase-free water.

qPCR array for miRNA Expression Profile

miRNA qPCR arrays were performed according to the manufacturer's instruction (SABiosciences, QIAGEN). First, reverse transcription reactions were performed in a special RT buffer mix that allowed selective conversion of mature miRNAs and certain small nucleolar RNAs (snoRNAs) and small nuclear RNAs (snRNAs) to cDNA and locked long RNAs in a conformation that rendered small RNAs to be selectively reverse transcribed. Mature miRNAs were polyadenylated by poly(A) polymerase and reverse transcribed into cDNA using oligo-dT primers. The oligo-dT primer (~65 nt) contains a 3' degenerate anchor and a universal tag sequence on the 5' end where the reverse primer binds promoting amplification of mature miRNAs in the qPCR step (Fig. 19).

cDNA was prepared in a reverse transcription reaction to serve as the template for qPCR analysis using the miRNA PCR arrays containing miRNA-specific forward primers arrayed in the plate (for whole miRNome/entire miRNA panels), universal primer (reverse primer) and SYBR Green PCR master mix. These PCR arrays were designed in 96-well plate formats (4 X 96-well plate) containing 277 canine miRNAs to be profiled. The assays were optimized based on sample RNA input and the detection system and each assay was validated using the QC report to determine reverse transcription efficiency and positive PCR control values passed or were within the correct range calculated for all samples analyzed.

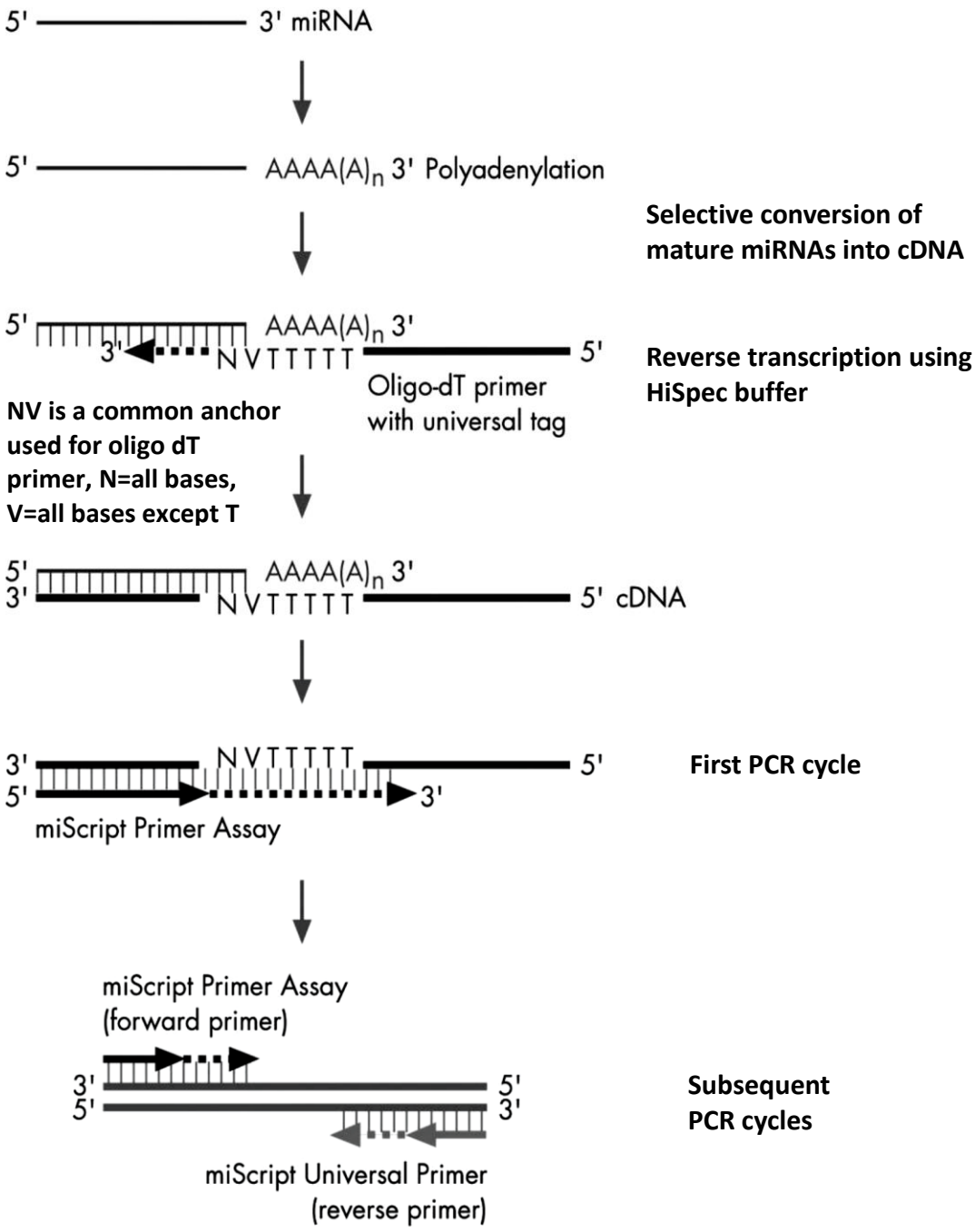

Fig. 19. Amplification of mature miRNAs in qPCR arrays. In a reverse transcription reaction using a special buffer, mature miRNAs and small RNAs are selectively polyadenylated by poly(A) polymerase and subsequently converted into cDNA by

reverse transcriptase with oligo-dT priming. The cDNA was then used as template for qPCR profiling of mature miRNA expression using the miRNA PCR array and the universal primer (adopted from the QIAGEN miScript miRNA PCR Array).

Reaction mix for a 96-well plate was prepared by adding 1375 µl 2X SYBR Green master mix, 275 µl 10X universal primer, 1075 µl RNase-free water and 25 µl template cDNA (previously diluted). Before addition to the reaction wells, the reaction mix was transferred to a loading reservoir. Using a multichannel pipettor, the array plate was loaded with 25 µl reaction mix per well. The plate was sealed with optical strips and centrifuged for 1 min at 1000x g at room temperature to remove bubbles. Cycling conditions for the qPCR array were initial activation of hotstart taq DNA polymerase at 95ºC for 15 min; 40 cycles of 3 step PCR amplification including denaturation at 94ºC for 15 sec, annealing at 55ºC for 30 sec and extension at 70ºC for 30 sec (fluorescence data was collected at this step in each cycle).

Data Analysis

There are two data analysis portals for the analysis of qPCR data. A web-based miRNA PCR Array data analysis tool (http://pcrdataanalysis.sabiosciences.com/mirna/arrayanalysis.php) was normally used to analyze the qPCR data from different samples with a number of replicates (2 to 4 for each sample). Once raw threshold cycle (Ct) data had been uploaded, the analysis tool automatically performed all fold-change calculations using the ΔΔCT method of relative quantification, and presented the results in several formats. A non-web based analysis could also be performed by using a downloadable Excel file containing the qPCR array data analysis template. Before the Ct value calculation, the baseline threshold was defined in the qPCR program. The baseline level was determined

based on assay noise levels in the early cycles, where there was no detectable increase in fluorescence due to specific PCR amplification products. Linear view of the amplification plot was used to determine the earliest visible amplification. The baseline was set from cycle 2 to 2 cycles before the earliest visible amplification which was never beyond cycle 15.

Following PCR amplification, Ct values of the positive PCR control wells (PPC) were examined. If the RNA sample was of high quality, the cycling program was correctly run, and the thresholds were correctly defined, the value of Ct^{PPC} should be 19 ± 2. Ct values of the reverse transcription control (miRTC) were also examined using the values for the positive PCR control (PPC) by calculating $\Delta Ct = AVG\ Ct^{miRTC} – AVG\ Ct^{PPC}$ -1.1 (correction factor). This calculation is particularly important for the quality control (QC) report of each array plate. If this value was less than 7, then no inhibition of the reverse-transcription reaction was apparent meaning RT efficiency passed the quality control specifications. If this value was greater than 7, there was evidence of impurities that may have inhibited the reverse transcription reaction and therefore RT efficiency. All CT values reported as greater than 35 or as N/A (not detected) were changed to 35 to allow calculation.

Calculation of fold-change in expression can be defined by the ΔΔCT method for relative quantification and described in the following diagram.

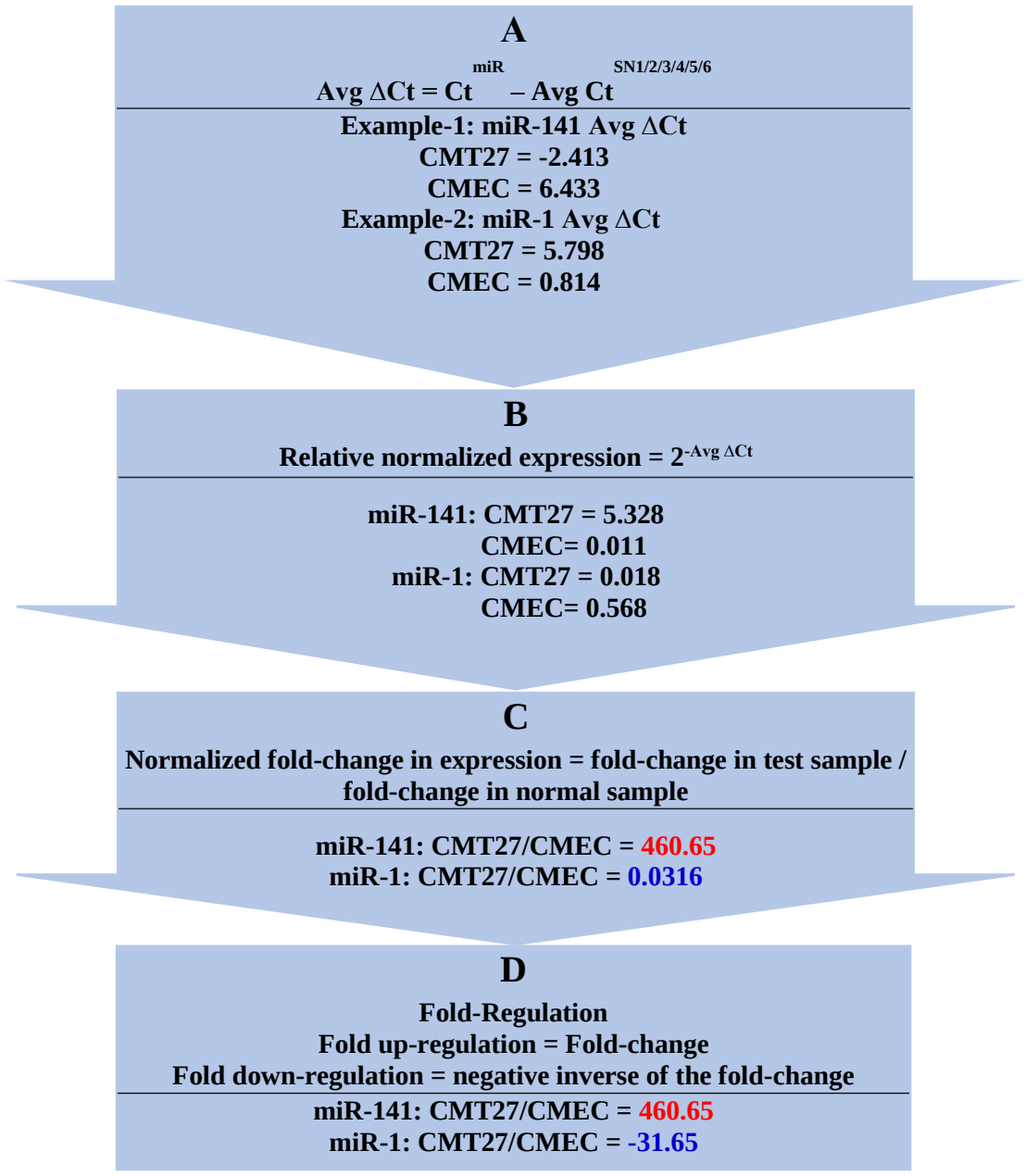

Fig. 20. Calculation of fold-change in expression. Representative examples of two miRNAs (miR-141 and miR-1) from miRNA qPCR arrays showing calculated values

of Avg ΔCt and fold-change or normalized fold-change in expression. Steps A, B, C and D in the diagram are indicated by corresponding successive steps in calculation of the fold-change which were performed using the data analysis tool (or formulated Excel sheet). The value in red indicates fold up-regulation which is equal to fold-change and in blue indicates down-regulation which is the negative inverse of the fold-change. Ct $^{SN1/2/3/4/5/6}$ = Average Ct of six Sno/SnRNAs (reference genes) used in the assay.

An important feature of miRNA qPCR array data analysis is called 'fold regulation'. Fold-regulation represents fold-change results in a biologically meaningful way. Fold-change values greater than one indicate a positive- or an up-regulation, and the fold-regulation is equal to the fold-change. Fold-change values less than one indicate a negative or down-regulation, and the fold-regulation is the negative inverse of the fold-change (indicated by Step C in Fig. 20). Fold-change and fold-regulation values greater than 2 are indicated in red; fold-change values less than 0.5 and fold-regulation values less than -2 are indicated in blue (Fig. 20). These threshold values have been arbitrarily defined by the data analysis tool. Many qPCR and microarray studies commonly adopted a >2-fold cut-off in the interpretation of differentially expressed genes when compared between control and tested samples (Dalman et al., 2012; LaConti et al., 2011; Shivapurkar et al., 2014; Song et al., 2014). Importantly, if the 2-fold cut-off is considered as the change in expression and biologically relevant it should reflect the experimental value from qPCR that corresponds to PCR cycle difference. In other words, experimentally it is a rule of a 1 cycle difference as a meaningful difference in qPCR in which there will be a 2-fold increase in the number of copies with each cycle (http://www.bio-

rad.com/webroot/web/pdf/lsr/literature/Bulletin_5279.pdf). Moreover, this convention is followed when the efficiency of the assay has been correctly determined during quality control and the reproducibility of Ct values has also been attained in replicate assays (Ahmed et al., 2008).

High Resolution Agarose Gel Electrophoresis

High resolution agarose has an intermediate melting temperature (75ºC) with twice the resolution capabilities of other agarose products, and can separate DNA fragments of 20-800 bp. High resolution agarose gels (4%) were prepared according to the manufacturer's instructions (MetaPhor agarose). Agarose powder was slowly added to a beaker containing 1X TBE buffer and a stir bar. The beaker was 2-4 times the volume of the gel. The agarose in the buffer was rapidly stirred at room temperature for 15 min before heating to reduce the tendency of the agarose solutions to foam during heating. The beaker was covered using a plastic wrap with a small hole for ventilation and heated in a microwave oven on medium power for 2 min. The beaker was removed from the microwave and gently swirled to resuspend any settled powder and gel pieces. The resulting solution was then reheated on high power until it boiled and was thoroughly mixed and cooled to 50-60ºC in a water bath prior to casting. The gel was incubated at 4ºC for 20 min (after casting) to obtain optimal resolution. The amplified miRNA products from qPCR arrays were run in 4% (w/v agarose) gels. The bands for each amplicons indicated the recovery of each miRNA amplification in CMT cells as well as their relative quantitation (Fig. 21).

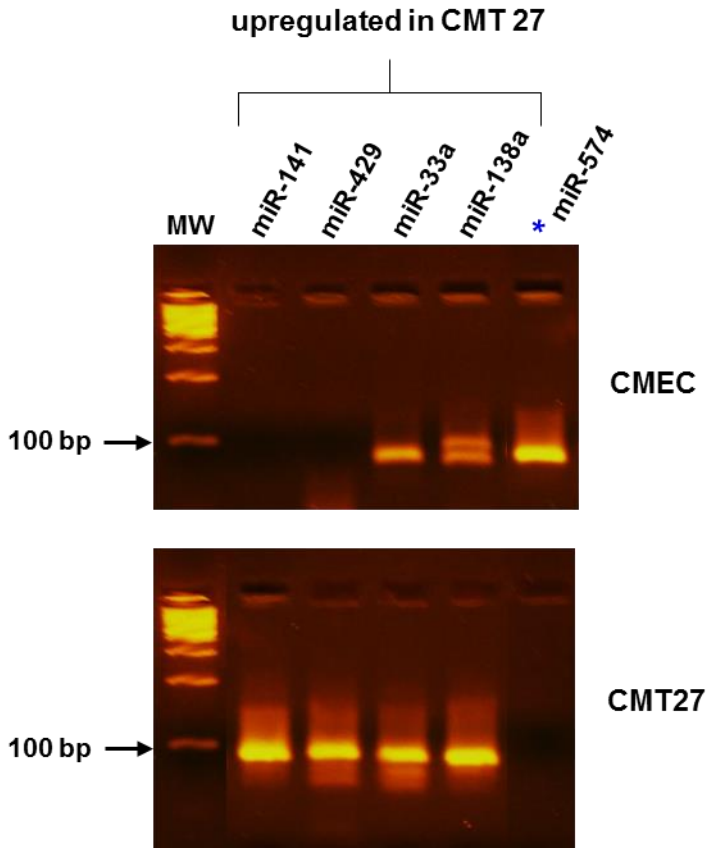

Fig. 21. 4% high resolution agarose gel electrophoresis of selected miRNA qPCR array products showing relative banding patterns. miR-141 and miR-429 were highly overexpressed in CMT27 cells by 460 and 1733 fold, respectively, compared to CMEC resulting in quantitative bands in CMT27 but not in CMEC. Similarly, miR-33a and miR-138 were overexpressed by 3 and 58 fold, respectively, as bands were amplified in both cell lines. In contrast, down-regulation of miR-574 (asterisk) in CMT27 cells (by ~5 fold) resulted in no detectable band in CMT27 but a clear amplification product was detectable in normal CMECs.

Prediction of miRNA Targets

TargetScan (Release 6.2) tool was used to search for predicted canine miRNA targets. TargetScan is the only available miRNA target prediction tool that retrieves predicted regulatory targets of miRNAs for a wide variety of mammals including human, chimpanzee, rhesus, cow, dog, mouse, rat, and opossum as well as for bird (chicken), amphibian (frog), fish (zebrafish), worm (C. elegans) and fly (D. melanogaster) (www.targetscan.org). Predicted miRNA targets were identified based on multiple algorithms that essentially searched for the presence of conserved 8mer (an exact match to positions 2-8 of the mature miRNA followed by an 'A') or 7mer (an exact match to positions 2-7 of the mature miRNA followed by an 'A') sites at the 3'-UTR sequence that match the seed region (position 2 to 7) of each miRNA (Lewis, et. al., 2005). This online prediction tool considers matches to annotated human orthologs as defined by UCSC whole genome alignments (http://genome.ucsc.edu/index.html).

For mammalian genome, predictions are ranked based on the predicted efficacy of targeting as calculated using the 'context score' of the sites. The context score for a specific site is the sum of the contribution of six features including, (1) site-type contribution, (2) 3' pairing contribution, (3) local AU (A and U bases flanking the target site) contribution, (4) position contribution, (5) target site abundance contribution and (6) seed-pairing stability contribution (Garcia et al., 2011; Grimson et al., 2007). These additional determinants beyond seed match help specify miRNA target sites (Grimson et al., 2007) as illustrated by two representative miRNAs (miR-145 and miR-214) evaluated in this study (Table 3). The site-type contribution reflects the average contribution of each site type while the 3' pairing contribution reflects consequential miRNA-target complementarity

outside the seed region (Grimson et al., 2007). The local AU content indicates the transcript AU content within 30 nucleotides upstream and downstream of predicted site. The position contribution reflects the distance to the nearest end of the annotated 3'-UTR of the target gene. In all these four features, a more negative score is associated with a more favorable site (Grimson et al., 2007). The target site abundance contribution to context score reflects the abundance of target sites of a miRNA family in the set of distinct 3' UTRs and a more negative score is associated with a lower abundance of the miRNA target site in the set of 3' UTRs (Garcia et al., 2011). Finally, the seed-pairing stability contribution (SPS) to context score implies the stability of a miRNA-target duplex, which is a function of the concentration of A and U bases in the seed region and a more negative score is associated with weaker seed-pairing stability (Garcia et al., 2011).

Table 3: Prediction of miRNA targets by using TargetScan (Part A)

mRNAs that target CDK6	predicted consequential pairing of target region (top) and miRNA (bottom)	seed match
Position 2354-2361 of CDK6 3' UTR cfa-miR-145	5' ...AAUGCAGCUGUUCUAAACUGGAA... 3' UCCCUAAGGACCCUU-UUGACCUG	8mer
Position 9723-9729 of CDK6 3' UTR cfa-miR-145	5' ...CACAAAUCCUUUGGAAACUGGAU... 3' UCCCUAAGGACCCUUUUGACCUG	7mer-m8
Position 282-288 of CDK6 3' UTR cfa-miR-214	5' ...CCAGAAGAAGAGAAGCUGCUGAC... 3' UGACGGACAGACACGGACGACA	7mer-1A
Position 6230-6236 of CDK6 3' UTR cfa-miR-214	5' ...CCGAGGUCCCCGUGCCCUGCUGC... 3' UGACGGACAGACACGGACGACA	7mer-m8

miRNA Seed Sequence

Table 3: Prediction of miRNA targets by using TargetScan (Part B)

mRNAs that target CDK6	site-type contri-bution	3' pairing contri-bution	local AU contri-bution	position contri-bution	TA contribution	SPS contribution	context+ score
Position 2354-2361 of CDK6 3' UTR cfa-miR-145	-0.247	-0.018	-0.068	0.265	0.014	-0.003	-0.06
Position 9723-9729 of CDK6 3' UTR cfa-miR-145	-0.120	-0.025	-0.019	-0.013	0.008	0.002	-0.17
Position 282-288 of CDK6 3' UTR cfa-miR-214	-0.074	0.015	0.000	-0.019	0.031	-0.047	-0.09
Position 6230-6236 of CDK6 3' UTR cfa-miR-214	-0.120	-0.007	0.095	0.151	0.031	-0.064	> -0.02

In Table 3, two representative miRNAs (miRNA-145 and miR-214) were selected to be analyzed for target prediction. They were predicted to bind different conserved 3'-UTR target sites of CDK6 mRNA. Each target sites were identified based on miRNA seed sequence match (either 8mer or 7mer as shown in Part A of Table 3) and were further assessed by a set of algorithms (Part B of Table 3). 8mer = an exact match to positions 2-8 of the mature miRNA followed by an 'A'; 7mer-m8 = an exact match to positions 2-8 of the mature miRNA (the seed + position 8); 7mer-1A = an exact match to positions 2-7 of the mature miRNA (the seed) followed by an 'A'.

3'-UTR amplification and sequencing

Total RNA was extracted from CMT cell lines and CMECs according to previously described methods (Chapter 2). The canine p16 3'-UTR sequence, including exons 2 and 3 derived from CMEC, was aligned with p16 sequences from other mammals. Primers (forward: 5' TTCCTGGACACGCTGGTGGTGCTGC 3', and reverse: 5' ATACAAATGGAAATTT AAGGGAAAGGGAAGGC 3') were designed using Vector

NTI primer design software. The canine p16 3'-UTR sequence was amplified by touch-down (TD) RT-PCR (Chapter 2). The TD-PCR protocol was RT (48ºC, 45 min), denaturation (94ºC, 2 min), and 10 cycles of denaturation (94ºC, 1 min), annealing 1 min (primer annealing temperature plus 10ºC decreasing 1ºC/cycle) and elongation (68ºC, 1 min) followed by 25 cycles of PCR amplification (Chapter 2). The TD-annealing temperature range for p16 3'-UTR was 67-77ºC. PCR products were analyzed semi-quantitatively on 2% agarose electrophoresis gels and gel-purified amplicons were analyzed and authenticated by DNA sequencing (Chapter 2 and 3).

Custom Constructs of Canine CDKN2A 3'-UTR and miRNA 3'-UTR Reporter Assay

miRNA 3'-UTR target clones were used for miRNA target identification and functional validation of predicted targets or to study the regulatory effect of miRNAs on target genes. Canine p16/CDKN2A 3'-UTR reporter clone constructs were designed and customized for miRNA 3'-UTR reporter assays. The canine p16/CDKN2A 3'-UTR sequence (441 bp including part of exon 2 and exon 3) was inserted downstream of the secreted *firefly* luciferase (fluc) reporter gene in the pEZX-MT01 vector system (GeneCopoeia Inc. Rockville, MD), with transcription driven by the SV40 promoter for expression in mammalian cells (Fig. 22). A chimeric mRNA was transcribed encoding the fluc protein and a 3' UTR target sequence. Besides using fluc as the miRNA 3' UTR target reporter, the *renilla* reporter driven by a CMV promoter, was also cloned into the same vector (pEZX-MT01) to serve as an internal control. The dual-reporter vector system enabled transfection-normalization for accurate cross-sample comparison. The cfa-miR-141 precursor clone was generated in another vector (pEZX-MR01, GeneCopoeia Inc. Rockville, MD) in order to exogenously synthesize mature miR-141 in transfected cells

(see Appendix 2 for detail information of each vector). All three CMT cell lines (CMT12, 27 and 28) and normal CMEC were co-transfected with either cfa-miR-141 precursor clone (pEZX-MR01-miR-141) or miRNA scrambled control clone (pEZX-MR01-Scramble) together with the CDKN2A 3'-UTR miRNA target clone (pEZX-MT01-3'UTR-CDKN2A) or miRNA target control (pEZX-MT01-Control that does not encode CDKN2A 3'-UTR). Both *firefly* luciferase and *renilla* luciferase activities expressed in the CDKN2A 3'-UTR miRNA target clone were measured to assess miRNA-dependent luciferase in this assay. *Renilla* luciferase activity was used to normalize the firefly luciferase signal in the same CMT cell line.

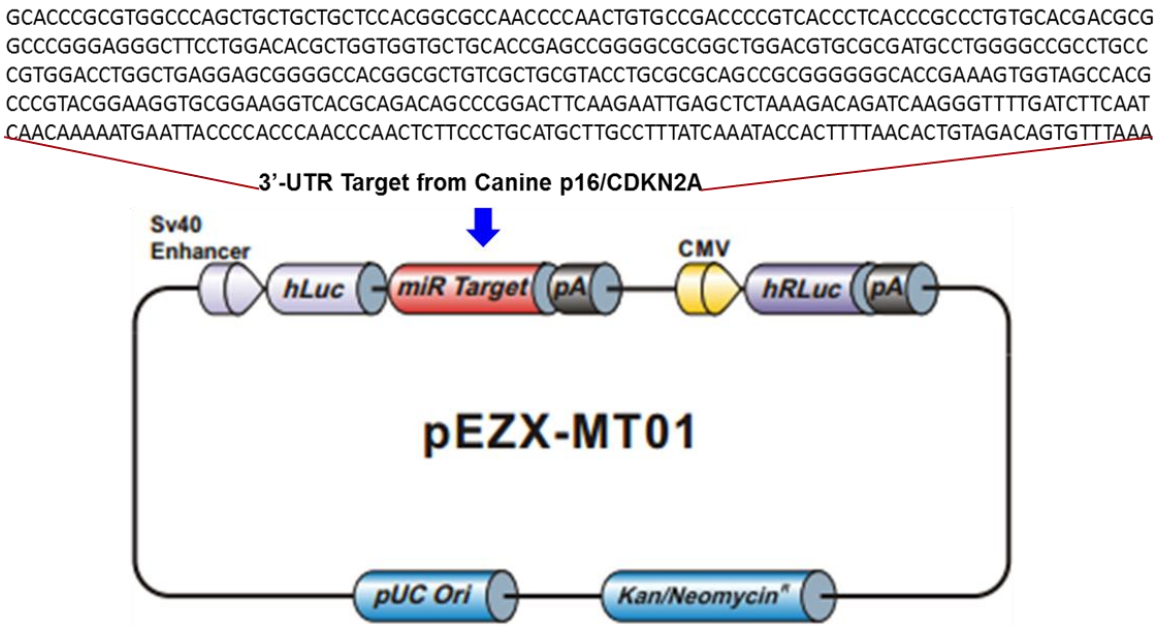

Fig. 22. Vector backbone of the miRNA 3'-UTR target clone. The vector encodes dual reporter genes. Expression of *firefly* luciferase is under SV40 and *renilla* luciferase is under control of the CMV promoter. The canine p16/CDKN2A 3'-UTR sequence was

inserted downstream from the firefly luciferase reporter gene as indicated (miR Target).

Normal CMEC and CMT Cells were grown in 24-well plates for 18-24 hours. Cells were ≥80% confluent prior to transfection. Cells were plated at a density of 1.5 - 6 x 10^4 cells/well. On the second day, cells were co-transfected with 0.1 μg of CDKN2A 3'-UTR miRNA target clone expression vector (or target control vector) and 0.2 μg of miR-141 precursor clone expression vector (or miRNA scramble control vector). These cloning vectors were prepared by incubating with 20-25 μl serum-free Minimum Essential Medium (MEM, Sigma Aldrich) and 1.0-1.5 μl transfection reagent (TransIT-LT1, Mirus Bio, Madison, WI) for 15-30 minutes at room temperature before adding to the cells. Cells were then transferred to 96-well plates (24-48 hours post-transfection) at a proportional concentration depending on the surface area of 96-well plate compared to 24-well plate (0.3 – 1.2 x 10^4 cells/well) and incubated for 24 hours. The *firefly* and *renilla* luciferase activities were measured in all transfected cells according to manufacturer instructions (GeneCopoeia Inc. Rockville, MD). Briefly, two working substrate solutions (Solution I and II) were prepared at 1:200 dilution immediately before adding to plate. The cell growth medium was removed from each well in the 96-well plate. For measuring the *firefly* activity, 100 μl working Solution I was added to each well and incubated for 10 minutes. The plate was read in a luminometer. For determining the *renilla* luminescence, 100 μl working Solution II was added to each well (already containing working Solution I) and the plate was read again after another 10 minutes.

Section 3. Results

Comprehensive Expression Profile of the 277 miRNAs from the Canine Genome

Comprehensive expression profile of miRNAs from canine genome was evaluated in CMTs by miRNA qPCR arrays. Three CMT cell lines (CMT12, CMT27 and CMT28) were used to profile the 277 best characterized and most abundantly expressed mature miRNAs from the canine genome (miRBase Release 16, www.mirbase.org). Each of these cell lines has been previously investigated for INK4 tumor suppressors that were differentially expressed and frequently deleted in these cell lines (Lutful Kabir et al., 2013). First, small RNAs including miRNAs were isolated from CMECs and CMT cells. The integrity of small RNA populations was validated by performing denaturing gel electrophoresis (Fig. 23).

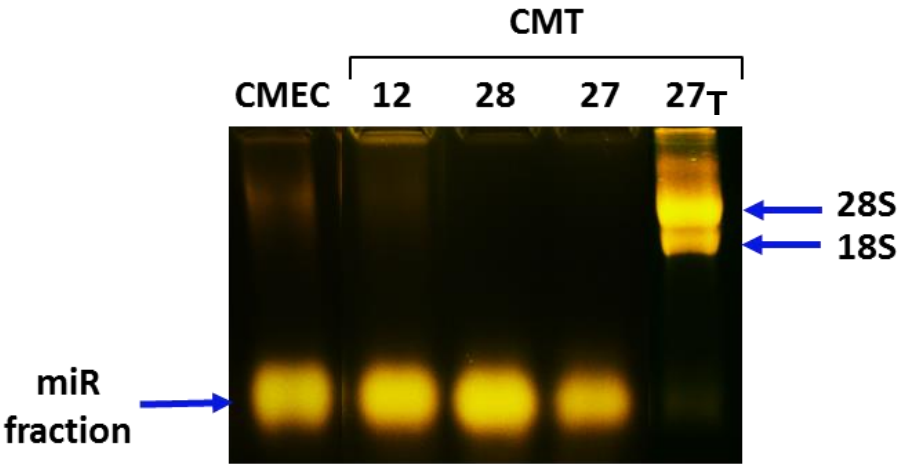

Fig. 23. 2% formaldehyde denaturing gel electrophoresis for miRNAs. Small RNA enriched RNA fraction including miRNAs isolated from CMEC and CMT (12, 28 and 27) cell lines was verified by formaldehyde denaturing gel electrophoresis. For comparison, total RNA from the CMT27 cell line (27T) was run in the same gel

showing distinct ribosomal RNA bands, characteristic of intact RNAs. miRNA bands were observed at the bottom of the gel because of their low molecular weight.

The miRNA qPCR arrays for the dog miRNome (defined by the full spectrum of miRNA content expressed in a specific genome) were performed to profile the expression of the 277 mature miRNA sequences in the CMT cell lines. A complete list of these miRNAs from the CanFam genome assembly has been provided (Appendix 3). Among this population of miRNAs, ~80% (220 out of 277) were deregulated in the CMT cell lines compared to normal CMEC and the expression of ~20% (57 out of 277) of the miRNAs remained nearly unchanged or was not detected in both CMEC and CMT cells (Fig. 24). In this study, the majority of the miRNAs whose expression was determined to be altered in the CMT cell lines could be divided into three groups including, up-/down-regulated, up-regulated and down-regulated miRNAs, in order to specify the biological importance of altered miRNAs from each group in regulating critical genes in canine breast cancer models. The up-/down-regulated group comprises a large number of miRNAs (151 out of 277) in which each miRNA was up- and/or down-regulated differentially in CMT cell lines rather than only up- or only down-regulated in all three CMT cell lines. A second group of miRNAs (45 out of 277) were up-regulated in all three CMT cell lines showing that each of these miRNAs was positively regulated (>2 fold change in expression) in all CMT cell lines suggesting that they may have an important contribution in cancer progression. A third category was the down-regulated miRNAs (24 out of 277) in which each miRNA was negatively regulated (<2 fold change in expression) in all three CMT cell lines (Fig. 24). These altered miRNAs were further investigated for their potential roles in targeting INK4

tumor suppressors and other genes expression defects, which have been evaluated in CMT models.

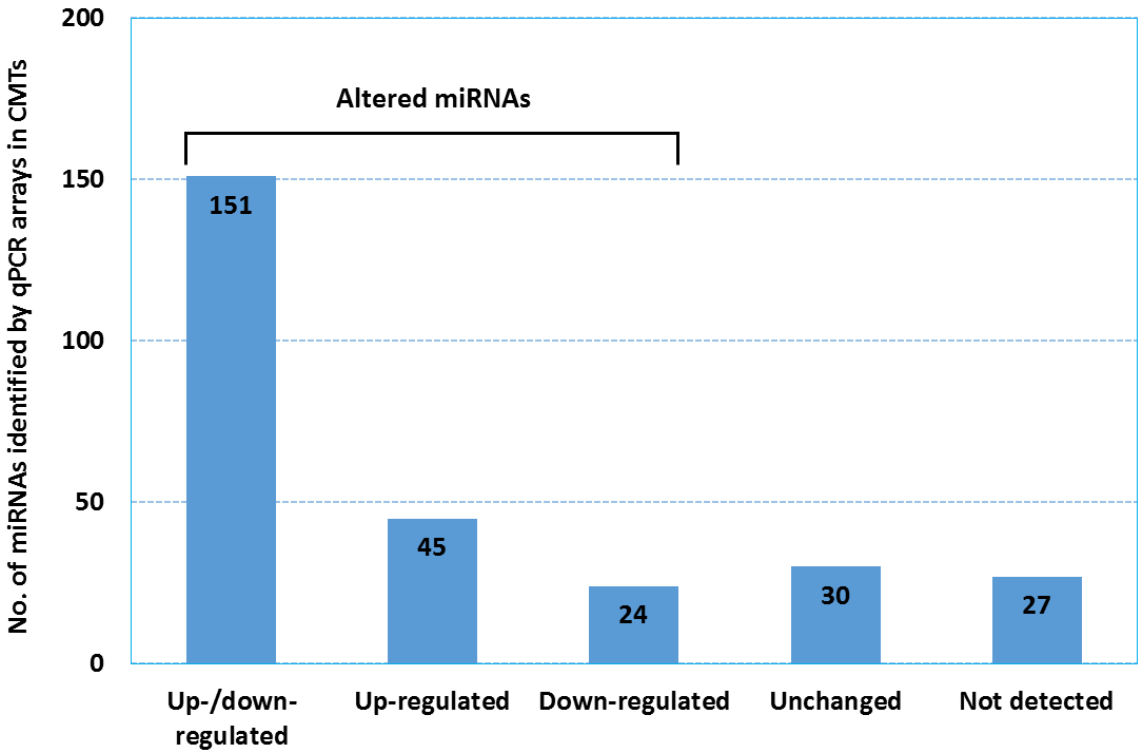

Fig. 24. Comprehensive expression profile of the dog miRNome. miRNAs identified by qPCR arrays were divided into altered and unchanged or not detected groups. A complete list of these altered and unchanged miRNAs with their quantitative fold-regulation values has been provided in the Appendix 4. 'Up-/down-regulated' = expression of each miRNA was up- and/or down-regulated differentially in CMT cells rather than only up- or only down-regulated in all three CMT cell lines; 'up-regulated' = expression of each miRNA was up-regulated (by >2 fold change) in all three CMT cell lines; 'down-regulated' = expression of each miRNA was down-regulated (by <2 fold change) in all three CMT cell lines; 'unchanged' = expression of each miRNA was not changed in normal CMEC and CMT cell lines; 'not detected'

= expression was undetectable or miRNAs were not found to be expressed in both CMEC and CMT cells.

Fold-change in expression of miRNAs in CMT Cells

Calculation of relative fold-change in miRNA expression was determined using the ΔΔCT method of relative quantification (described in the Methods and Materials). The fold-difference in expression from the array data was determined following two layers of normalization, one performed using the reference genes and another by comparing levels in normal cells. The results from miRNA expression profile in terms of fold-change or fold-regulation can be represented by graphical analyses. In heat maps, the fold-change values are calculated as log2 transformed values that could be represented by a color intensity scale (Fig. 25).

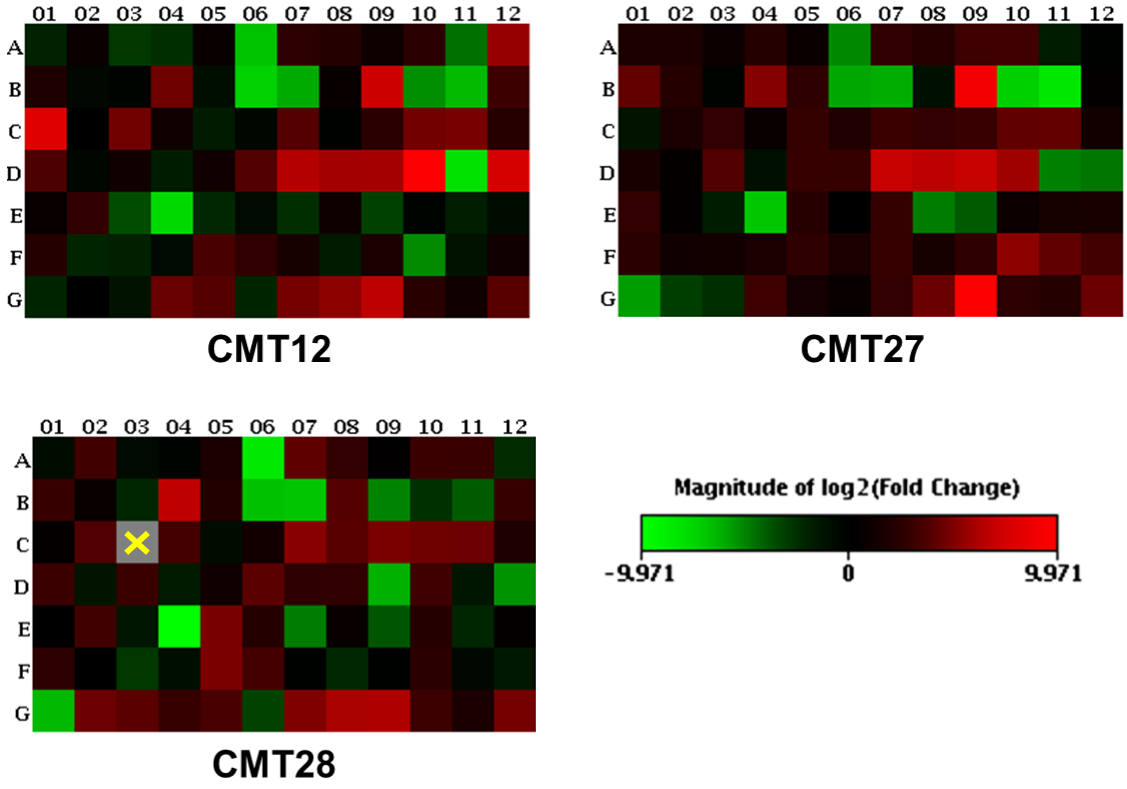

Fig. 25. Heat map visualization of log2 (fold-change) level of expression of miRNAs in CMT cell lines. Fold-change in expression of miRNAs is indicated by color-coded cells in the heat map array. The more red the cell the higher the fold-change in expression of the particular miRNA. Conversely, the brighter green the cell the lower the fold-change in expression and is regarded as down-regulated. The dark black cells (comparable to the middle region in the log2 scale) were close to or equal to '0' indicating very small or no change in expression. Cells in the heat map corresponding to miRNAs with erroneous fold-change, that is whose average threshold cycle is either not determined or greater than the defined cut-off value (35), are colored grey (indicated by 'X'). Plate 1 (out of 4) from each CMT cell line is shown as

representative heat maps. (See Appendix 5 for complete heat maps from each CMT cell line).

As described in the Materials and Methods, a 2-fold change threshold has been defined by the data analysis program and it is an arbitrary cut-off commonly practiced in the data analysis of microarrays and qPCR assays. There is a critical issue in the data analysis of differentially expressed genes using a defined fold-change threshold and also statistical cut-off (p-values <0.05) which may significantly alter the biological interpretation of fold-change (Dalman et al., 2012). For example, in the current miRNA qPCR arrays, a number of miRNAs were identified as differentially expressed by more than 10 to 100 fold-change but with a p-value >0.05 (Appendix 8), although the calculated relative normalized gene expression from three replicate experiments clearly differed between CMEC and CMT cell lines. Striking experimental evidence was the functional validation (target-binding) of miR-141 which was identified as differentially expressed in CMT cell lines by >100 fold-change but with a p-value >0.05 (described below). In addition, when the relative normalized gene expression of miRNAs, whose fold-change values fall between <2 to 1 is plotted, they demonstrate comparable expression profiles with either nearly similar values or very close to baseline values in both CMEC and CMT cell lines (Fig. 26). For this reason, it may be biologically relevant to graphically represent the data applying only a defined fold-change threshold (>2-fold) and also to identify a separate group of miRNAs with higher fold-change values (>10-fold) indicating their potential regulatory functions in CMT cells (described below in further analysis).

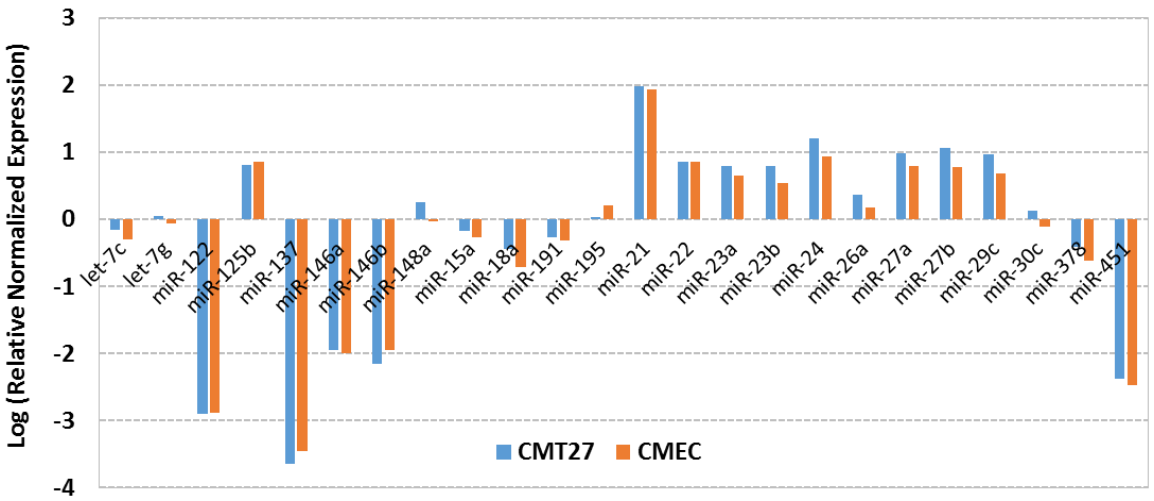

Fig. 26. Comparison of relative normalized expression [$\log_{10}$(fold-change)] of individual miRNAs between CMEC and CMT27 cells. Relative normalized expression of a group of representative miRNAs whose fold-change expression was determined qPCR arrays to be close to 1 and less than 2, was calculated and plotted for CMEC and CMT27 cells. Similar comparative expression analysis was performed for CMEC and CMT12/CMT28 (Appendix 6).

An important graphical representation of fold-change in expression is the scatter plot that compares expression level **($2^{-\Delta Ct}$)** of each gene in the test sample (CMT cells) versus the control sample (CMEC) (Fig. 27). The scatter plot represents miRNA expression in CMT cells in a biologically significant way by defining relative expression in terms of either more than 2 fold up-regulation or down-regulation compared to normal CMEC. The scatter plot from each cell line distinguishes the three altered groups of miRNAs as shown in Fig. 24. For example, miR-203, miR-9, miR-429 or miR-200a/b were highly up-regulated in all three CMT cell lines (Fig. 27, marked by triangles and in red) whereas miR-1, miR-133a/b/c or miR-214 were prominently down-regulated in all CMT cell lines (Fig.

27, indicated by blue arrows). miR-141 and miR-200c were shown to be differentially expressed in these cells as they were highly up-regulated in CMT12 and CMT27 cell lines but were identified as down-regulated in the CMT28 cell line. The miRNAs that are plotted in between the boundaries of 2 fold change (black circles in between the two diagonal boundary lines) indicate small or no change in expression (Fig.27).

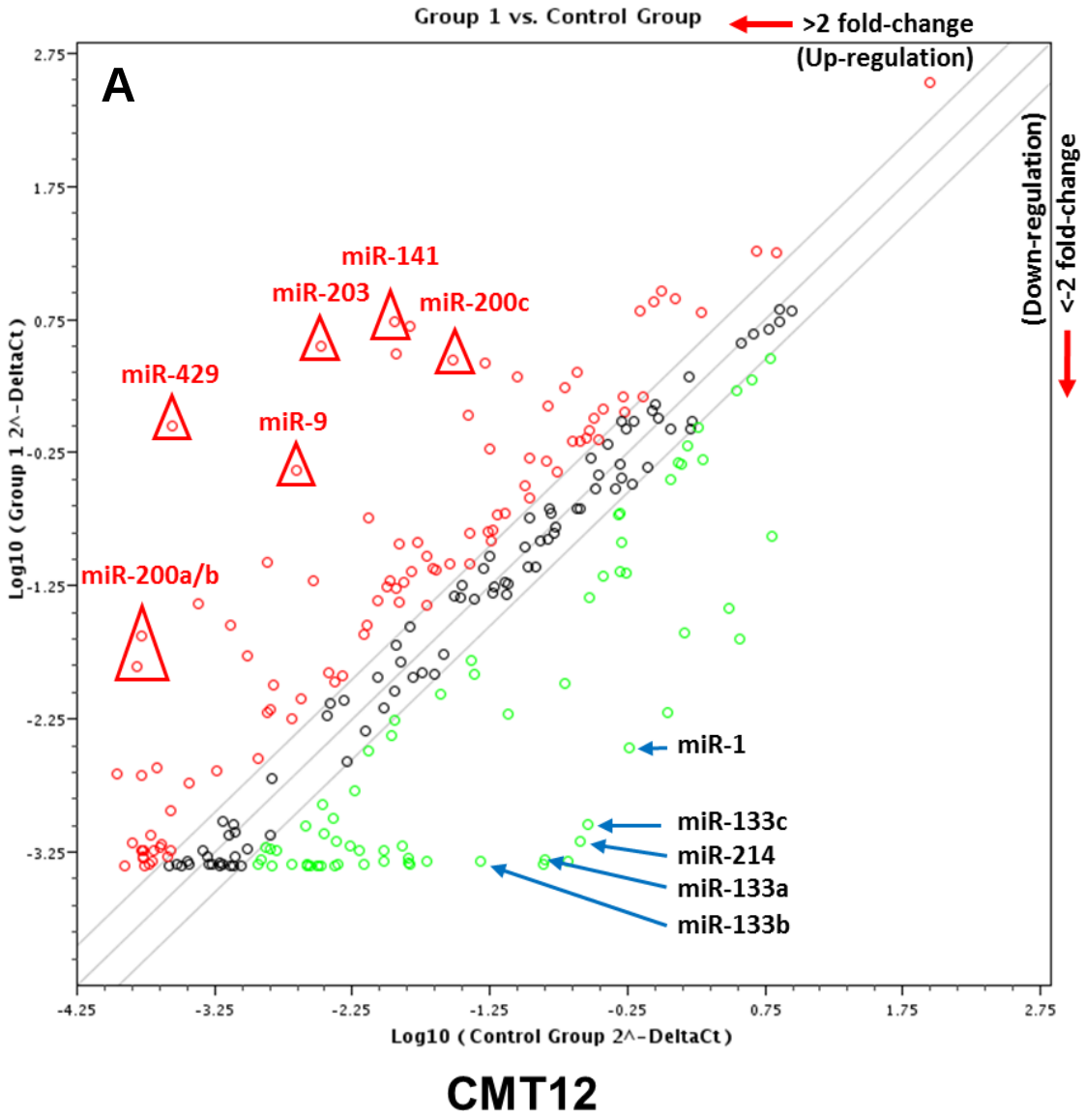

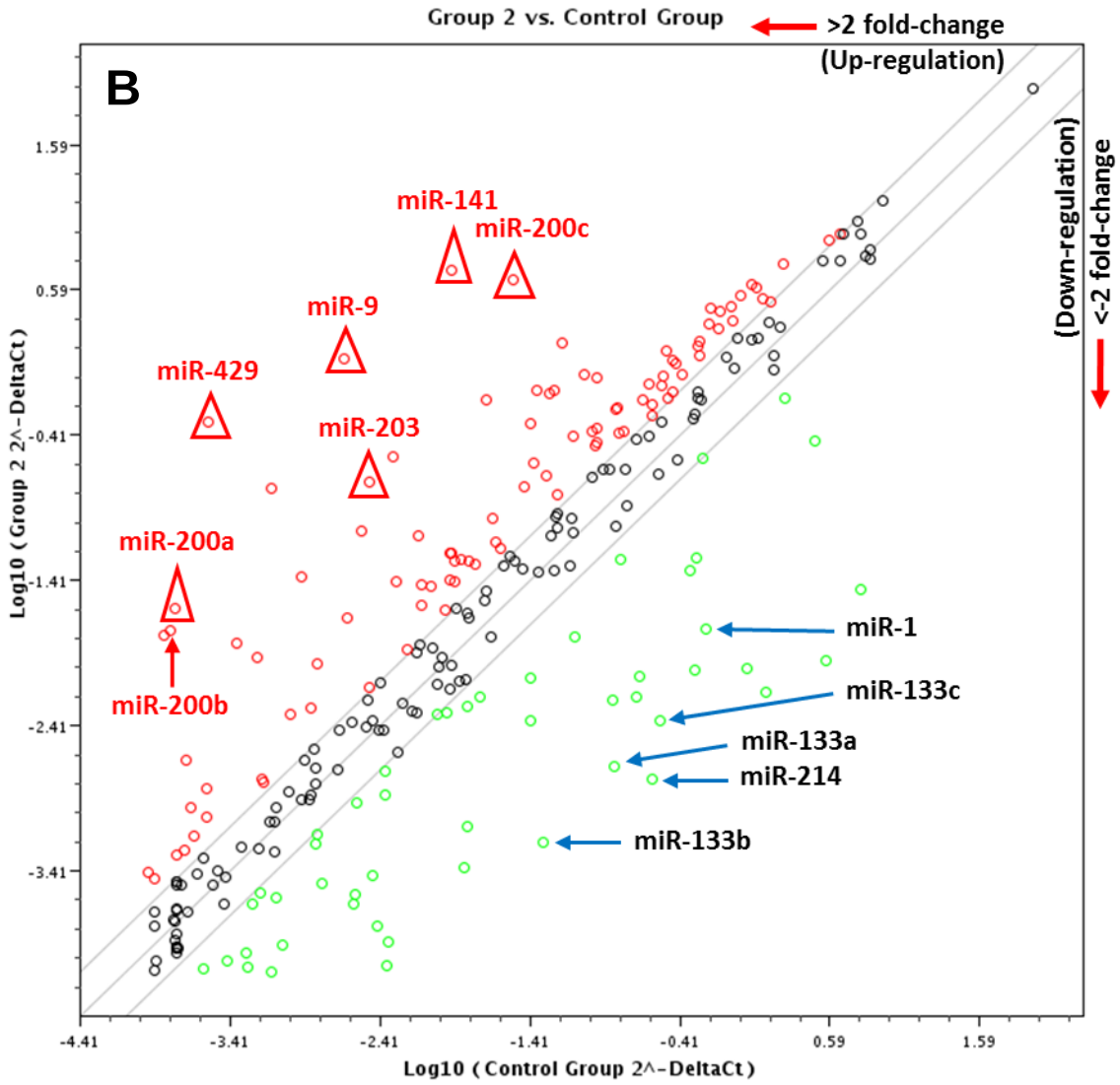
Group 2 vs. Control Group
>2 fold-change
(Up-regulation)
B
(Down-regulation)
<-2 fold-change
miR-141
miR-200c
miR-9
miR-429
miR-203
miR-200a
miR-200b
miR-1
miR-133c
miR-133a
miR-214
miR-133b
Log10 (Group 2 2^-DeltaCt)
Log10 (Control Group 2^-DeltaCt)
1.59
0.59
-0.41
-1.41
-2.41
-3.41
-4.41
-3.41
-2.41
-1.41
-0.41
0.59
1.59

CMT27

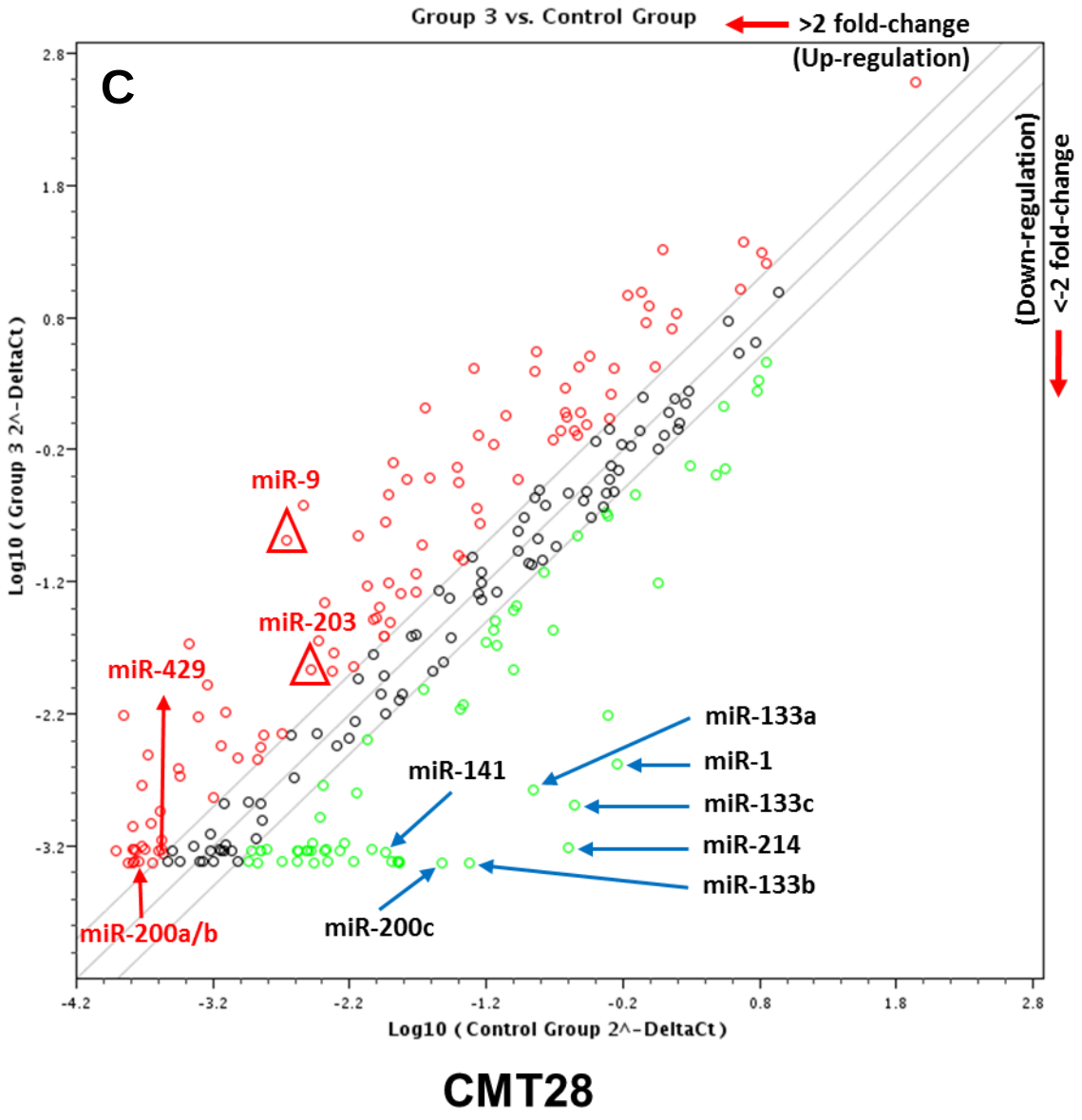

Fig. 27. Scatter plots of CMT vs CMEC log ($2^{-\Delta Ct}$) showing fold-change in miRNA expression. The diagonal line in the center indicates a fold change value ($2^{-\Delta\Delta Ct}$) of 1 or no change in expression. The two diagonal boundary lines drawn above and below the center line indicate the desired fold-change in gene expression threshold (as defined by 2). Each circle is plotted by a given coordinates (x,y) in which point along X-axis denoted by log ($2^{-\Delta Ct}$) or relative normalized expression of a miRNA in CMEC

and point along Y-axis obtained from log ($2^{-\Delta Ct}$) or relative normalized expression of a miRNA in a respective CMT cell line. Therefore, each circle indicates a miRNA's fold-regulation. All miRNAs indicated by red circles are up-regulated and those by green circles are down-regulated in CMT cell lines. The miRNAs that fall in between the two diagonal boundary lines (above and below the middle line respectively) are nearly unchanged in expression (fold-change is 1 or close to 1 and less than 2) and are designated by black circles. Several common and highly up-regulated miRNAs are indicated by either red triangles or red arrows whereas downregulated miRNAs are indicated by blue arrows. Fig. A, B, and C indicate the individual scatter plot for CMT12, CMT27, and CMT28, respectively.

The expression of miRNAs in CMT cells can also be represented by 3D-profiles that graph the fold difference in expression of each gene between the two samples in the 96-well format of the PCR Array. The major difference between fold-change representation by scatter plots and 3D profiles is that scatter plots depict log transformation plot of expression level whereas 3D profiles graph fold-difference in expression using direct values calculated from $2^{-\Delta\Delta Ct}$ for each miRNA**.** In a representative 3D profile for CMT27, a group of miRNAs were identified as highly up- or highly down-regulated in all three CMT cell lines (Fig. 28 and Appendix 7). Many of these deregulated miRNAs were analyzed for targeting sequence (3'-UTR) in critical tumor suppressor or oncogenes and shown to have sequence similarities sufficient to allow regulation (see below). An important feature of this 3D profile is that there is no defined threshold fold-change and any miRNA with a value >1 indicates up-regulation and <1 means down-regulation. Although it shows global fold-regulation of miRNA expression, a number of miRNAs with

fold change less than 2 or very close to 1 may be insignificant biologically as their relative normalized expression are very similar (Fig. 26).

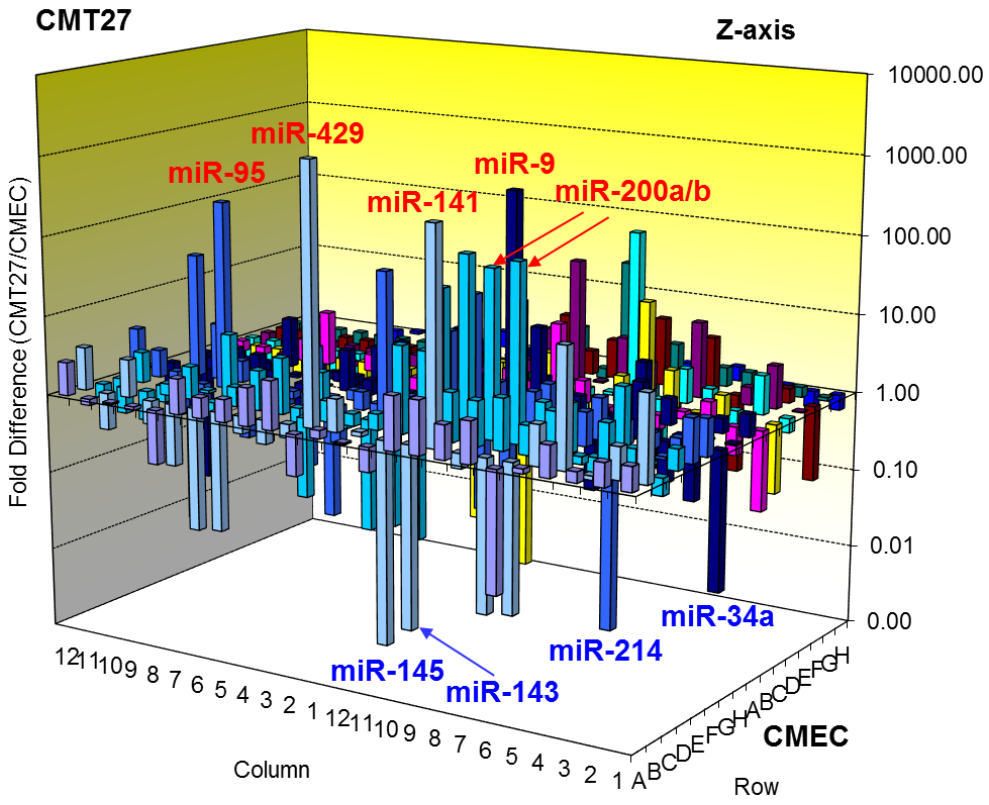

Fig. 28. Representative 3D profile showing fold difference in expression of miRNAs in CMT27 cell line. Columns in the 3D profile pointing up (with z-axis values > 1) indicate an up-regulation of gene expression, and columns pointing down (with z-axis values < 1) indicate a down-regulation of gene expression in CMT27 relative to CMEC. The miRNAs indicated in red text (for columns pointing up) are highly up-regulated and in blue text (for columns pointing down) are highly down-regulated in all 3 CMT cell lines except miR-141 which is up-regulated in CMT12 and CMT27 but down-regulated in CMT28.

Identification of Experimentally Validated Altered miRNAs in CMTs

The three altered miRNA expression profiles described (Fig. 24, up-/down-regulated miRNAs in CMT cell lines, only up-regulated and only down-regulated miRNAs in all three CMT cell lines) were further refined from the comprehensive expression profile. These new groups were devoid of any technical error emanating from qPCR array analysis narrowing down the numbers of miRNAs which were up-regulated (40 out of 45) and down-regulated (22 out of 24) in all three CMT models (Fig. 29A-B). qPCR array quantitation may generate errors when a miRNA's average threshold cycle is either not determined or greater than the defined cut-off (default 35 cycles), in both CMT and normal CMECs meaning that its expression was undetected, making this fold-change result erroneous and un-interpretable. Therefore, up- or down-regulation of miRNAs in all three CMT cell lines were screened for such technical precision. Another group of differentially expressed miRNAs (25 out of 151 up-/down-regulated miRNAs) were taken into consideration from all three CMT cell lines as their fold regulation range was from 10 to several hundred suggesting that they may have important regulatory functions in cancer development (Fig. 29C). However, the rest of the differentially expressed miRNAs were also analyzed to predict potential miRNA targets.

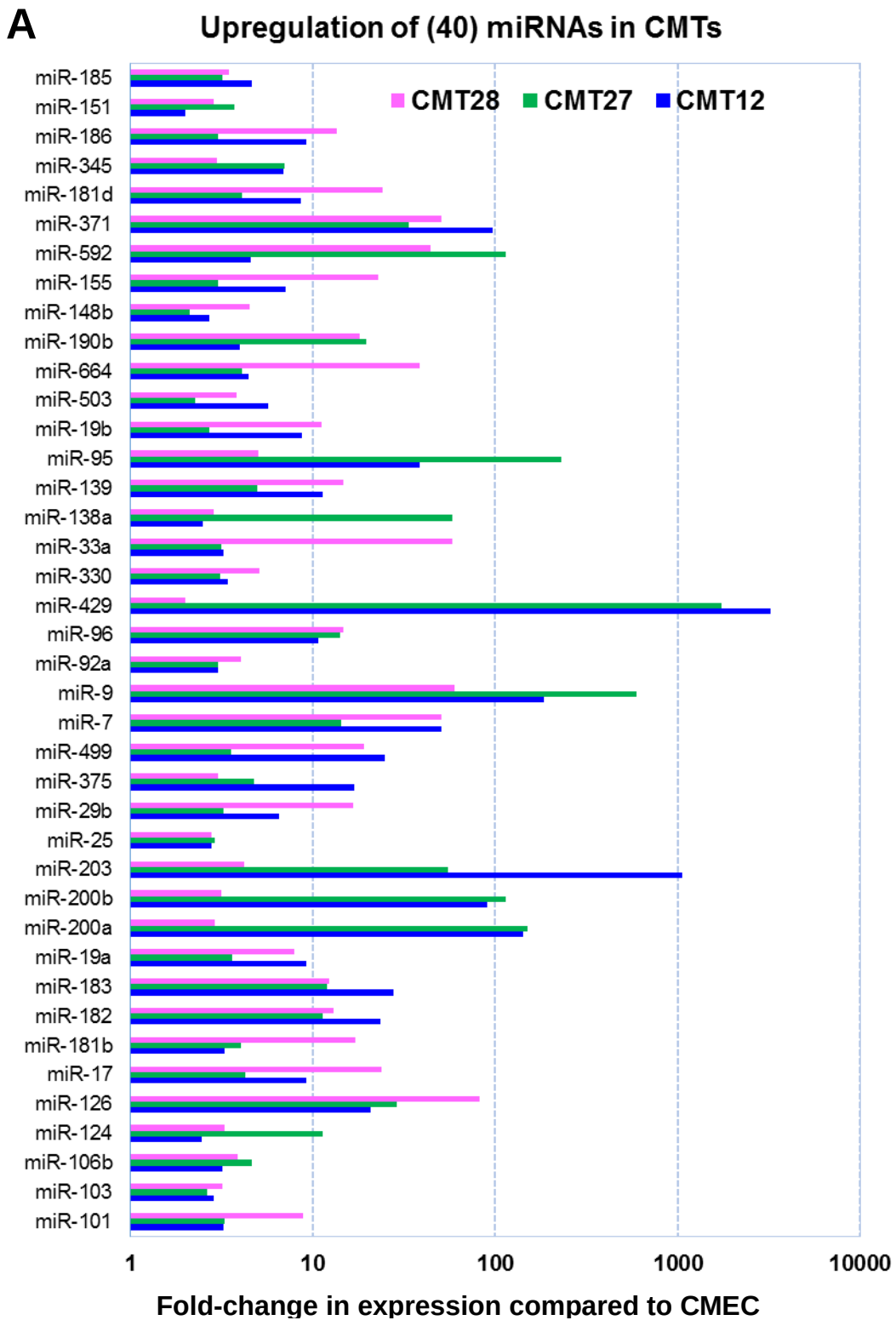
A
Upregulation of (40) miRNAs in CMTs
CMT28
CMT27
CMT12
miR-185
miR-151
miR-186
miR-345
miR-181d
miR-371
miR-592
miR-155
miR-148b
miR-190b
miR-664
miR-503
miR-19b
miR-95
miR-139
miR-138a
miR-33a
miR-330
miR-429
miR-96
miR-92a
miR-9
miR-7
miR-499
miR-375
miR-29b
miR-25
miR-203
miR-200b
miR-200a
miR-19a
miR-183
miR-182
miR-181b
miR-17
miR-126
miR-124
miR-106b
miR-103
miR-101
1
10
100
1000
10000
Fold-change in expression compared to CMEC

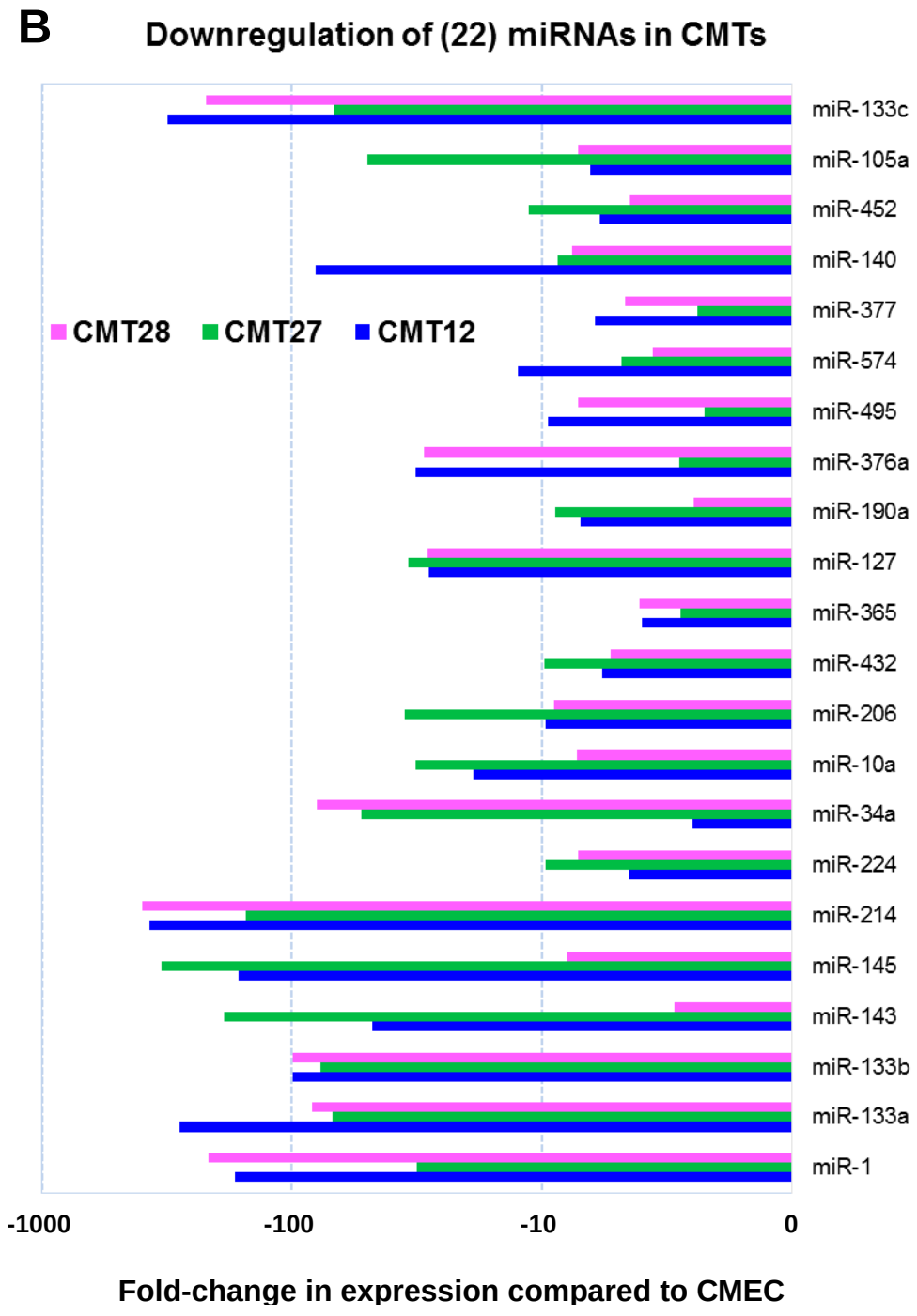
B
Downregulation of (22) miRNAs in CMTs
CMT28
CMT27
CMT12
miR-133c
miR-105a
miR-452
miR-140
miR-377
miR-574
miR-495
miR-376a
miR-190a
miR-127
miR-365
miR-432
miR-206
miR-10a
miR-34a
miR-224
miR-214
miR-145
miR-143
miR-133b
miR-133a
miR-1
-1000
-100
-10
0
Fold-change in expression compared to CMEC

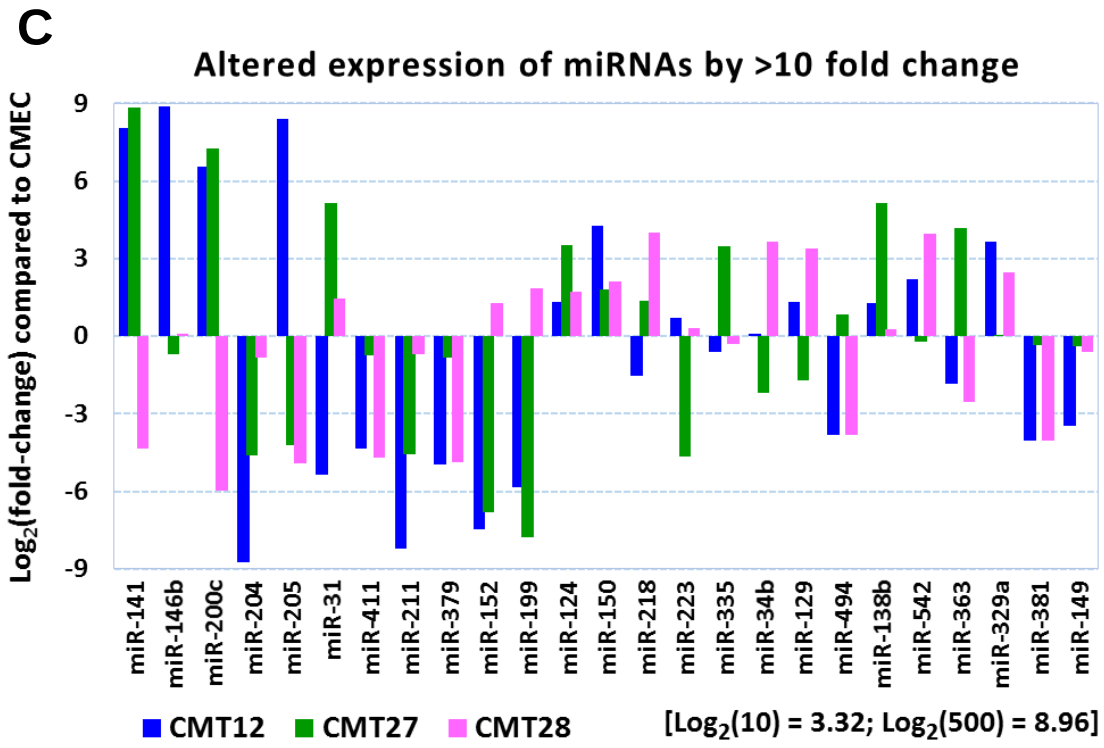

Fig. 29. Altered miRNA expression profiles in CMT cell lines. Among experimentally validated miRNAs devoid of technical errors, (A) 40 miRNAs were up-regulated, (B) 22 were down-regulated in all three CMT cell lines. (C) Another group of differentially expressed miRNAs were selected based on their altered expression by more than 10-fold change in CMT cell lines compared to CMECs. [All values are log_2 transformed and log_2(10-fold) = 3.32]

miRNA Target Prediction and Recovery of Target Site in Newly Characterized p16/p14 3'-UTR

Online-based tools are commonly used for miRNA target prediction. Only two of the recently developed online resources such as TargetScan (www.targetscan.org) and miRDB (www.mirdb.org) are available for target prediction based on the canine genome. We used TargetScan 6.2 which is one of the most widely used miRNA target prediction

programs that predicts miRNA binding sites through the identification of complementary seed sequence matches in the 3'-UTR of mRNAs and the assessment of their evolutionary conservation (Reczko et al., 2011).

The primary goal of this target prediction was to identify miRNAs from the altered expression panel in CMT models that could potentially target INK4 tumor suppressor genes. This would identify potential post-transcriptional regulation mechanisms pertinent to the regulation of individual INK4 tumor suppressor genes. The TargetScan tool identified several miRNA target sites from putative 3'-UTR sequences generated from mammalian sequence alignments. We found that miR-141, miR-300, miR-514 and miR-653 potentially target p16/p14ARF while miR-375 could target p15 mRNA. However, all these miRNAs were determined as differentially expressed in CMTs except miR-375 which was up-regulated in all three cell lines (Fig. 29). From the canine p16 sequence alignments, these miRNAs binding complementary sequences were located in the 3'-UTR of the p16 mRNA. However, p16 from CMEC was found to have a shorter length 3'-UTR in the sequence alignment thereby missing the target site for miR-141 (Fig. 30A). Apart from the 3'-UTR, the coding region of p16 also gave rise to additional target sites for three up-regulated miRNAs including miR-503, miR-103 and miR-29b through direct seed sequence match searching (Fig. 30B).

Although p16 mRNAs from CMEC and CMT28 have definite 3'-UTR length with poly (A) tail as determined by 3' RACE-PCR (Chapter 2), these were found to have shorter lengths compared to published canine p16 3'-UTR (GenBank: AB675384). Since p16 and p14 are alternatively spliced and the p14ARF 3'-UTR have never been defined, amplification of missing 3'-UTR could allow identification of miRNA target sites as well

as additional information of these alternatively spliced transcripts. For this purpose primers were designed to amplify the region of the p16 mRNA that could span the highly conserved exon 2 and 3'-UTR with ~100 bp additional downstream region (Fig. 30A).

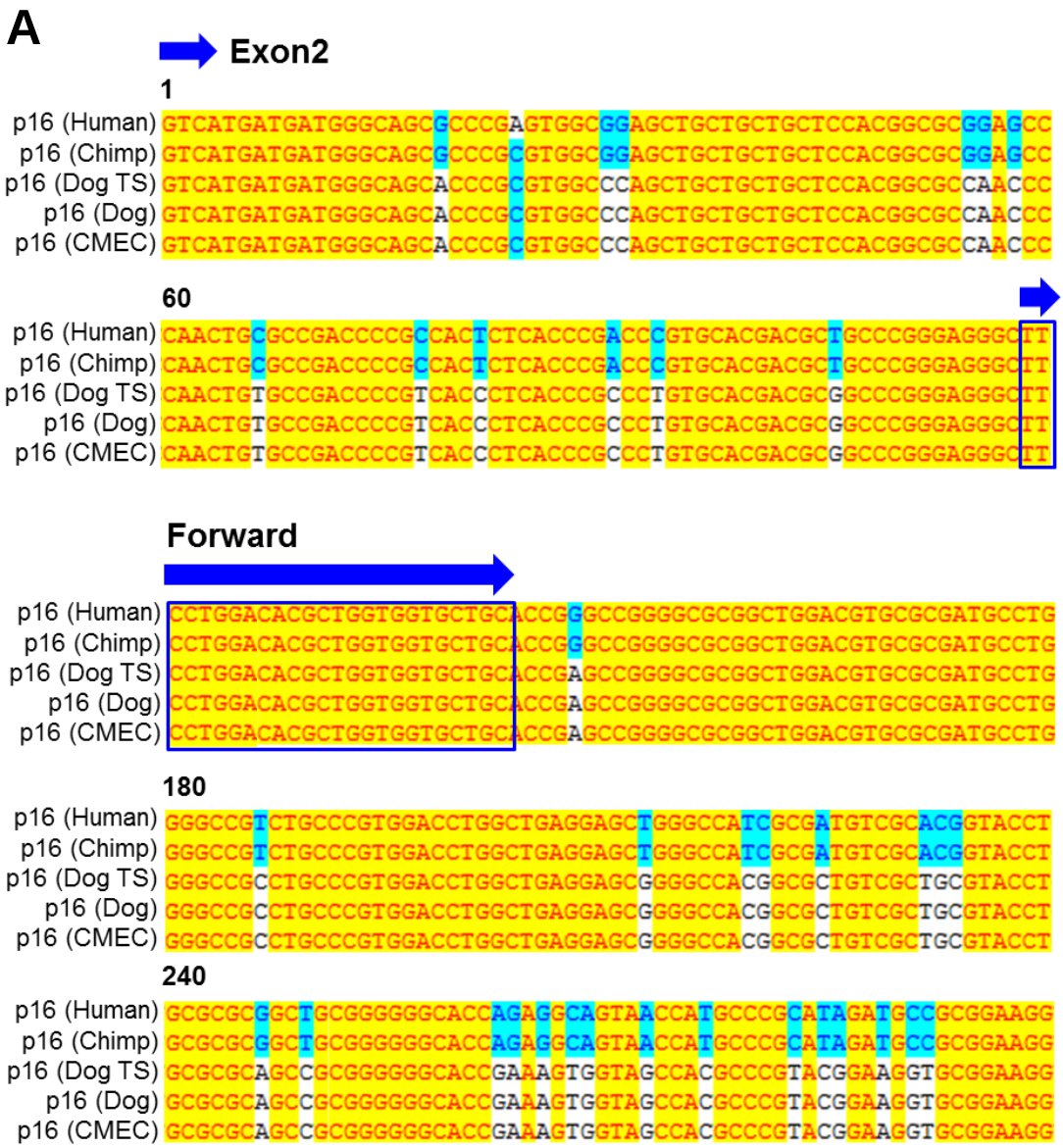

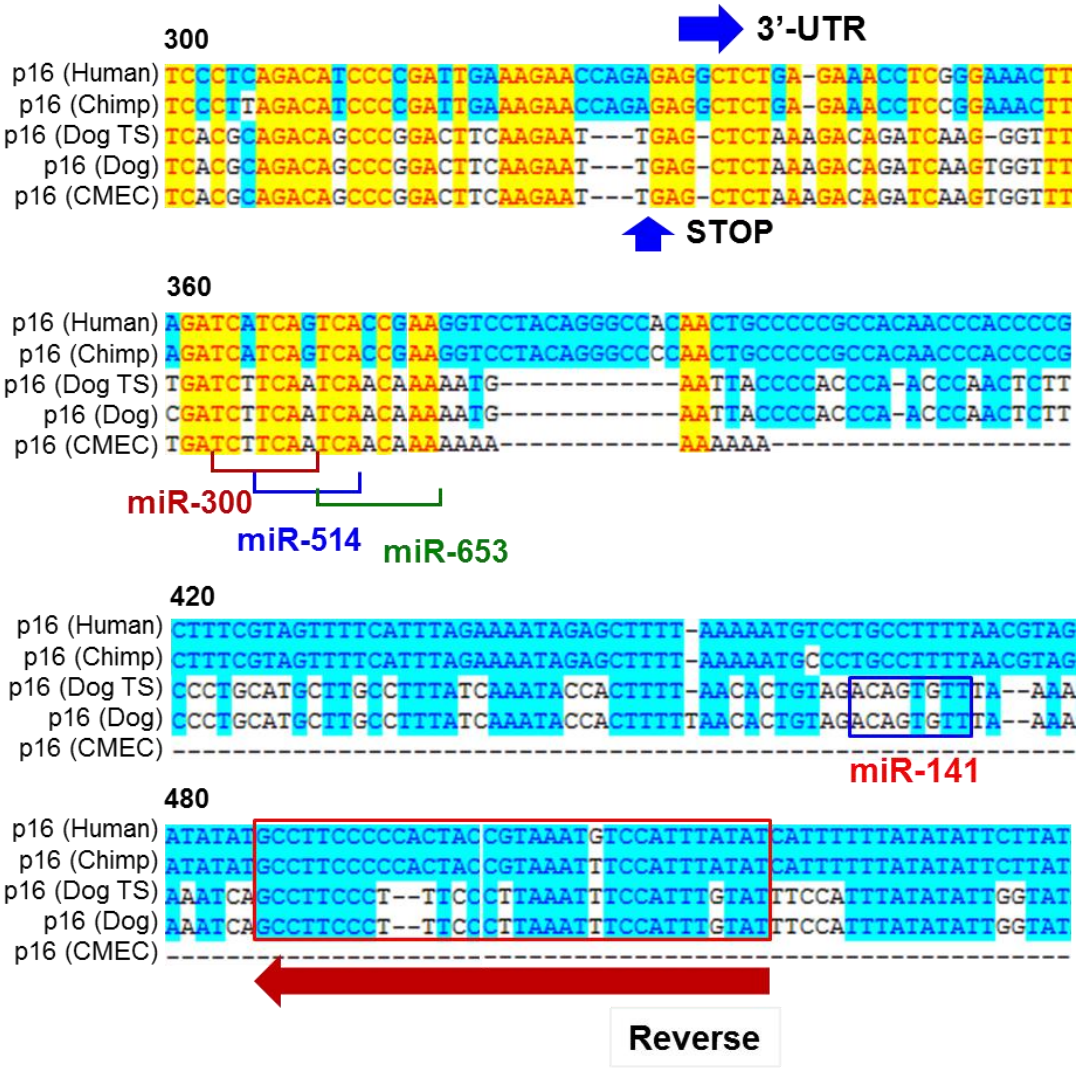

Fig. 30. Prediction of miRNA target binding sites in p16 mRNA sequence. (A) Alignments of p16 sequence spanning exon 2 to the 3'-UTR from different species. Canine p16 exon 2 – 3'-UTR sequences including putatively generated canine p16 sequence from genome alignments obtained from TargetScan (as indicated by Dog TS), published p16 sequences from thymic lymphoma indicated by 'p16 (Dog)' (GenBank: AB675384) and from canine mammary epithelium (CMEC) or normal canine fibroblasts (NCF) (GenBank: JQ796919) show variable lengths of 3'-UTR.

The sequence alignments indicated highly conserved exon 2 and at the start and stop codons for all dog sequences and 3'-UTR regions. The forward and reverse primers are shown by the forward arrow in blue and reverse arrow in red, respectively. Several predicted miRNA binding sites are indicated in the 3'-UTR. The binding site for miR-141 is missing in p16 3'-UTR from CMEC.

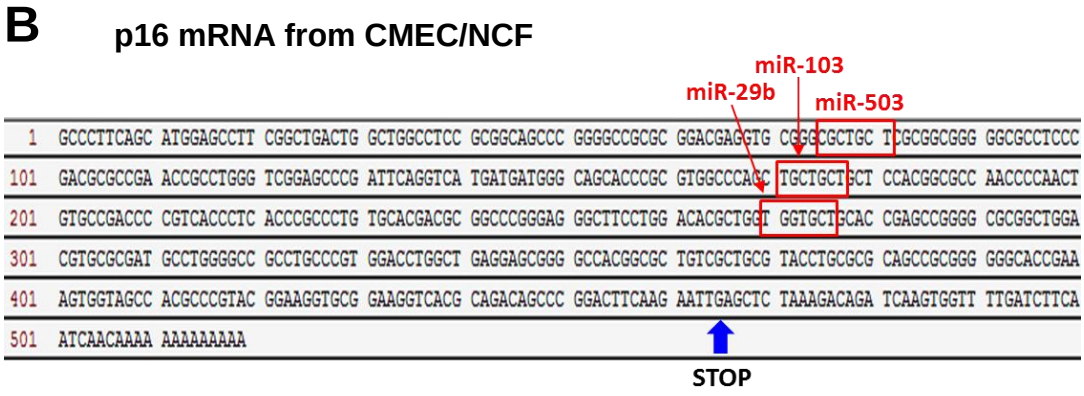

Fig. 30. (B) miRNA binding sites in wild-type canine p16 mRNA for three up-regulated miRNAs were identified by direct searching for seed sequence matches in the p16 mRNA from CMEC.

Surprisingly, touch-down RT-PCR assay demonstrated 3'-UTR expression (including the extended downstream region) in CMEC and CMT28 cells detecting longer 3'-UTR amplification although this was unexpected given the truncated sequence of the p16 mRNAs from these cell lines (Chapter 2, Lutful Kabir et. al., 2013). Similar PCR amplification was then performed in other CMT cell lines that were defective for both p16 and p14 expression (CMT12 and CMT27) or only p16 expression (CMT9). CMT9 (not CMT12 or CMT27) that never expressed p16 but did express p14, was found to amplify

this elongated 3'UTR similar to CMEC and CMT28 (Fig. 31) suggesting that this longer 3'-UTR is expressed as part of the p14 mRNA but not p16 mRNA in CMEC or in CMT cells. Sequencing of the amplicons also revealed that the new 3'-UTR for the INK4 message was more likely to be the part of the p14 mRNA. The alignment of the longer 3'-UTR from p14 mRNA recovered the miR-141 target site that was previously absent from the existing p16 3'-UTR from CMEC (Fig. 32). This experimental evidence demonstrated that how one miRNA regulates the two genes with the common target site in the 3'-UTR while cells regulate the variable 3'-UTR lengths between two alternatively spliced INK4A transcripts for fine tuning their expression in a tissue-specific manner and possibly for an escape from miRNA-mediated silencing.

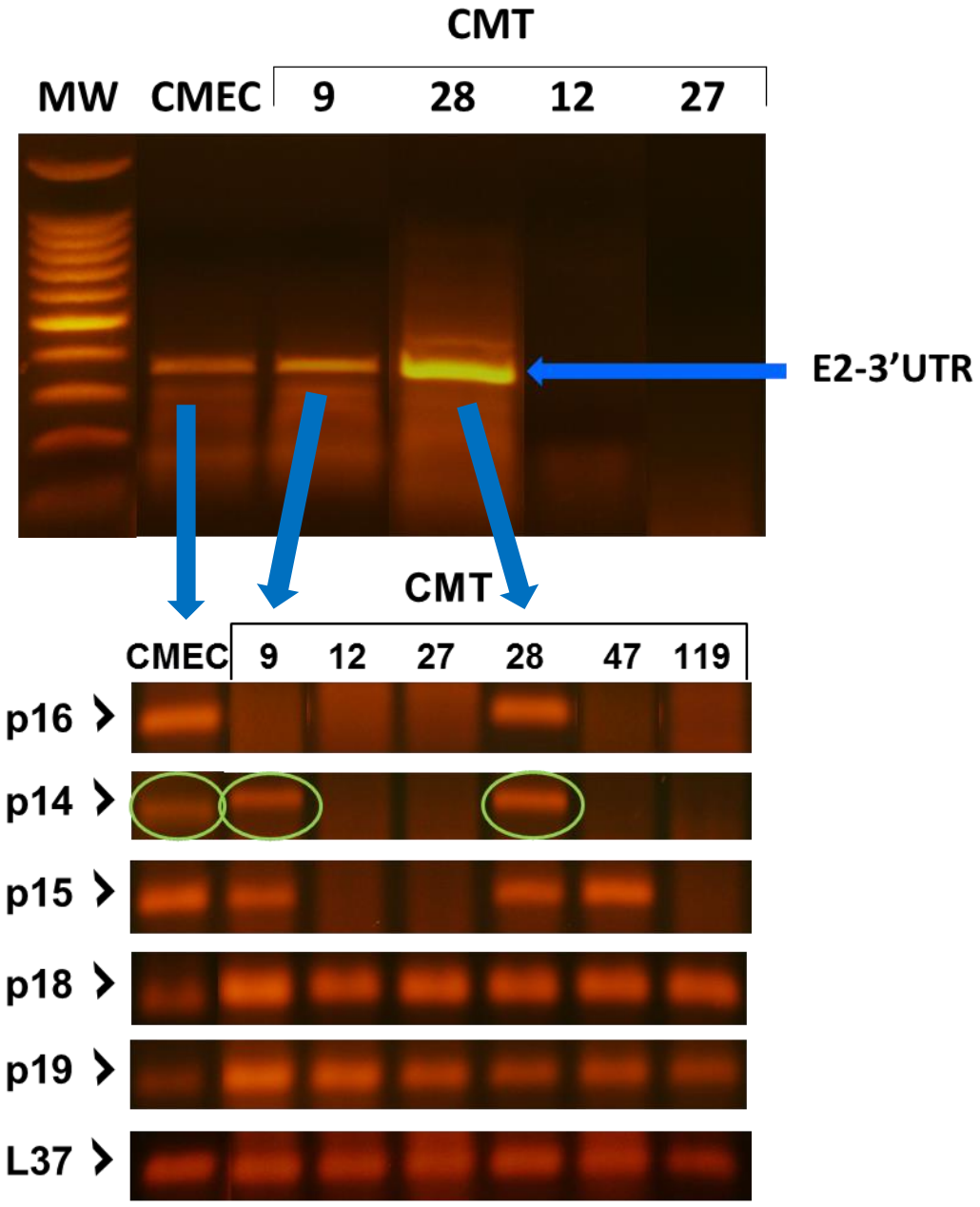

Fig. 31. Amplification of exon2-3'UTR (E2-3'UTR) sequence in CMECs, CMT9, CMT12, CMT28, and CMT27 cell lines. The forward primer for this new 3'-UTR amplification was designed from common exon 2 of p16 and p14 and the reverse primer was designed from the conserved 3'-UTR of the p16 sequence alignments (Fig. 30A). The authenticity of the amplicons was validated by sequencing and NCBI

BLAST analysis. In the upper panel, the ~380 bp E2-3'-UTR amplicon bands were observed in CMEC, CMT9 and CMT28. The expression of the longer 3'-UTR in these cell lines correspond to p14 expression in the lower panel (circled green).

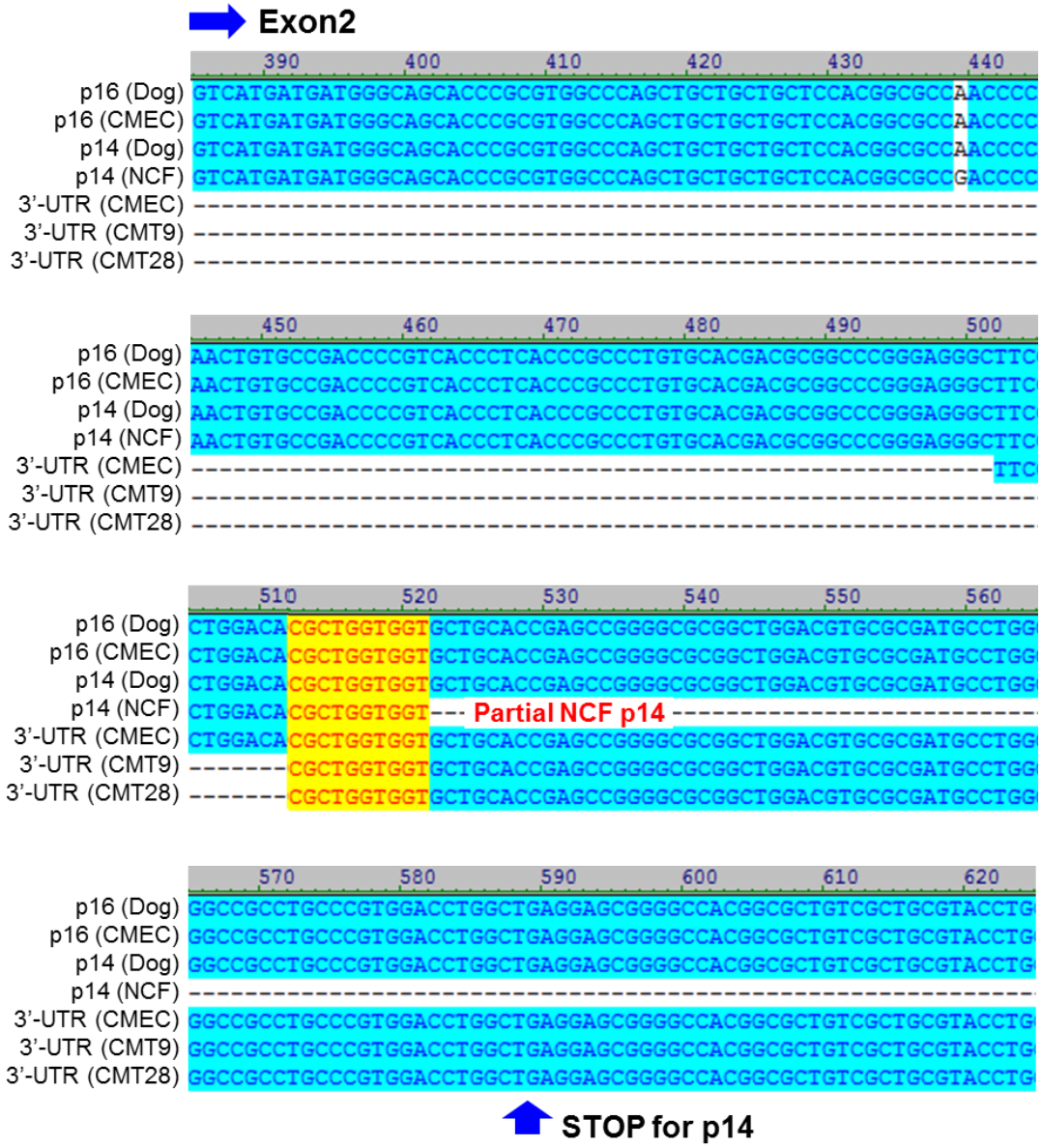

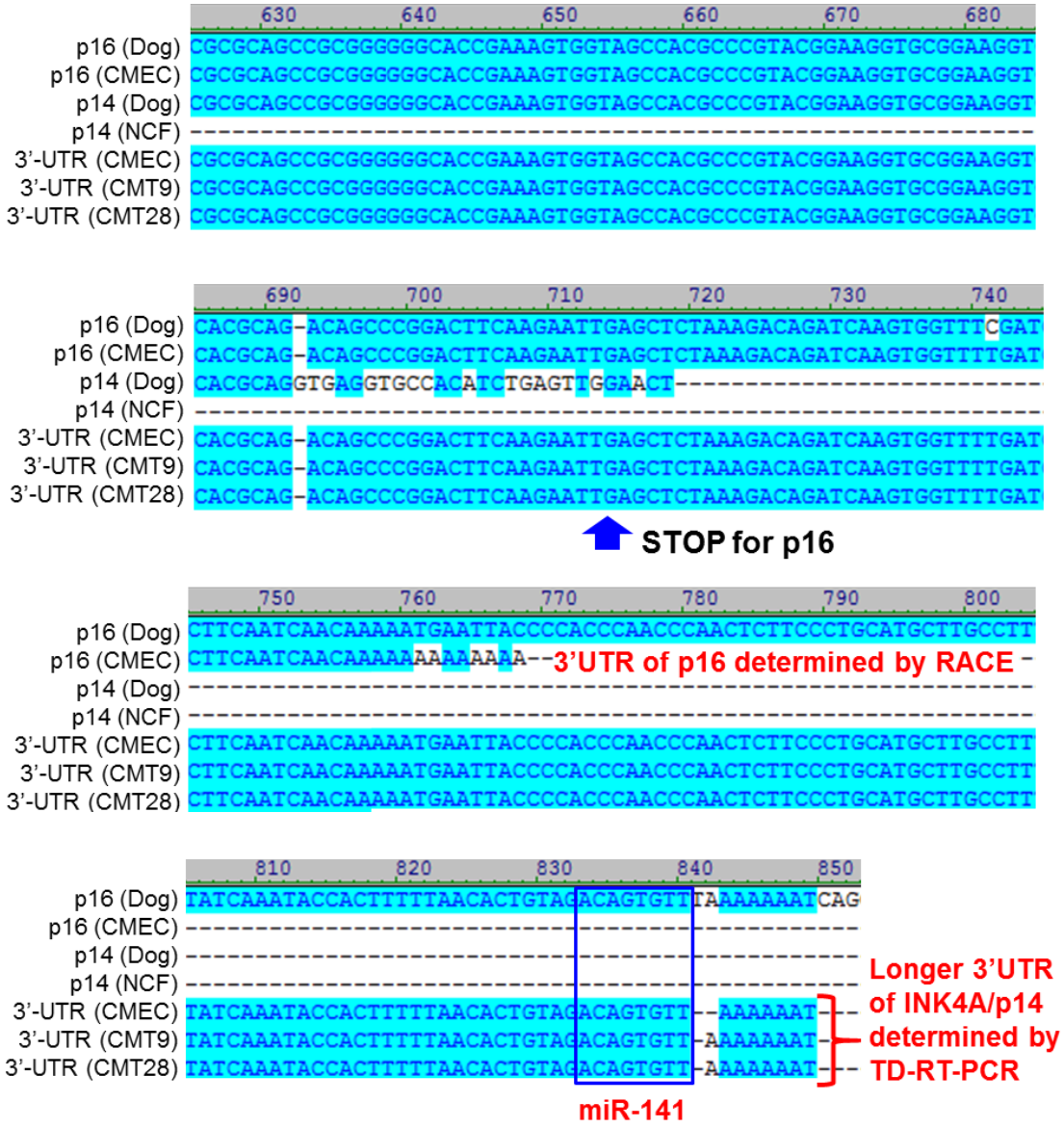

Fig. 32. Sequencing and alignment of the longer 3'-UTR of INK4A or p14ARF mRNA amplified in CMEC, CMT9 and CMT28. The published p16 sequences from dog (thymic lymphoma) and CMEC/NCF were compared as was the predicted p14 mRNA from dog (GenBank: FM883643) and the partial p14 sequence from NCF (GenBank: JQ801342) with newly discovered INK4A 3'-UTR sequences. The longer

3'-UTR sequences of the INK4A gene that are likely to be spliced to p14ARF obtained from CMEC, CMT9 and CMT28 are shown to harbor the predicted miR-141 target site. [TD-RT-PCR = Touch Down Reverse Transcription PCR].

Functional Validation of miR-141 Target-binding in CMT Cells

As the newly discovered 3'-UTR of the canine CDKN2A (INK4A/p14) mRNA was found to harbor a miR-141 target sequence (Fig. 32), the miR-141 target (CDKN2A 3'-UTR) binding was validated by 3'-UTR reporter assay. CMEC and CMT cell lines including CMT12, CMT27 and CMT28 were co-transfected with a CDKN2A 3'-UTR miRNA target clone expression vector (or target control vector) encoding *firefly* and *renilla* luciferase reporters and a miR-141 precursor clone expression vector (or miRNA scrambled control vector) encoding a GFP reporter (described in Methods and Materials). Transfection and expression of these genes in the CMEC and CMT cell lines were assessed by the respective reporter gene expression. First, the transfection and expression of miR-141 in the CMEC and CMT cells were confirmed by GFP expression prior to reporter assay following cell lysis (Fig. 33).

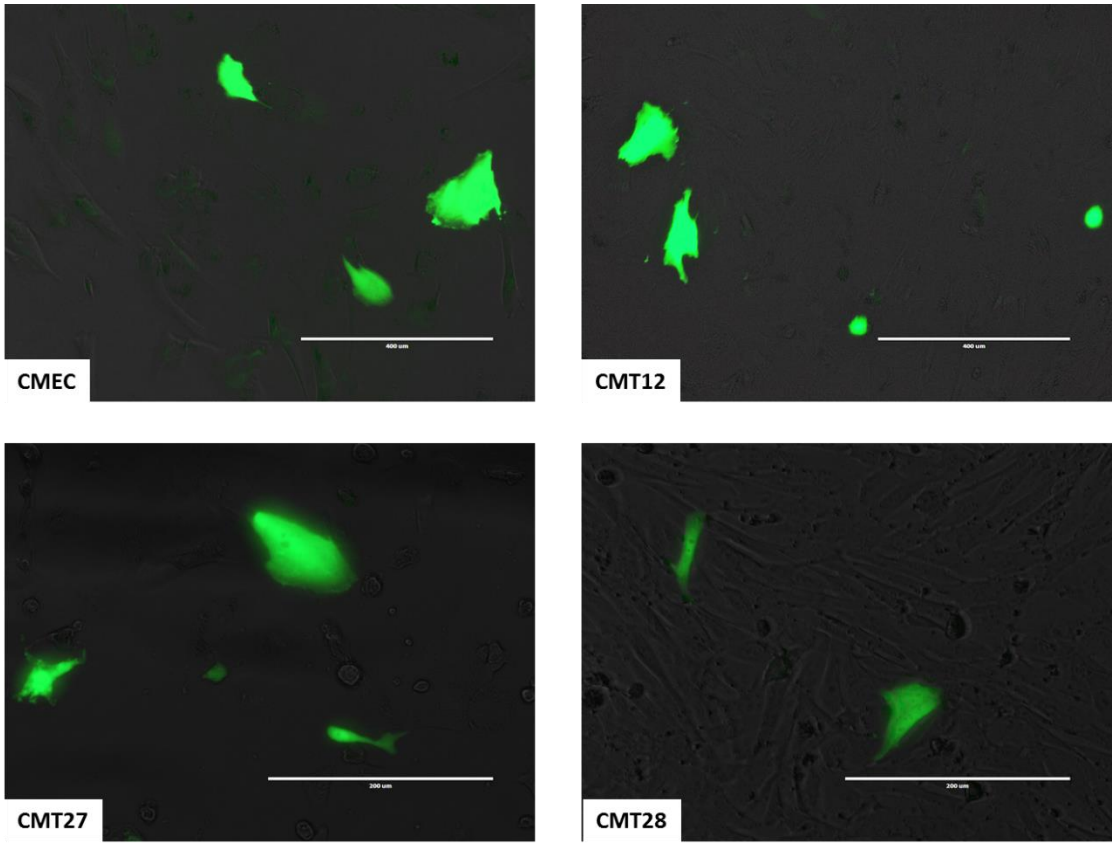

Fig. 33. Transfection of CMEC and CMT cell lines by miR-141. Each cell line was co-transfected with the miR-141 precursor clone expression vector and CDKN2A 3'-UTR target clone expression vector. After transfection, cells were grown for 24 hours and checked for GFP expression. Each cell line in a 24-well plate was examined under fluorescence microscopy using 10X and 20X objectives (EVOS AMG, Life Technologies). Representative fields of cells are shown for each cell type from culture. The magnification bar of 400 µm indicates the scale for CMEC and CMT12 (upper panel) and 200 µm indicates the scale for CMT27 and CMT28 cell lines (bottom panel).

The silencing of the CDKN2A 3'-UTR target by miR-141 (resulting from its seed sequence binding to the matched target sequence) was analyzed by comparing the diminished activity of *firefly* luciferase which was inserted upstream from the 3'-UTR sequence in the expression vector (Fig. 22). Expression of miR-141 caused variable level of suppression of target 3'-UTR in CMEC and CMT cell lines. When miR-141 was overexpressed in CMEC and CMT28 by transfecting with a higher concentration, it caused reduction in luciferase expression (up to 60%) thereby silencing 3'-UTR target and validating the miR-141 CDKN2A target binding (Fig. 34A).

On the other hand, miR-141 expression in CMT12 and CMT27 could suppress the target 3'-UTR to a more modest level (Fig. 34B). However these two cell lines were found to express higher endogenous miR-141 by several hundred fold (described earlier, Fig. 29). A control target 3'-UTR clone (lacking miR-141 target binding site) was designed and used to assess the inhibitory effect of endogenously expressed miR-141 on the cells transfected with CDKN2A 3'-UTR target. Transfecting the CMT12 and CMT27 cell line with the control target 3'-UTR sequence revealed that endogenously expressed miR-141 knocked down CDKN2A 3'-UTR target expression in these cells (Fig. 34B, when compared the 'control' green bars with the 'mock' blue bars) suggesting a dominant competitive function of endogenously expressed miR-141 in silencing the CDKN2A 3'-UTR target sequence in these cells. Similar treatment in the CMT28 cell line demonstrated no endogenous inhibitory effect on the CDKN2A 3'-UTR target (Fig. 34A), reconfirming the down-regulation of miR-141 in this cell line. Additionally, this experimental evidence suggests that lack of miR-141 mediated silencing in the CMT28 cell line was permissive for

INK4A/p14 mRNA expression leading to the discovery of the longer 3'-UTR sequence containing the miR-141 target site in these cells.

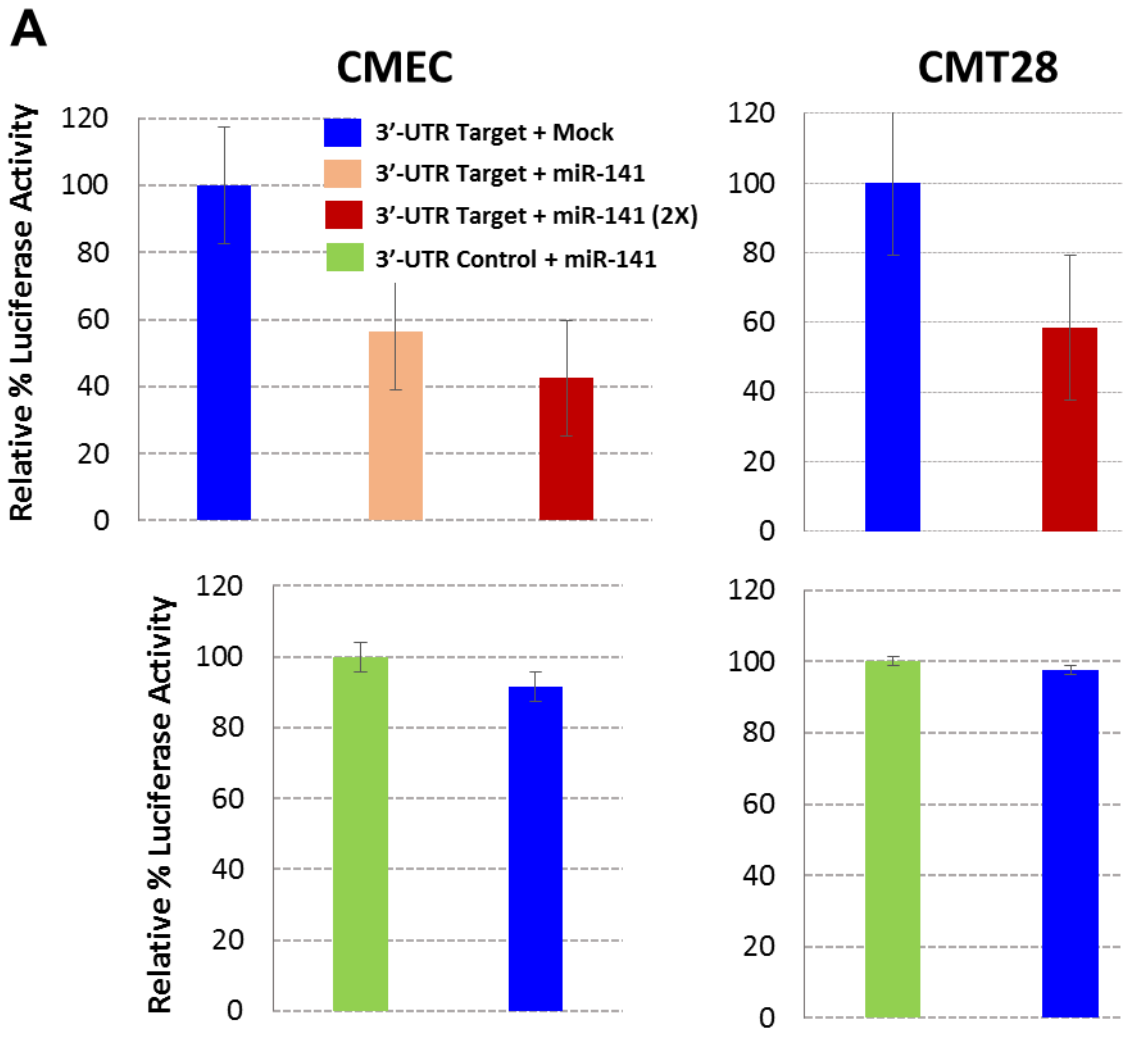

Fig. 34. Validation of miR-141 target binding by 3'-UTR luciferase assay. (A) CMEC and CMT28 cells were co-transfected with either CDKN2A 3'-UTR target cloning vector (or target control vector without miR-141 binding sequence) encoding *firefly* and *renilla* luciferase reporter expression and miR-141 precursor cloning vector encoding GFP expression. 90 ng of 3'-UTR target clone and two different concentrations of miR-141 (120 ng and 240 ng as indicated by 2X) were used to

transfect the cells grown in 24-well plates. Cells were also mock transfected (3'-UTR target clone + transfection reagent with serum-free medium) to assess the endogenous miR-141 function. In each case, relative percent luciferase activity was calculated by measuring the ratio of the *firefly* to *renilla* luciferase activities in the assay. The r*enilla* luciferase activity was used to normalize the firefly luciferase signal in the same CMEC or CMT28 cell line.

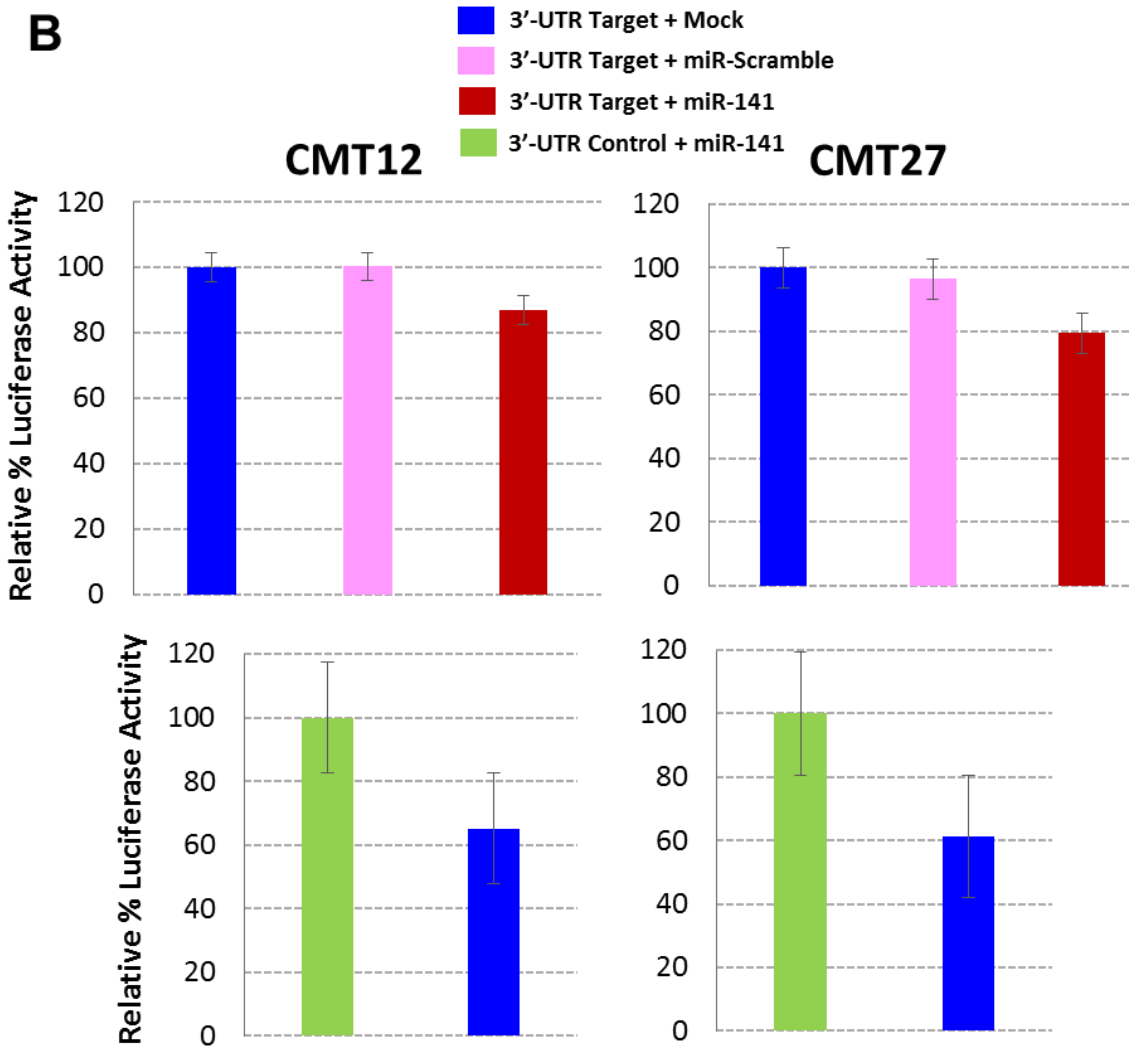

Fig. 34. (B) CMT12 and CMT27 cell lines were similarly transfected and assayed for the validation of miR-141 3'-UTR target binding. These cells were also co-transfected

with the 3'-UTR target clone and the miRNA scrambled control clone in addition to mock transfection to determine the specific binding of endogenous miR-141 with the 3'-UTR target sequence. Error bars indicate standard error for each experimental value.

Prediction of other Potential Canine miRNA Targets Including Cell Cycle Regulators

Several other miRNAs whose expression was altered in CMT cells, were investigated for targeting of other genes known to regulate the cell cycle. A group of down-regulated miRNAs were predicted to target the cyclin-CDK genes and E2F transcription factors that function downstream of the p16 in the same regulatory pathway suggesting that these miRNAs may act as potential tumor suppressors in canine breast cancer (Fig. 35).

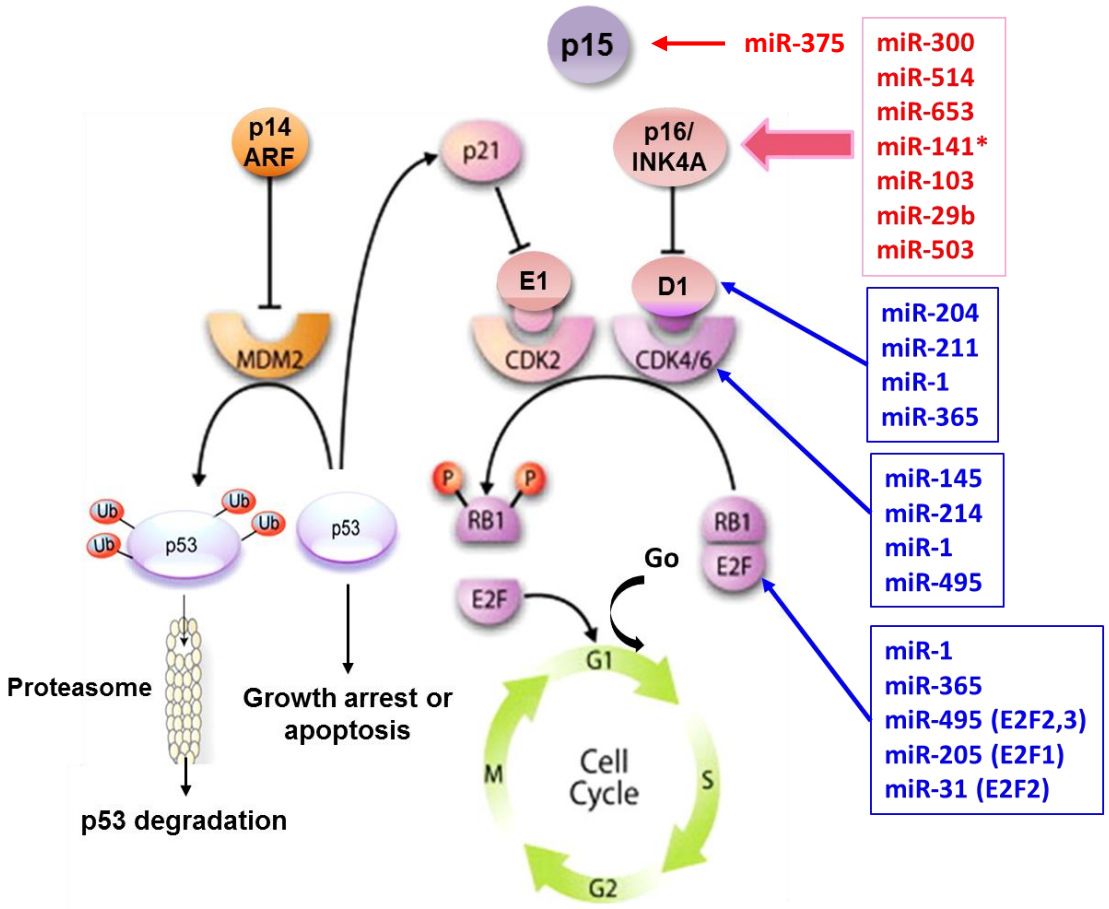

Fig. 35. Prediction of targets of deregulated miRNA among key cell cycle regulatory genes. A group of up- and down-regulated miRNAs in CMT cells identified by qPCR arrays, are shown to target different genes in the p16-Rb regulatory pathway. miRNAs in red were up-regulated and in blue were down-regulated in all three CMT cell lines. miR-141 (red asterisk) belongs to the group of altered and differentially expressed miRNAs and its expression was up-regulated in CMT12 and CMT27 but down-regulated in CMT28.

In an extended target prediction analysis, we identified more miRNA candidates from the deregulated panel (Fig. 29) that could potentially target other genes in CMT cell

models. Among these genes were included luminal epithelial specific markers and hormone receptors including estrogen receptor 1 (ESR1), progesterone receptor (PR) and proto-oncogenes such as the epidermal growth factor receptors (EGFR/Her-2 family) (Table 4). Most of these miRNAs are down-regulated in CMT cells verifying their important roles in silencing oncogenes that are involved in tumor progression.

Table 4: Deregulated miRNAs targeting oncogene growth factors and hormone receptors in the context of CMT models

Target genes	EGFR	Her-2/ERBB2	ESR1	PR
miRNAs	miR-1 miR-206	miR-376a miR-432 miR-214 miR-140 miR-199	miR-203	miR-190a

One miRNA family was found to be very highly up-regulated in CMT cell lines. This family includes miR-429 (>1000 fold-change in expression in CMT12 and CMT27) and miR-200c (100-150 fold-change in expression in CMT12 and CMT27) (Fig. 29). These two miRNAs were predicted to target a gene known as the ERBB receptor feedback inhibitor (ERRFI1) in a highly conserved fashion (the target sites are conserved across mammalian species). ERRFI1 has been characterized by many studies as a potent tumor suppressor gene that inhibits the kinase domain of ERBB (Fig. 36) (Anastasi et al., 2005; Zhang et al., 2007; Zhang et al., 2007). Therefore, these highly up-regulated miRNAs in CMT cells have the potential to promote potent oncogenic functions by targeting and down-regulating key tumor suppressor genes.

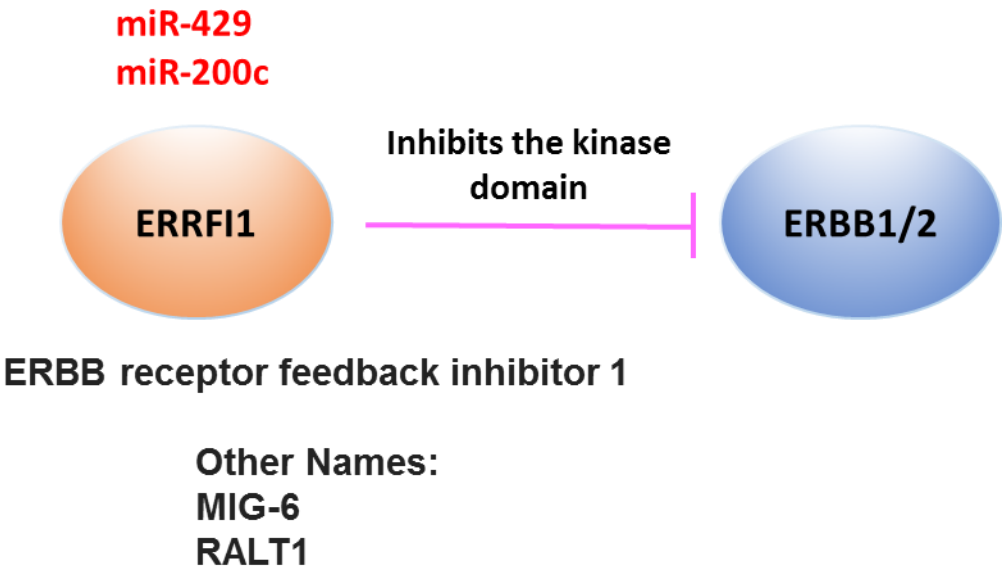

Fig. 36. Novel targets of miR-429 and miR-200c predicted by TargetScan. A potent tumor suppressor (ERRFI1) has been identified by the TargetScan program to be targeted (and potentially down-regulated) by highly up-regulated miR-429 and miR-200c in CMT cell lines. The alternative names of this gene are MIG-6 and RALT1 and it inhibits the kinase domain of the oncogenes ERBB1/2 which are key oncogenes in both human and canine breast cancers (Beck et al., 2013, Gama et. al., 2008; Sassi et al., 2010; DeInnocentes et al., 2014, manuscript in preparation).

Section 4. Discussion and Conclusions

The emergence of miRNAs as critical cancer-related genes is likely to contribute important therapeutic targets in advanced cancer gene therapy. Their predominant presence in the genome clearly indicates regulatory functions in gene expression that can manipulate a diverse areas of cellular processes including disease mechanisms. Large scale expression and screens in cancer versus normal cells that identify important regulatory and frequently dysfunctional miRNAs and their potential targets will be useful in understanding novel cancer mechanisms. This is the first evidence of comprehensive expression profiles of the best characterized miRNAs from the canine genome that have been evaluated in CMT models. This expression profile and fold-regulation of the 277 canine miRNAs in three CMT cell lines compared to normal CMECs were determined by using a quantitative PCR array strategy.

For comprehensive expression profiling of miRNAs, only small RNAs (less than 200 nucleotide long) including miRNAs and snoRNAs or snRNAs were isolated from the CMEC and CMT cell lines and used as the starting material in the initial step of the qPCR reaction. For accurate and reproducible results in miRNA quantitation by qPCR array, it was necessary to normalize the amount of target miRNA using suitable endogenous reference genes. The endogenous control RNAs, including small nucleolar or snoRNAs and small nuclear or snRNAs that are highly conserved and widely expressed in different tissues, are commonly used in the normalization of miRNA expression. Recent evidence has shown that these small control RNAs can be differentially expressed and frequently play roles in cancer prognosis and pathogenesis (Gee et al., 2011). Therefore using a single snoRNA or snRNA as a reference gene may introduce variability in results and analysis.

In order to overcome this problem, a panel of six snoRNAs/snRNAs were used as reference genes or endogenous controls. These genes together have been validated to give an average measure of relatively stable expression levels across tissues and cell types (Davoren et al., 2008; Gee et al., 2011).

The comparative expression of miRNAs was mathematically evaluated as fold-change or fold-regulation applying the ΔΔCT method of relative quantitation. A threshold fold-difference in miRNA expression was defined by 2-fold change in the data analysis and interpretation of results. Although it is arbitrarily designated but practically, a 2-fold difference indicates one Ct value in the qPCR assay when the efficiency of the experiment is equal to or close to 100%. In addition, 2-fold cut-off in the data analysis highlighted potentially interesting targets. However, a group of altered miRNAs identified to be differentially expressed by higher fold-change (>10 fold) were also represented as biologically significant candidates in the canine breast cancer mechanisms.

The quantitative expression profile estimated that nearly 80% of total miRNAs are differentially expressed in all three CMT cell lines compared to CMEC. These estimated numbers of altered miRNAs were narrowed down by considering only higher fold-change regulation and avoiding any technical errors generated from qPCR amplification such as abnormal threshold cycles. This refined group (up-/down-regulated miRNAs) was subjected to investigation for their potential roles in CMTs and targeting of INK4 tumor suppressors and other cancer related genes. Differentially expressed miRNAs also highly correlate the expression defects of predicted target mRNAs in CMTs. For example miR-141 was differentially expressed in CMT cell lines showing its sharp up-regulation in CMT12 and CMT27 (by ~266 and ~460 fold, respectively) but down-regulation in CMT28

(by ~20 fold). Up-regulated miR-141 was predicted to target p16/INK4A mRNA and this gene expression was missing in CMT12 and CMT27. In contrast, CMT28 cells down-regulated miR-141 and did express p16 mRNA though as a mutant message (chapter 2; Lutful Kabir et al., 2013). This suggests that expression of p16 in CMT12 and CMT27 cells may be post-transcriptionally regulated by miR-141.

Hunting for miRNA target sites in 3'-UTRs of INK4A mRNAs revealed striking evidence of potential regulation and expression of INK4 3'-UTRs in CMTs. As miR-141 was predicted to target the p16 mRNA, we intended to identify the target site from the 3'-UTR sequence alignments. The complementary target site in the 3'-UTR for the matched seed sequence of miR-141 was found in the published p16 mRNA sequences but missing in the sequences obtained from CMT28 and CMEC because this message was expressed in these cells with a shortened 3'-UTR. This could be because the p16 mRNA 3'-UTR sequence and length had been previously determined by 3'-RACE PCR in CMEC and CMT28 cells line. We have now shown that truncated p16 mRNAs that do not include the miR-141 binding site are frequently expressed in CMT cells and may be a common aspect of the breast cancer phenotype. A number of reports have suggested that 3'-UTR length variability may be the result of a mechanism to avoid miRNA target sites possessed in proliferating cells (Sandberg et al., 2008; Shrout, 2013). Surprisingly, the longer 3'-UTR sequence of p16 was found to be expressed in CMT28. To verify this unlikely expression of an extended 3'-UTR as part of p16 mRNA in CMT28, PCR amplification was performed in other CMT cell lines that were previously examined for p16 and p14 expression. This gene expression analysis identified that the longer 3'-UTR was also expressed in the CMT9 cell line that does not express p16, but only p14, suggesting that this mRNA sequence is

expressed as the 3'UTR of p14 but not of p16. This evidence demonstrated how particular cells can shift the 3'-UTR length from longer to shorter forms between two alternatively spliced transcripts and as a consequence eliminating the miRNA target sites in the dominant tumor suppressor gene p16. This newly discovered 3'-UTR and miR-141 target site in INK4A/p14 was further validated by miRNA 3'-UTR reporter assay. This experimental evidence demonstrated that miR-141 endogenously knocked down INK4A/p14 mRNA (containing 3'-UTR target site) when over-expressed in CMT12 and CMT27 cell lines. In contrast, down-regulation of miR-141 in CMT28 cells could not suppress p14 mRNA expression in this cell line.

miRNA expression profiles from the canine genome are not only associated with CMT cells but are also highly correlated with that found in human breast cancer. A number of miRNAs that are altered in both canine and human breast cancers have been identified in the current study and in several human studies (Table 5), suggesting conserved regulation of their potential oncogenic and tumor suppressive functions. Several well-known miRNAs have proven to be oncogenic and upregulated in human breast cancers including miR-21 (Iorio et al., 2005), miR-155 (Zhang et al., 2013), and miR-9 (Ma et al., 2010). Whereas miRNAs that function as tumor suppressors and are down-regulated in breast cancers have included miR-34a (Li et al., 2013), miR-143/145 (Iorio et al., 2005) and miR-31 (Laurila and Kallioniemi, 2013). In Table 5, these miRNAs have been shown to reflect a similar altered regulation in canine breast cancer models.

Table 5. Altered expression of miRNAs that are associated with canine and human breast cancers (Diff. Ex = differentially expressed)

miRNAs	Regulation in breast cancer	
	Human	Dog
miR-21	Up-regulated (oncogenic)	Up-regulated/Diff. Ex
miR-155	Up-regulated (oncogenic)	Up-regulated
miR-9	Up-regulated (oncogenic)	Up-regulated
miR-34a	Down-regulated (tumor suppressor)	Down-regulated
miR-143/145	Down-regulated (tumor suppressor)	Down-regulated
miR-31	Down-regulated (tumor suppressor)	Down-regulated/Diff. Ex

These correlations further strengthen the validity and use of canine cancers as appropriate models for the study of human cancers. However, there are certain miRNAs that were abnormally regulated in both human and canine cancers but were unique to each respective model system. For example, the miR-141 or miR-200 family were differentially regulated and may be involved in different mechanisms in canine and human breast cancers (Burk et al., 2008; Ye et al., 2014). Functional validation of these miRNA-target binding potentials in canine breast cancer models is necessary to further decipher the complex regulatory mechanisms involving miRNAs in breast cancer.

Chapter 5: Conclusions

Dogs are one of the very few animal species that develops cancers spontaneously with molecular features and clinical representations mimicking those of human cancers more closely than other mammalian species. Significant similarities in cancer genetics between human and dog have made the canine cancers an appropriate and valuable model system for the study of human cancer biology and development of future therapeutics. A large number of canine cancer-associated genes, including the cell cycle regulators which are clear human orthologs, are mostly unknown with respect to their regulatory mechanisms due to a lack of adequate studies in canine cancer genetics. The current study focuses on the development of canine mammary carcinoma as an important intermediate model for human breast cancer in terms of genetic defects and critical regulatory mechanisms controlling function of a family of cyclin-dependent kinase inhibitors, or INK4 tumor suppressor genes, that play vital roles in cell cycle regulation.

Three members of the INK4 cell cycle regulators including p16, p14ARF and p15, encoded by the INK4A/ARF/INK4B locus, are highly conserved between human and dog, not only for their genomic organization in orthologous regions of chromosomes 9 and 11, respectively, but also for their frequent deletion/mutation in many cancers (Chapter 1 and 2). It is important to characterize these genetic defects in the INK4 tumor suppressor genes in canine cancers to determine how closely they reflect lesions found in human cancers. The three members of the INK4 family (p16, p14 and p15) were found to be differentially

expressed while two other members (p18 and p19) were normally expressed or overexpressed when compared to normal canine fibroblasts (NCF). Evaluation of INK4 expression profiles in established CMT cell lines, which have been employed continuously in the current study, suggested that defects in these tumor suppressor genes occurred recurrently removing cell cycle check point control (at the G1 to S phase transition) and thereby promoting uncontrolled cell proliferation (Lutful Kabir et. al., 2013; DeInnocentes et al., 2009; Chapter 2).

Amplification and sequencing of the entire p16 coding sequence from NCF and CMT28 cell line led to the discovery of key genetic alterations including the novel frameshift mutation in p16 exon 1α in CMT28 providing a transforming mechanism in the CMT models. Analysis of the p16 mRNA sequence and frameshift mutation predicted altered reading frame and aberrant protein expression in the CMT28 cell line. These findings, including determination of the full-length p16 coding sequence and its mutation in the CMT28 as well as the differential expression of INK4 genes in CMT cell lines, provided valuable platform for further studies on the regulation of these tumors suppressor genes in canine breast cancer.

Although using cancer cell lines as models of human cancers gives essential gene expression profile and mutation data that could be selected for in cell culture, these cell lines still remain powerful experimental tools for studying many features of spontaneous cancers in humans as these types of expression defects were also observed in freshly isolated tumor derived cells. Another important factor is the cellular heterogeneity when using tissues (instead of cell lines) from animals or clinical samples as this will greatly enhance biological heterogeneity (Wurmbach et al., 2002). In order to authenticate the

differential expression of the INK4 genes in the CMT cell lines, a number of primary tumor biopsies collected from patient dogs were investigated in this study. In addition, normal canine mammary epithelial cells (CMEC) were developed and derived from normal mammary biopsy samples. These normal CMECs were used to serve as normal or control cells in the gene expression profiling and were compared with cancer cell lines. The INK4 gene expression profiles and defects in primary canine mammary carcinomas closely reflected those found in the CMT cell lines suggesting that these expression data were not merely an artifact of cell culture.

The INK4 gene expression and defects were also evaluated in canine malignant melanoma cell lines in which p16, p14 and p15 were even more frequently defective compared to their loss of expression in the CMT cell lines and primary tumors. These discoveries provided strong evidence for the loss of the INK4A/ARF/INK4B locus in both canine cancer models. Additionally, similar recurrent loss of p16, p14 and p15 expression was also evident in a panel of prominent human breast cancer cell lines comprising three major subclasses such as MCF7 (luminal A), ZR75 (luminal B) and MDA231 (triple negative). This firm correlation suggests conserved expression defects in p16, p14ARF and p15 tumor suppressors in both canine and human breast cancers.

The next major goal in this study was to elucidate the post-transcriptional regulation of the INK4 genes by miRNAs. Since the expression of the INK4 mRNAs were frequently lost in the CMT and canine melanoma models, it was hypothesized that these genes might be post-transcriptionally silenced in cancers. For the first time, the comprehensive expression profile of the 277 miRNAs from the canine genome was evaluated in the canine breast cancer models. These validated mature miRNAs represent the best characterized and

most abundantly expressed miRNAs identified from the CanFam genome assembly (miRBase v16, www.mirbase.org). Nearly 80% of these miRNAs were identified as differentially expressed based with a threshold defined as a 2-fold change in expression. Among these altered miRNAs, 40 miRNAs were found to be completely upregulated while 22 miRNAs were down-regulated in all three CMT cell lines (Chapter 4). In addition, the current study also reported a group of 25 miRNAs that were differentially expressed in the different CMT cell lines by more than a 10-fold change suggesting that they may possess potential regulatory functions in these cells. The altered fold-change in expression of these miRNAs could be biologically significant in cancer cells although all of them would not be statistically significant. One remarkable example was the identification of miR-141 which was highly up-regulated in the CMT12 and CMT27 cell lines (by >200 fold-change; p-value >0.05) but down-regulated in the CMT28 cell line and was predicted to target the p16/INK4A 3'-UTR. Interestingly, the target sequence of miR-141 was recovered in a newly discovered 3'-UTR which was shown to be expressed as part of the p14ARF but not the p16/INK4A mRNAs. Although these two genes share large overlapping exons 2 and 3, they were found to be expressed with variable lengths of 3'-UTR. The binding of miR-141 with its INK4A 3'-UTR target was validated by developing a 3'-UTR reporter assay. This evidence confirmed the post-transcriptional regulation of leading INK4 genes (p16 and p14/INK4A) by miR-141 and also revealed their transcriptional regulation through alternative splicing and shifting of critical 3'-UTR sequence from p16 to p14 in canine breast cancer.

The miRNA target prediction tool identified a number of deregulated miRNAs that target a panel of genes including cell cycle regulators involved in the p16-Rb pathway

(including cyclin D, CDK4/6 and E2F transcription factors) and several cancer biomarkers (oncogenic growth factors and hormone receptors including epidermal growth factor receptor families, estrogen receptor alpha, and progesterone receptor). A number of differentially expressed miRNAs in this study were also identified to be commonly dysregulated in both human and canine breast cancers (Chapter 4). These include miR-21, miR-155, miR-9, miR-34, miR-143/145 and miR-31. Importantly, miR-31 identified in this study has been reported to be located near the same chromosomal regions harboring the INK4A/ARF/INK4B locus and therefore, co-deleted in many human and canine cancers (Chapter 1).

Finally, this study shed light on the critical molecular mechanisms of the INK4 cyclin-dependent kinase inhibitors and potent tumor suppressor genes in terms of their expression, defects and regulation by miRNAs which were largely unexplored in the context of canine cancers. Particularly, these differentially expressed tumor suppressor genes encoded by the INK4A/ARF/INK4B locus showed great promise as potential therapeutic targets in breast cancers. The very first evidence of the comprehensive expression profile of the 277 canine miRNAs in the CMT cells revealed a large number of altered miRNAs (up-/down-regulated) that might serve as potential oncogenic and tumor suppressor targets for advancing the development of future therapeutic reagents. Moreover, the strong correlation between human and dog for INK4 gene expression, defects and regulation by miRNAs further reinforces the rationale of utilizing canine cancers as appropriate models for the study of human breast cancer.

References

1. Aaronson, S. A. (1991). Growth factors and cancer. Science 254(5035): 1146-53.

2. Agarwal P, Lutful Kabir FM, DeInnocentes P, Bird, R. C. (2012). Tumor suppressor gene p16/INK4A/CDKN2A and its role in cell cycle exit, differentiation, and determination of cell fate. In: Cheng Y., editor. Tumor Suppressor Genes. Rijeka, Croatia: InTech Open Access Pub. pp. 1-34.

3. Agarwal, P., Sandey, M., DeInnocentes, P., Bird, R. C. (2013). Tumor suppressor gene p16/INK4A/CDKN2A-dependent regulation into and out of the cell cycle in a spontaneous canine model of breast cancer. J Cell Biochem 114(6): 1355-63.

4. Aguirre-Hernandez, J., Milne, B. S., Queen, C., O'Brien, P. C., Hoather, T., et al. (2009). Disruption of chromosome 11 in canine fibrosarcomas highlights an unusual variability of CDKN2B in dogs. BMC Vet Res 5(27.

5. Ahern, T. E., Bird, R. C., Bird, A. E., Wolfe, L. G. (1996). Expression of the oncogene c-erbB-2 in canine mammary cancers and tumor-derived cell lines. Am J Vet Res 57(5): 693-6.

6. Ahmed, M. M., Sheldon, D., Fruitwala, M. A., Venkatasubbarao, K., Lee, E. Y., et al. (2008). Downregulation of PAR-4, a pro-apoptotic gene, in pancreatic tumors harboring K-ras mutation. Int J Cancer 122(1): 63-70.

7. Akao, Y., Nakagawa, Y., Naoe, T. (2006). let-7 microRNA functions as a potential growth suppressor in human colon cancer cells. Biol Pharm Bull 29(5): 903-6.

8. Alcorta, D. A., Xiong, Y., Phelps, D., Hannon, G., Beach, D., et al. (1996). Involvement of the cyclin-dependent kinase inhibitor p16 (INK4a) in replicative senescence of normal human fibroblasts. Proc Natl Acad Sci U S A 93(24): 13742-7.

9. Ambros, V. (2003). MicroRNA pathways in flies and worms: growth, death, fat, stress, and timing. Cell 113(6): 673-6.

10. American Veterinary Medical Association (2008). US pet ownership and demographics sourcebook 2007. Schaumburg, Illinois: American Veterinary Medical Association.

11. Anastasi, S., Sala, G., Huiping, C., Caprini, E., Russo, G., et al. (2005). Loss of RALT/MIG-6 expression in ERBB2-amplified breast carcinomas enhances ErbB-2 oncogenic potency and favors resistance to Herceptin. Oncogene 24(28): 4540-8.

12. Bartel, D. P. (2004). MicroRNAs: genomics, biogenesis, mechanism, and function. Cell 116(2): 281-97.

13. Bates, S., Parry, D., Bonetta, L., Vousden, K., Dickson, C., et al. (1994). Absence of cyclin D/cdk complexes in cells lacking functional retinoblastoma protein. Oncogene 9(6): 1633-40.

14. Beck, J., Hennecke, S., Bornemann-Kolatzki, K., Urnovitz, H. B., Neumann, S., et al. (2013). Genome aberrations in canine mammary carcinomas and their detection in cell-free plasma DNA. PLoS One 8(9): e75485.

15. Bergman, P. J. (2007). Canine oral melanoma. Clin Tech Small Anim Pract 22(2): 55-60.

16. Bird, R. C., Deinnocentes, P., Lenz, S., Thacker, E. E., Curiel, D. T., et al. (2008). An allogeneic hybrid-cell fusion vaccine against canine mammary cancer. Vet Immunol Immunopathol 123(3-4): 289-304.

17. Birney, E., Stamatoyannopoulos, J. A., Dutta, A., Guigo, R., Gingeras, T. R., et al. (2007). Identification and analysis of functional elements in 1% of the human genome by the ENCODE pilot project. Nature 447(7146): 799-816.

18. Blagosklonny, M. V. (2011). Cell cycle arrest is not senescence. Aging (Albany NY) 3(2): 94-101.

19. Boggs, R. M., Wright, Z. M., Stickney, M. J., Porter, W. W., Murphy, K. E. (2008). MicroRNA expression in canine mammary cancer. Mamm Genome 19(7-8): 561-9.

20. Bringold, F., Serrano, M. (2000). Tumor suppressors and oncogenes in cellular senescence. Exp Gerontol 35(3): 317-29.

21. Bueno, M. J., Malumbres, M. (2011). MicroRNAs and the cell cycle. Biochim Biophys Acta 1812(5): 592-601.

22. Burk, U., Schubert, J., Wellner, U., Schmalhofer, O., Vincan, E., et al. (2008). A reciprocal repression between ZEB1 and members of the miR-200 family promotes EMT and invasion in cancer cells. EMBO Rep 9(6): 582-9.

23. Byeon, I. J., Li, J., Ericson, K., Selby, T. L., Tevelev, A., et al. (1998). Tumor suppressor p16INK4A: determination of solution structure and analyses of its interaction with cyclin-dependent kinase 4. Mol Cell 1(3): 421-31.

24. Cairns, P., Mao, L., Merlo, A., Lee, D. J., Schwab, D., et al. (1994). Rates of p16 (MTS1) mutations in primary tumors with 9p loss. Science 265(5170): 415-7.

25. Caldas, C., Hahn, S. A., da Costa, L. T., Redston, M. S., Schutte, M., et al. (1994). Frequent somatic mutations and homozygous deletions of the p16 (MTS1) gene in pancreatic adenocarcinoma. Nat Genet 8(1): 27-32.

26. Calin, G. A., Dumitru, C. D., Shimizu, M., Bichi, R., Zupo, S., et al. (2002). Frequent deletions and down-regulation of micro- RNA genes miR15 and miR16 at 13q14 in chronic lymphocytic leukemia. Proc Natl Acad Sci U S A 99(24): 15524-9.

27. Calin, G. A., Ferracin, M., Cimmino, A., Di Leva, G., Shimizu, M., et al. (2005). A MicroRNA signature associated with prognosis and progression in chronic lymphocytic leukemia. N Engl J Med 353(17): 1793-801.

28. Calin, G. A., Liu, C. G., Sevignani, C., Ferracin, M., Felli, N., et al. (2004a). MicroRNA profiling reveals distinct signatures in B cell chronic lymphocytic leukemias. Proc Natl Acad Sci U S A 101(32): 11755-60.

29. Calin, G. A., Sevignani, C., Dumitru, C. D., Hyslop, T., Noch, E., et al. (2004). Human microRNA genes are frequently located at fragile sites and genomic regions involved in cancers. Proc Natl Acad Sci U S A 101(9): 2999-3004.

30. Campbell, I., Magliocco, A., Moyana, T., Zheng, C., Xiang, J. (2000). Adenovirus-mediated p16INK4 gene transfer significantly suppresses human breast cancer growth. Cancer Gene Ther 7(9): 1270-8.

31. Campisi, J. (2000). Cancer, aging and cellular senescence. In Vivo 14(1): 183-8.

32. Campisi, J. (2001). Cellular senescence as a tumor-suppressor mechanism. Trends Cell Biol 11(11): S27-31.

33. Carrera, C. J., Eddy, R. L., Shows, T. B., Carson, D. A. (1984). Assignment of the gene for methylthioadenosine phosphorylase to human chromosome 9 by mouse-human somatic cell hybridization. Proc Natl Acad Sci U S A 81(9): 2665-8.

34. Carthew, R. W. (2006). Gene regulation by microRNAs. Curr Opin Genet Dev 16(2): 203-8.

35. Chan, F. K., Zhang, J., Cheng, L., Shapiro, D. N., Winoto, A. (1995). Identification of human and mouse p19, a novel CDK4 and CDK6 inhibitor with homology to p16ink4. Mol Cell Biol 15(5): 2682-8.

36. Chan, J. A., Krichevsky, A. M., Kosik, K. S. (2005). MicroRNA-21 is an antiapoptotic factor in human glioblastoma cells. Cancer Res 65(14): 6029-33.

37. Chang, T. C., Wentzel, E. A., Kent, O. A., Ramachandran, K., Mullendore, M., et al. (2007). Transactivation of miR-34a by p53 broadly influences gene expression and promotes apoptosis. Mol Cell 26(5): 745-52.

38. Cheetham, S. W., Gruhl, F., Mattick, J. S., Dinger, M. E. (2013). Long noncoding RNAs and the genetics of cancer. Br J Cancer 108(12): 2419-25.

39. Chendrimada, T. P., Gregory, R. I., Kumaraswamy, E., Norman, J., Cooch, N., et al. (2005). TRBP recruits the Dicer complex to Ago2 for microRNA processing and gene silencing. Nature 436(7051): 740-4.

40. Chin, L., Pomerantz, J., Polsky, D., Jacobson, M., Cohen, C., et al. (1997). Cooperative effects of INK4a and ras in melanoma susceptibility in vivo. Genes Dev 11(21): 2822-34.

41. Chiyomaru, T., Fukuhara, S., Saini, S., Majid, S., Deng, G., et al. (2014). Long non-coding RNA HOTAIR is targeted and regulated by miR-141 in human cancer cells. J Biol Chem 289(18): 12550-65.

42. Ciafre, S. A., Galardi, S., Mangiola, A., Ferracin, M., Liu, C. G., et al. (2005). Extensive modulation of a set of microRNAs in primary glioblastoma. Biochem Biophys Res Commun 334(4): 1351-8.

43. Coller, H. A., Sang, L., Roberts, J. M. (2006). A new description of cellular quiescence. PLoS Biol 4(3): e83.

44. Collins, K., Jacks, T., Pavletich, N. P. (1997). The cell cycle and cancer. Proc Natl Acad Sci U S A 94(7): 2776-8.

45. Costa, F. F. (2010). Non-coding RNAs: Meet thy masters. Bioessays 32(7): 599-608.

46. Creighton, C. J., Fountain, M. D., Yu, Z., Nagaraja, A. K., Zhu, H., et al. (2010). Molecular profiling uncovers a p53-associated role for microRNA-31 in inhibiting the proliferation of serous ovarian carcinomas and other cancers. Cancer Res 70(5): 1906-15.

47. Croce, C. M., Calin, G. A. (2005). miRNAs, cancer, and stem cell division. Cell 122(1): 6-7.

48. Cullen, B. R. (2004). Transcription and processing of human microRNA precursors. Mol Cell 16(6): 861-5.

49. Cullen, J. M., Page, R., Misdorp, W. (2002). An overview of cancer pathogenesis, diagnosis and management. In: Moulton D. J., editor. Tumors in Domestic Animals. Iowa State Press, USA: Blackwell Publishing Company. pp. 3-45.

50. Cummins, J. M., He, Y., Leary, R. J., Pagliarini, R., Diaz, L. A., Jr., et al. (2006). The colorectal microRNAome. Proc Natl Acad Sci U S A 103(10): 3687-92.

51. Dalman, M. R., Deeter, A., Nimishakavi, G., Duan, Z. H. (2012). Fold change and p-value cutoffs significantly alter microarray interpretations. BMC Bioinformatics 13 (Suppl 2): S11.

52. Davoren, P. A., McNeill, R. E., Lowery, A. J., Kerin, M. J., Miller, N. (2008). Identification of suitable endogenous control genes for microRNA gene expression analysis in human breast cancer. BMC Mol Biol 9(76).

53. DeInnocentes, P., Agarwal, P., Bird, R. C. (2009). Phenotype-rescue of cyclin-dependent kinase inhibitor p16/INK4A defects in a spontaneous canine cell model of breast cancer. J Cell Biochem 106(3): 491-505.

54. DeInnocentes, P., Li, L. X., Sanchez, R. L., Bird, R. C. (2006). Expression and sequence of canine SIRT2 and p53 genes in canine mammary tumour cells - effects on downstream targets Wip1 and p21/Cip1. Vet Comp Oncol 4(3): 161-77.

55. Diaz, M. O., Ziemin, S., Le Beau, M. M., Pitha, P., Smith, S. D., et al. (1988). Homozygous deletion of the alpha- and beta 1-interferon genes in human leukemia and derived cell lines. Proc Natl Acad Sci U S A 85(14): 5259-63.

56. Dreyling, M. H., Bohlander, S. K., Adeyanju, M. O., Olopade, O. I. (1995). Detection of CDKN2 deletions in tumor cell lines and primary glioma by interphase fluorescence in situ hybridization. Cancer Res 55(5): 984-8.

57. Du, T., Zamore, P. D. (2005). microPrimer: the biogenesis and function of microRNA. Development 132(21): 4645-52.

58. Ebert, M. S., Neilson, J. R., Sharp, P. A. (2007). MicroRNA sponges: competitive inhibitors of small RNAs in mammalian cells. Nat Methods 4(9): 721-6.

59. el-Deiry, W. S., Tokino, T., Velculescu, V. E., Levy, D. B., Parsons, R., et al. (1993). WAF1, a potential mediator of p53 tumor suppression. Cell 75(4): 817-25.

60. Elledge, S. J. (1996). Cell cycle checkpoints: preventing an identity crisis. Science 274(5293): 1664-72.

61. England, N. L., Cuthbert, A. P., Trott, D. A., Jezzard, S., Nobori, T., et al. (1996). Identification of human tumour suppressor genes by monochromosome transfer: rapid growth-arrest response mapped to 9p21 is mediated solely by the cyclin-D-dependent kinase inhibitor gene, CDKN2A (p16INK4A). Carcinogenesis 17(8): 1567-75.

62. Esquela-Kerscher, A., Slack, F. J. (2006). Oncomirs - microRNAs with a role in cancer. Nat Rev Cancer 6(4): 259-69.

63. Esteller, M. (2011). Non-coding RNAs in human disease. Nat Rev Genet 12(12): 861-74.

64. Esteller, M., Cordon-Cardo, C., Corn, P. G., Meltzer, S. J., Pohar, K. S., et al. (2001). p14ARF silencing by promoter hypermethylation mediates abnormal intracellular localization of MDM2. Cancer Res 61(7): 2816-21.

65. Esteller, M., Tortola, S., Toyota, M., Capella, G., Peinado, M. A., et al. (2000). Hypermethylation-associated inactivation of p14(ARF) is independent of p16(INK4a) methylation and p53 mutational status. Cancer Res 60(1): 129-33.

66. Fabian, M. R., Sonenberg, N., Filipowicz, W. (2010). Regulation of mRNA translation and stability by microRNAs. Annu Rev Biochem 79(351-79).

67. Foote, J. B., Kabir, F. M., Graff, E. C., Cattley, R. C., DeInnocentes, P., et al. (2014). Engraftment of canine peripheral blood lymphocytes into nonobese diabetic-severe combined immune deficient IL-2R common gamma chain null mice. Vet Immunol Immunopathol 157(3-4): 131-41.

68. Fosmire, S. P., Thomas, R., Jubala, C. M., Wojcieszyn, J. W., Valli, V. E., et al. (2007). Inactivation of the p16 cyclin-dependent kinase inhibitor in high-grade canine non-Hodgkin's T-cell lymphoma. Vet Pathol 44(4): 467-78.

69. Frankel, L. B., Christoffersen, N. R., Jacobsen, A., Lindow, M., Krogh, A., et al. (2008). Programmed cell death 4 (PDCD4) is an important functional target of the microRNA miR-21 in breast cancer cells. J Biol Chem 283(2): 1026-33.

70. Friedman, R. C., Farh, K. K., Burge, C. B., Bartel, D. P. (2009). Most mammalian mRNAs are conserved targets of microRNAs. Genome Res 19(1): 92-105.

71. Gama, A., Alves, A., Schmitt, F. (2008). Identification of molecular phenotypes in canine mammary carcinomas with clinical implications: application of the human classification. Virchows Arch 453(2): 123-32.

72. Garcia, D. M., Baek, D., Shin, C., Bell, G. W., Grimson, A., et al. (2011). Weak seed-pairing stability and high target-site abundance decrease the proficiency of lsy-6 and other microRNAs. Nat Struct Mol Biol 18(10): 1139-46.

73. Gartel, A. L., Tyner, A. L. (2002). The role of the cyclin-dependent kinase inhibitor p21 in apoptosis. Mol Cancer Ther 1(8): 639-49.

74. Garzon, R., Calin, G. A., Croce, C. M. (2009). MicroRNAs in Cancer. Annu Rev Med 60(167-79.

75. Garzon, R., Garofalo, M., Martelli, M. P., Briesewitz, R., Wang, L., et al. (2008). Distinctive microRNA signature of acute myeloid leukemia bearing cytoplasmic mutated nucleophosmin. Proc Natl Acad Sci U S A 105(10): 3945-50.

76. Gasteiger, E., Hoogland, C., Gattiker, A., Duvaud, S., Wilkins, M. R., et al. (2005). Protein Identification and Analysis Tools on the ExPASy Server. In: Walker J. M., editor. The Proteomics Protocols Handbook New Jersey: Humana Press. pp. 571-607.

77. Gee, H. E., Buffa, F. M., Camps, C., Ramachandran, A., Leek, R., et al. (2011). The small-nucleolar RNAs commonly used for microRNA normalisation correlate with tumour pathology and prognosis. Br J Cancer 104(7): 1168-77.

78. Gibb, E. A., Brown, C. J., Lam, W. L. (2011). The functional role of long non-coding RNA in human carcinomas. Mol Cancer 10(38.

79. Gilbertson, S. R., Kurzman, I. D., Zachrau, R. E., Hurvitz, A. I., Black, M. M. (1983). Canine mammary epithelial neoplasms: biologic implications of morphologic characteristics assessed in 232 dogs. Vet Pathol 20(2): 127-42.

80. Gilley, J., Fried, M. (2001). One INK4 gene and no ARF at the Fugu equivalent of the human INK4A/ARF/INK4B tumour suppressor locus. Oncogene 20(50): 7447-52.

81. Goldstein, S. (1990). Replicative senescence: the human fibroblast comes of age. Science 249(4973): 1129-33.

82. Gottardis, M. M., Robinson, S. P., Jordan, V. C. (1988). Estradiol-stimulated growth of MCF-7 tumors implanted in athymic mice: a model to study the tumoristatic action of tamoxifen. J Steroid Biochem 30(1-6): 311-4.

83. Grimson, A., Farh, K. K., Johnston, W. K., Garrett-Engele, P., Lim, L. P., et al. (2007). MicroRNA targeting specificity in mammals: determinants beyond seed pairing. Mol Cell 27(1): 91-105.

84. Gu, Y., Turck, C. W., Morgan, D. O. (1993). Inhibition of CDK2 activity in vivo by an associated 20K regulatory subunit. Nature 366(6456): 707-10.

85. Guan, K. L., Jenkins, C. W., Li, Y., Nichols, M. A., Wu, X., et al. (1994). Growth suppression by p18, a p16INK4/MTS1- and p14INK4B/MTS2-related CDK6 inhibitor, correlates with wild-type pRb function. Genes Dev 8(24): 2939-52.

86. Guan, K. L., Jenkins, C. W., Li, Y., O'Keefe, C. L., Noh, S., et al. (1996). Isolation and characterization of p19INK4d, a p16-related inhibitor specific to CDK6 and CDK4. Mol Biol Cell 7(1): 57-70.

87. Gupta, R. A., Shah, N., Wang, K. C., Kim, J., Horlings, H. M., et al. (2010). Long non-coding RNA HOTAIR reprograms chromatin state to promote cancer metastasis. Nature 464(7291): 1071-6.

88. Guruprasad, K., Reddy, B. V., Pandit, M. W. (1990). Correlation between stability of a protein and its dipeptide composition: a novel approach for predicting in vivo stability of a protein from its primary sequence. Protein Eng 4(2): 155-61.

89. Haga, S., Nakayama, M., Tatsumi, K., Maeda, M., Imai, S., et al. (2001). Overexpression of the p53 gene product in canine mammary tumors. Oncol Rep 8(6): 1215-9.

90. Hahn, K. A., Bravo, L., Adams, W. H., Frazier, D. L. (1994). Naturally occurring tumors in dogs as comparative models for cancer therapy research. In Vivo 8(1): 133-43.

91. Hammond, S. M., Bernstein, E., Beach, D., Hannon, G. J. (2000). An RNA-directed nuclease mediates post-transcriptional gene silencing in Drosophila cells. Nature 404(6775): 293-6.

92. Hannon, G. J., Beach, D. (1994). p15INK4B is a potential effector of TGF-beta-induced cell cycle arrest. Nature 371(6494): 257-61.

93. Hara, E., Smith, R., Parry, D., Tahara, H., Stone, S., et al. (1996). Regulation of p16CDKN2 expression and its implications for cell immortalization and senescence. Mol Cell Biol 16(3): 859-67.

94. Harper, J. W., Adami, G. R., Wei, N., Keyomarsi, K., Elledge, S. J. (1993). The p21 Cdk-interacting protein Cip1 is a potent inhibitor of G1 cyclin-dependent kinases. Cell 75(4): 805-16.

95. Harper, J. W., Elledge, S. J. (1996). Cdk inhibitors in development and cancer. Curr Opin Genet Dev 6(1): 56-64.

96. Harquail, J., Benzina, S., Robichaud, G. A. (2012). MicroRNAs and breast cancer malignancy: an overview of miRNA-regulated cancer processes leading to metastasis. Cancer Biomark 11(6): 269-80.

97. Harris, H. (1988). The analysis of malignancy by cell fusion: the position in 1988. Cancer Res 48(12): 3302-6.

98. Harrow, J., Frankish, A., Gonzalez, J. M., Tapanari, E., Diekhans, M., et al. (2012). GENCODE: the reference human genome annotation for The ENCODE Project. Genome Res 22(9): 1760-74.

99. Hartwell, L. (1992). Defects in a cell cycle checkpoint may be responsible for the genomic instability of cancer cells. Cell 71(4): 543-6.

100. Hatfield, S. D., Shcherbata, H. R., Fischer, K. A., Nakahara, K., Carthew, R. W., et al. (2005). Stem cell division is regulated by the microRNA pathway. Nature 435(7044): 974-8.

101. Hatta, Y., Hirama, T., Miller, C. W., Yamada, Y., Tomonaga, M., et al. (1995). Homozygous deletions of the p15 (MTS2) and p16 (CDKN2/MTS1) genes in adult T-cell leukemia. Blood 85(10): 2699-704.

102. Hayflick, L. (1965). The Limited in Vitro Lifetime of Human Diploid Cell Strains. Exp Cell Res 37(614-36.

103. He, L., He, X., Lim, L. P., de Stanchina, E., Xuan, Z., et al. (2007). A microRNA component of the p53 tumour suppressor network. Nature 447(7148): 1130-4.

104. Herzog, C. R., Noh, S., Lantry, L. E., Guan, K. L., You, M. (1999). Cdkn2a encodes functional variation of p16INK4a but not p19ARF, which confers selection in mouse lung tumorigenesis. Mol Carcinog 25(2): 92-8.

105. Hirai, H., Roussel, M. F., Kato, J. Y., Ashmun, R. A., Sherr, C. J. (1995). Novel INK4 proteins, p19 and p18, are specific inhibitors of the cyclin D-dependent kinases CDK4 and CDK6. Mol Cell Biol 15(5): 2672-81.

106. Holliday, D. L., Speirs, V. (2011). Choosing the right cell line for breast cancer research. Breast Cancer Res 13(4): 215.

107. Hsu, P. W., Huang, H. D., Hsu, S. D., Lin, L. Z., Tsou, A. P., et al. (2006). miRNAMap: genomic maps of microRNA genes and their target genes in mammalian genomes. Nucleic Acids Res 34(Database issue): D135-9.

108. Hunter, T., Pines, J. (1994). Cyclins and cancer. II: Cyclin D and CDK inhibitors come of age. Cell 79(4): 573-82.

109. Hussussian, C. J., Struewing, J. P., Goldstein, A. M., Higgins, P. A., Ally, D. S., et al. (1994). Germline p16 mutations in familial melanoma. Nat Genet 8(1): 15-21.

110. Hutvagner, G., Zamore, P. D. (2002). A microRNA in a multiple-turnover RNAi enzyme complex. Science 297(5589): 2056-60.

111. Iorio, M. V., Ferracin, M., Liu, C. G., Veronese, A., Spizzo, R., et al. (2005). MicroRNA gene expression deregulation in human breast cancer. Cancer Res 65(16): 7065-70.

112. Ishikawa, F., Yasukawa, M., Lyons, B., Yoshida, S., Miyamoto, T., et al. (2005). Development of functional human blood and immune systems in NOD/SCID/IL2 receptor {gamma} chain(null) mice. Blood 106(5): 1565-73.

113. James, C. D., He, J., Carlbom, E., Nordenskjold, M., Cavenee, W. K., et al. (1991). Chromosome 9 deletion mapping reveals interferon alpha and interferon beta-1 gene deletions in human glial tumors. Cancer Res 51(6): 1684-8.

114. Jemal, A., Siegel, R., Ward, E., Murray, T., Xu, J., et al. (2007). Cancer statistics, 2007. CA Cancer J Clin 57(1): 43-66.

115. Jenkins, D. E., Hornig, Y. S., Oei, Y., Dusich, J., Purchio, T. (2005). Bioluminescent human breast cancer cell lines that permit rapid and sensitive in vivo detection of mammary tumors and multiple metastases in immune deficient mice. Breast Cancer Res 7(4): R444-54.

116. Jin, X., Nguyen, D., Zhang, W. W., Kyritsis, A. P., Roth, J. A. (1995). Cell cycle arrest and inhibition of tumor cell proliferation by the p16INK4 gene mediated by an adenovirus vector. Cancer Res 55(15): 3250-3.

117. Johnson, S. M., Grosshans, H., Shingara, J., Byrom, M., Jarvis, R., et al. (2005). RAS is regulated by the let-7 microRNA family. Cell 120(5): 635-47.

118. Jovanovic, M., Hengartner, M. O. (2006). miRNAs and apoptosis: RNAs to die for. Oncogene 25(46): 6176-87.

119. Kamb, A., Gruis, N. A., Weaver-Feldhaus, J., Liu, Q., Harshman, K., et al. (1994). A cell cycle regulator potentially involved in genesis of many tumor types. Science 264(5157): 436-40.

120. Kamb, A., Shattuck-Eidens, D., Eeles, R., Liu, Q., Gruis, N. A., et al. (1994a). Analysis of the p16 gene (CDKN2) as a candidate for the chromosome 9p melanoma susceptibility locus. Nat Genet 8(1): 23-6.

121. Kamijo, T., Weber, J. D., Zambetti, G., Zindy, F., Roussel, M. F., et al. (1998). Functional and physical interactions of the ARF tumor suppressor with p53 and Mdm2. Proc Natl Acad Sci U S A 95(14): 8292-7.

122. Kamijo, T., Zindy, F., Roussel, M. F., Quelle, D. E., Downing, J. R., et al. (1997). Tumor suppression at the mouse INK4a locus mediated by the alternative reading frame product p19ARF. Cell 91(5): 649-59.

123. Kao, J., Salari, K., Bocanegra, M., Choi, Y. L., Girard, L., et al. (2009). Molecular profiling of breast cancer cell lines defines relevant tumor models and provides a resource for cancer gene discovery. PLoS One 4(7): e6146.

124. Kelley, L. A., MacCallum, R. M., Sternberg, M. J. (2000). Enhanced genome annotation using structural profiles in the program 3D-PSSM. J Mol Biol 299(2): 499-520.

125. Kelley, L. A., Sternberg, M. J. (2009). Protein structure prediction on the Web: a case study using the Phyre server. Nat Protoc 4(3): 363-71.

126. Kent, O. A., Mendell, J. T. (2006). A small piece in the cancer puzzle: microRNAs as tumor suppressors and oncogenes. Oncogene 25(46): 6188-96.

127. Khanna, C., Lindblad-Toh, K., Vail, D., London, C., Bergman, P., et al. (2006). The dog as a cancer model. Nat Biotechnol 24(9): 1065-6.

128. King, M., Pearson, T., Shultz, L. D., Leif, J., Bottino, R., et al. (2008). A new Hu-PBL model for the study of human islet alloreactivity based on NOD-scid mice bearing a targeted mutation in the IL-2 receptor gamma chain gene. Clin Immunol 126(3): 303-14.

129. Kinzler, K. W., Vogelstein, B. (1997). Cancer-susceptibility genes. Gatekeepers and caretakers. Nature 386(6627): 761, 63.

130. Klopfleisch, R., Gruber, A. D. (2009). Differential expression of cell cycle regulators p21, p27 and p53 in metastasizing canine mammary adenocarcinomas versus normal mammary glands. Res Vet Sci 87(1): 91-6.

131. Klopfleisch, R., Lenze, D., Hummel, M., Gruber, A. D. (2010). Metastatic canine mammary carcinomas can be identified by a gene expression profile that partly overlaps with human breast cancer profiles. BMC Cancer 10(618.

132. Kluiver, J., Poppema, S., de Jong, D., Blokzijl, T., Harms, G., et al. (2005). BIC and miR-155 are highly expressed in Hodgkin, primary mediastinal and diffuse large B cell lymphomas. J Pathol 207(2): 243-9.

133. Koenig, A., Bianco, S. R., Fosmire, S., Wojcieszyn, J., Modiano, J. F. (2002). Expression and significance of p53, rb, p21/waf-1, p16/ink-4a, and PTEN tumor suppressors in canine melanoma. Vet Pathol 39(4): 458-72.

134. Koh, J., Enders, G. H., Dynlacht, B. D., Harlow, E. (1995). Tumour-derived p16 alleles encoding proteins defective in cell-cycle inhibition. Nature 375(6531): 506-10.

135. Korbie, D. J., Mattick, J. S. (2008). Touchdown PCR for increased specificity and sensitivity in PCR amplification. Nat Protoc 3(9): 1452-6.

136. Krimpenfort, P., Quon, K. C., Mooi, W. J., Loonstra, A., Berns, A. (2001). Loss of p16Ink4a confers susceptibility to metastatic melanoma in mice. Nature 413(6851): 83-6.

137. LaConti, J. J., Shivapurkar, N., Preet, A., Deslattes Mays, A., Peran, I., et al. (2011). Tissue and serum microRNAs in the Kras(G12D) transgenic animal model and in patients with pancreatic cancer. PLoS One 6(6): e20687.

138. Lagos-Quintana, M., Rauhut, R., Lendeckel, W., Tuschl, T. (2001). Identification of novel genes coding for small expressed RNAs. Science 294(5543): 853-8.

139. Lal, A., Kim, H. H., Abdelmohsen, K., Kuwano, Y., Pullmann, R., Jr., et al. (2008). p16(INK4a) translation suppressed by miR-24. PLoS One 3(3): e1864.

140. Laurila, E. M., Kallioniemi, A. (2013). The diverse role of miR-31 in regulating cancer associated phenotypes. Genes Chromosomes Cancer 52(12): 1103-13.

141. Lee, R. C., Feinbaum, R. L., Ambros, V. (1993). The C. elegans heterochronic gene lin-4 encodes small RNAs with antisense complementarity to lin-14. Cell 75(5): 843-54.

142. Lee, Y., Ahn, C., Han, J., Choi, H., Kim, J., et al. (2003). The nuclear RNase III Drosha initiates microRNA processing. Nature 425(6956): 415-9.

143. Lee, Y. S., Dutta, A. (2007). The tumor suppressor microRNA let-7 represses the HMGA2 oncogene. Genes Dev 21(9): 1025-30.

144. Levine, R. A., Fleischli, M. A. (2000). Inactivation of p53 and retinoblastoma family pathways in canine osteosarcoma cell lines. Vet Pathol 37(1): 54-61.

145. Lewis, B. P., Burge, C. B., Bartel, D. P. (2005). Conserved seed pairing, often flanked by adenosines, indicates that thousands of human genes are microRNA targets. Cell 120(1): 15-20.

146. Li, L., Yuan, L., Luo, J., Gao, J., Guo, J., et al. (2013). MiR-34a inhibits proliferation and migration of breast cancer through down-regulation of Bcl-2 and SIRT1. Clin Exp Med 13(2): 109-17.

147. Lilischkis, R., Sarcevic, B., Kennedy, C., Warlters, A., Sutherland, R. L. (1996). Cancer-associated mis-sense and deletion mutations impair p16INK4 CDK inhibitory activity. Int J Cancer 66(2): 249-54.

148. Lindblad-Toh, K., Wade, C. M., Mikkelsen, T. S., Karlsson, E. K., Jaffe, D. B., et al. (2005). Genome sequence, comparative analysis and haplotype structure of the domestic dog. Nature 438(7069): 803-19.

149. Linsley, P. S., Schelter, J., Burchard, J., Kibukawa, M., Martin, M. M., et al. (2007). Transcripts targeted by the microRNA-16 family cooperatively regulate cell cycle progression. Mol Cell Biol 27(6): 2240-52.

150. Liu, L., Lassam, N. J., Slingerland, J. M., Bailey, D., Cole, D., et al. (1995). Germline p16INK4A mutation and protein dysfunction in a family with inherited melanoma. Oncogene 11(2): 405-12.

151. Liu, Q., Fu, H., Sun, F., Zhang, H., Tie, Y., et al. (2008). miR-16 family induces cell cycle arrest by regulating multiple cell cycle genes. Nucleic Acids Res 36(16): 5391-404.

152. Llanos, S., Clark, P. A., Rowe, J., Peters, G. (2001). Stabilization of p53 by p14ARF without relocation of MDM2 to the nucleolus. Nat Cell Biol 3(5): 445-52.

153. Lomas, J., Martin-Duque, P., Pons, M., Quintanilla, M. (2008). The genetics of malignant melanoma. Front Biosci 13(5071-93.

154. Loughran, O., Edington, K. G., Berry, I. J., Clark, L. J., Parkinson, E. K. (1994). Loss of heterozygosity of chromosome 9p21 is associated with the immortal phenotype of neoplastic human head and neck keratinocytes. Cancer Res 54(19): 5045-9.

155. Loughran, O., Malliri, A., Owens, D., Gallimore, P. H., Stanley, M. A., et al. (1996). Association of CDKN2A/p16INK4A with human head and neck keratinocyte replicative senescence: relationship of dysfunction to immortality and neoplasia. Oncogene 13(3): 561-8.

156. Lu, J., Getz, G., Miska, E. A., Alvarez-Saavedra, E., Lamb, J., et al. (2005). MicroRNA expression profiles classify human cancers. Nature 435(7043): 834-8.

157. Lujambio, A., Ropero, S., Ballestar, E., Fraga, M. F., Cerrato, C., et al. (2007). Genetic unmasking of an epigenetically silenced microRNA in human cancer cells. Cancer Res 67(4): 1424-9.

158. Lukas, J., Parry, D., Aagaard, L., Mann, D. J., Bartkova, J., et al. (1995). Retinoblastoma-protein-dependent cell-cycle inhibition by the tumour suppressor p16. Nature 375(6531): 503-6.

159. Lund, E., Guttinger, S., Calado, A., Dahlberg, J. E., Kutay, U. (2004). Nuclear export of microRNA precursors. Science 303(5654): 95-8.

160. Lundberg, A. S., Hahn, W. C., Gupta, P., Weinberg, R. A. (2000). Genes involved in senescence and immortalization. Curr Opin Cell Biol 12(6): 705-9.

161. Lutful Kabir, F. M., Agarwal, P., Deinnocentes, P., Zaman, J., Bird, A. C., et al. (2013). Novel frameshift mutation in the p16/INK4A tumor suppressor gene in canine breast cancer alters expression from the p16/INK4A/p14ARF locus. J Cell Biochem 114(1): 56-66.

162. Ma, L., Young, J., Prabhala, H., Pan, E., Mestdagh, P., et al. (2010). miR-9, a MYC/MYCN-activated microRNA, regulates E-cadherin and cancer metastasis. Nat Cell Biol 12(3): 247-56.

163. MacEwen, E. G. (1990). Spontaneous tumors in dogs and cats: models for the study of cancer biology and treatment. Cancer Metastasis Rev 9(2): 125-36.

164. Malhas, A., Saunders, N. J., Vaux, D. J. (2010). The nuclear envelope can control gene expression and cell cycle progression via miRNA regulation. Cell Cycle 9(3): 531-9.

165. Mao, L., Merlo, A., Bedi, G., Shapiro, G. I., Edwards, C. D., et al. (1995). A novel p16INK4A transcript. Cancer Res 55(14): 2995-7.

166. Mareel, M., Leroy, A. (2003). Clinical, cellular, and molecular aspects of cancer invasion. Physiol Rev 83(2): 337-76.

167. Martello, G., Rosato, A., Ferrari, F., Manfrin, A., Cordenonsi, M., et al. (2010). A MicroRNA targeting dicer for metastasis control. Cell 141(7): 1195-207.

168. Matsuoka, S., Edwards, M. C., Bai, C., Parker, S., Zhang, P., et al. (1995). p57KIP2, a structurally distinct member of the p21CIP1 Cdk inhibitor family, is a candidate tumor suppressor gene. Genes Dev 9(6): 650-62.

169. McConnell, B. B., Gregory, F. J., Stott, F. J., Hara, E., Peters, G. (1999). Induced expression of p16(INK4a) inhibits both CDK4- and CDK2-associated kinase activity by reassortment of cyclin-CDK-inhibitor complexes. Mol Cell Biol 19(3): 1981-9.

170. McKeller, R. N., Fowler, J. L., Cunningham, J. J., Warner, N., Smeyne, R. J., et al. (2002). The Arf tumor suppressor gene promotes hyaloid vascular regression during mouse eye development. Proc Natl Acad Sci U S A 99(6): 3848-53.

171. Medema, R. H., Herrera, R. E., Lam, F., Weinberg, R. A. (1995). Growth suppression by p16ink4 requires functional retinoblastoma protein. Proc Natl Acad Sci U S A 92(14): 6289-93.

172. Meng, F., Henson, R., Wehbe-Janek, H., Ghoshal, K., Jacob, S. T., et al. (2007). MicroRNA-21 regulates expression of the PTEN tumor suppressor gene in human hepatocellular cancer. Gastroenterology 133(2): 647-58.

173. Mercer, T. R., Dinger, M. E., Sunkin, S. M., Mehler, M. F., Mattick, J. S. (2008). Specific expression of long noncoding RNAs in the mouse brain. Proc Natl Acad Sci U S A 105(2): 716-21.

174. Merlo, D. F., Rossi, L., Pellegrino, C., Ceppi, M., Cardellino, U., et al. (2008). Cancer incidence in pet dogs: findings of the Animal Tumor Registry of Genoa, Italy. J Vet Intern Med 22(4): 976-84.

175. Metzler, M., Wilda, M., Busch, K., Viehmann, S., Borkhardt, A. (2004). High expression of precursor microRNA-155/BIC RNA in children with Burkitt lymphoma. Genes Chromosomes Cancer 39(2): 167-9.

176. Meyerrose, T. E., Herrbrich, P., Hess, D. A., Nolta, J. A. (2003). Immune-deficient mouse models for analysis of human stem cells. Biotechniques 35(6): 1262-72.

177. Migone, F., Deinnocentes, P., Smith, B. F., Bird, R. C. (2006). Alterations in CDK1 expression and nuclear/nucleolar localization following induction in a spontaneous canine mammary cancer model. J Cell Biochem 98(3): 504-18.

178. Misdorp, W. (2002). Tumors of the mammary gland. In: Meuten D. J., editor. Tumors in Domestic Animals. Ames, Iowa: Iowa State Press. pp. 575-606.

179. Morey, L., Helin, K. (2010). Polycomb group protein-mediated repression of transcription. Trends Biochem Sci 35(6): 323-32.

180. Morgan, D. O. (1997). Cyclin-dependent kinases: engines, clocks, and microprocessors. Annu Rev Cell Dev Biol 13(261-91.

181. Nairn, R. S., Kazianis, S., McEntire, B. B., Della Coletta, L., Walter, R. B., et al. (1996). A CDKN2-like polymorphism in Xiphophorus LG V is associated with UV-B-induced melanoma formation in platyfish-swordtail hybrids. Proc Natl Acad Sci U S A 93(23): 13042-7.

182. Nelson, P. T., Baldwin, D. A., Scearce, L. M., Oberholtzer, J. C., Tobias, J. W., et al. (2004). Microarray-based, high-throughput gene expression profiling of microRNAs. Nat Methods 1(2): 155-61.

183. Niemeyer, G. P., Hudson, J., Bridgman, R., Spano, J., Nash, R. A., et al. (2001). Isolation and characterization of canine hematopoietic progenitor cells. Exp Hematol 29(6): 686-93.

184. Nobori, T., Miura, K., Wu, D. J., Lois, A., Takabayashi, K., et al. (1994). Deletions of the cyclin-dependent kinase-4 inhibitor gene in multiple human cancers. Nature 368(6473): 753-6.

185. Nobori, T., Takabayashi, K., Tran, P., Orvis, L., Batova, A., et al. (1996). Genomic cloning of methylthioadenosine phosphorylase: a purine metabolic enzyme deficient in multiple different cancers. Proc Natl Acad Sci U S A 93(12): 6203-8.

186. O'Donnell, K. A., Wentzel, E. A., Zeller, K. I., Dang, C. V., Mendell, J. T. (2005). c-Myc-regulated microRNAs modulate E2F1 expression. Nature 435(7043): 839-43.

187. Oesterreich, S., Fuqua, S. A. (1999). Tumor suppressor genes in breast cancer. Endocr Relat Cancer 6(3): 405-19.

188. Ogawa, S., Hirano, N., Sato, N., Takahashi, T., Hangaishi, A., et al. (1994). Homozygous loss of the cyclin-dependent kinase 4-inhibitor (p16) gene in human leukemias. Blood 84(8): 2431-5.

189. Okamoto, A., Demetrick, D. J., Spillare, E. A., Hagiwara, K., Hussain, S. P., et al. (1994). Mutations and altered expression of p16INK4 in human cancer. Proc Natl Acad Sci U S A 91(23): 11045-9.

190. Osborne, C. K., Hobbs, K., Clark, G. M. (1985). Effect of estrogens and antiestrogens on growth of human breast cancer cells in athymic nude mice. Cancer Res 45(2): 584-90.

191. Otterson, G. A., Kratzke, R. A., Coxon, A., Kim, Y. W., Kaye, F. J. (1994). Absence of p16INK4 protein is restricted to the subset of lung cancer lines that retains wildtype RB. Oncogene 9(11): 3375-8.

192. Owen, L. N. (1979). A comparative study of canine and human breast cancer. Invest Cell Pathol 2(4): 257-75.

193. Paoloni, M., Khanna, C. (2008). Translation of new cancer treatments from pet dogs to humans. Nat Rev Cancer 8(2): 147-56.

194. Pardee, A. B. (1989). G1 events and regulation of cell proliferation. Science 246(4930): 603-8.

195. Parry, D., Mahony, D., Wills, K., Lees, E. (1999). Cyclin D-CDK subunit arrangement is dependent on the availability of competing INK4 and p21 class inhibitors. Mol Cell Biol 19(3): 1775-83.

196. Perez-Sayans, M., Suarez-Penaranda, J. M., Gayoso-Diz, P., Barros-Angueira, F., Gandara-Rey, J. M., et al. (2011). p16(INK4a)/CDKN2 expression and its relationship with oral squamous cell carcinoma is our current knowledge enough? Cancer Lett 306(2): 134-41.

197. Pines, J., Hunter, T. (1991). Cyclin-dependent kinases: a new cell cycle motif? Trends Cell Biol 1(5): 117-21.

198. Pinho, S. S., Carvalho, S., Cabral, J., Reis, C. A., Gartner, F. (2012). Canine tumors: a spontaneous animal model of human carcinogenesis. Transl Res 159(3): 165-72.

199. Polyak, K., Kato, J. Y., Solomon, M. J., Sherr, C. J., Massague, J., et al. (1994). p27Kip1, a cyclin-Cdk inhibitor, links transforming growth factor-beta and contact inhibition to cell cycle arrest. Genes Dev 8(1): 9-22.

200. Pomerantz, J., Schreiber-Agus, N., Liegeois, N. J., Silverman, A., Alland, L., et al. (1998). The Ink4a tumor suppressor gene product, p19Arf, interacts with MDM2 and neutralizes MDM2's inhibition of p53. Cell 92(6): 713-23.

201. Prensner, J. R., Chinnaiyan, A. M. (2011). The emergence of lncRNAs in cancer biology. Cancer Discov 1(5): 391-407.

202. Qi, L., Bart, J., Tan, L. P., Platteel, I., Sluis, T., et al. (2009). Expression of miR-21 and its targets (PTEN, PDCD4, TM1) in flat epithelial atypia of the breast in relation to ductal carcinoma in situ and invasive carcinoma. BMC Cancer 9(163.

203. Quelle, D. E., Ashmun, R. A., Hannon, G. J., Rehberger, P. A., Trono, D., et al. (1995). Cloning and characterization of murine p16INK4a and p15INK4b genes. Oncogene 11(4): 635-45.

204. Quesnel, B., Preudhomme, C., Philippe, N., Vanrumbeke, M., Dervite, I., et al. (1995). p16 gene homozygous deletions in acute lymphoblastic leukemia. Blood 85(3): 657-63.

205. Ranade, K., Hussussian, C. J., Sikorski, R. S., Varmus, H. E., Goldstein, A. M., et al. (1995). Mutations associated with familial melanoma impair p16INK4 function. Nat Genet 10(1): 114-6.

206. Randerson-Moor, J. A., Harland, M., Williams, S., Cuthbert-Heavens, D., Sheridan, E., et al. (2001). A germline deletion of p14(ARF) but not CDKN2A in a melanoma-neural system tumour syndrome family. Hum Mol Genet 10(1): 55-62.

207. Rao, N. A., van Wolferen, M. E., van den Ham, R., van Leenen, D., Groot Koerkamp, M. J., et al. (2008). cDNA microarray profiles of canine mammary tumour cell lines reveal deregulated pathways pertaining to their phenotype. Anim Genet 39(4): 333-45.

208. Reczko, M., Maragkakis, M., Alexiou, P., Papadopoulos, G. L., Hatzigeorgiou, A. G. (2011). Accurate microRNA Target Prediction Using Detailed Binding Site Accessibility and Machine Learning on Proteomics Data. Front Genet 2(103.

209. Ressel, L., Millanta, F., Caleri, E., Innocenti, V. M., Poli, A. (2009). Reduced PTEN protein expression and its prognostic implications in canine and feline mammary tumors. Vet Pathol 46(5): 860-8.

210. Reznikoff, C. A., Yeager, T. R., Belair, C. D., Savelieva, E., Puthenveettil, J. A., et al. (1996). Elevated p16 at senescence and loss of p16 at immortalization in human

papillomavirus 16 E6, but not E7, transformed human uroepithelial cells. Cancer Res 56(13): 2886-90.

211. Rizos, H., Darmanian, A. P., Holland, E. A., Mann, G. J., Kefford, R. F. (2001). Mutations in the INK4a/ARF melanoma susceptibility locus functionally impair p14ARF. J Biol Chem 276(44): 41424-34.

212. Rocco, J. W., Sidransky, D. (2001). p16(MTS-1/CDKN2/INK4a) in cancer progression. Exp Cell Res 264(1): 42-55.

213. Ronnov-Jessen, L., Petersen, O. W., Bissell, M. J. (1996). Cellular changes involved in conversion of normal to malignant breast: importance of the stromal reaction. Physiol Rev 76(1): 69-125.

214. Rovira, C., Guida, M. C., Cayota, A. (2010). MicroRNAs and other small silencing RNAs in cancer. IUBMB Life 62(12): 859-68.

215. Rowell, J. L., McCarthy, D. O., Alvarez, C. E. (2011). Dog models of naturally occurring cancer. Trends Mol Med 17(7): 380-8.

216. Ruas, M., Peters, G. (1998). The p16INK4a/CDKN2A tumor suppressor and its relatives. Biochim Biophys Acta 1378(2): F115-77.

217. Russo, A. A., Tong, L., Lee, J. O., Jeffrey, P. D., Pavletich, N. P. (1998). Structural basis for inhibition of the cyclin-dependent kinase Cdk6 by the tumour suppressor p16INK4a. Nature 395(6699): 237-43.

218. Saal, L. H., Johansson, P., Holm, K., Gruvberger-Saal, S. K., She, Q. B., et al. (2007). Poor prognosis in carcinoma is associated with a gene expression signature of aberrant PTEN tumor suppressor pathway activity. Proc Natl Acad Sci U S A 104(18): 7564-9.

219. Sage, J., Miller, A. L., Perez-Mancera, P. A., Wysocki, J. M., Jacks, T. (2003). Acute mutation of retinoblastoma gene function is sufficient for cell cycle re-entry. Nature 424(6945): 223-8.

220. Saito, Y., Liang, G., Egger, G., Friedman, J. M., Chuang, J. C., et al. (2006). Specific activation of microRNA-127 with downregulation of the proto-oncogene BCL6 by chromatin-modifying drugs in human cancer cells. Cancer Cell 9(6): 435-43.

221. Sampson, V. B., Rong, N. H., Han, J., Yang, Q., Aris, V., et al. (2007). MicroRNA let-7a down-regulates MYC and reverts MYC-induced growth in Burkitt lymphoma cells. Cancer Res 67(20): 9762-70.

222. Sandberg, R., Neilson, J. R., Sarma, A., Sharp, P. A., Burge, C. B. (2008). Proliferating cells express mRNAs with shortened 3' untranslated regions and fewer microRNA target sites. Science 320(5883): 1643-7.

223. Santamaria, D., Ortega, S. (2006). Cyclins and CDKS in development and cancer: lessons from genetically modified mice. Front Biosci 11(1164-88.

224. Sarkar, S., Dey, B. K., Dutta, A. (2010). MiR-322/424 and -503 are induced during muscle differentiation and promote cell cycle quiescence and differentiation by down-regulation of Cdc25A. Mol Biol Cell 21(13): 2138-49.

225. Sarli, G., Preziosi, R., Benazzi, C., Castellani, G., Marcato, P. S. (2002). Prognostic value of histologic stage and proliferative activity in canine malignant mammary tumors. J Vet Diagn Invest 14(1): 25-34.

226. Sassi, F., Benazzi, C., Castellani, G., Sarli, G. (2010). Molecular-based tumour subtypes of canine mammary carcinomas assessed by immunohistochemistry. BMC Vet Res 6(5.

227. Schickel, R., Boyerinas, B., Park, S. M., Peter, M. E. (2008). MicroRNAs: key players in the immune system, differentiation, tumorigenesis and cell death. Oncogene 27(45): 5959-74.

228. Schmittgen, T. D., Jiang, J., Liu, Q., Yang, L. (2004). A high-throughput method to monitor the expression of microRNA precursors. Nucleic Acids Res 32(4): e43.

229. Serrano, M. (1997). The tumor suppressor protein p16INK4a. Exp Cell Res 237(1): 7-13.

230. Serrano, M. (2000). The INK4a/ARF locus in murine tumorigenesis. Carcinogenesis 21(5): 865-9.

231. Serrano, M., Gomez-Lahoz, E., DePinho, R. A., Beach, D., Bar-Sagi, D. (1995). Inhibition of ras-induced proliferation and cellular transformation by p16INK4. Science 267(5195): 249-52.

232. Serrano, M., Hannon, G. J., Beach, D. (1993). A new regulatory motif in cell-cycle control causing specific inhibition of cyclin D/CDK4. Nature 366(6456): 704-7.

233. Serrano, M., Lee, H., Chin, L., Cordon-Cardo, C., Beach, D., et al. (1996). Role of the INK4a locus in tumor suppression and cell mortality. Cell 85(1): 27-37.

234. Sharpless, E., Chin, L. (2003). The INK4a/ARF locus and melanoma. Oncogene 22(20): 3092-8.

235. Sharpless, N. E. (2005). INK4a/ARF: a multifunctional tumor suppressor locus. Mutat Res 576(1-2): 22-38.

236. Sharpless, N. E., Bardeesy, N., Lee, K. H., Carrasco, D., Castrillon, D. H., et al. (2001). Loss of p16Ink4a with retention of p19Arf predisposes mice to tumorigenesis. Nature 413(6851): 86-91.

237. Sharpless, N. E., DePinho, R. A. (1999). The INK4A/ARF locus and its two gene products. Curr Opin Genet Dev 9(1): 22-30.

238. Sharpless, N. E., DePinho, R. A. (2004). Telomeres, stem cells, senescence, and cancer. J Clin Invest 113(2): 160-8.

239. Shearin, A. L., Hedan, B., Cadieu, E., Erich, S. A., Schmidt, E. V., et al. (2012). The MTAP-CDKN2A locus confers susceptibility to a naturally occurring canine cancer. Cancer Epidemiol Biomarkers Prev 21(7): 1019-27.

240. Sherr, C. J. (1993). Mammalian G1 cyclins. Cell 73(6): 1059-65.

241. Sherr, C. J. (1994). G1 phase progression: cycling on cue. Cell 79(4): 551-5.

242. Sherr, C. J. (1996). Cancer cell cycles. Science 274(5293): 1672-7.

243. Sherr, C. J., Roberts, J. M. (1995). Inhibitors of mammalian G1 cyclin-dependent kinases. Genes Dev 9(10): 1149-63.

244. Sherr, C. J., Roberts, J. M. (1999). CDK inhibitors: positive and negative regulators of G1-phase progression. Genes Dev 13(12): 1501-12.

245. Shinoda, H., Legare, M. E., Mason, G. L., Berkbigler, J. L., Afzali, M. F., et al. (2014). Significance of ERalpha, HER2, and CAV1 expression and molecular subtype classification to canine mammary gland tumor. J Vet Diagn Invest 26(3): 390-403.

246. Shivapurkar, N., Weiner, L. M., Marshall, J. L., Madhavan, S., Deslattes Mays, A., et al. (2014). Recurrence of early stage colon cancer predicted by expression pattern of circulating microRNAs. PLoS One 9(1): e84686.

247. Shrout, T. A. (2013). Post-Transcriptional Regulation of Cardiac Sarcomere Protein Titin Through 3'Untranslated Regions. Vanderbilt Undergraduate Research Journal 9(Summer 2013): 1-12.

248. Shultz, L. D., Ishikawa, F., Greiner, D. L. (2007). Humanized mice in translational biomedical research. Nat Rev Immunol 7(2): 118-30.

249. Shultz, L. D., Lyons, B. L., Burzenski, L. M., Gott, B., Chen, X., et al. (2005). Human lymphoid and myeloid cell development in NOD/LtSz-scid IL2R gamma null mice engrafted with mobilized human hemopoietic stem cells. J Immunol 174(10): 6477-89.

250. Sleeckx, N., de Rooster, H., Veldhuis Kroeze, E. J., Van Ginneken, C., Van Brantegem, L. (2011). Canine mammary tumours, an overview. Reprod Domest Anim 46(6): 1112-31.

251. Smith, B. F., Bird, R. C. (2010). Hematologic Neoplasia - Gene Therapy. In: Weiss D. J., Wardrop K. J., editors. Schalm's Veterinary Hematology. Iowa: Wiley-Blackwell. pp. 550-57.

252. Smith, J. R., Pereira-Smith, O. M. (1996). Replicative senescence: implications for in vivo aging and tumor suppression. Science 273(5271): 63-7.

253. Song, D., Cui, M., Zhao, G., Fan, Z., Nolan, K., et al. (2014). Pathway-based analysis of breast cancer. Am J Transl Res 6(3): 302-11.

254. Sorenmo, K. (2003). Canine mammary gland tumors. Vet Clin North Am Small Anim Pract 33(3): 573-96.

255. Spillare, E. A., Okamoto, A., Hagiwara, K., Demetrick, D. J., Serrano, M., et al. (1996). Suppression of growth in vitro and tumorigenicity in vivo of human carcinoma cell lines by transfected p16INK4. Mol Carcinog 16(1): 53-60.

256. Spruck, C. H., 3rd, Gonzalez-Zulueta, M., Shibata, A., Simoneau, A. R., Lin, M. F., et al. (1994). p16 gene in uncultured tumours. Nature 370(6486): 183-4.

257. Stefani, G., Slack, F. J. (2008). Small non-coding RNAs in animal development. Nat Rev Mol Cell Biol 9(3): 219-30.

258. Stein, G. H., Drullinger, L. F., Soulard, A., Dulic, V. (1999). Differential roles for cyclin-dependent kinase inhibitors p21 and p16 in the mechanisms of senescence and differentiation in human fibroblasts. Mol Cell Biol 19(3): 2109-17.

259. Stone, S., Dayananth, P., Jiang, P., Weaver-Feldhaus, J. M., Tavtigian, S. V., et al. (1995a). Genomic structure, expression and mutational analysis of the P15 (MTS2) gene. Oncogene 11(5): 987-91.

260. Stone, S., Jiang, P., Dayananth, P., Tavtigian, S. V., Katcher, H., et al. (1995). Complex structure and regulation of the P16 (MTS1) locus. Cancer Res 55(14): 2988-94.

261. Strandberg, J. D., Goodman, D. G. (1974). Animal model of human disease: canine mammary neoplasia. Am J Pathol 75(1): 225-8.

262. Sun, F., Fu, H., Liu, Q., Tie, Y., Zhu, J., et al. (2008). Downregulation of CCND1 and CDK6 by miR-34a induces cell cycle arrest. FEBS Lett 582(10): 1564-8.

263. Sweet-Cordero, A., Mukherjee, S., Subramanian, A., You, H., Roix, J. J., et al. (2005). An oncogenic KRAS2 expression signature identified by cross-species gene-expression analysis. Nat Genet 37(1): 48-55.

264. Takeshita, F., Patrawala, L., Osaki, M., Takahashi, R. U., Yamamoto, Y., et al. (2010). Systemic delivery of synthetic microRNA-16 inhibits the growth of metastatic prostate tumors via downregulation of multiple cell-cycle genes. Mol Ther 18(1): 181-7.

265. Taylor, G. N., Shabestari, L., Williams, J., Mays, C. W., Angus, W., et al. (1976). Mammary neoplasia in a closed beagle colony. Cancer Res 36(8): 2740-3.

266. Thuroczy, J., Reisvaag, G. J., Perge, E., Tibold, A., Szilagyi, J., et al. (2007). Immunohistochemical detection of progesterone and cellular proliferation in canine mammary tumours. J Comp Pathol 137(2-3): 122-9.

267. Toyoshima, H., Hunter, T. (1994). p27, a novel inhibitor of G1 cyclin-Cdk protein kinase activity, is related to p21. Cell 78(1): 67-74.

268. Tripathy, D., Benz, C. C. (1992). Activated oncogenes and putative tumor suppressor genes involved in human breast cancers. Cancer Treat Res 63(15-60.

269. Tsai, M. C., Manor, O., Wan, Y., Mosammaparast, N., Wang, J. K., et al. (2010). Long noncoding RNA as modular scaffold of histone modification complexes. Science 329(5992): 689-93.

270. Uva, P., Aurisicchio, L., Watters, J., Loboda, A., Kulkarni, A., et al. (2009). Comparative expression pathway analysis of human and canine mammary tumors. BMC Genomics 10(135.

271. Vail, D. M., MacEwen, E. G. (2000). Spontaneously occurring tumors of companion animals as models for human cancer. Cancer Invest 18(8): 781-92.

272. van 't Veer, L. J., Dai, H., van de Vijver, M. J., He, Y. D., Hart, A. A., et al. (2002). Gene expression profiling predicts clinical outcome of breast cancer. Nature 415(6871): 530-6.

273. Venkataramani, R., Swaminathan, K., Marmorstein, R. (1998). Crystal structure of the CDK4/6 inhibitory protein p18INK4c provides insights into ankyrin-like repeat structure/function and tumor-derived p16INK4 mutations. Nat Struct Biol 5(1): 74-81.

274. Vidal, A., Koff, A. (2000). Cell-cycle inhibitors: three families united by a common cause. Gene 247(1-2): 1-15.

275. Vojta, P. J., Barrett, J. C. (1995). Genetic analysis of cellular senescence. Biochim Biophys Acta 1242(1): 29-41.

276. Volinia, S., Calin, G. A., Liu, C. G., Ambs, S., Cimmino, A., et al. (2006). A microRNA expression signature of human solid tumors defines cancer gene targets. Proc Natl Acad Sci U S A 103(7): 2257-61.

277. Wang, F., Fu, X. D., Zhou, Y., Zhang, Y. (2009). Down-regulation of the cyclin E1 oncogene expression by microRNA-16-1 induces cell cycle arrest in human cancer cells. BMB Rep 42(11): 725-30.

278. Wang, P., Zou, F., Zhang, X., Li, H., Dulak, A., et al. (2009). microRNA-21 negatively regulates Cdc25A and cell cycle progression in colon cancer cells. Cancer Res 69(20): 8157-65.

279. Wang, Y., Blelloch, R. (2009). Cell cycle regulation by MicroRNAs in embryonic stem cells. Cancer Res 69(10): 4093-6.

280. Wass, M. N., Kelley, L. A., Sternberg, M. J. (2010). 3DLigandSite: predicting ligand-binding sites using similar structures. Nucleic Acids Res 38(Web Server issue): W469-73.

281. Watanabe, S., Terashima, K., Ohta, S., Horibata, S., Yajima, M., et al. (2007). Hematopoietic stem cell-engrafted NOD/SCID/IL2Rgamma null mice develop human lymphoid systems and induce long-lasting HIV-1 infection with specific humoral immune responses. Blood 109(1): 212-8.

282. Weber, J. D., Jeffers, J. R., Rehg, J. E., Randle, D. H., Lozano, G., et al. (2000). p53-independent functions of the p19(ARF) tumor suppressor. Genes Dev 14(18): 2358-65.

283. Weinberg, R. A. (1991). Tumor suppressor genes. Science 254(5035): 1138-46.

284. Weinberg, R. A. (1995). The retinoblastoma protein and cell cycle control. Cell 81(3): 323-30.

285. Wesierska-Gadek, J., Schmid, G. (2006). Dual action of the inhibitors of cyclin-dependent kinases: targeting of the cell-cycle progression and activation of wild-type p53 protein. Expert Opin Investig Drugs 15(1): 23-38.

286. Winter, J., Jung, S., Keller, S., Gregory, R. I., Diederichs, S. (2009). Many roads to maturity: microRNA biogenesis pathways and their regulation. Nat Cell Biol 11(3): 228-34.

287. Withrow, S. J., MacEwen, E. G. (1996). Small animal clinical oncology. Philadelphia: WB Saunders.

288. Wolfe, L. G., Oliver, J. L., Smith, B. B., Toivio-Kinnucan, M. A., Powers, R. D., et al. (1987). Biologic characterization of canine melanoma cell lines. Am J Vet Res 48(11): 1642-8.

289. Wolfe, L. G., Smith, B. B., Toivio-Kinnucan, M. A., Sartin, E. A., Kwapien, R. P., et al. (1986). Biologic properties of cell lines derived from canine mammary carcinomas. J Natl Cancer Inst 77(3): 783-92.

290. Wong, H., Riabowol, K. (1996). Differential CDK-inhibitor gene expression in aging human diploid fibroblasts. Exp Gerontol 31(1-2): 311-25.

291. Wright, F. A., Lemon, W. J., Zhao, W. D., Sears, R., Zhuo, D., et al. (2001). A draft annotation and overview of the human genome. Genome Biol 2(7): RESEARCH0025.

292. Wurmbach, E., Gonzalez-Maeso, J., Yuen, T., Ebersole, B. J., Mastaitis, J. W., et al. (2002). Validated genomic approach to study differentially expressed genes in complex tissues. Neurochem Res 27(10): 1027-33.

293. Xiong, Y., Hannon, G. J., Zhang, H., Casso, D., Kobayashi, R., et al. (1993). p21 is a universal inhibitor of cyclin kinases. Nature 366(6456): 701-4.

294. Yanaihara, N., Caplen, N., Bowman, E., Seike, M., Kumamoto, K., et al. (2006). Unique microRNA molecular profiles in lung cancer diagnosis and prognosis. Cancer Cell 9(3): 189-98.

295. Ye, F., Tang, H., Liu, Q., Xie, X., Wu, M., et al. (2014). miR-200b as a prognostic factor in breast cancer targets multiple members of RAB family. J Transl Med 12(17.

296. Yeudall, W. A., Crawford, R. Y., Ensley, J. F., Robbins, K. C. (1994). MTS1/CDK4I is altered in cell lines derived from primary and metastatic oral squamous cell carcinoma. Carcinogenesis 15(12): 2683-6.

297. Yi, R., Qin, Y., Macara, I. G., Cullen, B. R. (2003). Exportin-5 mediates the nuclear export of pre-microRNAs and short hairpin RNAs. Genes Dev 17(24): 3011-6.

298. You, J., Bird, R. C. (1995). Selective induction of cell cycle regulatory genes cdk1 (p34cdc2), cyclins A/B, and the tumor suppressor gene Rb in transformed cells by okadaic acid. J Cell Physiol 164(2): 424-33.

299. Yusuf, I., Fruman, D. A. (2003). Regulation of quiescence in lymphocytes. Trends Immunol 24(7): 380-6.

300. Zariwala, M., Xiong, Y. (1996). Lack of mutation in the cyclin-dependent kinase inhibitor, p19INK4d, in tumor-derived cell lines and primary tumors. Oncogene 13(9): 2033-8.

301. Zdobnov, E. M., Apweiler, R. (2001). InterProScan--an integration platform for the signature-recognition methods in InterPro. Bioinformatics 17(9): 847-8.

302. Zeng, Y., Wagner, E. J., Cullen, B. R. (2002). Both natural and designed micro RNAs can inhibit the expression of cognate mRNAs when expressed in human cells. Mol Cell 9(6): 1327-33.

303. Zhang, C. M., Zhao, J., Deng, H. Y. (2013). MiR-155 promotes proliferation of human breast cancer MCF-7 cells through targeting tumor protein 53-induced nuclear protein 1. J Biomed Sci 20(79.

304. Zhang, H., Cai, K., Wang, J., Wang, X., Cheng, K., et al. (2014). MiR-7, Inhibited Indirectly by LincRNA HOTAIR, Directly Inhibits SETDB1 and Reverses the EMT of Breast Cancer Stem Cells by Downregulating the STAT3 Pathway. Stem Cells 32(11): 2858-68.

305. Zhang, S., Ramsay, E. S., Mock, B. A. (1998). Cdkn2a, the cyclin-dependent kinase inhibitor encoding p16INK4a and p19ARF, is a candidate for the plasmacytoma susceptibility locus, Pctr1. Proc Natl Acad Sci U S A 95(5): 2429-34.

306. Zhang, S. L., DuBois, W., Ramsay, E. S., Bliskovski, V., Morse, H. C., 3rd, et al. (2001). Efficiency alleles of the Pctr1 modifier locus for plasmacytoma susceptibility. Mol Cell Biol 21(1): 310-8.

307. Zhang, X., Pickin, K. A., Bose, R., Jura, N., Cole, P. A., et al. (2007). Inhibition of the EGF receptor by binding of MIG6 to an activating kinase domain interface. Nature 450(7170): 741-4.

308. Zhang, Y., Xiong, Y., Yarbrough, W. G. (1998). ARF promotes MDM2 degradation and stabilizes p53: ARF-INK4a locus deletion impairs both the Rb and p53 tumor suppression pathways. Cell 92(6): 725-34.

309. Zhang, Y. W., Staal, B., Su, Y., Swiatek, P., Zhao, P., et al. (2007). Evidence that MIG-6 is a tumor-suppressor gene. Oncogene 26(2): 269-76.

310. Zhang, Z., Jones, A., Sun, C. W., Li, C., Chang, C. W., et al. (2011). PRC2 complexes with JARID2, MTF2, and esPRC2p48 in ES cells to modulate ES cell pluripotency and somatic cell reprogramming. Stem Cells 29(2): 229-40.

311. Zhang, Z. J., Ma, S. L. (2012). miRNAs in breast cancer tumorigenesis (Review). Oncol Rep 27(4): 903-10.

312. Zhu, S., Si, M. L., Wu, H., Mo, Y. Y. (2007). MicroRNA-21 targets the tumor suppressor gene tropomyosin 1 (TPM1). J Biol Chem 282(19): 14328-36.

313. Zhu, S., Wu, H., Wu, F., Nie, D., Sheng, S., et al. (2008). MicroRNA-21 targets tumor suppressor genes in invasion and metastasis. Cell Res 18(3): 350-9.

314. Zuo, L., Weger, J., Yang, Q., Goldstein, A. M., Tucker, M. A., et al. (1996). Germline mutations in the p16INK4a binding domain of CDK4 in familial melanoma. Nat Genet 12(1): 97-9.

Appendix 1: GenBank accession numbers for INK4 proteins from different species.

Species	Gene	GenBank Accession#
Human	p16	AFN61598
	p14ARF	NP_478102
	p15	AGC10270
	p18	AAH00598
	p19	AAH01822
Chimp	p16	NP_001139762 XP_520513
	p15	XP_003312069
	p18	XP_524704
	p19	XP_001165514
Dog	p16	AFX98054
	p14ARF	CAT05765
	p15	NP_001139741 XP_538685
	p18	XP_005629070
	p19	XP_853946
Cat	p16	NP_001277177 XP_006939246
	p15	XP_003995565
	p18	XP_003990137
	p19	XP_003981908
Pig	p16	CAC87046
	p15	NP_999289
Mouse	p16	NP_034007
	p19ARF	Q64364
	p15	NP_031696 XP_994982
	p18	NP_031697
	p19	NP_034008
Opossum	p16	NP_001029248
	p15	XP_007498133
	p18	XP_001373169
	p19	XP_001366834
Chicken	p15	NP_989764
Fugu	p16/p15	CAC12808
	p19	CAC12811

Appendix 2: (A) miTarget™ miRNA CDKN2A 3' UTR Target Clone datasheet.

Clone Information

Catalog No.: CS-MIT318J-MT01-REP

UTR Length: 441bp

Description: Custom UTR clone

Vector: pEZX-MT01 Whole Plasmid Size: 7814 bp

Antibiotic: Kanamycin Stable Selection Marker: Neomycin

Reporter Genes: hLuc,Rluc Promoter: SV40

5' Cutting Site: AsiSI,EcoRI 3' Cutting Site: XhoI,SpeI

Suggested Sequencing Primers-

Forward: 5'-GATCCGCGAGATCCTGAT-3'

Reverse: 5'-CCTATTGGCGTTACTATG-3'

Restriction Enzyme Information for CS-MIT318J-MT01-REP

Restriction enzymes that do not cleave CS-MIT318J-MT01-REP

AclI	AflIII	AhdI	AscI	AseI	BaeI	BaeI	BlpI
BstEII	BstZ17I	MluI	NheI	NotI	PacI	PciI	PflMI
PmlI	PpuMI	PshAI	SanDI	SapI	SbfI	SgrAI	SrfI
SwaI	XcmI						

Restriction enzymes that cleave CS-MIT318J-MT01-REP once

AccIII	838	AdeI	1055	AfeI	6654	AflII	5498	AgeI	1802	AhlI	7809	AjuI	2077	AloI	6497
Aor13HI	838	Aor51HI	6654	ArsI	6327	AsiGI	1802	AsiSI	7346	Asp700I	1401	AssI	5832	AsuII	3821
BamHI	238	BbsI	821	BbvCI	7548	BcuI	7809	BfrI	5498	BglII	853	BmcAI	5832	BpiI	821
Bpu10I	7548	Bpu14I	3821	BpuAI	821	BseAI	838	BsePI	7585	BshTI	1802	BsiWI	7625	BsmBI	776
Bsp119I	3821	Bsp13I	838	BspEI	838	BspT104I	3821	BspTI	5498	BssHII	7585	BstAFI	5498	BstBI	3821
BstSNI	527	BstV2I	821	BstXI	6785	Cfr42I	7596	Cfr9I	7452	CpoI	3655	CspAI	1802	CspCI	563
CspI	3655	DraIII	1055	Eco105I	527	Eco47III	6654	EcoRI	7350	Esp3I	776	FseI	7078	HindIII	5485
Kpn2I	838	KspI	7596	MroI	838	MroXI	1401	MspCI	5498	MssI	7799	NspV	3821	PaeR7I	7803
PauI	7585	PdmI	1401	Pfl23II	7625	PinAI	1802	PmeI	7799	PspLI	7625	PteI	7585	RgaI	7346
RigI	7078	Rsr2I	3655	RsrII	3655	SacII	7596	SalI	5060	ScaI	5832	SfaAI	7346	Sfr274I	7803
Sfr303I	7596	SfuI	3821	SgfI	7346	SgrBI	7596	SlaI	7803	SmaI	7454	SnaBI	527	SpeI	7809
StrI	7803	TspMI	7452	Vha464I	5498	XbaI	7324	XhoI	7803	XmaI	7452	XmnI	1401	ZrmI	5832

Note: The numbers after each restriction enzyme indicates the start position which is the vector backbone start site.

>CS-MIT318J-MT01-REP

tcgagcagacatgataagatacattgatgagtttggacaaaccacaactagaatgcagtg
aaaaaaatgctttatttgtgaaatttgtgatgctattgctttatttgtaaccattataag
ctgcaataaacaagttaacaacaacaattgcattcattttatgtttcaggttcaggggga
ggtgtgggaggttttttaaagcaagtaaaacctctacaaatgtggtaaaatcgataagga
tccatgtcgttacataacttacggtaaatggcccgcctggctgaccgcccaacgacccccc
gcccattgacgtcaataatgacgtatgttcccatagtaacgccaatagggactttccatt
gacgtcaatgggtggagtatttacggtaaactgcccacttggcagtacatcaagtgtatc
atatgccaagtacgccccctattgacgtcaatgacggtaaatggcccgcctggcattatg
cccagtacatgaccttatgggactttcctacttggcagtacatctacgtattagtcatcg
ctattaccatggtgatgcggttttggcagtacatcaatgggcgtggatagcggtttgact
cacggggatttccaagtctccaccccattgacgtcaatgggagtttgttttggcaccaaa
atcaacgggactttccaaaatgtcgtaacaactccgccccattgacgcaaatgggcggta
ggcgtgtacggtgggaggtctatataagcagagctcgtttagtgaaccgtcagatcgcct
ggagacgccatccacgctgttttgacctccatagaagacaccgggaccgatccagcctcc
ggactctagcctagatcttcggtaccatggcttccaaggtgtacgaccccgagcaacgca
aacgcatgatcactgggcctcagtggtgggctcgctgcaagcaaatgaacgtgctggact
ccttcatcaactactatgattccgagaagcacgccgagaacgccgtgatttttctgcatg
gtaacgctgcctccagctacctgtggaggcacgtcgtgcctcacatcgagcccgtggcta
gatgcatcatccctgatctgatcggaatgggtaagtccggcaagagcgggaatggctcat
atcgcctcctggatcactacaagtacctcaccgcttggttcgagctgctgaaccttccaa
agaaaatcatctttgtgggccacgactgggggcttgtctggcctttcactactcctacg
agcaccaagacaagatcaaggccatcgtccatgctgagagtgtcgtggacgtgatcgagt
cctgggacgagtggcctgacatcgaggaggatatcgccctgatcaagagcgaagagggcg
agaaaatggtgcttgagaataacttcttcgtcgagaccatgctcccaagcaagatcatgc
ggaaactggagcctgaggagttcgctgcctacctggagccattcaaggagaagggcgagg
ttagacggcctaccctctcctggcctcgcgagatccctctcgttaagggaggcaagcccg
acgtcgtccagattgtccgcaactacaacgcctaccttcgggccagcgacgatctgccta
agatgttcatcgagtccgaccctgggttcttttccaacgctattgtcgagggagctaaga
agttccctaacaccgagttcgtgaaggtgaagggcctccacttcagccaggaggacgctc
cagatgaaatgggtaagtacatcaagagcttcgtggagcgcgtgctgaagaacgagcagt
aaccggtcgagtgcggccctagcttgggatctttgtgaaggaaccttacttctgtggtgt
gacataattggacaaactacctacagagatttaaagctctaaggtaaatataaaatttttt
aagtgtataatgtgttaaactagctgcatatgcttgctgcttgagagttttgcttactga
gtatgatttatgaaaatattatacacaggagctagtgattctaattgtttgtgtatttta
gattcacagtcccaaggctcatttcaggcccctcagtcctcacagtctgttcatgatcat
aatcagccataccacatttgtagaggttttacttgctttaaaaaacctcccacacctccc
cctgaacctgaaacataaaatgaatgcaattgttgttgttaacttgtttattgcagctta
taatggttacaaataaagcaatagcatcacaaatttcacaaataaagcatttttttcact
gcattctagttgtggtttgtccaaactcatcaatgtatcttatcatgtctggatcgatcg
atccggtcgcagtggccgcaaagggaacccagctttcttgtacaaagttggcattataag
aaagcattgcttatcaatttgttgcaacgaacaggtcactatcagtcaaaataaaatcat
tatttgccatccagctgatatcccctagatccgcacttttcggggaaatgtgcgcggaac
ccctatttgtttatttttctaaatacattcaaatatgtatccgctcatgagacaataacc
ctgataaatgcttcaataatattgaaaaaggaagaatcctgaggcggaaagaaccagctg
tggaatgtgtgtcagttagggtgtggaaagtccccaggctccccagcaggcagaagtatg
caaagcatgcatctcaattagtcagcaaccaggtgtggaaagtccccaggctccccagca
ggcagaagtatgcaaagcatgcatctcaattagtcagcaaccatagtcccgcccctaact
ccgcccatcccgcccctaactccgcccagttccgcccattctccgccccatggctgacta
attttttttatttatgcagaggccgaggccgcctcggcctctgagctattccagaagtag
tgaggaggctttttggaggcctaggcttttgcaaagatcgatcaagagacaggatgagg
atcgtttcgcatgattgaacaagatggattgcacgcaggttctccggccgcttgggtgga
gaggctattcggctatgactgggcacaacagacaatcggctgctctgatgccgccgtgtt
ccggctgtcagcgcaggggcgcccggttctttttgtcaagaccgacctgtccggtgccct
gaatgaactgcaagacgaggcagcgcggctatcgtggctggccacgacgggcgttccttg
cgcagctgtgctcgacgttgtcactgaagcgggaagggactggctgctattgggcgaagt

gccggggcaggatctcctgtcatctcaccttgctcctgccgagaaagtatccatcatggc
tgatgcaatgcggcggctgcatacgcttgatccggctacctgcccattcgaccaccaagc
gaaacatcgcatcgagcgagcacgtactcggatggaagccggtcttgtcgatcaggatga
tctggacgaagaacatcaggggctcgcgccagccgaactgttcgccaggctcaaggcgag
catgcccgacggcgaggatctcgtcgtgacccatggcgatgcctgcttgccgaatatcat
ggtggaaaatggccgcttttctggattcatcgactgtggccggctgggtgtggcggaccg
ctatcaggacatagcgttggctacccgtgatattgctgaagaacttggcggcgaatgggc
tgaccgcttcctcgtgctttacggtatcgccgctcccgattcgcagcgcatcgccttcta
tcgccttcttgacgagttcttctgagcgggactctggggttcgaaatgaccgaccaagcg
acgcccaacctgccatcacgagatttcgattccaccgccgccttctatgaaaggttgggc
ttcggaatcgttttccgggacgccggctggatgatcctccagcgcggggatctcatgctg
gagttcttcgcccaccctagggggaggctaactgaaacacggaaggagacaataccggaa
ggaacccgcgctatgacggcaataaaaagacagaataaaacgcacggtgttgggtcgttt
gttcataaacgcggggttcggtcccagggctggcactctgtcgataccccaccgagaccc
cattggggccaatacgcccgcgtttcttccttttccccacccccacccccccaagttcgggt
gaaggcccagggctcgcagccaacgtcggggcggcaggccctgccatagcctcaggttac
tcatatatactttagattgatttaaaacttcatttttaatttaaaaggatctaggtgaag
atccttttttgataatctcatgaccaaaatcccttaacgtgagttttcgttccactgagcg
tcagaccccgtagaaaagatcaaaggatcttcttgagatcctttttttctgcgcgtaatc
tgctgcttgcaaacaaaaaaaccaccgctaccagcggtggtttgtttgccggatcaagag
ctaccaactctttttccgaaggtaactggcttcagcagagcgcagataccaaatactgtc
cttctagtgtagccgtagttaggccaccacttcaagaactctgtagcaccgcctacatac
ctcgctctgctaatcctgttaccagtggctgctgccagtggcgataagtcgtgtcttacc
gggttggactcaagacgatagttaccggataaggcgcagcggtcgggctgaacggggggt
tcgtgcacacagcccagcttggagcgaacgacctacaccgaactgagatacctacagcgt
gagctatgagaaagcgccacgcttcccgaagggagaaaggcggacaggtatccggtaagc
ggcagggtcggaacaggagagcgcacgagggagcttccagggggaaacgcctggtatctt
tatagtcctgtcgggtttcgccacctctgacttgagcgtcgatttttgtgatgctcgtca
gggggggcggagcctatggaaaaacgccagcaacgcggccttttacggttcctggccttt
tgctggccttttgctcacagtcgactgatctgcgcagcaccatggcctgaaataacctct
gaaagaggaacttggttaggtaccttctgaggcggaaagaaccagctgtggaatgtgtgt
cagttagggtgtggaaagtccccaggctccccagcaggcagaagtatgcaaagcatgcat
ctcaattagtcagcaaccaggtgtggaaagtccccaggctccccagcaggcagaagtatg
caaagcatgcatctcaattagtcagcaaccatagtcccgcccctaactccgcccatcccg
cccctaactccgcccagttccgcccattctccgccccatggctgactaatttttttttatt
tatgcagaggccgaggccgcctcggcctctgagctattccagaagtagtgaggaggcttt
tttggaggcctaggcttttgcaaaaagcttggccagtcttaagctcgggccccaaataat
gattttattttgactgatagtgacctgttcgttgcaacaaattgatgagcaatgcttttt
tataatgccaactttgtacaaaaaagcaggcttgcccttcacactgcggccgagcttggc
attccggtactgttggtaaagccaccatggccgatgctaagaacattaagaagggccctg
ctcccttctaccctctggaggatggcaccgctggcgagcagctgcacaaggccatgaaga
ggtatgccctggtgcctggcaccattgccttcaccgatgcccacattgaggtggacatca
cctatgccgagtacttcgagatgtctgtgcgcctggccgaggccatgaagaggtacggcc
tgaacaccaaccaccgcatcgtggtgtgctctgagaactctctgcagttcttcatgccag
tgctgggcgccctgttcatcggagtggccgtggcccctgctaacgacatttacaacgagc
gcgagctgctgaacagcatgggcatttctcagcctaccgtggtgttcgtgtctaagaagg
gcctgcagaagatcctgaacgtgcagaagaagctgcctatcatccagaagatcatcatca
tggactctaagaccgactaccagggcttccagagcatgtacacattcgtgacatctcatc
tgcctcctggcttcaacgagtacgacttcgtgccagagtctttcgacagggacaaaacca
ttgccctgatcatgaacagctctgggtctaccggcctgcctaagggcgtggccctgcctc
atcgcaccgcctgtgtgcgcttctctcacgcccgcgaccctattttcggcaaccagatca
tccccgacaccgctattctgagcgtggtgccattccaccacggcttcggcatgttcacca
ccctgggctacctgatttgcggctttcgggtggtgctgatgtaccgcttcgaggaggagc
tgttcctgcgcagcctgcaagactacaaaattcagtctgccctgctggtgccaaccctgt
tcagcttcttcgctaagagcaccctgatcgacaagtacgacctgtctaacctgcacgaga
ttgcctctggcggcgccccactgtctaaggaggtgggcgaagccgtggccaagcgctttc
atctgccaggcatccgccagggctacggcctgaccgagacaaccagcgccattctgatta

ccccagagggcgacgacaagcctggcgccgtgggcaaggtggtgccattcttcgaggcca
aggtggtggacctggacaccggcaagaccctgggagtgaaccagcgcggcgagctgtgtg
tgcgcggccctatgattatgtccggctacgtgaataaccctgaggccacaaacgccctga
tcgacaaggacggctggctgcactctggcgacattgcctactgggacgaggacgagcact
tcttcatcgtggaccgcctgaagtctctgatcaagtacaagggctaccaggtggccccag
ccgagctggagtctatcctgctgcagcaccctaacattttcgacgccggagtggccggcc
tgcccgacgacgatgccggcgagctgcctgccgccgtcgtcgtgctggaacacggcaaga
ccatgaccgagaaggagatcgtggactatgtggccagccaggtgacaaccgccaagaagc
tgcgcggcggagtggtgttcgtggacgaggtgcccaagggcctgaccggcaagctggacg
cccgcaagatccgcgagatcctgatcaaggctaagaaaggcggcaagatcgccgtgtaat
aattctagagtcggggcgcccGCGATCGCGAATTCCGTACCGCACCCGCGTGGCCCAGCT
GCTGCTGCTCCACGGCGCCAACCCCAACTGTGCCGACCCCGTCACCCTCACCCGCCCTGT
GCACGACGCGGCCCGGGAGGGCTTCCTGGACACGCTGGTGGTGCTGCACCGAGCCGGGGC
GCGGCTGGACGTGCGCGATGCCTGGGGCCGCCTGCCCGTGGACCTGGCTGAGGAGCGGGG
CCACGGCGCTGTCGCTGCGTACCTGCGCGCAGCCGCGGGGGGCACCGAAAGTGGTAGCCA
CGCCCGTACGGAAGGTGCGGAAGGTCACGCAGACAGCCCGGACTTCAAGAATTGAGCTCT
AAAGACAGATCAAGGGTTTTGATCTTCAATCAACAAAAATGAATTACCCCACCCAACCCA
ACTCTTCCCTGCATGCTTGCCTTTATCAAATACCACTTTTAACACTGTAGACAGTGTTTA
AACTCGAGACTAGT

Note: The sequence in blue is the canine p16/CDKN2A 3'-UTR. Sequences in red are the linkers/cloning sites used to construct the plasmid.

(B) cfa-miR-141 precursor clone Datasheet

Clone Information

Catalog No.: CS-MIR241J-MR01

Description: cfa-miR-141 precursor clone in pEZX-MR01 vector

Whole Plasmid Size: 8112 bp

Vector: pEZX-MR01

Antibiotic: Ampicillin Stable Selection Marker: Neomycin

Suggested Sequencing Primers:

Forward: 5'-GCCCTGCAATATTTGCATGTCGCT-3'

Reverse: 5'-GTAACCATTATAAGCTGCAA-3'

Vector Information for CS-MIR241J-MR01

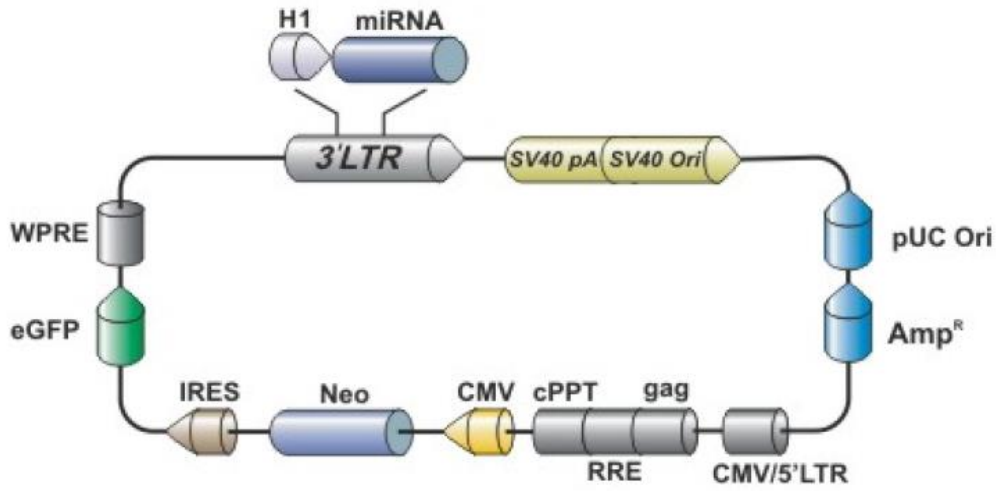

Restriction Enzyme Information for CS-MIR241J-MR01

Restriction enzymes that do not cleave CS-MIR241J-MR01

AfeI	AgeI	AscI	BaeI	BaeI	BclI	BglII	BsaBI
BsiWI	BspEI	BsrGI	BstBI	BstEII	BstZ17I	Bsu36I	EcoNI
EcoRV	HpaI	MfeI	MluI	NheI	NotI	NruI	NsiI
PacI	PmeI	Ppu10I	PshAI	SbfI	SgfI	SgrAI	SrfI
SwaI							

Restriction enzymes that cleave CS-MIR241J-MR01 once

AccI	6859	AdeI	5880	AflII	4177	AhdI	1784	AhlI	4349	AspA2I	5668	AspEI	1784	AssI	2264
AvrII	5668	BamHI	7820	BbvCI	8020	BcgI	2289	BcuI	4349	BfrI	4177	BlnI	5668	BlpI	6273
BmcAI	2264	BmeRI	1784	Bpu10I	8020	Bpu1102I	6273	BpvUI	2154	Bsa29I	7598	BseCI	7598	BsePI	7669
BshVI	7598	Bsp1720I	6273	BspDI	7598	BspTI	4177	BssHII	7669	BstAFI	4177	BstXI	3834	Bsu15I	7598
CelII	6273	Cfr42I	7367	Cfr9I	8006	ClaI	7598	CpoI	5353	CsiI	3861	CspI	5353	DraIII	5880
DriI	1784	Eam1105I	1784	EcoRI	16	FauNDI	2955	FblI	6859	FseI	6442	KflI	7881	KspI	7367
MabI	3861	MspCI	4177	MvrI	2154	NdeI	2955	PaeI	5242	PaeR7I	3588	PauI	7669	Ple19I	2154
PpuMI	7881	Psp5II	7881	PspPPI	7881	PspXI	3588	PstI	6676	PteI	7669	PvuI	2154	RigI	6442
Rsr2I	5353	RsrII	5353	SacII	7367	SalI	6858	ScaI	2264	SexAI	3861	SfiI	464	Sfr274I	3588
Sfr303I	7367	SgrBI	7367	SlaI	3588	SmaI	8008	SpeI	4349	SphI	5242	StrI	3588	TspMI	8006
Vha464I	4177	XhoI	3588	XmaI	8006	XmaJI	5668	XmiI	6859	ZrmI	2264				

>CS-MIR241J-MR01
aattgaagctttttgaattctagcgtccataagcattctttctttcgatagcttccagt
gctttgtgaaacttcgaggagtctctttgttgaggacttttgagttctcccttgaggctc
ccacagatacaataaatatttgagattgaaccctgtcgagtatctgtgtaatctttttta
cctgtgaggtctcggaatccgggccgagaacttcgcagcgagctcattgtaccgcgaact
tgtttattgcagcttataatggttacaaataaagcaatagcatcacaaatttcacaaata
aagcatttttttcactgcattctagttgtggtttgtccaaactcatcaatgtatcttatc
atgtctggctctagctatcccgcccctaactccgcccagttccgcccattctccgcccca
tggctgactaatttttttttatttatgcagaggccgaggccgcctcggcctctgagctatt
ccagaagtagtgaggaggctttttggaggcctagacttttgcagagacggcccaaattc
gtaatcatggtcatagctgtttcctgtgtgaaattgttatccgctcacaattccacacaa
catacgagccggaagcataaagtgtaaagcctggggtgcctaatgagtgagctaactcac
attaattgcgttgcgctcactgcccgctttccagtcgggaaacctgtcgtgccagctgca
ttaatgaatcggccaacgcgcggggagaggcggtttgcgtattgggcgctcttccgcttc
ctcgctcactgactcgctgcgctcggtcgttcggctgcggcgagcggtatcagctcactc
aaaggcggtaatacggttatccacagaatcaggggataacgcaggaaagaacatgtgagc
aaaaggccagcaaaaggccaggaaccgtaaaaaggccgcgttgctggcgtttttccatag
gctccgcccccctgacgagcatcacaaaaatcgacgctcaagtcagaggtggcgaaaccc
gacaggactataaagataccaggcgtttccccctggaagctccctcgtgcgctctcctgt
tccgaccctgccgcttaccggatacctgtccgcctttctcccttcgggaagcgtggcgct
ttctcatagctcacgctgtaggtatctcagttcggtgtaggtcgttcgctccaagctggg
ctgtgtgcacgaaccccccgttcagcccgaccgctgcgccttatccggtaactatcgtct
tgagtccaacccggtaagacacgacttatcgccactggcagcagccactggtaacaggat
tagcagagcgaggtatgtaggcggtgctacagagttcttgaagtggtggcctaactacgg
ctacactagaaggacagtatttggtatctgcgctctgctgaagccagttaccttcggaaa
aagagttggtagctcttgatccggcaaacaaaccaccgctggtagcggtggtttttttgt
ttgcaagcagcagattacgcgcagaaaaaaaggatctcaagaagatcctttgatcttttc
tacggggtctgacgctcagtggaacgaaaactcacgttaagggattttggtcatgagatt
atcaaaaaggatcttcacctagatccttttaaattaaaaatgaagttttaaatcaatcta
aagtatatatgagtaaacttggtctgacagttaccaatgcttaatcagtgaggcacctat
ctcagcgatctgtctatttcgttcatccatagttgcctgactccccgtcgtgtagataac
tacgatacgggagggcttaccatctggccccagtgctgcaatgataccgcgagacccacg
ctcaccggctccagatttatcagcaataaaccagccagccggaagggccgagcgcagaag
tggtcctgcaactttatccgcctccatccagtctattaattgttgccgggaagctagagt
aagtagttcgccagttaatagtttgcgcaacgttgttgccattgctacaggcatcgtggt
gtcacgctcgtcgtttggtatggcttcattcagctccggttcccaacgatcaaggcgagt
tacatgatcccccatgttgtgcaaaaaagcggttagctccttcggtcctccgatcgttgt
cagaagtaagttggccgcagtgttatcactcatggttatggcagcactgcataattctct
tactgtcatgccatccgtaagatgcttttctgtgactggtgagtactcaaccaagtcatt
ctgagaatagtgtatgcggcgaccgagttgctcttgcccggcgtcaatacgggataatac
cgcgccacatagcagaactttaaaagtgctcatcattggaaaacgttcttcggggcgaaa
actctcaaggatcttaccgctgttgagatccagttcgatgtaacccactcgtgcacccaa
ctgatcttcagcatcttttactttcaccagcgtttctgggtgagcaaaaacaggaaggca
aaatgccgcaaaaaagggaataagggcgacacggaaatgttgaatactcatactcttcct
ttttcaatattattgaagcatttatcagggttattgtctcatgagcggatacatatttga
atgtatttagaaaaataaacaaatagggggttccgcgcacatttccccgaaaagtgccacc
tgacgtctaagaaaccattattatcatgacattaacctataaaaataggcgtatcacgag
gccctttcgtctcgcgcgtttcggtgatgacggtgaaaacctctgacacatgcagctccc
ggagacggtcacagcttgtctgtaagcggatgccgggagcagacaagcccgtcagggcgc
gtcagcgggtgttggcgggtgtcggggctggcttaactatgcggcatcagagcagattgt
actgagagtgcaccatatgccaagtacgccccctattgacgtcaatgacggtaaatggcc
cgcctggcattatgcccagtacatgaccttatgggactttcctacttggcagtacatcta
cgtattagtcatcgctattaccatggtgatgcggttttggcagtacatcaatgggcgtgg
atagcggtttgactcacggggatttccaagtctccaccccattgacgtcaatgggagttt

gttttggcaccaaaatcaacgggactttccaaaatgtcgtaacaactccgccccattgac
gcaaatgggcggtaggcgtgtacggtgggaggtctatataagcagagcttgtgaaacttc
gaggagtctctttgttgaggacttttgagttctcccttgaggctcccacagatacaataa
atatttgagattgaaccctgtcgagtatctgtgtaatctttttacctgtgaggtctcgg
aatccgggccgagaacttcgcagttggcgcccgaacagggacttgattgagagtgattga
ggaagtgaagctagagcaatagaaagctgttaagcagaactcctgctgacctaaataggg
aagcagtagcagacgctgctaacagtgagtatctctagtgaagcagactcgagctcataa
tcaagtcattgtttaaaggcccagataaattacatctggtgactcttcgcggaccttcaa
gccaggagattcgccgagggacagtcaacaaggtaggagagattctacagcaacatgggg
aatggacaggggcgagattggaaaatggccattaagagatgtagtaatgttgctgtagga
gtaggggggaagagtaaaaaatttggagaagggaatttcagatgggccattagaatggct
aatgtatctacaggacgagaacctggtgatataccagagactttagatcaactaaggttg
gttatttgcgatttacaagaaagaagagaaaaatttggatctagcaaagaaattgatatg
gcaattcctgcattgaggagaaatggtaggcaatgtggcatgtctgaaaaagaggaggaa
tgatgaagtatctcagacttattttataagggagatactgtgctgagttcttccctttga
ggaaggtatgtcatatcctagacatagtctcaattttaaaagaagaggtaggataggagg
gatggccccttatgaattattagcacaacaagaatccttaagaatacaagattatttttc
tgcaataccacaaaaattgcaagcacagtggatttattataaagatcaaaaagataagaa
atggaaaggaccaatgagagtagaatactggggacagggatcagtattattaaaggatga
agagaagggatattttcttataatcggtactagtattatgcccagtacatgaccttatgg
gactttcctacttggcagtacatctacgtattagtcatcgctattaccatggtgatgcgg
ttttggcagtacatcaatgggcgtggatagcggtttgactcacggggatttccaagtctc
caccccattgacgtcaatgggagtttgttttggcaccaaaatcaacgggactttccaaaa
tgtcgtaacaactccgccccattgacgcaaatgggcggtaggcgtgtacggtgggaggtc
tatataagcagagctcgtttagtgaaccgtcagatcgcctggagacgccatccacgctgt
tttgacctccatagaagattctagctagatgattgaacaagatggattgcacgcaggttc
tccggccgcttgggtggagaggctattcggctatgactgggcacaacagacaatcggctg
ctctgatgccgccgtgttccggctgtcagcgcaggggcgcccggttctttttgtcaagac
cgacctgtccggtgccctgaatgaactgcaagacgaggcagcgcggctatcgtggctggc
cacgacgggcgttccttgcgcagctgtgctcgacgttgtcactgaagcgggaagggactg
gctgctattgggcgaagtgccggggcaggatctcctgtcatctcaccttgctcctgccga
gaaagtatccatcatggctgatgcaatgcggcggctgcatacgcttgatccggctacctg
cccattcgaccaccaagcgaaacatcgcatcgagcgagcacgtactcggatggaagccgg
tcttgtcgatcaggatgatctggacgaagagcatcaggggctcgcgccagccgaactgtt
cgccaggctcaaggcgagcatgcccgacggcgaggatctcgtcgtgacccatggcgatgc
ctgcttgccgaatatcatggtggaaaatggccgcttttctggattcatcgactgtggccg
gctgggtgtggcggaccgctatcaggacatagcgttggctacccgtgatattgctgaaga
gcttggcggcgaatgggctgaccgcttcctcgtgctttacggtatcgccgctcccgattc
gcagcgcatcgccttctatcgccttcttgacgagttcttctgatctagaaattccgcccc
tctccctcccccccccctaacgttactggccgaagccgcttggaataaggccggtgtgcg
tttgtctatatgtgattttccaccatattgccgtcttttggcaatgtgagggcccggaaa
cctggccctgtcttcttgacgagcattcctaggggtctttcccctctcgccaaaggaatg
caaggtctgttgaatgtcgtgaaggaagcagttcctctggaagcttcttgaagacaaaca
acgtctgtagcgacccttgcaggcagcggaacccccacctggcgacaggtgcctctgc
ggccaaaagccacgtgtataagatacacctgcaaaggcggcacaaccccagtgccacgtt
gtgagttggatagttgtggaaagagtcaaatggctctcctcaagcgtattcaacaagggg
ctgaaggatgcccagaaggtaccccattgtatgggatctgatctggggcctcggtgcaca
tgctttacatgtgtttagtcgaggttaaaaaaacgtctaggccccccgaaccacggggac
gtggttttcctttgaaaaacacgatgataagctctagaatggagagcgacgagagcggcc
tgcccgccatggagatcgagtgccgcatcaccggcaccctgaacggcgtggagttcgagc
tggtgggcggcggagagggcacccccaagcagggccgcatgaccaacaagatgaagagca
ccaaaggcgccctgaccttcagcccctacctgctgagccacgtgatgggctacggcttct
accacttcggcacctaccccagcggctacgagaaccccttcctgcacgccatcaacaacg
gcggctacaccaacacccgcatcgagaagtacgaggacggcggcgtgctgcacgtgagct

tcagctaccgctacgaggccggccgcgtgatcggcgacttcaaggtggtgggcaccggct
tccccgaggacagcgtgatcttcaccgacaagatcatccgcagcaacgccaccgtggagc
acctgcaccccatgggcgataacgtgctggtgggcagcttcgcccgcaccttcagcctgc
gcgacggcggctactacagcttcgtggtggacagccacatgcacttcaagagcgccatcc
accccagcatcctgcagaacgggggccccatgttcgccttccgccgcgtggaggagctgc
acagcaacaccgagctgggcatcgtggagtaccagcacgccttcaagacccccatcgcct
tcgccagatcccgcgctcagtcgtccaattctgccgtggacggcaccgccggacccggct
ccaccggatctcgctaagtcgacaatcaacctctggattacaaaatttgtgaaagattga
ctggtattcttaactatgttgctccttttacgctatgtggatacgctgctttaatgcctt
tgtatcatgctattgcttcccgtatggctttcattttctcctccttgtataaatcctggt
tgctgtctctttatgaggagttgtggcccgttgtcaggcaacgtggcgtggtgtgcactg
tgtttgctgacgcaacccccactggttggggcattgccaccacctgtcagctcctttccg
ggactttcgctttccccctccctattgccacggcggaactcatcgccgcctgccttgccc
gctgctggacaggggctcggctgttgggcactgacaattccgtggtgttgtcggggaaat
catcgtcctttccttggctgctcgcctgtgttgccacctggattctgcgcgggacgtcct
tctgctacgtcccttcggccctcaatccagcggaccttccttcccgcggcctgctgccgg
ctctgcggcctcttccgcgtctccgccttcgccctcagacgagtcggatctccctttggg
ccgcctccccgcctggtaccgatgacagagttagaagatcgcttcaggaagctatttggc
acgacttctacaacgggagacagcacagtagattctgaagatgaacctcctaaaaaagaa
aaaagggtggactgggatgagtattggaaccctgaaatcgatgaacgctgacgtcatcaa
cccgctccaaggaatcgcgggcccagtgtcactaggcgggaacacccagcgcgcgtgcgc
cctggcaggaagatggctgtgagggacaggggagtggcgccctgcaatatttgcatgtcg
ctatgtgttctgggaaatcaccataaacgtgaaatgtctttggatttgggaatcttataa
gttctgtatgagaccacttggatcCTTGAGCTTGGGATTGGCTACATCCTCTCAAGAGGC
CTCACCTGGCCTGCGGCCAGGGTCCCTGTAGCAACTGGTCAGCTCTGGCCTGGAGCTGCA
CGTCCGCCGGCTCTGGGTCCATCTTCCAGTACAGTGTTGGATGGTCTAGTCACGAAGCTC
CTAACACTGTCTGGTAAAGATGGCCCCCGGGCCGGTTCCCTCAGCAGTGACCTTCAGGGC
GCCCTGAAGACCATGGAGGCCTCCTGATGAATCACCTCTGACCTTTAGCCCCTGGATGGG
GGTATAAATCAG

Note: The highlighted sequence in yellow indicates the miR-141 mature sequence and the highlighted in green + yellow indicates the complete sequence of miR-141 step-loop precursor.

Appendix 3: List of the 277 miRNAs from the canine genome

#	Plate	Position	miRBase or NCBI Accession No.	Mature miRNA ID or Gene Symbol
1	1	A01	MIMAT0006594	cfa-let-7a
2	1	A02	MIMAT0009836	cfa-let-7b
3	1	A03	MIMAT0006669	cfa-let-7c
4	1	A04	MIMAT0006610	cfa-let-7f
5	1	A05	MIMAT0006637	cfa-let-7g
6	1	A06	MIMAT0006656	cfa-miR-1
7	1	A07	MIMAT0006600	cfa-miR-101
8	1	A08	MIMAT0006687	cfa-miR-103
9	1	A09	MIMAT0006749	cfa-miR-106a
10	1	A10	MIMAT0006695	cfa-miR-106b
11	1	A11	MIMAT0009837	cfa-miR-10b
12	1	A12	MIMAT0006619	cfa-miR-122
13	1	B01	MIMAT0006657	cfa-miR-124
14	1	B02	MIMAT0006609	cfa-miR-125a
15	1	B03	MIMAT0006670	cfa-miR-125b
16	1	B04	MIMAT0006730	cfa-miR-126
17	1	B05	MIMAT0006631	cfa-miR-130a
18	1	B06	MIMAT0009834	cfa-miR-133a
19	1	B07	MIMAT0009835	cfa-miR-133b
20	1	B08	MIMAT0006702	cfa-miR-137
21	1	B09	MIMAT0009876	cfa-miR-141
22	1	B10	MIMAT0006682	cfa-miR-143
23	1	B11	MIMAT0009863	cfa-miR-145
24	1	B12	MIMAT0006684	cfa-miR-146a
25	1	C01	MIMAT0006667	cfa-miR-146b
26	1	C02	MIMAT0006622	cfa-miR-148a
27	1	C03	MIMAT0006602	cfa-miR-150
28	1	C04	MIMAT0006647	cfa-miR-15a
29	1	C05	MIMAT0006676	cfa-miR-15b
30	1	C06	MIMAT0006648	cfa-miR-16
31	1	C07	MIMAT0006649	cfa-miR-17
32	1	C08	MIMAT0006707	cfa-miR-181a
33	1	C09	MIMAT0006708	cfa-miR-181b
34	1	C10	MIMAT0009841	cfa-miR-182
35	1	C11	MIMAT0006621	cfa-miR-183
36	1	C12	MIMAT0009842	cfa-miR-184

37	1	D01	MIMAT0009832	cfa-miR-18a
38	1	D02	MIMAT0006638	cfa-miR-191
39	1	D03	MIMAT0006632	cfa-miR-192
40	1	D04	MIMAT0006692	cfa-miR-195
41	1	D05	MIMAT0006662	cfa-miR-196a
42	1	D06	MIMAT0006650	cfa-miR-19a
43	1	D07	MIMAT0009865	cfa-miR-200a
44	1	D08	MIMAT0009864	cfa-miR-200b
45	1	D09	MIMAT0006664	cfa-miR-200c
46	1	D10	MIMAT0009866	cfa-miR-203
47	1	D11	MIMAT0006598	cfa-miR-204
48	1	D12	MIMAT0009845	cfa-miR-205
49	1	E01	MIMAT0006651	cfa-miR-20a
50	1	E02	MIMAT0006741	cfa-miR-21
51	1	E03	MIMAT0009846	cfa-miR-210
52	1	E04	MIMAT0009847	cfa-miR-214
53	1	E05	MIMAT0006672	cfa-miR-218
54	1	E06	MIMAT0006733	cfa-miR-22
55	1	E07	MIMAT0009851	cfa-miR-222
56	1	E08	MIMAT0009852	cfa-miR-223
57	1	E09	MIMAT0006744	cfa-miR-224
33358	1	E10	MIMAT0006640	cfa-miR-23a
59	1	E11	MIMAT0006612	cfa-miR-23b
60	1	E12	MIMAT0006614	cfa-miR-24
61	1	F01	MIMAT0006697	cfa-miR-25
62	1	F02	MIMAT0006595	cfa-miR-26a
63	1	F03	MIMAT0006641	cfa-miR-27a
64	1	F04	MIMAT0006613	cfa-miR-27b
65	1	F05	MIMAT0006625	cfa-miR-29b
66	1	F06	MIMAT0006705	cfa-miR-29c
67	1	F07	MIMAT0006617	cfa-miR-30b
68	1	F08	MIMAT0006605	cfa-miR-30c
69	1	F09	MIMAT0006616	cfa-miR-30d
70	1	F10	MIMAT0006599	cfa-miR-31
71	1	F11	MIMAT0006624	cfa-miR-335
72	1	F12	MIMAT0006709	cfa-miR-342
73	1	G01	MIMAT0006690	cfa-miR-34a
74	1	G02	MIMAT0009838	cfa-miR-34b
75	1	G03	MIMAT0006693	cfa-miR-34c
76	1	G04	MIMAT0009871	cfa-miR-375
77	1	G05	MIMAT0006683	cfa-miR-378

78	1	G06	MIMAT0009870	cfa-miR-451
79	1	G07	MIMAT0006655	cfa-miR-499
80	1	G08	MIMAT0006634	cfa-miR-7
81	1	G09	MIMAT0006674	cfa-miR-9
82	1	G10	MIMAT0006653	cfa-miR-92a
83	1	G11	MIMAT0006696	cfa-miR-93
84	1	G12	MIMAT0009861	cfa-miR-96
85	2	A01	MIMAT0006629	cfa-miR-383
86	2	A02	MIMAT0006623	cfa-miR-129
87	2	A03	MIMAT0010196	cfa-miR-135a-5p
88	2	A04	MIMAT0009923	cfa-miR-632
89	2	A05	MIMAT0006729	cfa-miR-219*
90	2	A06	MIMAT0009905	cfa-miR-494
91	2	A07	MIMAT0009869	cfa-miR-208b
92	2	A08	MIMAT0009930	cfa-miR-874
93	2	A09	MIMAT0001544	cfa-miR-449
94	2	A10	MIMAT0009843	cfa-miR-187
95	2	A11	MIMAT0009936	cfa-miR-761
96	2	A12	MIMAT0006630	cfa-miR-1837
97	2	B01	MIMAT0009895	cfa-miR-331
98	2	B02	MIMAT0001539	cfa-miR-429
99	2	B03	MIMAT0009940	cfa-miR-872
100	2	B04	MIMAT0009859	cfa-miR-367
101	2	B05	MIMAT0006716	cfa-miR-411
102	2	B06	MIMAT0006737	cfa-miR-10
103	2	B07	MIMAT0006606	cfa-miR-206
104	2	B08	MIMAT0009907	cfa-miR-504
105	2	B09	MIMAT0009855	cfa-miR-302a
106	2	B10	MIMAT0006596	cfa-miR-1835
107	2	B11	MIMAT0006735	cfa-miR-193a
108	2	B12	MIMAT0006681	cfa-miR-194
109	2	C01	MIMAT0009927	cfa-miR-454
110	2	C02	MIMAT0009910	cfa-miR-544
111	2	C03	MIMAT0009904	cfa-miR-432
112	2	C04	MIMAT0009921	cfa-miR-628
113	2	C05	MIMAT0009893	cfa-miR-330
114	2	C06	MIMAT0006717	cfa-miR-380
115	2	C07	MIMAT0006762	cfa-miR-676
116	2	C08	MIMAT0006700	cfa-miR-590
117	2	C09	MIMAT0006608	cfa-let-7e
118	2	C10	MIMAT0009906	cfa-miR-496

119	2	C11	MIMAT0006712	cfa-miR-433
120	2	C12	MIMAT0009933	cfa-miR-885
121	2	D01	MIMAT0009867	cfa-miR-211
122	2	D02	MIMAT0006752	cfa-miR-384
123	2	D03	MIMAT0006593	cfa-miR-33
124	2	D04	MIMAT0009850	cfa-miR-217
125	2	D05	MIMAT0006740	cfa-miR-1844
126	2	D06	MIMAT0006726	cfa-miR-409
127	2	D07	MIMAT0009831	cfa-miR-18b
128	2	D08	MIMAT0006720	cfa-miR-543
129	2	D09	MIMAT0006756	cfa-miR-98
130	2	D10	MIMAT0006592	cfa-miR-216b
131	2	D11	MIMAT0009909	cfa-miR-539
132	2	D12	MIMAT0006699	cfa-miR-193b
133	2	E01	MIMAT0006654	cfa-miR-138a
134	2	E02	MIMAT0009901	cfa-miR-483
135	2	E03	MIMAT0006748	cfa-miR-450b
136	2	E04	MIMAT0006645	cfa-miR-139
137	2	E05	MIMAT0009937	cfa-miR-764
138	2	E06	MIMAT0009856	cfa-miR-302b
139	2	E07	MIMAT0009932	cfa-miR-876
140	2	E08	MIMAT0009878	cfa-miR-95
141	2	E09	MIMAT0009914	cfa-miR-568
142	2	E10	MIMAT0001540	cfa-miR-365
143	2	E11	MIMAT0009916	cfa-miR-582
144	2	E12	MIMAT0009911	cfa-miR-545
145	2	F01	MIMAT0006755	cfa-miR-421
146	2	F02	MIMAT0006715	cfa-miR-379
147	2	F03	MIMAT0006661	cfa-miR-1306
148	2	F04	MIMAT0006713	cfa-miR-127
149	2	F05	MIMAT0009872	cfa-miR-190a
150	2	F06	MIMAT0006675	cfa-miR-28
151	2	F07	MIMAT0009875	cfa-miR-490
152	2	F08	MIMAT0006633	cfa-miR-128
153	2	F09	MIMAT0009830	cfa-miR-20b
154	2	F10	MIMAT0006646	cfa-miR-138b
155	2	F11	MIMAT0006722	cfa-miR-376a
156	2	F12	MIMAT0006626	cfa-miR-29a
157	2	G01	MIMAT0006734	cfa-miR-144
158	2	G02	MIMAT0009938	cfa-miR-759
159	2	G03	MIMAT0006759	cfa-miR-500

160	2	G04	MIMAT0006635	cfa-miR-181c
161	2	G05	MIMAT0006745	cfa-miR-424
162	2	G06	MIMAT0009929	cfa-miR-300
163	2	G07	MIMAT0009899	cfa-miR-329b
164	2	G08	MIMAT0009877	cfa-miR-514
165	2	G09	MIMAT0009853	cfa-miR-301a
166	2	G10	MIMAT0006665	cfa-miR-1307
167	2	G11	MIMAT0006738	cfa-miR-152
168	2	G12	MIMAT0009897	cfa-miR-325
169	3	A01	MIMAT0006698	cfa-miR-197
170	3	A02	MIMAT0006604	cfa-miR-30a
171	3	A03	MIMAT0009913	cfa-miR-551b
172	3	A04	MIMAT0009885	cfa-miR-299
173	3	A05	MIMAT0006686	cfa-miR-1841
174	3	A06	MIMAT0006747	cfa-miR-542
175	3	A07	MIMAT0010198	cfa-miR-105b
176	3	A08	MIMAT0006644	cfa-miR-1838
177	3	A09	MIMAT0006746	cfa-miR-503
178	3	A10	MIMAT0006750	cfa-miR-363
179	3	A11	MIMAT0006728	cfa-miR-410
180	3	A12	MIMAT0006680	cfa-miR-664
181	3	B01	MIMAT0006691	cfa-miR-497
182	3	B02	MIMAT0006721	cfa-miR-495
183	3	B03	MIMAT0006723	cfa-miR-487b
184	3	B04	MIMAT0009917	cfa-miR-589
185	3	B05	MIMAT0009919	cfa-miR-599
186	3	B06	MIMAT0006731	cfa-miR-212
187	3	B07	MIMAT0009902	cfa-miR-487a
188	3	B08	MIMAT0006639	cfa-miR-425
189	3	B09	MIMAT0009908	cfa-miR-505
190	3	B10	MIMAT0006627	cfa-miR-30e
191	3	B11	MIMAT0006611	cfa-miR-219
192	3	B12	MIMAT0006760	cfa-miR-660
193	3	C01	MIMAT0006714	cfa-miR-136
194	3	C02	MIMAT0009894	cfa-miR-326
195	3	C03	MIMAT0006724	cfa-miR-382
196	3	C04	MIMAT0009848	cfa-miR-215
197	3	C05	MIMAT0006757	cfa-miR-221
198	3	C06	MIMAT0009873	cfa-miR-190b
199	3	C07	MIMAT0006663	cfa-miR-148b
200	3	C08	MIMAT0006704	cfa-miR-350

201	3	C09	MIMAT0006763	cfa-let-7j
202	3	C10	MIMAT0006671	cfa-miR-155
203	3	C11	MIMAT0006642	cfa-miR-199
204	3	C12	MIMAT0006742	cfa-miR-423a
205	3	D01	MIMAT0001548	cfa-miR-450a
206	3	D02	MIMAT0009854	cfa-miR-301b
207	3	D03	MIMAT0009915	cfa-miR-578
208	3	D04	MIMAT0006743	cfa-miR-652
209	3	D05	MIMAT0006652	cfa-miR-19b
210	3	D06	MIMAT0006673	cfa-miR-574
211	3	D07	MIMAT0009918	cfa-miR-592
212	3	D08	MIMAT0009858	cfa-miR-302d
213	3	D09	MIMAT0009860	cfa-miR-489
214	3	D10	MIMAT0009840	cfa-miR-153
215	3	D11	MIMAT0009903	cfa-miR-488
216	3	D12	MIMAT0006628	cfa-miR-135a-3p
217	3	E01	MIMAT0009887	cfa-miR-376b
218	3	E02	MIMAT0009926	cfa-miR-671
219	3	E03	MIMAT0006758	cfa-miR-532
220	3	E04	MIMAT0009890	cfa-miR-377
221	3	E05	MIMAT0009839	cfa-miR-135b
222	3	E06	MIMAT0009924	cfa-miR-653
223	3	E07	MIMAT0006753	cfa-miR-374a
224	3	E08	MIMAT0006701	cfa-miR-1842
225	3	E09	MIMAT0006719	cfa-miR-329a
226	3	E10	MIMAT0007747	cfa-miR-371
227	3	E11	MIMAT0006636	cfa-miR-181d
228	3	E12	MIMAT0009896	cfa-miR-324
229	3	F01	MIMAT0006689	cfa-miR-140
230	3	F02	MIMAT0006618	cfa-miR-1836
231	3	F03	MIMAT0006597	cfa-miR-32
232	3	F04	MIMAT0006603	cfa-miR-455
233	3	F05	MIMAT0006677	cfa-miR-1839
234	3	F06	MIMAT0006732	cfa-miR-132
235	3	F07	MIMAT0006710	cfa-miR-345
236	3	F08	MIMAT0006751	cfa-miR-361
237	3	F09	MIMAT0006694	cfa-miR-186
238	3	F10	MIMAT0006761	cfa-miR-502
239	3	F11	MIMAT0006703	cfa-miR-92b
240	3	F12	MIMAT0009928	cfa-miR-802
241	3	G01	MIMAT0009888	cfa-miR-376c

242	3	G02	MIMAT0006711	cfa-miR-493
243	3	G03	MIMAT0009880	cfa-miR-188
244	3	G04	MIMAT0009931	cfa-miR-875
245	3	G05	MIMAT0006754	cfa-miR-374b
246	3	G06	MIMAT0006615	cfa-miR-151
247	3	G07	MIMAT0009844	cfa-miR-202
248	3	G08	MIMAT0009900	cfa-miR-452
249	3	G09	MIMAT0006739	cfa-miR-338
250	3	G10	MIMAT0006658	cfa-miR-320
251	3	G11	MIMAT0006660	cfa-miR-185
252	3	G12	MIMAT0009935	cfa-miR-207
253	4	A01	MIMAT0006725	cfa-miR-485
254	4	A02	MIMAT0001535	cfa-miR-448
255	4	A03	MIMAT0006736	cfa-miR-142
256	4	A04	MIMAT0006659	cfa-miR-130b
257	4	A05	MIMAT0009891	cfa-miR-381
258	4	A06	MIMAT0009886	cfa-miR-362
259	4	A07	MIMAT0006688	cfa-miR-328
260	4	A08	MIMAT0006607	cfa-miR-99b
261	4	A09	MIMAT0009892	cfa-miR-340
262	4	A10	MIMAT0006678	cfa-miR-26b
263	4	A11	MIMAT0006727	cfa-miR-369
264	4	A12	MIMAT0009879	cfa-miR-105a
265	4	B01	MIMAT0006643	cfa-miR-708
266	4	B02	MIMAT0009849	cfa-miR-216a
267	4	B03	MIMAT0009925	cfa-miR-758
268	4	B04	MIMAT0009884	cfa-miR-149
269	4	B05	MIMAT0006601	cfa-miR-491
270	4	B06	MIMAT0009883	cfa-miR-134
271	4	B07	MIMAT0006685	cfa-miR-1271
272	4	B08	MIMAT0009912	cfa-miR-551a
273	4	B09	MIMAT0009868	cfa-miR-208a
274	4	B10	MIMAT0009934	cfa-miR-665
275	4	B11	MIMAT0006620	cfa-miR-196b
276	4	B12	MIMAT0006668	cfa-miR-99a
277	4	C01	MIMAT0009833	cfa-miR-133c
	4	H01	MIMAT0000010	cel-miR-39
	4	H02	MIMAT0000010	cel-miR-39
	4	H03	NR_002735	SNORD61
	4	H04	NR_002450	SNORD68
	4	H05	NR_002583	SNORD72

	4	H06	NR_002591	SNORD95
	4	H07	NR_002592	SNORD96A
	4	H08	NR_002752	RNU6-2
	4	H09	miRTC	
	4	H10	miRTC	
	4	H11	PPC	
	4	H12	PPC	

Note: All the reference genes (snoRNAs/snRNAs), negative control (cel-miR-39), reverse transcription control (miRTC), positive PCR control (PPC) are indicated in plate 4 (position H1 – H12). This set of controls are repeated in each plate at position H1 – H12.

Appendix 4: List of total altered miRNAs identified in 3 CMT cell lines. Fold-change >2 is indicated by values in red and <-2 indicated by values in blue. Those are <2 but >-2 are in black.

miR ID	CMT12	CMT27	CMT28
cfa-let-7a	-2.33	2.06	-1.31
cfa-let-7b	1.33	2.06	4.43
cfa-let-7c	-4.29	1.36	-1.34
cfa-let-7f	-3.04	2.44	-1.15
cfa-miR-1	-169.25	-31.65	-216.1
cfa-miR-101	3.23	3.28	8.9
cfa-miR-103	2.85	2.63	3.18
cfa-miR-106a	1.56	4.62	1.11
cfa-miR-106b	3.21	4.64	3.88
cfa-miR-10b	-19.53	-2.01	3.53
cfa-miR-122	62.7	-1.05	-2.76
cfa-miR-124	2.47	11.4	3.28
cfa-miR-125a	-1.21	2.47	1.17
cfa-miR-125b	-1.07	-1.12	-2.46
cfa-miR-126	20.75	28.75	81.7
cfa-miR-130a	-1.42	3.14	2.16
cfa-miR-133a	-281.62	-68.47	-83.29
cfa-miR-133b	-98.99	-77.05	-98.82
cfa-miR-137	1.36	-1.52	6.92
cfa-miR-141	266.21	460.66	-20.27
cfa-miR-143	-47.78	-187.73	-2.94
cfa-miR-145	-163.21	-334.18	-7.93
cfa-miR-146a	5.42	1.13	3.38
cfa-miR-146b	474.16	-1.62	1.08
cfa-miR-148a	1.1	1.94	6.29

cfa-miR-150	19.41	3.46	4.37
cfa-miR-15a	1.57	1.24	4.9
cfa-miR-15b	-1.87	3.77	-1.36
cfa-miR-16	-1.03	2.28	1.59
cfa-miR-17	9.26	4.3	23.88
cfa-miR-181a	-1.14	3.57	7.72
cfa-miR-181b	3.31	4.02	17.01
cfa-miR-182	23.45	11.27	13.03
cfa-miR-183	27.6	11.95	12.29
cfa-miR-184	2.73	1.58	2.08
cfa-miR-18a	8.7	1.82	3.82
cfa-miR-192	1.59	7.71	3.79
cfa-miR-196a	1.64	3.92	1.41
cfa-miR-19a	9.18	3.6	7.98
cfa-miR-200a	142.87	149.33	2.9
cfa-miR-200b	89.99	114.2	3.15
cfa-miR-200c	93.18	153.19	-62.06
cfa-miR-203	1051.2	55.44	4.19
cfa-miR-204	-428.58	-24.33	-1.74
cfa-miR-205	335.92	-18.82	-30.5
cfa-miR-20a	1.37	3.47	1.03
cfa-miR-21	3.87	1.08	4.41
cfa-miR-210	-7.91	-2.04	-1.76
cfa-miR-214	-370.25	-152.72	-398.9
cfa-miR-218	-2.88	2.6	16.12
cfa-miR-22	-1.35	1.01	2.27
cfa-miR-222	-3.34	3.65	-18.4
cfa-miR-223	1.61	-22.89	1.24
cfa-miR-224	-4.5	-9.61	-7.17
cfa-miR-23a	-1.06	1.34	2.29
cfa-miR-23b	-2.14	1.75	-2.6
cfa-miR-25	2.8	2.9	2.78
cfa-miR-26a	-2.46	1.5	1.02
cfa-miR-27a	-2.15	1.54	-3.53
cfa-miR-29b	6.51	3.23	16.69
cfa-miR-29c	3.75	1.96	4.87
cfa-miR-30b	2.02	3.8	-1.06
cfa-miR-30c	-1.82	1.7	-2.7
cfa-miR-30d	2.14	3.24	-1.08
cfa-miR-31	-40.82	34.99	2.7
cfa-miR-335	-1.55	11.17	-1.23

cfa-miR-342	1.71	5.17	-1.8
cfa-miR-34a	-2.5	-52.86	-79.47
cfa-miR-34b	1.06	-4.65	12.53
cfa-miR-34c	-1.52	-3.12	8.21
cfa-miR-375	16.97	4.74	3.05
cfa-miR-378	9.5	1.61	5.14
cfa-miR-451	-2.71	1.21	-5.06
cfa-miR-499	24.73	3.55	19.23
cfa-miR-7	50.81	14.31	50.9
cfa-miR-9	184.3	595.34	59.85
cfa-miR-92a	3.04	3.04	4.02
cfa-miR-93	1.63	2.5	1.83
cfa-miR-96	10.79	14.16	14.82
cfa-miR-129	2.53	-3.25	10.49
cfa-miR-135a-5p	1.1	4.07	-2.56
cfa-miR-632	2.72	2.99	4.21
cfa-miR-494	-14.87	1.8	-13.82
cfa-miR-208b	3.92	2.78	9.76
cfa-miR-874	3.55	-4.79	2.57
cfa-miR-449a	-2.13	-1.1	-1.79
cfa-miR-187	3.28	-1.04	6.11
cfa-miR-1837	1.48	2.63	2.38
cfa-miR-331	-1.18	2.56	-1.72
cfa-miR-429	3205.6	1733	2.01
cfa-miR-411	-20.54	-1.65	-26.25
cfa-miR-10a	-18.82	-32.07	-7.23
cfa-miR-206	-9.64	-35.38	-8.95
cfa-miR-504	-1.11	-6	-1.03
cfa-miR-1835	3.41	2.99	2.93
cfa-miR-193a	1.23	-2.92	2
cfa-miR-194	-1.26	3.48	2.18
cfa-miR-454	-1.21	1.41	-2.62
cfa-miR-432	-5.72	-9.81	-5.32
cfa-miR-628	-2.27	4.99	1.63
cfa-miR-330	3.43	3.12	5.14
cfa-miR-380	-4.47	1.74	-4.15
cfa-miR-590	-1.08	2.55	-1.26
cfa-let-7e	-2.74	1.39	-1.58
cfa-miR-496	-1.18	-2.34	-1.09
cfa-miR-433	1.35	-2.12	-1.47
cfa-miR-211	-300.01	-23.89	-1.62

cfa-miR-33a	3.23	3.14	57.89
cfa-miR-1844	3.49	-1.36	5.73
cfa-miR-409	-2.55	1.03	-2.37
cfa-miR-18b	-2.68	6.16	-5.94
cfa-miR-98	-2.51	1.05	-2.24
cfa-miR-539	-1.41	2.43	-1.31
cfa-miR-138a	2.5	58.25	2.87
cfa-miR-483	2.49	1.69	2.68
cfa-miR-450b	-1.44	-2.93	1.39
cfa-miR-139	11.32	4.95	14.74
cfa-miR-876	1.25	-3.99	1.34
cfa-miR-95	38.73	229.9	5.03
cfa-miR-365	-3.97	-2.78	-4.08
cfa-miR-582	-3.62	2.22	-8.57
cfa-miR-545	4.62	3.82	2.15
cfa-miR-379	-30.79	-1.78	-29.11
cfa-miR-127	-28.44	-34.34	-28.72
cfa-miR-190a	-7.01	-8.87	-2.46
cfa-miR-20b	-1.54	5.08	-2.29
cfa-miR-138b	2.45	35.81	1.19
cfa-miR-376a	-32.05	-2.82	-29.78
cfa-miR-29a	2.67	-1	2.95
cfa-miR-500	5	1.53	6.96
cfa-miR-181c	1.69	3.3	8.98
cfa-miR-301a	-1.09	2.12	-1.23
cfa-miR-1307	2.03	1.43	1.31
cfa-miR-152	-176.14	-113.03	2.46
cfa-miR-299	-7.48	2.13	-5.65
cfa-miR-1841	4.21	5.35	2.64
cfa-miR-542	4.6	-1.16	15.68
cfa-miR-105b	-1.64	-9.35	-1.24
cfa-miR-1838	3.59	-1.43	2.13
cfa-miR-503	5.74	2.26	3.82
cfa-miR-363	-3.59	18.35	-5.78
cfa-miR-410	-3.24	1.38	-2.45
cfa-miR-664	4.43	4.08	38.64
cfa-miR-497	-1.5	-9.87	-1.91
cfa-miR-495	-9.42	-2.24	-7.13
cfa-miR-487b	-7.16	1.83	-5.42
cfa-miR-589	-6.99	1.23	-5.29
cfa-miR-212	-1.38	-2.27	1.27

cfa-miR-487a	-2.43	-2.41	-2.42
cfa-miR-425	3.13	1.94	-7.26
cfa-miR-505	3.41	9.1	1.87
cfa-miR-219-5p	1.21	1.97	2.52
cfa-miR-660	2.49	1.91	1.06
cfa-miR-136	-1.96	-7.2	-1.48
cfa-miR-326	-4.12	-1.14	-2.21
cfa-miR-382	-2.5	1.86	-2.08
cfa-miR-215	5.07	-1.03	6.03
cfa-miR-221	3.31	3.05	-1.09
cfa-miR-190b	3.98	19.69	18.08
cfa-miR-148b	2.73	2.11	4.52
cfa-miR-350	-5.52	-1.42	-1.89
cfa-let-7j	2.57	-1.52	3.4
cfa-miR-155	7.06	3.05	22.82
cfa-miR-199	-57.42	-216.88	3.65
cfa-miR-423a	2.11	1.87	3.05
cfa-miR-450a	2.73	-1.49	9.75
cfa-miR-301b	-1.37	3.07	-2.53
cfa-miR-19b	8.79	2.7	11.19
cfa-miR-574	-12.44	-4.8	-3.61
cfa-miR-592	4.6	114.63	44.16
cfa-miR-489	-2.61	-2.28	-1.2
cfa-miR-153	1.9	1.98	-3.65
cfa-miR-488	3.56	-1.34	4.7
cfa-miR-376b	-8.71	1.02	-9.28
cfa-miR-671	-1.33	3.45	-1.7
cfa-miR-532	4.76	1.66	3.74
cfa-miR-377	-6.15	-2.4	-4.65
cfa-miR-135b	2.37	8.84	1.01
cfa-miR-374a	1.12	2.22	-1.1
cfa-miR-1842	1.36	4.18	-2.07
cfa-miR-329a	12.66	1.04	5.45
cfa-miR-371	96.96	33.66	50.83
cfa-miR-181d	8.6	4.11	24.28
cfa-miR-324	2.62	1.46	4.23
cfa-miR-140	-80.55	-8.65	-7.53
cfa-miR-32	3.92	1.92	-4.5
cfa-miR-455	2.07	-9.46	9.18
cfa-miR-1839	1.57	4.86	-1.47
cfa-miR-132	2.76	-1.05	2.25

cfa-miR-345	6.88	7.03	3
cfa-miR-361	1.01	1.02	2.12
cfa-miR-186	9.24	3.04	13.51
cfa-miR-502	2.83	2	1.9
cfa-miR-92b	-2.08	5.31	2.19
cfa-miR-802	1.72	-3.13	4.56
cfa-miR-188	4.76	1.42	3.41
cfa-miR-151	2.01	3.71	2.86
cfa-miR-452	-5.86	-11.26	-4.43
cfa-miR-338	3.05	26.5	-2.84
cfa-miR-320	2.54	-1.33	3.21
cfa-miR-185	4.65	3.18	3.48
cfa-miR-207	2.04	1.86	2.28
cfa-miR-485	2.84	1.02	2.97
cfa-miR-142	2.12	3.37	2.22
cfa-miR-130b	1.4	2.67	-1.11
cfa-miR-381	-16.33	-1.26	-15.62
cfa-miR-99b	1.49	4.12	1.94
cfa-miR-340	2.31	-1.36	1.4
cfa-miR-369	3.42	-1.3	3.58
cfa-miR-105a	-6.39	-49.65	-7.15
cfa-miR-708	-6.48	1.61	-2.05
cfa-miR-216a	-2.77	-5	-2.64
cfa-miR-149	-10.96	-1.3	-1.52
cfa-miR-491	-2.91	1.63	-1.21
cfa-miR-1271	-1.8	4.76	-2.23
cfa-miR-551a	4.72	1.92	2.56
cfa-miR-208a	3.53	1.09	3.66
cfa-miR-196b	-1.11	1.35	-2.26
cfa-miR-99a	-2.1	1.17	-1.28
cfa-miR-133c	-313.74	-67.83	-219.7

miRNAs whose expression were nearly unchanged compared to CMEC

miR ID	CMT12	CMT27	CMT28
cfa-let-7g	1.45	1.28	1.82
cfa-miR-191	-1.07	1.11	-1.63
cfa-miR-195	-1.92	-1.5	-1.8
cfa-miR-24	-1.34	1.84	1.13

cfa-miR-27b	-1.28	1.91	-1.46
cfa-miR-676	1.16	-1.46	1.73
cfa-miR-543	-1.33	1.08	-1.44
cfa-miR-193b	-1.9	-1.99	-1.4
cfa-miR-421	1.84	1.56	-1.82
cfa-miR-1306	1.34	1.34	1.4
cfa-miR-28	-1.17	-1.61	1.91
cfa-miR-490	1.54	1.03	1.65
cfa-miR-128	-1.54	1.87	1.66
cfa-miR-424	-1.41	1.04	1.91
cfa-miR-329b	-1.61	1.43	-1.94
cfa-miR-197	-1.51	1.9	-1.89
cfa-miR-30a	-1.38	1.52	-1.77
cfa-miR-30e	-1.2	1.54	1.3
cfa-miR-652	1.51	1.69	-1.93
cfa-miR-302d	-1.29	-1.09	-1.03
cfa-miR-135a-3p	1.39	1.21	1.84
cfa-miR-1836	1.91	1.51	1.79
cfa-miR-376c	-1.75	1.1	-1.32
cfa-miR-493	1.01	1.33	-1.2
cfa-miR-374b	-1.09	1.73	-1.49
cfa-miR-362	1.66	-1.22	-1.07
cfa-miR-328	-1.88	1.09	-1.06
cfa-miR-26b	-1.69	-1.19	-1.62
cfa-miR-134	1.04	1.18	-1.19
cfa-miR-665	1.26	1.25	1.4

Appendix 5: Heat map visualization of log2 (fold-change) level of expression of miRNAs in 3 CMT cell lines (for array plates 2, 3 and 4)

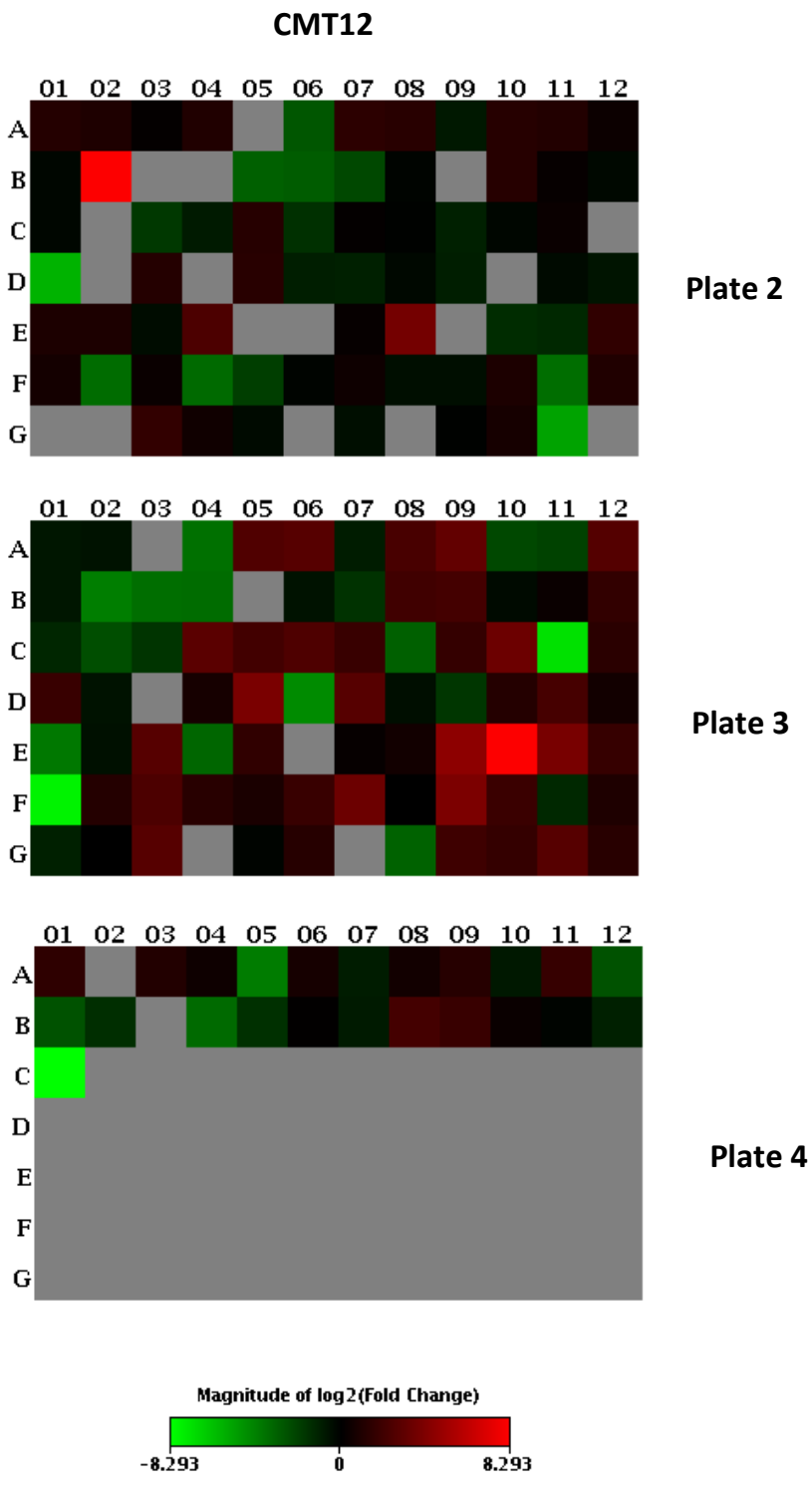

CMT27

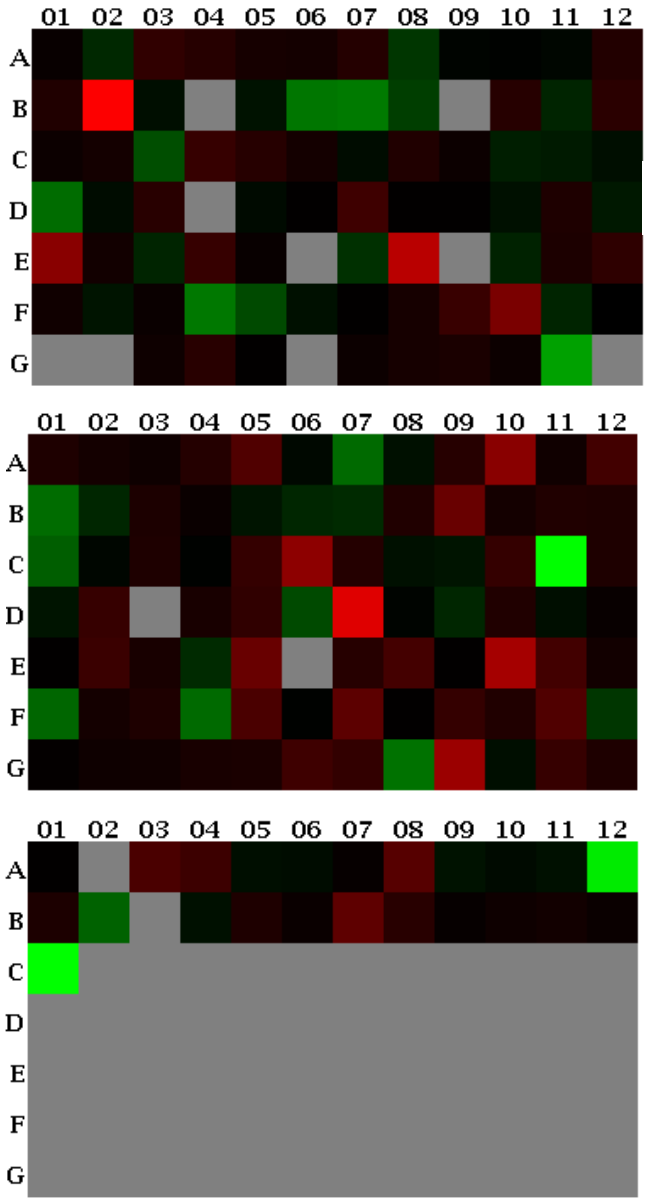

Plate 2

Plate 3

Plate 4

CMT28

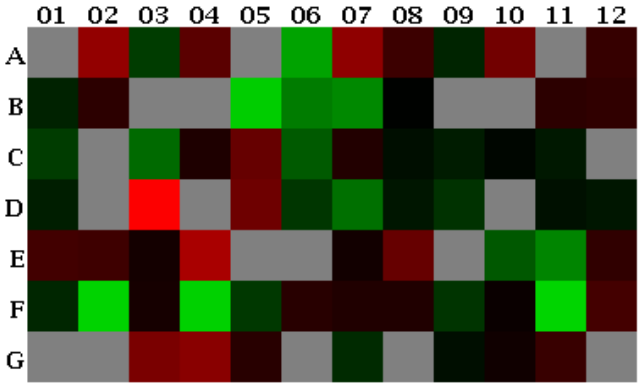

Plate 2

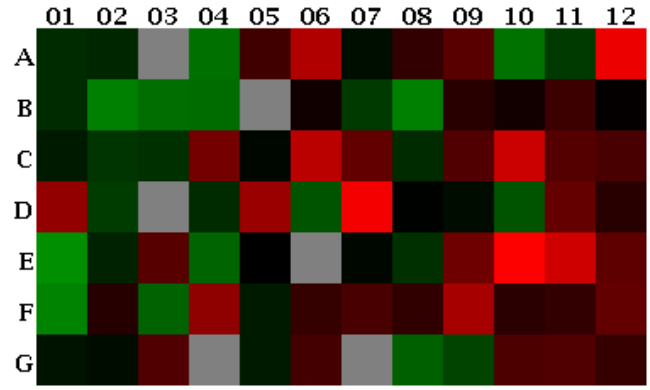

Plate 3

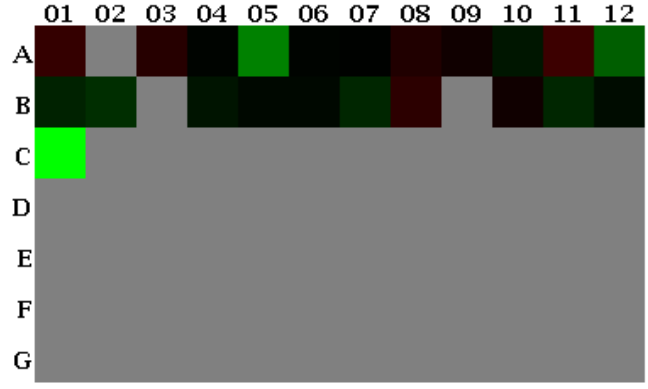

Plate 4

Appendix 6: Comparison of miRNA relative normalized expression between CMEC and CMT cells. Relative normalized expression of a group of representative miRNAs whose fold-change expression was determined as close to 1 or less than 2, was calculated and plotted for CMEC and CMT12 (upper panel) or CMT28 cells (bottom panel).

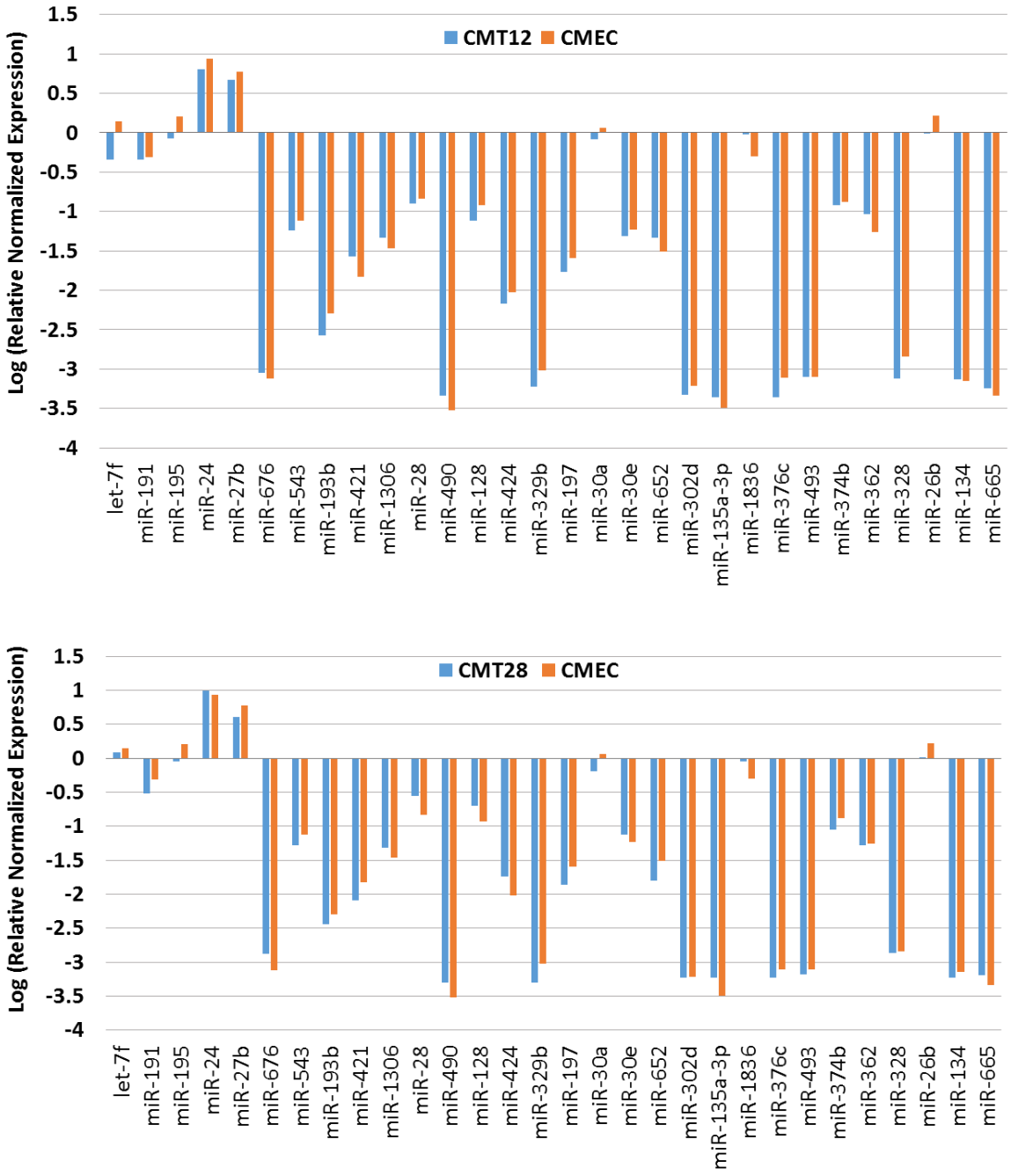

Appendix 7: 3D profile showing fold difference in expression of miRNAs in CMT12 (upper panel) and CMT28 (bottom) cell lines. Columns in the 3D profile pointing up (with z-axis values > 1) indicate an up-regulation of gene expression, and columns pointing down (with z-axis values < 1) indicate a down-regulation of gene expression in CMT cells relative to CMEC.

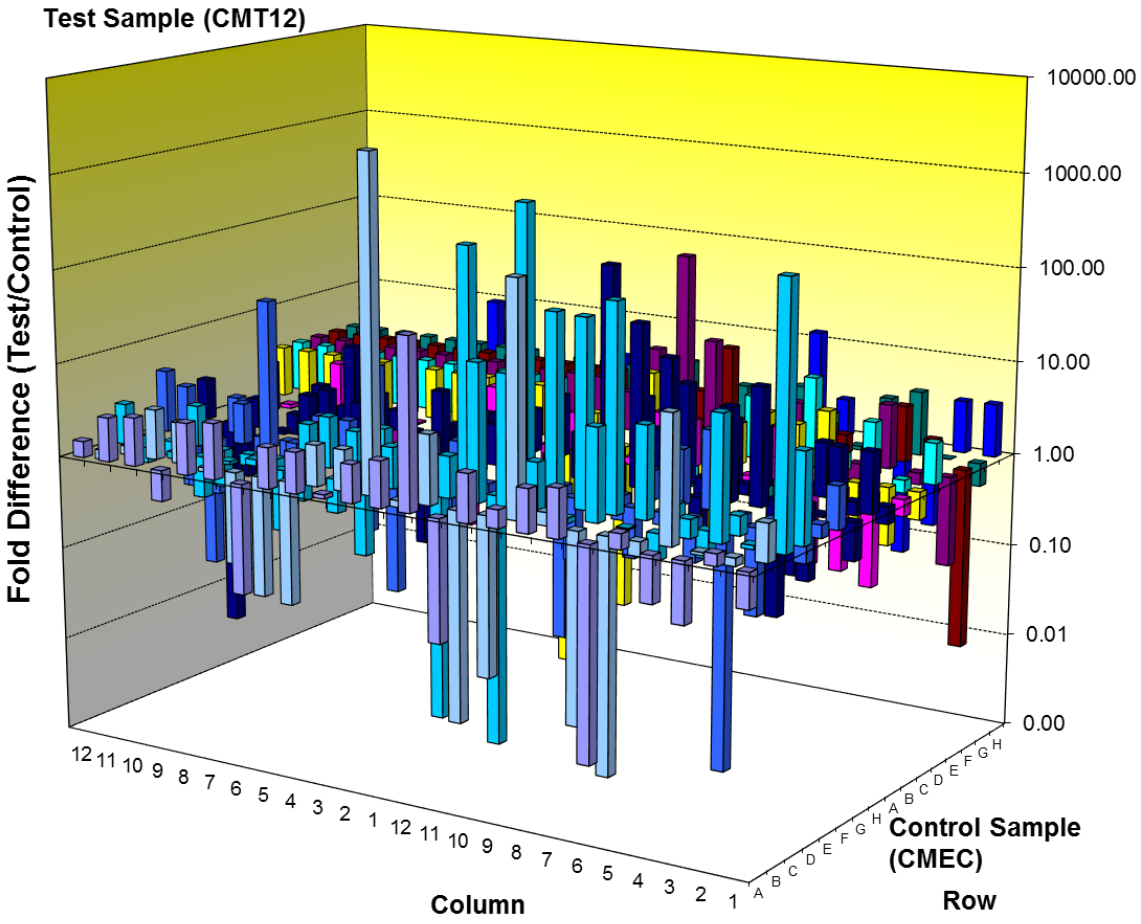

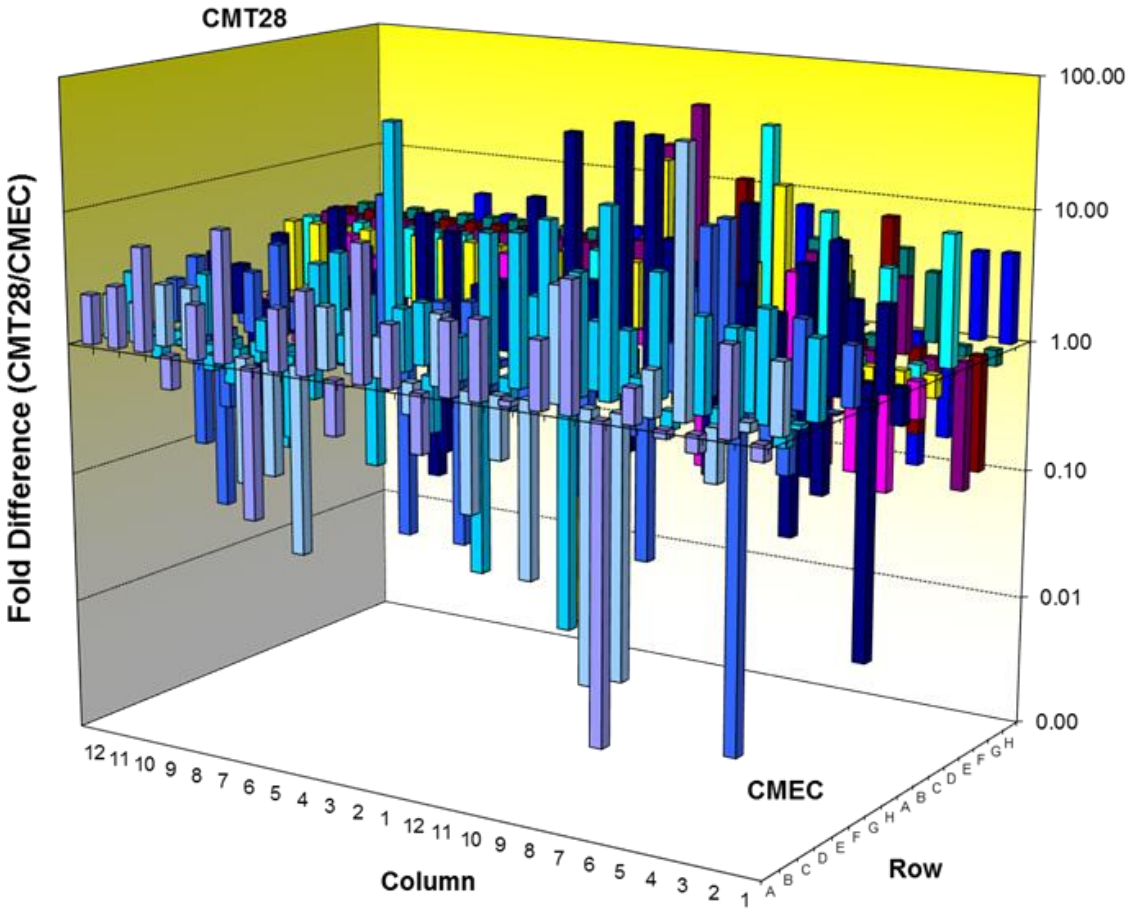
CMT28
Fold Difference (CMT28/CMEC)
100.00
10.00
1.00
0.10
0.01
0.00
12 11 10 9 8 7 6 5 4 3 2 1 12 11 10 9 8 7 6 5 4 3 2 1
Column
CMEC
A B C D E F G H A B C D E F G H
Row

Appendix 8: Volcano plots for CMT27 vs CMEC. The Volcano plot graphs the log2 of the fold change in each gene expression between the samples versus its $\log_{10}$(p-value) from the t-test. The center vertical line indicates fold changes of 1. The two boundary lines vertically to the central line indicate the desired fold-change in gene expression threshold by 2-fold. The blue horizontal line indicates the desired p-value (0.05) from the t-test. Up-regulated miRNAs are in red; down-regulated miRNAs are in green. miRNAs in red and green (just above the respective circles) are shown as both biologically and statistically significant with either higher fold change (by >> 2) or p-value (<<0.05) or both. Group 1 vs. Control Group = CMT27 vs CMEC.

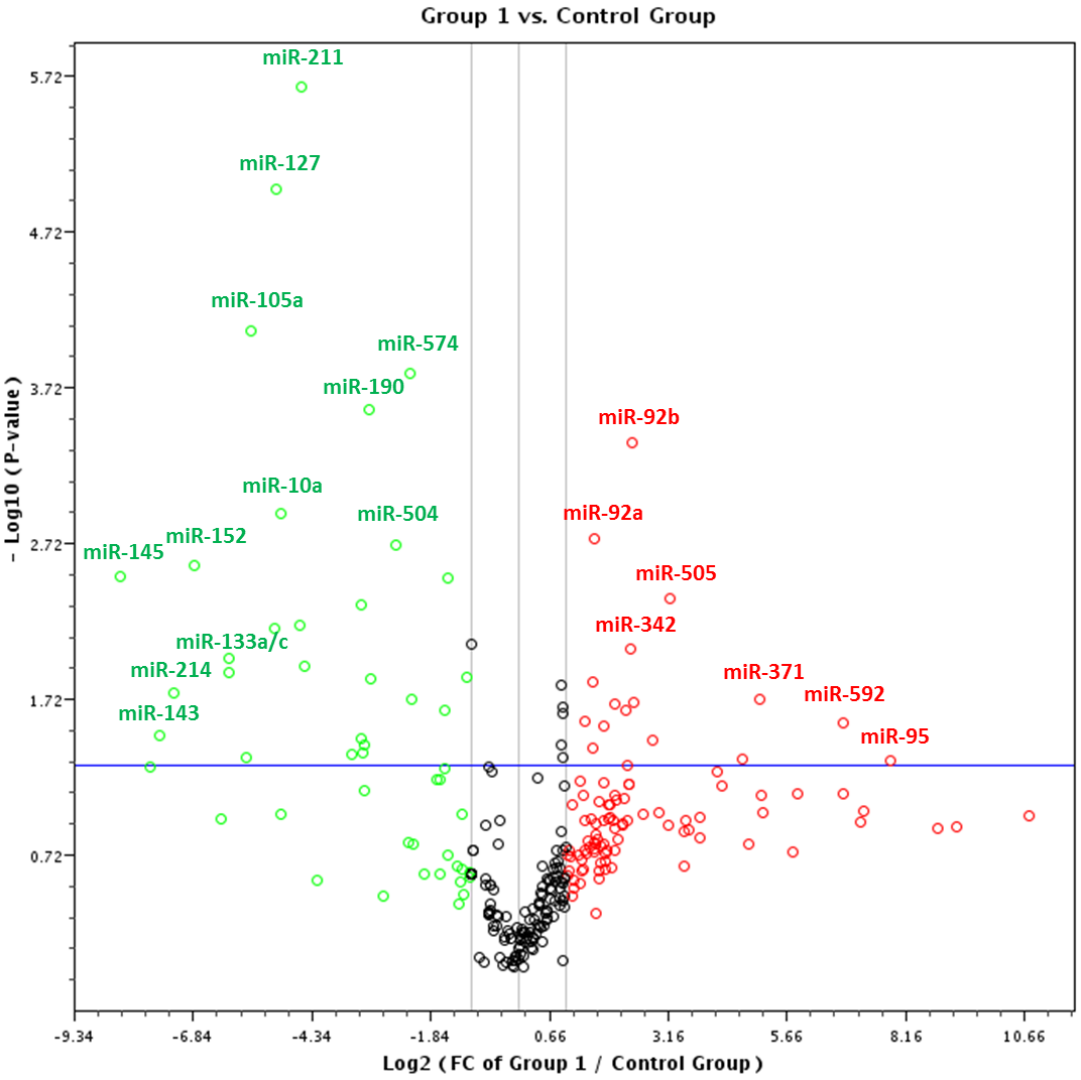

Appendix 9: Single Cell Sorting of Normal Canine Mammary Epithelial Cells. Epitheloid single cell populations were isolated from the bulk mixed cell populations (derived directly from the primary biopsies) using side scatter by size analysis and single cell sorted into 96-well culture plates containing 100 µl growth media per well in a MoFlo XDP Cell Sorter. Each gate was set to separate cell populations based on their sizes. Cells from each gate were recovered following culture in the growth medium and specific mammary epitheloid cells were recognized by observing their morphologies under phase contrast microscopy.